



**University of
Sunderland**

Naik, Swapna G. (2017) Molecular cloning, purification, and characterization of the *Caenorhabditis elegans* Phosphodiesterase 3 (CEPDE3) gene. Doctoral thesis, The University of Sunderland.

Downloaded from: <http://sure.sunderland.ac.uk/id/eprint/16545/>

Usage guidelines

Please refer to the usage guidelines at <http://sure.sunderland.ac.uk/policies.html> or alternatively contact sure@sunderland.ac.uk.

**Molecular cloning, purification, and characterization
of the *Caenorhabditis elegans* Phosphodiesterase 3
(*CEPDE3*) gene**

Swapna G. Naik

**A thesis submitted in partial fulfilment of the requirements of the
University of Sunderland for the degree of Doctor of Philosophy**

Ph.D.

May, 2017

**This research programme was carried out in collaboration with the
National Institutes of Health, National Heart, Lung, and Blood
Institute, Bethesda, MD, USA**

Abstract of Research

Cyclic nucleotide phosphodiesterases (PDEs) are enzymes that regulate the cellular levels of the second messenger molecules cAMP and cGMP by controlling their rates of degradation. In humans, there are 11 different PDE genes, and each gene produces several different isoforms and splice variants. The PDEs are a medically important class of proteins that regulate signaling across a range of tissues, and inhibition of these enzymes is clinically important in a wide array of human diseases. The human PDE3 gene produces two distinct, but related isoforms PDE3A and PDE3B. PDE3A is further subdivided into three isoforms with masses averaging at ~125 kDa. PDE3 play an important role in insulin signaling pathways, cardiovascular tissues, platelets, adipocytes, and oocyte maturation. In particular, PDE3A isoforms are prominently expressed in myocardium and vascular smooth muscle cells, hence, the inhibition of PDE3 activity is particularly useful in treatment of cardiac disease. The focus of this project is the PDE3 gene present in *C. elegans*. Although PDE3 activity has been widely studied from cell and tissue extracts from mammals, there is little data on purified protein for detailed biochemical analysis and characterization of the PDE3 gene and, based on the literature, it suggests that these are difficult proteins to express and purify. There is also very little structural data on the PDE family of enzymes. What exists is mostly on partial proteins, and none at all on the PDE3s.

The aims of this project were to clone and overexpress affinity-tagged recombinant proteins of isoforms of the *C. elegans* PDE3 gene to analyze their catalytic properties and attempt crystallization of the isoforms. The *CEPDE3* gene is a homolog of the mammalian PDE3 family encoding two different CEPDE3 isoforms; CEPDE3-LF (long form) codes for a 63.5 kDa protein, and CEPDE3-SF (short form) codes for a 54.2 kDa protein. Sequence homology alignments of CEPDE3 with human PDE sequences indicate the mammalian and the nematode gene have ~47% homology. The advantages of this approach are that the *C. elegans* isoforms are smaller in mass, making them potentially easier to purify. Preliminary experimental data has suggested that the nematode *CEPDE3* gene exhibits catalytic properties and inhibitor sensitivities that are characteristic of the mammalian PDE3 gene family. A crystal structure would enable the determination of structural elements of the PDE3 catalytic pocket which could contribute to the design of more effective small molecule modulators of PDE3 catalytic activity.

Initially, the CEPDE3-SF isoform was expressed as a His-tag protein from an existing clone. However, due to low protein expression, solubility, and enzyme activity, the use of a GST-tag was attempted since GST-tags are reported to improve solubility in some studies. Initial cloning using traditional PCR and restriction/ligation cloning was attempted to clone both isoforms into the plasmid pGEX-6P1 with little success. To overcome the problem, two alternative approaches to traditional cloning were attempted. The long form was amplified by PCR and was cloned by recombination using the TOPO vector system, prior to subcloning into the expression vector pGEX-6P1. The short form was made synthetically and shipped as a codon optimized insert in a vector and also subcloned into the expression vector pGEX-6P1. Both isoforms were expressed as a GST-tag protein in *E. coli* and, despite the change of affinity tag, the solubility was still poor using standard expression conditions. The solubility of these proteins was a significant barrier to purification, and this was improved by the optimization

of the growth conditions, IPTG concentration, and cell lysis. Optimal solubility was achieved by a novel expression protocol which included an incubation of cells at 4°C prior to expression. Both isoforms were then purified by optimizing conditions using the batch method of purification and using glutathione sepharose 4B. Cleavage of the GST-tag was achieved using PreScission Protease. The purified CEPDE3-LF and CEPDE3-SF after enzymatic cleavage from GST-tag correspond to the predicted size of 63.5 kDa and 54.2 kDa, respectively. Some initial biochemistry was performed on the proteins. CEPDE3-LF and SF lysate and purified protein were assayed for PDE3 enzyme activity by measuring breakdown of cAMP to adenosine. CEPDE3-SF purified protein showed an increase in enzyme activity (24 pmoles/min/mg) compared to crude lysate (5.6 pmoles/min/mg), which is a ~5-fold increase. CEPDE3-LF showed an increase from 2.8 pmoles/min/mg in lysate to 37.5 pmoles/min/mg in purified protein; a ~ 7-fold increase in PDE3 enzyme activity. The CEPDE3-LF and SF isoforms expressed in Sf21 insect cells were assayed with a range of doses of the PDE3 specific inhibitor cilostamide to determine the capacity of enzyme inhibition. A 0.01 μM cilostamide treatments showed a 10-20% inhibition of activity and 5 μM of cilostamide showed ~95% inhibition. Hence both isoforms were inhibited by PDE3 specific inhibitor. The CEPDE3 isoforms expressed in insect cells were also assayed for cAMP and cGMP hydrolysis. The CEPDE3-LF actively hydrolyzed cAMP substrate with a V_{max} of 70.4 pmoles/min/mg, K_m of 0.11 μM and K_{cat} of 0.26 seconds⁻¹. In comparison, the CEPDE3-SF assay did not reach saturation under the same experimental conditions. Therefore, CEPDE3-SF was less efficient in cAMP hydrolysis. Meanwhile, CEPDE3-SF actively hydrolyzed cGMP substrate with a V_{max} of 232 pmoles/min/mg, K_m of 0.37 μM and K_{cat} of 0.84 seconds⁻¹. However, CEPDE3-LF assay did not reach saturation under the same experimental conditions. While both CEPDE3 isoforms have dual specificity for cAMP and cGMP, in this study, the long isoform hydrolyzes cAMP more efficiently short isoform more efficiently hydrolyzes

Acknowledgments

I am very thankful to the University of Sunderland, UK and the National Institutes of Health, USA for accepting me for the prestigious Graduate Partnership Program and for the Intramural Research Fellowship Award.

I am sincerely grateful and very thankful to my supervisor and director of studies Dr. Noel Carter. His guidance, support, kindness and expertise throughout my research work and under difficult circumstances have been very encouraging in completion of my thesis.

I wish to posthumously commemorate my supervisor at NIH, late Dr. Vincent Manganiello (Chief, Biochemical Physiology, Laboratory of Cardiovascular Pulmonary Branch, NHLBI, NIH) for accepting me as a predoctoral research fellow in his laboratory. His valuable supervision on my research work until his last days is deeply appreciated. I specially thank Mrs. Caroline Manganiello for helping Dr. Manganiello go through my experimental data during his time at the hospital. His passing away has been a sad moment. However, what I gained from his teachings in science and outside will always be cherished.

I would like to specially thank Dr. Faiyaz Ahmad (Staff Scientist at the NIH-NHLBI) for supervising my research work throughout and guiding me with molecular and cell biology techniques, enzyme kinetics experiments and presentation of research data. I would like to thank Dr. Arun Samidurai for his help with the *C. elegans* research project.

I would like to specially thank my annual monitoring review committee, Professor Rozaleen Anderson and Dr. Lewis Bingle. Their feedback and comments on my annual monitoring review meetings at the University of Sunderland helped me improve in several ways.

I am very grateful to Dr. Rhee Dong Keun at the NHLBI-NIH for his generous help and teaching me valuable research techniques and precision with subcloning, protein expression and protein purification. I am very thankful to Mr. Steve Hockman at NIH for his outstanding technical support and help with molecular biology techniques.

I specially appreciate and am very thankful to Dr. Gail Seabold (Scientific Skills Coach at NIH-Office of Intramural Training and Education) for her support, guidance and intense proofreading and valuable feedback on my thesis and research work.

I would specially like to thank Dr. Jiro Kato (Staff Scientist at NIH-NHLBI) for his expertise, and guidance with the TOPO cloning procedure, PCR and general molecular biology techniques, also helping me with reagents. I am very thankful to Mrs. Linda Stevens at NIH for her help with protein expression experiments.

I would specially like to thank Dr. Sharon Milgram for her extensive support and guidance and helping with the collaboration of my graduate partnership program. I am very thankful to Dr. John Lough at the University of Sunderland for helping me set up the graduate partnership program. I am thankful to Dr. Mark Proctor for his extensive help with training programmes.

I would like to thank Dr. Kim Guemsoo at the NIH for his help with protein expression experiments and French Press equipment. I am very thankful to Mrs. Yi Hi at the NIH facility for her kindness and help in setting up large bacterial cultures and using the facility. I specially thank Dr. Medha Bhagwat at the NIH library for bioinformatics consultation. I would specially like to thank Dr. Joel Moss for the data club meetings at NIH in absence of Dr. Manganiello. I would like to thank my family and friends for their guidance, support and encouragement.

Above all, I thank God for this life and letting me through all difficulties, guiding me throughout and for giving me the opportunity to write this thesis.

List of Abbreviations

Arg	Arginine
AFD	Amphid neurons with finger like ciliated endings
AWC	Amphic wing C
ASI	Amphid neuron single
BL21	Strain of <i>E. coli</i> supports lac promoter driven gene expression
BL21 (DE3)	Strain of <i>E. coli</i> that contain additional gene for T7 polymerase
BAY60-7650	2-[(3,4-dimethoxyphenyl) methyl]-7-[(1R)-1-hydroxyethyl] 4phenyl-butyl]-5-methyl-imidazo[5,1-f][1,2,4]triazin-4(1H)-one)
BAP	Biotin acceptor peptide
cAMP	Cyclic adenosine monophosphate
CaM	Calmodulin domain
cGMP	Cyclic guanosine monophosphate
c-di-GMP	Cyclic diguanylate
Ca²⁺	Calcium ion
CNG	Cyclic nucleotide gated
CNGC	Cyclic nucleotide gated-channels
CNS	Central nervous system
Cn3D	Macromolecular crystal structure viewer software
COPD	Chronic obstructive pulmonary disease
CBP	Calmodulin binding peptide
Csp	Cold shock proteins
Cpm	Counts per minute
DMPP0	1,3 dimethyl-6-(2-propoxy-5methane sulphonylamidophenyl)-pyrazolo[3,4-d]pyrimidin-4-(5H)-one
DTT	Dithiothreitol
DEAE	Diethylaminoethanol anion exchange
DW	Distilled water
EDTA	Ethylenediaminetetraacetic acid
EGL-4	Egg-laying 4
EHNA	Erythro-9-(2-hydroxy-3-nonyl) adenine
endA	Endonuclease I deficient
FLAG	Asp-Tyr-Lys-Asp-Asp-Asp-Asp-Lys
Gb-1	Protein G B1 domain
GC	Guanosine cytosine
GCAPs	Guanylate cyclase-activating proteins
Glu	Glutamic acid
Gor	Glutathione reductase
GPCR	G protein coupled receptors
GST	Glutathione S transferase
³H-5'-cAMP	Tritium labelled cyclic AMP substrate
³H-3-5' cGMP	Tritium labelled cyclic GMP substrate
HCl	Hydrochloric acid
Hdc	Conserved HD domain
HPC	Heavy chain of protein C
HRP	Horseradish peroxidase
His6	Polyhistidine tag with 6 histidine residues
IPTG	Isopropyl β-D-1 thiogalactopyranoside
IC₅₀	Half maximal inhibitory concentration

IBMX	3-isobutyl-1-methylxanthine
IC224	Selective inhibitor of PDE1
kDa	Kilodalton
K_m	Michaelis constant
MBP	Maltose binding protein
MW	Molecular weight
Mg²⁺	Magnesium Ion
MK1	PDE3 inhibitor
NaCl	Sodium chloride
NHR	N terminal hydrophobic membrane association region
NusA	N-utilization substance
NCS-1	Neuronal calcium sensor-1
NPP	Nucleotide pyrophosphatase/phosphodiesterase
OmpT	Omptin protease mutation in outer membrane protein protease
OD	Optical Density
ON	Overnight
pLysS	Plasmid carrying chloramphenicol resistance and phage T7
PCR	Polymerase chain reaction
Pfam	Protein family database
PDE	Phosphodiesterase
pIDT	Plasmid Integrated DNA Technologies
PBS	Phosphate buffer saline
pH	Potential of hydrogen
pI	Isoelectric point
PSI	Pound-force per square inch
PKB-Akt	Protein kinase B
PKA	Protein kinase A
QIA	Qiagen
QG	Buffer provided with QIAGEN gel purification kit to dissolve DNA
rGCs	Receptor guanylate cyclases
RNase E	Endoribonuclease (endo-RNase)
RPM	Revolutions per minute
RPGR	Retinitis pigmentosa GTPase regulator
Sf9	<i>Spodoptera frugiperda-9</i>
Sf21	<i>Spodoptera frugiperda-21</i>
SNPs	Single nucleotide polymorphisms
SDS-PAGE	Sodium dodecyl sulfate polyacrylamide gel electrophoresis
SGC	Soluble guanylate cyclase
TNF-α	Tumor necrosis factor
tRNA	Transfer ribonucleic acid
tonA	Outer membrane receptor
USFDA	United States Food & Drugs Administration
UCR	Upstream conserved region
Tac	'trp' and 'lac'
T7	T7 bacteriophage
TAP	Tandem affinity purification
Tris-HCl	Tris-HCl (hydroxymethyl) aminomethane buffer
Trx	Thioredoxin
trxb	Thioredoxin reductase b
ThRCs	Thermoreceptor currents
TCA	Trichloroacetic acid

UV

V_{max}

Xap2

Zn²⁺

ZZ-domain

Ultraviolet

Maximum velocity

X associated protein 2

Zinc

Double Z domain

List of Figures

Serial No	Name	Page No
Figure 1.1	Cyclic nucleotide molecule	2
Figure 1.2	Catalytic domain alignment of CEPDE3-SF and CEPDE3-LF with mammalian PDE3B	7
Figure 1.3	Classification of mammalian PDEs	8
Figure 1.4	Domain arrangement of PDE families	9
Figure 1.5	Crystal structure of catalytic domains of PDE3B	13
Figure 1.6	Diagrammatic representation of human-PDE3 isoforms	17
Figure 1.7	Diagrammatic representation of the structural organization of <i>C. elegans</i> PDE3 gene	27
Figure 1.8	Diagrammatic representation of HD Domain in <i>CEPDE3</i> gene	28
Figure 2.1	Experimental design for the study of CEPDE3 isoforms	30
Figure 2.2	Protein fractionation by ultracentrifugation	43
Figure 3.1	Subcloning workflow in recombination cloning	52
Figure 3.2	Overview of TOPO cloning workflow	55
Figure 3.3	TOPO vector blunt map	56
Figure 3.4	Diagram of subcloning vector map for CEPDE3 isoforms	59
Figure 3.5	Agarose gel analysis of subcloning with CEPDE3-LF	60
Figure 3.6	Agarose gel analysis of subcloning with CEPDE3-SF	61
Figure 3.7	Primers designed for CEPDE3-SF and CEPDE3-LF for PCR	62
Figure 3.8	Analysis of PCR samples in CEPDE3-LF and CEPDE3-SF	63
Figure 3.9	Amplification of CEPDE3-LF fragments by PCR	64
Figure 3.10	Agarose gel analysis of the resultant CEPDE3-LF PCR product	65
Figure 3.11	Restriction analysis of recombinant TOPO cloning in CEPDE3-LF	66
Figure 3.12	Subcloning analysis of CEPDE3-LF and pGEX-6P1	67
Figure 3.13	Gene synthesis of CEPDE3-SF sequence for codon optimization	69
Figure 3.14	Workflow for subcloning of CEPDE3-SF gene in pGEX-6P1	70
Figure 3.15	Agarose gel analysis of CEPDE3-SF plasmid	71
Figure 3.16	Agarose gel analysis of codon optimized CEPDE3-SF and pGEX-6P1	72
Figure 4.1	Western blot analysis of CEPDE3-LF and SF his-tag CEPDE3 isoform	83
Figure 4.2	Western blot analysis to detect expression of ARH protein	84
Figure 4.3	Western blot analysis for buffer optimization study with CEPDE3-LF	85
Figure 4.4	Western blot analysis to test specificity of antibody with anti-GST antibody	87
Figure 4.5	Western blot analysis to detect specificity of CEPDE3-SF C terminus antibody	88
Figure 4.6	Western blot analysis for specificity of CEPDE3-SF N terminus antibody	89
Figure 4.7	Western blot analysis for specificity of CEPDE3-LF C terminus antibody	90
Figure 4.8	Western blot analysis for specificity of CEPDE3-LF N terminus antibody	91
Figure 4.9	Western blot analysis to detect common antibody	92
Figure 4.10	Western blot analysis of CEPDE3-LF protein expression	93
Figure 4.11	Western blot and coomassie gel analysis of CEPDE3-LF expression at 37°C	94
Figure 4.12	Western blot and coomassie gel analysis of CEPDE3-LF at lower temperature	96

Figure 4.13	Western blot with CEPDE3-LF expression at large scale (anti-GST antibody)	100
Figure 4.14	CEPDE3-SF protein expressions at 20°C and 25°C	102
Figure 4.15	CEPDE3-SF and LF expression at 20°C	104
Figure 5.1	Representation of affinity chromatography process	110
Figure 5.2	Overview of affinity chromatography through various stages	112
Figure 5.3	Chart of the purification study representing the experimental outcome	115
Figure 5.4	Western blot analysis of GST-spin trap purification	116
Figure 5.5	Western blot from CEPDE3-LF batch purification	117
Figure 5.6	Western bot for buffer optimization in CEPDE3-LF	119
Figure 5.7	Western blot of optimization study using GST-fusion protein	120
Figure 5.8	Western blot analysis with enzyme cleavage CEPDE3-LF	122
Figure 5.9	Detection of CEPDE3-LF protein purification using glutathione sepharose 4B	123
Figure 5.10	Optimization of enzymatic cleavage of CEPDE3-LF using enzyme Precision protease	124
Figure 5.11	CEPDE-LF purification using BL21	126
Figure 5.12	Analysis of CEPDE3-LF purification by regeneration	127
Figure 5.13	Diagrammatic representation for CEPDE3-LF purification using ultracentrifugation	128
Figure 5.14	Analysis of CEPDE3-LF purification fractions by ultracentrifugation	130
Figure 5.15	Analysis of enzymatic cleavage with direct enzyme incubation in CEPDE3-LF	132
Figure 5.16	Enzymatic cleavage using batch method	133
Figure 5.17	Analysis of purification using DEAE columns	135
Figure 5.18	Optimization with DEAE sepharose optimizing with buffers	136
Figure 5.19	Western blot and coomassie gel of CEPDE3-SF purification using glutathione sepharose 4B by batch method	138
Figure 5.20	Analysis of CEPDE3-SF purification fractionation by ultracentrifugation	141
Figure 5.21	Analysis of enzymatic cleavage samples from PreScission protease using direct enzyme incubation	142
Figure 5.22	Analysis of enzymatic cleavage samples from PreScission protease using batch method	143
Figure 5.23	Native gel analysis with CEPDE3 purification fractions	145
Figure 5.24	Coomassie gel analysis with CEPDE3 purification samples	146
Figure 6.1	Percentage of inhibition using cilostamide in CEPDE3-LF protein expressed in insect cells	162
Figure 6.2	Percentage of inhibition using cilostamide in CEPDE3-LF protein expressed in bacteria	163
Figure 6.3	Percentage of inhibition using cilostamide in CEPDE3-SF expressed in <i>E. coli</i>	164
Figure 6.4	Hydrolysis of cAMP by CEPDE3-LF insect cells	168
Figure 6.5	Hydrolysis of cAMP by CEPDE3-SF insect cells	170
Figure 6.6	Hydrolysis of cGMP by CEPDE3-LF insect cells	173
Figure 6.7	Hydrolysis of cGMP by CEPDE3-SF insect cells	175
Figure 6.8	Process of enzymatic reactions	177
Figure 7.1	Predicted crystal structure for CEPDE3-SF	189
Figure 7.2	Predicted crystal structure for CEPDE3-LF	190

List of Tables

Serial No	Name	Page No
Table 1.1	Class I mammalian PDE inhibitors	15
Table 2.1	PCR mastermix reaction	34
Table 2.2	PCR program cycle for CEPDE3 amplification	34
Table 2.3	TOPO cloning reaction mix	35
Table 2.4	Primary and secondary antibody in CEPDE3	40
Table 2.5	Preparation of assay buffer	46
Table 2.6	Preparation of stop solution	46
Table 2.7	Preparation of snake venom	46
Table 2.8	Preparation of neutralization solution	47
Table 2.9	Preparation of ³ H-cAMP assay substrate	47
Table 2.10	Preparation of a standard reaction mix in the PDE enzyme assay	48
Table 4.1	Advantages and disadvantages in <i>E. coli</i> protein expression	80
Table 4.2	Characteristics of <i>E. coli</i> strains	81
Table 4.3	Effect of lower temperature on protein expression and solubility	98
Table 6.1	Summary of PDE activity in protein fractions in the early phase of CEPDE3 protein study	157
Table 6.2	PDE3 enzyme activity of CEPDE3-LF protein expression	159
Table 6.3	Analysis of PDE3 enzyme activity in CEPDE3-LF protein purification fractions	160
Table 6.4	Analysis of purified fractions of CEPDE3-SF	160
Table 6.5	Protein fractions from ultracentrifugation assayed for PDE activity	161
Table 6.6	Effects of dialysis on CEPDE3 enzyme activity	165
Table 6.7	Preparation of substrate for cAMP hydrolysis	166
Table 6.8	Experimental data for CEPDE3-LF cAMP hydrolysis	167
Table 6.9	Experimental data for CEPDE3-SF cAMP hydrolysis	169
Table 6.10	Preparation of substrate for cGMP hydrolysis in CEPDE3-SF	171
Table 6.11	Experimental data for CEPDE3-LF cGMP hydrolysis	171
Table 6.12	Experimental data for CEPDE3-SF cGMP hydrolysis	174
Table 6.13	cAMP and cGMP hydrolysis by CEPDE3-SF and LF	176

Table of contents

Chapter 1: Introduction	1
1.1: Background	1
1.1.1: <i>Classes of PDEs</i>	2
1.1.2: <i>Bacterial PDEs</i>	3
1.1.3: <i>Yeast PDEs</i>	4
1.1.4: <i>Dictyostelium PDEs</i>	4
1.1.5: <i>PDEs in Metazoa</i>	5
1.2: PDE catalytic domain.....	5
1.2.1: <i>Function of PDE catalytic domain</i>	6
1.2.2: <i>Regulatory domain</i>	10
1.2.3: <i>Mechanism for PDE regulation</i>	10
1.2.3.1: PDE protein interactions	11
1.2.4: <i>Interactions of PDE inhibitors with the catalytic domain</i>	11
1.2.4.1: <i>Inhibitor potencies in PDE families</i>	12
1.2.4.2: <i>Factors affecting inhibitor functions</i>	12
1.2.4.3: Commonly used PDE Inhibitors	14
1.3: PDE3 Gene.....	16
1.3.1: <i>Regulation of PDE3A and PDE3B</i>	17
1.3.2: <i>Pattern of expression</i>	18
1.3.3: <i>Structural organization</i>	19
1.3.4: <i>Biological role of PDE3</i>	20
1.4. <i>C. elegans</i> as a model organism for study of diseases	21
1.5 Studies of cyclic nucleotides and PDEs in <i>C. elegans</i>	21
1.5.1 <i>Phototransduction in the worm and upregulation of second messenger cGMP</i>	21
1.5.2 <i>Study of regulation of cGMP levels in AWC neurons in C. elegans</i>	22
1.5.3: <i>The study of human phosphodiesterase PDE10A gene in C. elegans</i>	22
1.5.4: <i>Study of human PDEδ and the C. elegans ortholog CEδ</i>	23
1.5.5: <i>Study of cGMP signaling in C. elegans sensory system</i>	24
1.5.6: <i>Role of cGMP dependent thermotransduction in the C. elegans thermotaxis</i>	24
1.6 PDE3 in <i>C. elegans</i> , an overview.....	25
Chapter 2: General Materials and Methods	30
2.1: Experimental design.....	30
2.2: General Materials.....	31
2.2.1: <i>PCR experiment</i>	31
2.2.2: <i>Subcloning experiment</i>	31
2.2.3: <i>CEPDE3 expression and cell lysis</i>	32
2.2.4: <i>Protein purification</i>	32
2.2.5: <i>PDE3 enzyme assay</i>	32
2.2.5.1 Cell samples	32
2.2.5.2: Equipment	33
2.3: General methods.....	33
2.3.1: <i>Preparation of plasmid DNA</i>	33

2.3.1.1: Experiment 1: PCR with CEPDE3-LF and SF	33
2.3.1.2: Experiment 2: ethanol precipitation.....	34
2.4: TOPO cloning reaction.....	35
2.5: Subcloning experimental method	35
2.5.1: Restriction double digest of CEPDE3-LF and SF.....	35
2.5.2: Agarose gel electrophoresis.....	35
2.5.3: Gel extraction of DNA fragments for cloning.....	36
2.5.3.1: Ligation for CEPDE3-LF and SF	36
2.5.4: Bacterial transformation.....	36
2.5.4.1: Experimental method 1.....	36
2.5.4.2: Experimental method 2.....	37
2.5.4.3: Experimental method for inoculation of colonies in liquid culture	37
2.6: CEPDE3-LF and SF expression.....	37
2.6.1: Cell-lysis using sonication.....	37
2.6.2: Recombinant CEPDE3 expression experiments (cold-shock process).....	38
2.6.3: Cell-lysis buffer optimization.....	38
2.6.4: Bacterial cell-lysis with French press.....	38
2.6.5: Separation of proteins by SDS-PAGE.....	39
2.6.5.1: Western blot analysis.....	39
2.7: Protein purification using GST-spin trap columns	40
2.7.1: GST-spin trap columns	40
2.7.2: Batch method using GST-spin trap columns	41
2.7.3: Protein purification with batch method using glutathione sepharose 4B.....	41
2.7.3.1: PreScission protease enzymatic cleavage.....	42
2.7.3.1.1: Preparation of cleavage buffer	42
2.7.3.1.2: On-column cleavage of fusion proteins.....	42
2.8: Homogenization of CEPDE3-LF and SF using ultracentrifuge	42
2.8.1: Experimental protocol for enzymatic cleavage.....	43
2.8.1.1: Direct incubation with PreScission Protease	44
2.8.1.2: Batch method incubation with PreScission Protease.....	44
2.9: Ion exchange chromatography.....	44
2.10: CEPDE3 enzyme activity assay.....	45
2.10.1: Preparation of QAE Sephadex-A-25 columns.....	45
2.10.2.2: Preparation of buffers for enzyme assay.....	46
2.10.3: Preparation of reaction mix	48
2.10.4: PDE assay calculations	49
2.10.4.1: Enzyme kinetic calculations	49
2.10.4.2: The Lineweaver-Burk method.....	49
Chapter 3: Cloning of CEPDE3-SF and CEPDE3-LF into pGEX-6P1.....	52
3.1: Introduction	52

3.1.1: Traditional cloning	52
3.1.2: Alternative methods of cloning	53
3.1.3: Plasmids for high level expression and purification of protein in <i>E. coli</i>	53
3.1.4: Cloning by recombination	54
3.1.4.1: TOPO cloning method: Function of Topoisomerase I	54
3.1.4.2: Gateway cloning	56
3.1.5: Gene synthesis	57
3.1.5.1: Applications of Gene synthesis	57
3.1.5.2: Importance of codon optimization	57
3.1.6: Background of CEPDE3 initial constructs	58
3.2: Aims.....	59
3.3: Results	60
3.3.1: Experimental design for subcloning of CEPDE3-SF and LF into pGEX-6P1	60
3.3.2: Sequence analysis of isoforms and improved primer design.....	61
3.3.3: PCR amplification of CEPDE3-SF and LF using new primers	63
3.3.4: TOPO cloning and analysis.....	65
3.3.5: Subcloning of CEPDE3-LF into pGEX-6P1.....	66
3.3.6: CEPDE3-SF gene synthesis.....	67
3.3.7: Cloning by gene synthesis	68
3.3.8: Subcloning of CEPDE3-SF with pGEX-6P1.....	71
3.3.9: Subcloning of CEPDE3-SF into pGEX-6P1.....	72
3.4 Discussion	73
3.4.1: Overview	73
3.4.2: Initial subcloning of CEPDE3 isoforms.....	73
3.4.3: Parameters in traditional cloning	74
3.4.3.1: Troubleshooting in PCR experiments	74
3.4.3.2: Analysis of restriction enzymes.....	75
3.4.3.3: Ligation	75
3.4.4: Alternative methods of cloning for CEPDE3 isoforms	76
3.4.4.2:Subcloning of CEPDE3 isoforms in to pGEX-6P1.....	77
3.4.4.1: Summary.....	77
Chapter 4: Protein expression of the <i>C. elegans</i> CEPDE3-SF and CEPDE3-LF isoforms	79
4.1: Introduction	79
4.1.1: The use of <i>E. coli</i> as a host organism for protein production	79
4.1.2: Advantages and disadvantages of <i>E. coli</i> for recombinant protein expression.....	80
4.1.2.1: Choosing the appropriate <i>E. coli</i> host.....	80
4.1.2.2: Affinity Tags	81
4.2: Aims.....	82
4.3: Histidine-tag protein expression	82
4.3.1: Expression of CEPDE3-SF and LF GST-tagged protein expression	84
4.3.2: Specificity of antibodies for expressed GST-tagged SF and LF proteins	85

4.3.3: Optimizing culture conditions	93
4.3.4: Effect of cold-shock therapy on CEPDE3-LF.....	95
4.3.5: Large-scale protein expression in CEPDE3-LF.....	99
4.3.6: CEPDE3-SF expression	102
4.3.7: CEPDE3-SF expression in comparison to CEPDE3-LF	103
4.4: Discussion.....	105
4.4.1: Overview	105
4.4.2: Background on CEPDE3 isoforms	105
4.4.3: Common factors influencing protein solubility	106
4.4.3.1: Protein solubility	106
4.4.3.2: Effect of temperature on protein expression.....	107
4.4.3.2.1: Effect of cold shock on CEPDE3 solubility.....	107
4.4.3.2.2: Effect of IPTG on protein expression	108
4.4.4: Summary.....	108
Chapter 5: Protein purification for <i>C. elegans</i> PDE3 isoforms.....	110
5.1: Introduction	110
5.1.1: Chromatography techniques.....	110
5.1.2: Types of Chromatography.....	110
5.1.3: Affinity Chromatography	111
5.1.3.1: Effect of affinity tags on protein purification	113
5.2: Aims.....	114
5.3: Results	114
5.3.1: Purification of CEPDE3 LF and SF	114
5.3.2: Experimental outcome for CEPDE3 LF and SF protein purification	115
5.3.3: CEPDE3-LF purification.....	115
5.3.3.1: CEPDE3-LF purification with GST-spin trap columns.....	115
5.3.3.2: CEPDE3-LF purification using batch method derived from GST-spin trap columns	117
5.3.4: CEPDE3-LF purification experiments using Tris-HCl and PBS buffers	118
5.3.4.1: Experimental method.....	118
5.3.5: GST control experiment.....	119
5.3.6: Scaling-up of CEPDE3-LF batch purification	121
5.3.6.1: Optimization study for effective enzyme cleavage	123
5.3.7: Measures for improved binding efficiency of CEPDE3-LF with batch method.....	125
5.3.7.1: Pre-incubation of glutathione sepharose 4B with BL21 culture	125
5.3.7.2: Regeneration of Glutathione Sepharose 4B	126
5.3.7.3: Protein fractionation using ultracentrifuge technique.....	128
5.3.7.3.1: CEPDE3-LF studies	128
5.3.7.3.2: Enzymatic cleavage of soluble samples of CEPDE3-LF and SF using PreScission Protease enzyme.....	131
5.3.8: Ion exchange chromatography	134

5.3.8.1: Optimization conditions for protein purification with range of pH buffers using IEX.....	135
5.3.9: CEPDE3-SF purification experiments.....	137
5.3. 9.1: Batch purification with CEPDE3-SF using glutathione sepharose 4B.....	137
5.3.9.2: CEPDE3-SF purification using ultracentrifugation.....	140
5.3.9.3: Enzymatic cleavage.....	140
5.3.10: Summary from protein purification experiments with CEPDE3-LF and SF isoforms.....	144
5.4: Discussion.....	147
5.4.1: Affinity Purification.....	147
5.4.2: Challenges with protein purification.....	147
5.4.3: GST fusion system.....	148
5.4.3.1: Challenges with small scale purification.....	148
5.4.3.2: Challenges with binding efficiency in GST-tag proteins.....	149
5.4.4: Importance of buffers and pH range in protein purification.....	150
5.4.5: PreScission protease cleavage.....	150
5.4.6: Study of Large scale purification using batch method.....	152
5.4.7: Alternative approaches for scaling up CEPDE3 protein purification.....	153
5.4.7.1: Protein fractionation by ultracentrifugation.....	153
Chapter 6: Enzyme kinetics of <i>C. elegans</i> Phosphodiesterase 3 short form and long form (CEPDE3-SF and LF).....	
6.1: Introduction.....	156
6.2: Aims.....	156
6.3: PDE enzyme assay.....	157
6.3.1: Earlier studies on PDE3 enzyme activity.....	157
6.3.2: PDE3 enzyme activity in CEPDE3-LF expressed in bacteria.....	158
6.3.3: Experimental results of CEPDE3-LF protein expression in bacteria.....	158
6.4: Study of PDE3 activity in purified CEPDE3-LF fractions.....	159
6.4.1: Study of PDE3 activity in purified CEPDE3-SF fractions.....	160
6.5: Study of enzyme activity in CEPDE3-LF expressed in insect cells.....	161
6.5.1: Study of IC_{50} in CEPDE3-LF proteins expressed in bacteria.....	162
6.5.2: Study of enzyme activity in CEPDE3-SF expressed in insect cells.....	163
6.5.3: Effects of dialysis on PDE3 activity.....	164
6.6: Study of enzyme kinetics in CEPDE3-LF and SF insect cell lysates.....	165
6.6.1: Experimental method.....	165
6.6.1.1: cAMP hydrolysis.....	165
6.6.1.2: cAMP hydrolysis with CEPDE3-LF and CEPDE3-SF.....	167
6.6.1.2.1: CEPDE3-LF.....	167
6.7.1.3: CEPDE3-SF.....	169
6.7.1.3.1: cAMP Hydrolysis CEPDE3-SF.....	169
6.7.2: cGMP hydrolysis by CEPDE3-LF and CEPDE3-SF.....	171
6.7.2.1: CEPDE3-LF.....	171

6.7.2.2: CEPDE3-SF cGMP hydrolysis	174
6.8 Discussion	176
6.8.1: PDE3 catalytic assay	176
6.8.1.1: Enzyme activity in CEPDE3 proteins	177
6.8.1.2: Enzyme activity of recombinant proteins from bacteria versus insect cells	178
6.8.2 cAMP and cGMP hydrolysis.....	178
6.8.3: K_{cat}/K_m ratio in CEPDE3 isoforms	180
6.8.3.1: Continued studies in CEPDE3 isoforms.....	181
6.8.3.2: Biological importance of CEPDE3 isoforms	181
Chapter 7	183
Chapter 7: Final Discussion	184
7.1: Overview	184
7.2: Studies on CEPDE3 isoforms.....	184
7.2.1: Soluble protein expression	185
7.2.2: Purifying GST-tagged proteins	186
7.2.3: CEPDE3 enzyme study.....	186
7.2.4: Structure of CEPDE3 isoforms	188
7.2.5: PDE3 inhibitors and functions	191
7.3: Future Studies	192

Chapter 1

Chapter 1: Introduction

1.1: Background

Cyclic nucleotide phosphodiesterases (PDEs) are a class of enzymes that catalyze hydrolysis of the 3' phosphodiester bond of second messengers cAMP (cyclic adenosine monophosphate) and cGMP (cyclic guanosine monophosphate) resulting in 5'AMP and 5'GMP. cAMP is derived from adenosine triphosphate and cGMP is derived from guanosine triphosphate. Second messengers are signaling molecules released by cells in response to exposure to extracellular signaling molecules, which are the first messengers, triggering physiological changes such as cell proliferation, differentiation, and apoptosis. In eukaryotes, cAMP and cGMP are involved in activation of protein kinases such as protein kinase A (PKA) and G (PKG), respectively and amplify the effects of the signal received from first messengers. For example, cAMP activation of PKA and the mitogen activated kinase (MAPK) pathway amplifies the allosteric activation of the transcription factors CREB and Myc (Thomas and Haganir, 2004). The intracellular levels of cAMP and cGMP are controlled by their rate of synthesis by cyclases and their degradation rates by phosphodiesterases. Hence PDEs play an important role in regulating the intracellular concentrations and compartmentalization of these second messengers, as well as their biological processes like myocardial contractility, platelet aggregation, vascular smooth muscle relaxation and proliferation of signal transducing molecules (Degerman et al., 2011; Murata et al., 2009). Since the discovery of cAMP by Earl Sutherland in 1958 (Blumenthal, 2012), the cyclic nucleotide system has been developed to explore the opportunities for therapeutic targets to inhibit or enhance PDEs (Pang, 1988), thus providing a mechanism for modulating cyclic nucleotide signaling. Due to advances in methods and technology in the recent years, there has been an increase in knowledge of the PDE families. The PDE families represent an important class of enzymes and constitute gene-related families (PDE1 to PDE11). Each member of the PDE family is characterized by its function, enzymatic characteristics and inhibitor properties. The different PDE families display regulation by distinct allosteric activators or inhibitors. For example, PDE5 contains a GAF domain which has an important role in enzyme allosteric binding to cGMP (Liu et al., 2010). Another example is that of the PDE3 family, which has affinity for both cAMP and cGMP. This difference in regulation allows for specific signaling within each family. Furthermore, PDE proteins within the different families are expressed in specific tissues, as well as distributed in specialized cellular and subcellular locations (Kenan et al., 2000). The human genome encodes twenty-one different PDE genes, the proteins encoded by them have been differentiated and characterized based on their physiochemical and regulatory properties (Soderling and Beavo, 2000). It is reported that there are over 100 isoforms generated through mRNA splicing in PDEs, which are known to exist in several human tissues (Houslay and Adams, 2003; Ahmad et al., 2015).

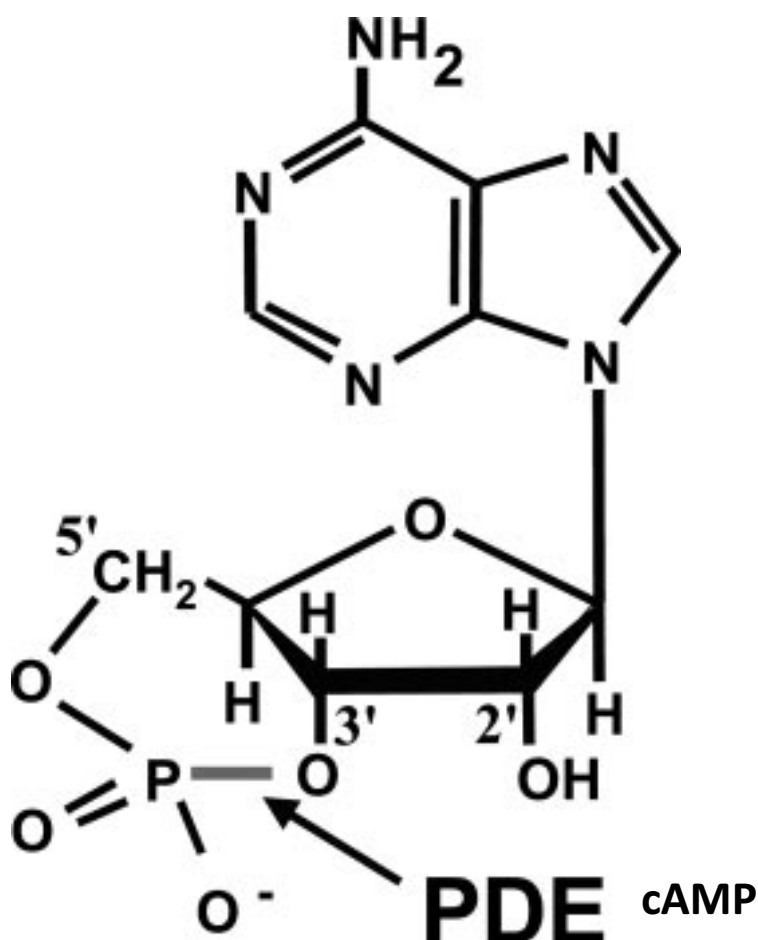


Figure 1.1: Diagrammatic representation of the cyclic nucleotide molecule cAMP

The cyclic nucleotide represents a cyclic bond between the phosphate and the sugar. Cyclic nucleotide molecule contains three functional groups, which includes a sugar, a nitrogenous base and a single phosphate group. There are two bonds between the phosphate group and the 3' and 5' hydroxyl group as seen in the diagram above. The 3' cyclic phosphate bond hydrolyzed by phosphodiesterases is indicated by the arrow (Bender and Beavo, 2006).

1.1.1: Classes of PDEs

The PDE families are known as a superfamily of enzymes that are classified based on their primary structures and homology among genes of the same family and different family genes, as well as substrate and inhibitor specificities. PDEs are subdivided into class I and class II. Class I contains all mammalian PDEs, also several genes identified in other lower organisms such as *Drosophila*, *Caenorhabditis elegans*, and yeast. The mammalian PDEs consist of 11 families (PDE1-PDE11) and are classified based on their relative sequences, mode of regulation, kinetic and pharmacological properties (Conti and Jin 1999). Each PDE molecule contains an N-terminus, regulatory domain, and catalytic domain located at the C-terminus (Ke and Wang, 2007). The mammalian PDE families have high substrate selectivity at physiological concentrations (Beavo and Heaslip, 1994).

Most of the PDEs from class I are encoded by genes consisting of a complex structure with multiple promoters. PDE isoforms are products of individual genes that have unique variants produced by alternative splicing or alternative transcription sites. Along with alternative splicing sites, a large number of transcripts are generated through the promoter region. Thus, genetic regulation results in diverse PDE proteins. Over 100 different human PDE open reading frames from class I have been reported (Conti and Beavo, 2007). The isoforms are biologically important due to their properties of regulation and exhibiting differential expression within the organism. For example, PDE4B and its splice variants showed differential expression in the acute immune response provoked by lipopolysaccharide. PDE4B2 showed increased expression and PDE4B3 showed decreased expression (Johansson et al., 2011). Another example of differential expression and function of PDE8 and PDE4 in T cells. PDE8A is selectively expressed in T effector cells. The PDE8-selective inhibitor PF-04957325 compared to the PDE4-selective inhibitor piclamilast (PICL) demonstrated that PDE8 inhibition did not suppress proliferation and cytokine gene expression in these cells. PDE4 inhibition showed partially opposite effects, thus both PDE8 and PDE4 play unique roles in the control of T effector cell functions (Vang et al., 2016).

Investigation of the differential expression in PDE3 isoforms has the potential to explore therapeutic interventions. The PDE class II consists of a few enzymes from *Saccharomyces cerevisiae*, *Dictyostelium discoideum*, *Schizosaccharomyces pombe*, *Candida albicans*, and periplasmic PDE from *Vibrio fischeri* (Richter, 2002). Yeast and protozoans also contain class I and class II enzymes. Not much is known about proteins that are classified as class III PDEs, since they have not yet been demonstrated to be specific for cyclic nucleotides. Eukaryotic organisms contain multiple genes encoding cyclic nucleotide PDEs. However, in complex species like mammalian class of enzymes, the complexity of the gene varies; e.g., in yeast only one gene of class I is present, however in a complex organism like *Caenorhabditis elegans* there are five genes of class I present. The mammalian PDEs have close homologs in the simple organisms and several genes found in lower species are homologous to some of the recently discovered PDEs. For example, the zebra fish PDE7 homologs, and *Drosophila* homologs of PDE8 and PDE11 (Beavo et al., 2010).

1.1.2: Bacterial PDEs

Cyclic nucleotide PDEs are expressed in several bacterial species. In *Vibrio fischeri*, class II PDE exhibit high expression and are localized in the periplasm. Unlike the class II PDEs, the enzyme present in bacteria is not completely selective for cAMP or cGMP, but is also known to hydrolyze other nucleotides and polynucleotides (Callahan et al., 1995). For example, cyclic diguanylate (c-di-GMP) is known as a ubiquitous second messenger in bacteria. It affects various cellular functions that are related to the transition between a motile single-cell state and an adhesive multicellular state, like cells in biofilm.

1.1.3: Yeast PDEs

The yeast, *Saccharomyces cerevisiae* and *Candida albicans* express a limited amount of PDEs. The PDE1 and PDE2 are known to be present in the *Saccharomyces cerevisiae*, PDE1 which belongs to class II and encodes a low affinity cAMP phosphodiesterase. PDE2 which belongs to class I encodes a high affinity cAMP phosphodiesterase (Hoyer et al., 1994). PDE1 in yeast controls glucose and intracellular acidification-induced cAMP signaling (Ma et al., 1999). It is also now been accepted that activation of the cAMP pathway affects cell wall and membrane structure and biosynthesis not only in *S. cerevisiae*, but also in the human fungal pathogen *C. albicans* (Jung et al., 2005).

1.1.4: Dictyostelium PDEs

Seven PDEs have been identified in *Dictyostelium discoideum*. Among them, three of the enzymes are known to belong to class I PDEs, commonly found in eukaryotes, while four of the enzymes present are in class II PDEs, which are usually found in bacteria and a few other eukaryotic organisms (Bader et al., 2007). PDEs expressed in the *Dictyostelium* play an important role during all aspects of social life (Insall et al., 1994). For example, *Dictyostelium* amoebae undergo chemotaxis in a different way as compared to mammalian cells. When starved, the amoebae begin to release cAMP, and other cells respond through chemotaxis by releasing more cAMP through a signal relay (Stephens et al., 2008). Chemotaxis in *Dictyostelium* involves directional sensing which associates its response to external gradient. The cell receptors and trimeric G proteins with *Dictyostelium* undergo directed cell migration in response to nutrients, platelet activating factor and cAMP. Four cAMP receptors have been identified which are associated with chemotaxis, and have different affinities for cAMP (Van Haastert and Devreotes, 2004). In initial development, during the four hours of starvation, cAMP binds to specific receptors and activates the signal transduction pathway that leads to chemotaxis, secretion of extra cAMP, synthesis and gene expression. During these mechanisms, cAMP is generated through AC (adenylyl cyclase), which shuts down, and the PDE (phosphodiesterase) secreted degrades the extracellular cAMP. These regulatory events help in aggregation of cells. In the later stages of development, the aggregates form a multicellular organism that gradually transforms into a slug structure that migrates along the essential gradients to adapt itself into a suitable environment for its further development (Bagorda et al., 2006). cAMP present in the extracellular region, is known to cause induction of chemotaxis during differential stages of development in slugs. The intracellular cAMP mediates the process of development and the intracellular cGMP in turn mediates chemotaxis. In *Dictyostelium*, different forms of class 1 PDEs were identified, e.g. DdPDE2, DdPDE3, and DdPDE4, and are known to be expressed during the life cycle at various stages of differentiation and development of this organism (Hall et al., 1993).

1.1.5: PDEs in Metazoa

Studies on genome sequences in Metazoa suggest that they show a homology with mammalian PDEs based on their class I catalytic domains. Infrequently, some mammalian orthologs are identified in metazoa, orthologs of mammalian forms are present in species such as *C. elegans*; the *Ciona* (sea squirt) genome also contain PDEs from PDE1, PDE3, PDE4, PDE8, PDE9 and PDE11 families. Meanwhile, *Drosophila* lack PDE2, PDE3, PDE7, and PDE10 (Day et al., 2005).

1.2: PDE catalytic domain

The 11 PDE families share most similarity in their sequence at the carboxy terminus based on the structural determinants among class I PDEs (Fig. 1.4). The catalytic domain is a highly conserved region located at the C terminus that has 25-40% homology with other mammalian PDE catalytic domains. Meanwhile, differences in the N-terminus regulatory domain characterizes each family and their variants. Crystal structures of the catalytic domains indicate that they contain three subdomains composed of 16 helices, which further contain an active site and is composed of two metal-binding sites. These sites form a deep hydrophobic pocket lined with highly conserved residues, most of which exist in all PDEs (Manganiello, 2013). The active site for binding amino acid residues is formed at the junction of the helices by the conserved amino acid residues in the PDEs and the pocket contains a signature histidine motif (HD(X₂) H(X₄) N). It also contains binding sites for Zn²⁺ and Mg²⁺, which are divalent ions important in PDE catalytic function (Wang et al., 2007). Mn²⁺ and Co²⁺ also have an active role in PDE catalytic activity (Francis et al., 2001). In addition, the catalytic pocket is lined with highly conserved and invariant residues, including an invariant glutamine (Ke et al., 2011). All PDE families have a uniform conformation, except PDE5 (Ahmad et al., 2007) The presence of the 3 subdomains allows for conformational changes within the catalytic domain, and contribute to the conformation variability detected by different binding substrates (Xu et al., 2000) It is likely that the conserved residues account for functional properties common to PDEs (Richter et al., 2001). The first PDE catalytic domain to be studied was PDE4B (Xu et al., 2000).

PDEs differ from each other in terms of their substrate specificity, inhibitor sensitivities and their distribution in various tissues and subcellular regions (Richter et al., 2001). The families of class I PDEs can be grouped according to their substrate specificity (see Fig. 1.3). PDEs 4, 7, 8 selectively hydrolyze cAMP, PDEs 5, 6 and 9 hydrolyze cGMP, while PDEs 1, 2, 3, 10 and 11 exhibit dual specificity and are known to hydrolyze both cAMP and cGMP (Ahmad et al., 2000). PDE3 and the other PDEs which hydrolyze both substrates are closely related in terms of substrate specificity. PDEs which hydrolyze cAMP are regulated by GAF domains. The name originates from the first three domains identified in almost all phyla, the mammalian cGMP binding PDEs, *Anabaena* adenylyl cyclases and plant *FhIA* transcription factors (GAF)(Martinez et al., 2005). Binding of cGMP on an allosteric binding site at the N-terminus of the PDE causes activation of PDE. PDE2, PDE5, PDE6, PDE10 and PDE11 all contain a GAF domain (Sette and Conti, 1996). PDE1 is the only

family among mammalian PDEs that is regulated by calcium. This is an allosteric regulation because PDE1 contains a Ca^{2+} /CaM calmodulin binding site at the N terminus, which stimulates the hydrolysis of the cyclic nucleotide. The PDE4 family contains a unique amino acid region known as upstream conserved region (UCR) 1 and 2. The UCR1 region contains a unique PKA phosphorylation site, and upon phosphorylation, UCR1 interacts with UCR2 and activates PDE4 (see Fig. 1.4) (Richter, 2002).

1.2.1: Function of PDE catalytic domain

Initially, the presence of zinc in the catalytic domain was observed in PDE5 (Conti and Beavo, 2007). It has since been observed that the function of zinc is indispensable in all PDEs for catalysis. On the other hand, magnesium (Mg^{2+}) binds loosely to the catalytic pocket compared to zinc, which may be due to the presence of water molecules coordinating with Mg^{2+} bind. (Xu et al., 2000). In addition, conserved residues present in the catalytic pocket are critical for enzyme function. The specificity for cyclic nucleotide at the catalytic domain is dependent on a specific invariant of glutamine. This key glutamine (Q) residue within the active site is critical to determine substrate specificity. For example, in PDE4B, which has specificity for cAMP, glutamine 443 (Q443) is orientated such that its amide group forms a hydrogen bond with adenine. This conformation is stabilized by the adenine also hydrogen bonding with a nearby asparagine (N321) (Hou et al., 2011). PDE5A is an example of a PDE that shows specificity for cGMP. In this case, glutamine 817 (Q817) has the amide in the opposite orientation, which allows hydrogen bonding with the guanidine. This orientation of the glutamine is restricted in part by its hydrogen bonding with another nearby glutamine (Q775). PDE5, has specific binding for cGMP at low substrate levels, but can show a very high catalytic capacity for cAMP as substrate when it is at high substrate levels. This difference in binding specificity is based on the crystal structure of the catalytic domain containing the 5'AMP or 5'GMP complex interacting with catalytic binding pocket site. It is not clear if the cyclic nucleotide substrates would also bind similarly (Li et al., 2012).

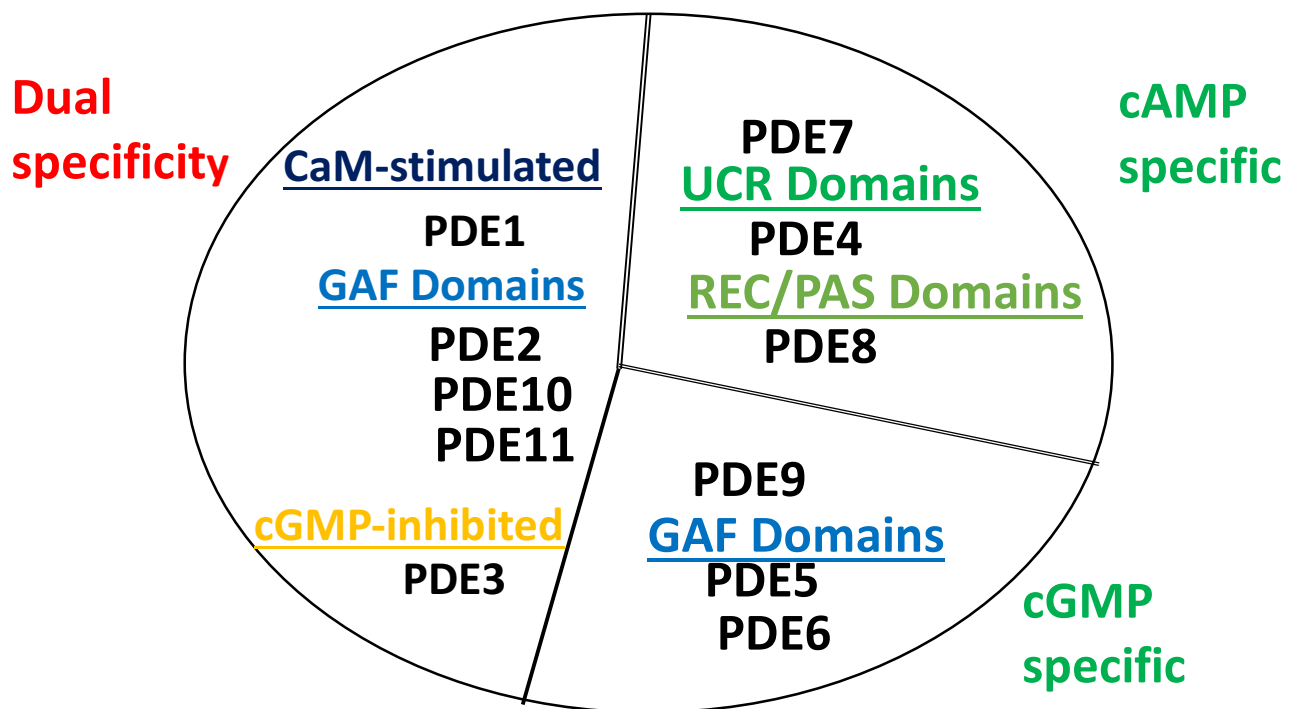


Figure 1.3: Classification of mammalian PDEs

Mammalian PDEs are characterized based on their primary structures, substrate affinity for cAMP and cGMP, their responses to specific effectors and inhibitors, and in relation to mechanisms for their regulation. Three main types of mammalian PDE families are identified depending on their specificity to cAMP and cGMP substrates. They are also classified based on the presence of specific regulatory regions, e.g., calmodulin-binding domain (PDE1) family is calcium dependent and regulated by calmodulin, GAF domains (PDEs 2, 5, 6, 10, and 11), and UCR regions (PDE4). UCR are upstream conserved regions present in PDE4 which are involved in activation and phosphorylation of PDE4. REC/PAS domains (PDE8) (Beavo et al., 2010).

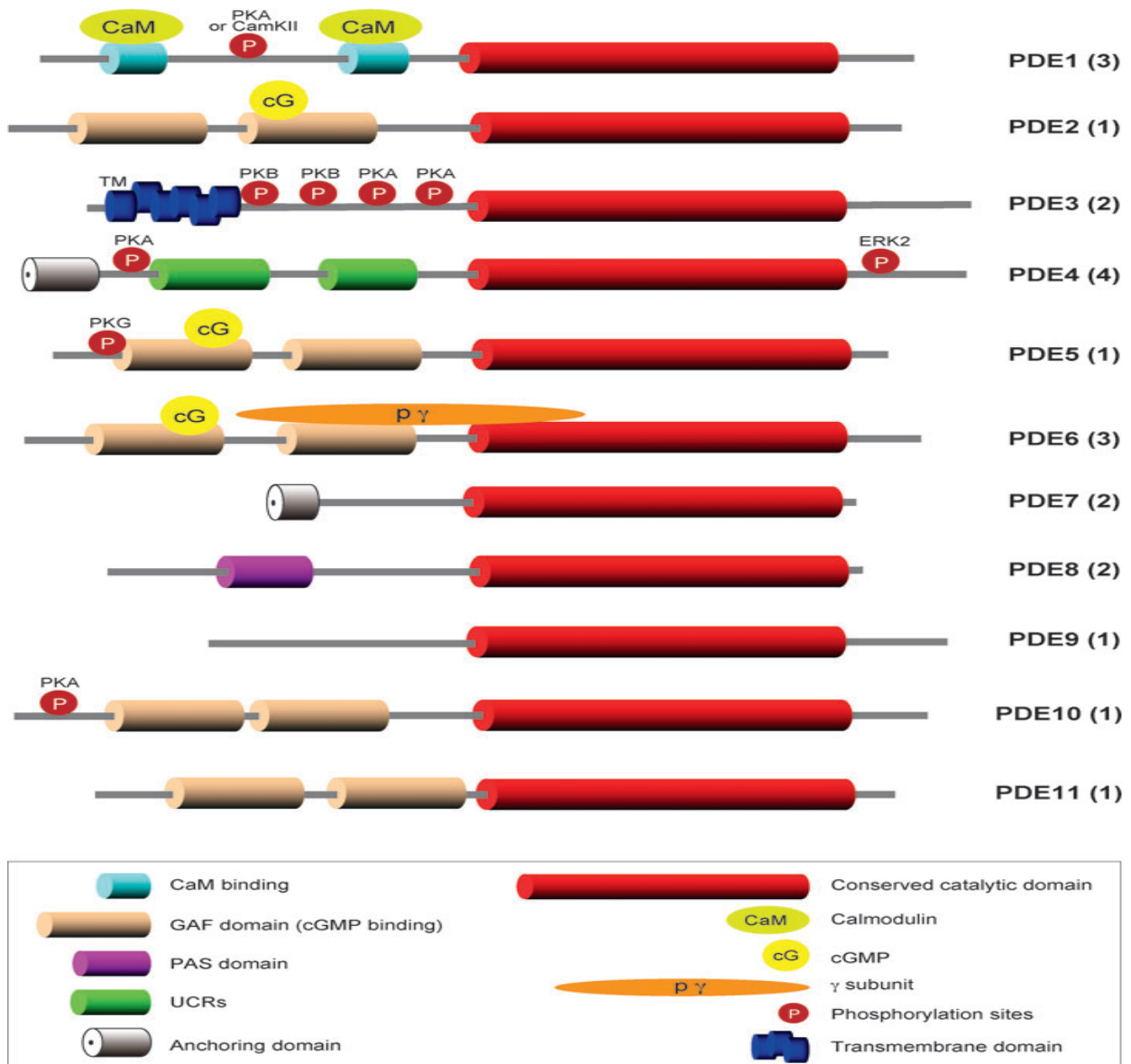


Figure 1.4: Diagrammatic representation of the domain arrangement present in the 11 phosphodiesterase (PDE) gene families

Alignment of the catalytic domains from each of the PDE families. On the right of each structure is the family name, the number in the parenthesis denotes the number of genes the family contains. Some of the families indicate one gene and some contain several genes. The red cylindrical area for each family is the conserved catalytic domain located at the carboxy terminal, representing homology among members of the same family, indicating approximately 25-52% amino acid sequence identity between different PDE families. The regulatory domain of PDEs is diverse. Binding proteins are reported in yellow, P marked in red shows phosphorylation sites. There are alternative splicing sites present in many of the genes generating a large number of mRNA transcripts. Many families contain variants that greatly differ in the regulatory domain and the functional domains. CaM binds to Ca^{2+} and activates PDE1, hence PDE1 family is known as CaM-PDEs. The PDE3 gene represents the 44-amino acid insert in the catalytic domain which is unique to the PDE3 gene family (Omori and Kotera, 2007). The upstream conserved regions (UCR1 and UCR2) are unique to PDE4 and are located in the amino-terminal portion of the enzymes.

1.2.2: Regulatory domain

The N-terminus of the PDE molecule contains the regulatory domain and is known to be highly divergent amongst family members (see Fig. 1.4). It contains structural determinants and specific amino acid sequences of PDEs which respond to specific regulatory signals (Manganiello, 2006). Hence, the regulatory functions at the N-terminus region of the PDEs are diverse as related to the catalytic region (Richter, 2002). The amino terminal sequences in PDEs contain distinct domains that provide for various modes of regulation of PDE functions, e.g.; allosteric cyclic nucleotide-binding sites, inhibitory protein binding sites, phosphorylation sites, Ca^{2+} /calmodulin binding, and autoinhibitory domain (Bender and Beavo, 2006). Autoinhibitory domains are regions present in proteins that negatively regulate the functions of other domains through intramolecular interactions. Autoinhibition involves a potent regulatory mechanism which involves tight-onsite repression. The presence of an autoinhibitory domain was reported in some PDEs, including PDEs 1, 2, 4, 5 and 6, which suggests remarkable homology in the PDE structure. The binding of Ca^{2+} to free calmodulin (CaM) activates the Ca^{2+} -CaM complex associated with the PDE1 isoforms, and relieves the autoinhibitory restrictions, which in turn activates PDE1. The autoinhibitory domains separate the CaM-binding domains from the catalytic site (Jin et al., 1992; Ahmad et al., 2015). Despite the divergent sequences in the N-terminus, recent studies have suggested that several PDE signaling domains can activate bacterial adenylyl cyclase, which participates in the production of cAMP. Therefore, a common mechanism for activation may be present (Martinez et al., 2005).

1.2.3: Mechanism for PDE regulation

PDEs are known as highly regulated enzymes. In general, the rate of cyclic nucleotide breakdown involves the following 1) substrate availability, 2) extracellular signal regulation, 3) short-term feedback regulation and 4) long-term changes in PDE protein levels. PDE enzyme assay methods determined the K_m values for several PDEs are relatively higher compared to cyclic nucleotide at cellular levels. It could be possible that these enzymes could function at lower than the maximum rates. Thus, the activity of PDE would increase due to mass action as cyclic nucleotide levels rise (Francis et al., 2001). The intracellular PDE activity is modified by extracellular signals through several signaling pathways like phosphorylation events, changes in small molecules (Ca^{2+} , phosphatidic acid, inositol phosphates), and protein-protein interactions (e.g., PDE3 activity regulated by insulin, leptin or insulin-like growth factor) (Zhao et al., 1998). Short-term feedback regulation of PDEs is an important and immediate physiological response, which involves several mechanisms, e.g. phosphorylation of PDE3 or PDE4 catalyzed by PKA (Sette and Conti, 1996). Long-term changes at the PDE protein level are caused due to constant changes of enzymes and substrate at the cellular levels, e.g., desensitization which occurs by increased PDE3 and PDE4 levels, followed by chronic exposure of cells to cAMP-elevating agents (Degerman et al 1997). Other examples of PDEs regulation include selective cellular compartmentation due to covalent modification or specific targeting sequences in the PDE primary structure (Houslay and Milligan, 1997).

1.2.3.1: PDE protein interactions

The presence of several PDE splicing variants and the diversity in their regulatory domains indicate that PDE families have the potential for varied protein-protein interactions. These interactions give the catalytic domain new regulatory properties and integrate its function. For example, the holoenzymes present in macromolecular complex. Holoenzymes are enzymes which requires a cofactor. They are complex of proteins that are inactive but are activated upon binding to the cofactor. The complex nature of PDEs and their various splice variants is that the divergent domains specify protein/protein interactions. These interactions give rise to a catalytic domain with new regulatory properties and the functions of holoenzyme is integrated within the macromolecular complexes located inside the cell. Some of these protein interactions have been characterized. For example, CaM interactions with PDE1 and γ subunit interactions with PDE6 influence regulatory protein binding, which affects the catalytic activity of the enzyme (Snyder et al., 1999). In addition, interactions between PDE4A5 and Xap2, a member of the immunophilin family, causes inhibition of the catalytic activity of the enzyme (Bolger et al., 2003). Although the physiological properties of this process have not been identified at the cellular level. Another example of protein interaction is seen with PDE3B and 14-3-3. PDE3B is phosphorylated by PKB/Akt (Degerman and Maganiello., 1997). and this phosphorylation of PDE3B induces 14-3-3 binding (Onuma et al., 2002). Co-immunoprecipitation studies indicate that PDE3B associates with 14-3-3 beta present in rat adipocytes, and this interaction is enhanced by insulin. Therefore, 14-3-3 beta could play a role as a scaffolding protein in the activation of PDE3B by insulin, as insulin receptors are also associated with 14-3-3 (Onuma et al., 2002). In another study conducted on PDE3B, PLC γ was found to bind to PDE3B in the heart, and its ablation had effects on cardiac function by altering cAMP homeostasis (Patruco et al., 2004).

1.2.4: Interactions of PDE inhibitors with the catalytic domain

PDE inhibitors exhibit two features that make them effective in blocking PDE catalytic activity: 1) a planar ring structure, which remains clasped at the active site by a pair of hydrophobic residues, forming a hydrophobic clamp. 2) Formation of hydrogen bond with the invariant glutamine residue that is involved with nucleotide selectivity. Studies based on the crystal structures detected from various PDEs have demonstrated the active binding sites for inhibitors. Studies with crystal structures of PDE4D, PDE4B and PDE5A with inhibitor revealed that the interaction of these inhibitors with these enzymes is through hydrogen bonds (Bender and Beavo, 2006). Identification of this mechanism has encouraged several studies in the therapeutic field. PDE family-selective inhibitors have been studied intensely for potential therapeutic uses. For example, PDE3 selective inhibitors are used in treatment of acute heart failure and intermittent claudication (see Table 1.1). PDE3 inhibitors also affect platelet aggregation, block oocyte maturation, increase myocardial contractility, and affect smooth muscle, as well as vascular, functions. In platelets, cyclic nucleotides can regulate platelet aggregation. For example, PDE3 plays a role in inducing aggregation and PDE3 specific inhibitor prevents platelet aggregation (Shakur et al., 2001). Although PDE families have specific inhibitors, the mechanism of how each family is recognized selectively by the different inhibitors is not very clear (Wang, et al., 2005).

Studies conducted on PDE4 and 7 suggest that there are four factors responsible for inhibitor selectivity: 1) Position and conformation of the invariant glutamine. 2) Scaffolding residues of the active site. 3) Residues that play a role in alteration of the shape and size of the binding pocket. 4) Interactions at the catalytic sites affected by the cellular environment (i.e. pH) (Wanf et al., 2005). Posttranslational modifications, activators such as calcium/calmodulin or cGMP, and binding with other proteins can also influence inhibitor specificity (Houslay et al., 2005). However, studies suggest that the information gained from crystal structures or protein assays using the isolated catalytic domains of PDE does not necessarily divulge all the important contact points that are present in the whole enzyme that could also be exploited when designing new inhibitors (Burgin et al., 2010).

1.2.4.1: Inhibitor potencies in PDE families

Often PDE inhibitors have different efficacy within the same family, or even cytosolic vs. membrane bound forms of the same PDE family member. For example, PDE4 inhibitors show significant differences in activity among the various members of this family. Cilomilast is known to be a highly selective PDE4 inhibitor, but it demonstrates higher potency for PDE4D, in comparison to PDE4A or PDE4C (Torphy et al., 1992). The differences in these closely related enzymes are not well known. However, they could be related to the differences in the catalytic pocket site, posttranslational modification, or their interactions with binding proteins (Burgin et al., 2010). On the other hand, while there are a large number of PDE3 selective inhibitors, which include amrinone, milrinone, cilostamide, and trequinsin (Manganiello, 2013), there are no inhibitors known to be specific for PDE3A or PDE3B, although OPC-33450 has demonstrated some selectivity (Sudo et al., 2000).

1.2.4.2: Factors affecting inhibitor functions

At the catalytic sites of PDEs there can be many changes at cellular levels including pH, posttranslational modifications, interactions with activators (for example, calcium/calmodulin, cGMP), and binding with other proteins (Houslay et al, 2005). However, regulation of the catalytic site is not entirely understood. It is not known why these regulatory changes affect the potency of one inhibitor, but not necessarily another. Experimental studies do not completely unfold the role of the catalytic domain in PDEs in designing new inhibitors (Burgin et al., 2010).

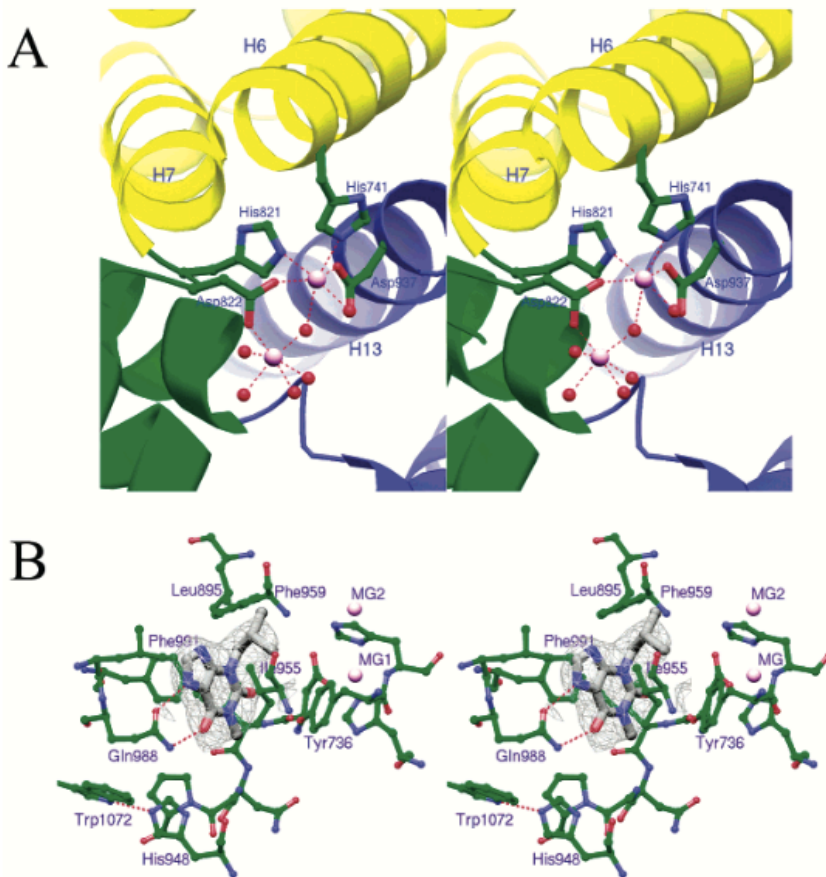


Figure 1.5: Crystal structure of catalytic domains of PDE3B

The crystal structure of the human PDE3B shows binding of metals (A) and inhibitor (B) to PDE3B. (A) All amino acid residues are indicated with their names and number, the helices (H) are also marked by numbers. Between the helices H6 and H7 there is a 44 amino acid insert, characteristic of PDE3B. Water molecules form hydrogen bond interactions (shown by red dashed lines) between the side chains of the catalytic domain residues and the Zn^{2+} and Mg^{2+} ions. (B) IBMX, a PDE3 inhibitor, bound to PDE3B. IBMX makes two hydrogen bond interactions with the side chain of highly conserved Gln988. Magnesium metal binding sites (MG1 and MG2) were observed. MG1 is coordinated by side chain of nitrogen connecting H6 and H7, and MG2 occupies a smaller area; it makes only one direct interaction with protein atoms through second side chain of Asp822.

1.2.4.3: Commonly used PDE Inhibitors

Commonly used PDE inhibitors include cardiostimulant agents, vasodilators, smooth muscle relaxants, anti-depressants, anti-thrombotic, anti-asthmatics, and therapeutic agents for chronic obstructive pulmonary disease (COPD), as well as the improvement of learning and memory (Manganiello, 2011). Several PDE inhibitors have been approved by the US Food and Drug Administration (FDA). The PDE5 selective inhibitors sildenafil (Viagra), vardenafil (Levitra) and tadalafil (Cialis) are some of the known therapeutic drugs in use for treatment of male erectile dysfunction (Wang et al., 2007). PDE5 inhibitors are also used in treatment of pulmonary hypertension. Although PDE5 and PDE11 have catalytic domains with a ~ 51% identical sequence, the differences in their sequences can affect their binding selectivity and catalytic activity. For example, their selectivity for cAMP and cGMP differ, however their hydrolysis rates are equal. Meanwhile, PDE5 shows a ~100 fold greater affinity for cGMP, than cAMP (Corbin and Francis, 1999). In comparison, PDE11 shows hydrolysis with equal affinities for both cAMP and cGMP. In addition, PDE5 and PDE11 show different affinities for the PDE5 inhibitors vardenafil, sildenafil, and tadalafil (Francis et al., 2011). In comparison, both PDE5 and PDE6 have specific binding for cGMP, and the amino acid sequences of their catalytic domains are similar by 42% sequence identity. However, the PDE6 catalytic site shows a ~14 μ M affinity for cGMP, while PDE5 has ~2 μ M affinity. In addition, the catalytic rate of PDE6 exceeds that of PDE5 by ~ 1000 fold (Blount et al., 2006). Similar to PDE5, PDE6 is highly inhibited by sildenafil, zaprinast, and vardenafil. However, while tadalafil is a potent inhibitor of PDE5, it weakly inhibits PDE6 (Zhang et al., 2006). Thus, it indicates that each of the inhibitor chemical characteristics and topography could also influence substrate specificity, catalytic efficiency and potencies of different family of genes to specific inhibitors (Francis et al., 2011).

Table 1.1: Class I mammalian PDE inhibitors.

PDE gene families 1-11 and their commonly used, family specific inhibitors are listed in the table with their clinical applications. Some of the drugs have been approved by USFDA are commonly used, such as PDE5 inhibitors and a few PDE3 inhibitors (Milrinone, Cilostamide), and some inhibitors have been under study for design and implications

PDE	Inhibitors	Clinical Applications
PDE1	IC224, SCH51866, Vinpocetine	Vinpocentine and SCH51866 are used in vitro, IC224 is not well known but may be permeable in intact cells.
PDE2	EHNA, PDP, IC933, Bay 60-7550	Used in function of memory and reducing endothelial permeability under inflammatory conditions.
PDE3	Trequinsin, OPC-33450, Cilostamide, Milrinone, Cilastazol	Milrinone for short-term treatment of congestive heart failure, cilastazol for intermittent claudication.
PDE4	Roflumilast, AWD12-281, SCH-351591, Cilomilast, Rolipram, Ro 20-1724.	These are drugs used for treatment of COPD but have limitations due to their side effects. Some conditions like CNS disorders including depression, schizophrenia, have been investigated.
PDE5	Vardenafil, Udenafil, Sildenafil, Tadalafil.	Sildenafil, Tadalafil Vardenafil, and have been used in treatment of erectile dysfunction, other conditions such as pulmonary hypertension and benign prostatic hyperplasia have been in research.
PDE6	Zaprinast, DMPPO, Sildenafil, Tadalafil, Vardenafil.	Sildenafil use may have known to cause visual side effects.
PDE7	BRL 50481	Anti-inflammatory agent, limited utility in vivo shown currently.
PDE8	PF-04957325	T-cell activation
PDE9	BAY-73-6691	Pre-clinical development for Alzheimer's disease.
PDE10	Papaverine, TP-10, MP-10	Cognitive deficits caused in Schizophrenia

1.3: PDE3 Gene

The PDE3 family hydrolyzes both cAMP and cGMP and are distinguished from the rest of the PDEs by their dual specificity to both substrates. The PDE3 family consists of two subfamilies, PDE3A and PDE3B that are encoded by two different, but related, genes (Degerman et al., 1996; Shakur et al., 2001). The PDE3 gene consists of C-terminus catalytic and N-terminus regulatory region (see Fig. 1.5). Although the conserved catalytic domains in PDE3A and PDE3B are similar, the 44-amino acid insert which is characteristic to PDE3 family, and encoded by exons 11 and 12, is different in PDE3A and PDE3B. This amino acid insert disrupts the first two metal-binding domains present in PDEs (Beavo, 2006). In addition, the N-terminus of PDE3A and PDE3B has two N-terminus hydrophobic regions (NHR1 and NHR2) with transmembrane helical segments. Thus, N-terminus portion of PDE3 is further subdivided into NHR1, containing 5-6 transmembrane helices encoded by amino acids 1-300, followed by NHR2, which contains a smaller hydrophobic region and is encoded by amino acids 300-500. While the PDE3A variants are mainly cytosolic, PDE3B is associated mainly with the membrane. This difference in localization is due to differences in their N-terminus region. Studies conducted with human PDE3A and mouse PDE3B recombinant protein expression performed in Sf9 insect cells and NIH 3006 cells demonstrated that structural determinants present in the NHR1 and NHR2 domains promote efficient membrane association (Shakur et al., 2001; Kenan and Manganiello, 2000). Truncations in both the domains resulted in the enzyme becoming cytosolic (Kenan et al., 2000). Meanwhile, induction of these sequences causes formation of elongated complexes, self-association of PDE3 molecules, and also the interaction of PDE3 recombinants with other proteins. There are also consensus sites for PKB/AKT and PKA phosphorylation in the NH1 and NH2 region of PDE3B (see section 1.3.1). These kinases are considered to be important enzymes involved in regulation of phosphorylation and activation of PDE3B in adipocytes (Degerman et al., 1997; Degerman et al., 1997; Kenan and Manganiello, 2000).

Human PDE3 Isoforms

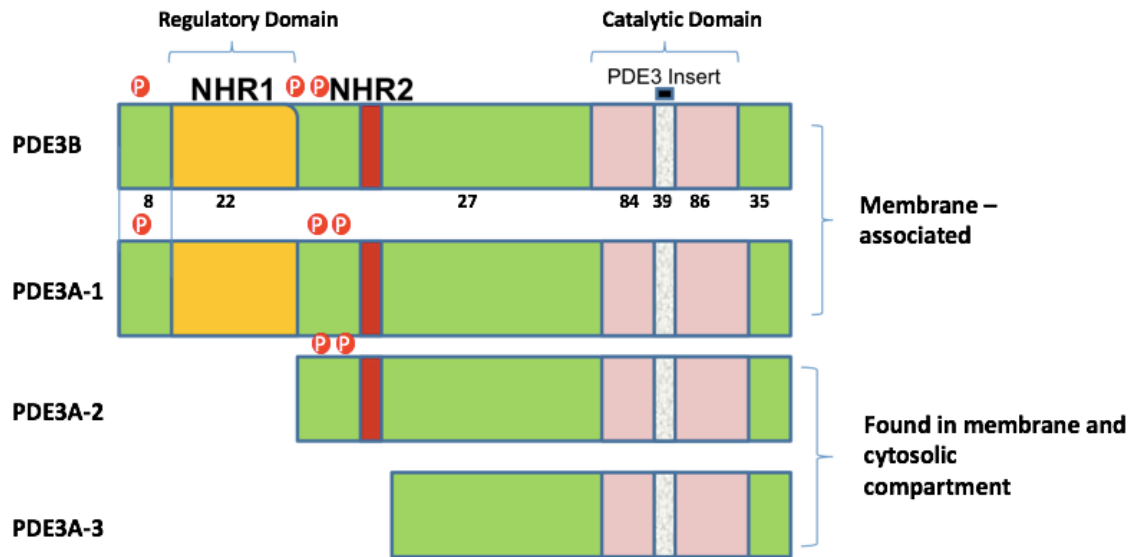


Figure 1.6. Diagrammatic representation of human PDE3 isoforms

PDE3 human gene consists of two sub-families PDE3A and PDE3B. PDE3A-1 PDE3A-2 and PDE3A-3 have identical aa sequences except for the indicated N-terminus deletions. PDE3B and PDE3A-1 are membrane associated isoforms; PDE3A-2 and PDE3A-3 are found in both membrane and cytosol compartments. The N-terminus and C terminus portions of PDE3A and PDE3B are divergent. The catalytic domain is highly conserved among all PDE3 isoforms. There is a 44-amino acid insert located in the catalytic domain, which is unique to the mammalian PDE3; the insert differs between PDE3A and PDE3B isoforms, and differentiates the catalytic domains of the PDE3A and PDE3B subfamilies. The numbers indicated are the % of conserved amino acids in each domain. Red circles indicate the PKA/PKB phosphorylation sites located between the NHR1 and NHR2 domains in the regulatory region of the PDE3A-1 and PDE3A-2 isoforms (Shakur et al., 2001).

1.3.1: Regulation of PDE3A and PDE3B

As mentioned above, PDE3A and PDE3B are two separate genes of the PDE3 family which are closely related, yet distinct. Both PDE3 isoforms are involved in many biological processes, and hence exist in many cells, however they have characteristic localizations (Kenan et al., 2000). They exhibit identical affinities for both cAMP and cGMP, but the cGMP hydrolysis is ~ 10% that of cAMP. At the catalytic site, the breakdown of cAMP is inhibited by the presence of cGMP which competes for binding. Therefore, changes in the levels of cGMP affects cAMP breakdown, and this leads to regulation of cAMP signaling (Shakur et al., 2001). PDE3B is activated and phosphorylated as a result of increased levels of cAMP in response to insulin, insulin-like growth factor (IGF) or leptin through PI3K and PKB signaling, which causes the phosphorylation of PDE3B

(Bender and Beavo, 2006). Importantly, phosphorylation of serines in the N-terminus of PDE3A or PDE3B activates catalysis. In human PDE3B, PKA modifies Ser-73, Ser-296 and Ser-318 (Palmer et al., 2007). In addition, the PKA phosphorylation of Ser-318 causes activation of enzyme, resulting in its interaction with 14-3-3 proteins. PKB phosphorylation of PDE3B also initiates its association with the 14-3-3 proteins (Palmer et al., 2007). As a result of this interaction, phosphorylated PDE3B can become more resistant to dephosphorylation by phosphatases. For example, the 14-3-3 bound, PKA-activated form of HSPDE3B (human phosphodiesterase 3B) was protected from inactivation by phosphatase, in comparison to unbound PKA-activated HSPDE3B. The 14-3-3 protein binds to some, but not all phosphorylated binding partners and may influence their rate of dephosphorylation. A difference in phosphatase catalyzed inactivation of the PKA versus PKB-activated forms of phosphorylated PDE3B may therefore represent a mechanism of activity regulation in cells.

Protein expression and activity of both PDE3B and PDE4D is regulated by insulin in 3T3-L1 adipocytes (Oknianska et al., 2007). In animal model studies of diabetes and obesity, PDE3B is downregulated by TNF- α , which is a cytokine that is increased in obesity and is known to be associated with insulin resistance in animal models, as well as obese individuals (Tang et al., 2001). The upregulation of PDE3B in response to insulin leads to an increase in phospho-CREB, which is mediated by PKA (Oknianska et al., 2007). In a study of human failing hearts, there is a decrease in PDE3A expression (Ding et al., 2005). Angiotensin II or isoproterenol causes downregulation of PDE3A, and thus upregulation of inducible cAMP early repressor (ICER) in cardiac myocytes (Degerman et al., 2011). ICER induction causes repression of PDE3A expression, which further results into activation of cAMP/PKA signaling and, in turn, helps increase ICER expression. However, sustained induction of ICER results in apoptosis of cardiomyocytes. This signaling mechanism is a distinctive autoregulatory positive feedback pathway known as the PDE3A-ICER feedback loop.

1.3.2: Pattern of expression

The two PDE3 isoforms are closely related and hence demonstrate close patterns of expression. PDE3A expression is detected in platelets, placental and vascular smooth muscles. It is also present in corpus cavernosum smooth muscles. PDE3A1 (8.2kb) and PDE3A2 (6.9 kb) are transcripts of the *PDE3* gene. Although they are expressed from the same gene, they carry characteristic 5' regions generated by separate downstream transcription sites located within exon 1. Both are expressed in the human cardiovascular system. It is known that the alternative transcription and post transcriptional processing of the *PDE3A* gene results in two mRNAs and three isoforms in cardiac myocytes (Wechsler et al., 2002). Both the transcripts encode the N-terminus variants PDE3A-(136kDa), PDE3A-(118kDa) and PDE3A-(94kDa). PDE3A1-encodes PDE3A-(136A), which contains the two hydrophobic N-terminus membranes associated domains (NH1 and NH2). PDE3A2 encodes PDE3A-118 and contains one membrane associated domain (NHR2), while a membrane associated domain is not present in PDE3A3 (Keravis and Lugnier, 2012).

In comparison to PDE3A, PDE3B is known to be expressed in cells and tissues related to metabolism, e.g., liver, adipose tissues, and pancreatic β -cells. It is also present in cells related to glucose metabolism, energy homeostasis, and the hypothalamus (Choi et al., 2006; Degerman et al., 2006). Thus, PDE3B expression is particularly high in cells involved in glucose and lipid metabolism (Conti and Beavo, 2007). In addition, PDE3B is present in white and brown adipocytes, hepatocytes, renal collecting duct, epithelium and developing spermatocytes in the rat (Shakur et al., 2001).

Both PDE3A and PDE3B are regulated by phosphorylation. Some biological effects of endogenous cGMP may be mediated by PDE3 inhibition, resulting in increased cAMP levels, which leads to PKA activation, and could also cause activation of other exchange proteins activated by cAMP such as GTP exchange factors (GEFs) (Springett et al., 2004). PDE3A1 and PDE3A2 both contain a PKA phosphorylation site. In contrast, a PKB/AKT phosphorylation site is located only on PDE3A1, while there are no PKA and PKB phosphorylation sites located in PDE3A3 (Wechsler et al., 2002). PKA phosphorylation causes activation of the *PDE3A* gene, which imparts a negative feedback regulation in cAMP signaling. At the same time, activation of PDE3A and PDE3B occurs due to PKB dependent phosphorylation. PKC also causes phosphorylation and activation in PDE3A (Pozuelo Rubio et al., 2005).

1.3.3: Structural organization

Molecular cloning studies conducted in various rat tissues, liver, bovine adipose tissues, human platelets have detected PDE3 isoforms, PDE3A and PDE3B (Beavo 2006). Sequence analysis of PDE3 isoforms demonstrated that both PDE3A and PDE3B in different species are more similar to each other than the amino acid identity of PDE3A and PDE3B present in the same species. The human isoforms PDE3A and PDE3B are located on chromosome 12 and 11 (Hambleton et al., 2005). PDE3A1 has two variants, PDE3A2 and PDE3A3 as alternate start site truncations. PDE3A2 is a shorter version of PDE3A1 due to an individual downstream transcriptional start site. PDE3A3 is a truncated version of PDE3A2, in which the translation begins at downstream ATG. No PDE3B splice variants have been identified. PDE3A and PDE3B exhibit differences in cell-specific locations based on properties, regulation and cell-specific functions (Wechsler et al., 2002). Alternative splicing is also observed in various cell specific regions. For example, as described above in section 1.3.2, three different isoforms can be derived from the *PDE3A1* gene, A vascular smooth muscle isoform (PDE3A2), a longer myocardial isoform (PDE3A1) and a short placental form (PDE3A3) (Choi et al., 2006). PDE3B exhibit regulatory differences based on alternative splicing in cell-specific regions and accordingly they could also have cell-specific functions (Bender and Beavo, 2006). Experimental data from in vitro transcription/translation indicate that alternative transcriptional and post-transcriptional processing of the *PDE3A* gene also results in the generation of two mRNAs and three protein isoforms in cardiacmyocytes (Wechsler et al., 2002). Thus, cell-specific regions from different tissues in PDE3 evoke alternative splicing (Imai et al., 1996).

1.3.4: Biological role of PDE3

PDE3s are located in several tissues, such as platelets, vascular smooth muscles, adipose and liver, PDE3s from adipocytes, hepatocytes and platelets are regulated by several hormones, including insulin, glucagon, catecholamines and prostaglandin (Francis et al., 2001).

In platelets, PDE3A regulates platelet aggregation.

The PDE3 inhibitors such as cilostamide and milrinone inhibit aggregation of platelets. The second messengers cAMP and cGMP are important intracellular second messengers that modulate the function of platelets (Colman, 2004). Thus, PDE3 plays an important role in regulating platelet function and regulate cAMP level, thus causing inhibition in platelet activation pathways. PDE3A inhibitors decrease platelet aggregation (Rondina and Weyrich, 2012). Platelets are considered drug targets for antiplatelet therapy in human diseases (Colman, 2004). The platelet aggregation also plays an important role in cancer metastasis, in circulating tumor cells and their adhesion to vascular endothelium appeared in early stages of metastatic process (Keravis and Lugnier, 2012; Gatspar, 1983).

PDE3A plays an important role in mice oocytes for hydrolysis of cAMP. PDE3A is known to be activated prior to resuming meiosis in the oocytes, an increase in PDE activity is observed during non-induced and LH induced oocyte maturation in vitro. This activation of PDE3A may be important in controlling the cAMP levels which cause resumption of meiosis (Richards, 2001). PDE3A deficient mice were infertile as ovulated oocytes were arrested at the germinal vesicle stage and fertilization failed. Injection with protein kinase inhibitor peptide (PKI) resulted in increased cAMP-PKA signaling, relieving meiotic blockade. As a result, the oocytes resumed meiosis, confirming the critical role of PDE3A in meiotic maturation and ovulation (Masciarelli et al., 2004; Conti, 2011).

The mammalian PDE3 isoforms exhibit distinct functions. Studies conducted on pancreatic β -cell demonstrated that PDE3B has a key role in stimulating the B-cell exocytosis, which thus results in the release of insulin. Due to this activity, PDE3 facilitates the stimulation of glucagon-like peptide 1 on the β -cells in pancreas (Ahmad et al., 2009). In adipocytes, PDE3 inhibitors are known to cause increase in lipolysis there are no PDE3B specific inhibitors yet, however, a PDE3B inhibitor would be important in studying the PDE3B inhibition in lipolysis and increase of metabolic rate, since these functions of PDE3B could have therapeutic effects in obesity (Snyder et al., 1999; Guirguis et al., 2013).

PDE3 specific inhibitor functions demonstrated that PDE3 plays an important function in contractility of myocardium, aggregation of platelets and relaxation of smooth muscle. PDE3 are also involved in contractility of vascular smooth muscle and regulation of cardiac contractility. PDE3 mRNA is greatly expressed in hearts from human, rats, rabbits and dogs. PDE3 variants are expressed in human, rat, pig and synthetic/activated VSMC (vascular smooth muscle cells) with evidence of both PDE3A and PDE3B gene products. (Liu and Maurice, 1998) In vivo studies with cAMP elevating agents increased both PDE3A2 and PDE3B in rats. In contrast, extended cAMP elevation increased PDE3B, but had no effect on PDE3A. The molecular mechanism for the differentiated induction of both PDE3A and PDE3B by cAMP-elevating agents in contractile and activated VSMC are however not completely understood, but may form a basis for selective

regulation of PDE3 variants. This induction of PDE3 may also lead to therapeutic importance, in conditions when cAMP dependent actions are required for vascular smooth muscle procedures, such as balloon angioplasty (Tilley and Maurice, 2002). PDE3B plays an important role in IGF1 insulin and leptin signaling. PDE3B activation affects antilipolytic and anti glycogenolytic actions of insulin, it also affects the release of glucagon like peptide-1 stimulated by insulin, which is released from the pancreas (Zhao et al., 2000). In addition, IGF1, leptin and insulin activation of PI3K stimulates the PKB phosphorylation in PDE3B, which in turn leads to activation of the enzyme (Zhao et al., 1998). The agents that cause rise in cAMP, insulin, IGF-1, leptin, IL-4 in various cells causes activation and phosphorylation of PDE3 isoforms.

1.4. *C. elegans* as a model organism for study of diseases

Caenorhabditis elegans is derived from the name Caeno (recent), rhabditis, (rod-like structure) elegans, (elegant) is a free-living nematode measuring 1 mm in length, it can be safely used in laboratory as a preferred model organism to study various diseases due to several advantages. It has a simple morphology and exhibits well differentiated cell systems, carries a short life span and has ease of manipulability (Harrington et al., 2010). In addition the nematode is biologically and genetically well characterized and can therefore divulge much information regarding the molecular basis of human diseases and thus this organism is amenable for use in research studies of human diseases (Hillier et al., 2005). There have been some important biomedical discoveries carried out in *C. elegans* research. With respect to Alzheimer's disease (AD) research, the protein presenilin was discovered in *C. elegans*, however mutations related to early-onset of familial AD were detected later (Markaki and Tavernarakis, 2010).

1.5 Studies of cyclic nucleotides and PDEs in *C. elegans*

1.5.1 Phototransduction in the worm and upregulation of second messenger cGMP

C. elegans do not have eyes, but are able to sense light, which is essential for the survival of the organism. In animals, photoreceptor cells detect light and the process of phototransduction occurs through electrical responses. Rods and cones absorb light through the rhodopsin family of GPCRs which activate the G protein transducin (Fu and Yau, 2007). In mammalian photoreceptor cells, light-activated transducin turns on PDE6 to cleave the second messenger cGMP, which decreases cGMP and causes closure of CNG channels, thus initiating phototransduction (Fu and Yau, 2007). In vertebrate parietal eye photoreceptor cells, light activated G proteins can inhibit PDEs leading to increase in cGMP levels and opening of CNG channels (Liu et al., 2010). The worm *C. elegans* has also been used widely to study sensory transduction. Nematodes are dependent on olfactory neurons (AWA and AWC) and gustatory neurons (ASE) in response to chemical stimulation (Bargmann, 2006). They react to mechanical forces via touch receptor neurons (ALM, AVM and PLM) and proprioceptor neurons (DVA) (Bounoutas and Chalfie, 2007). *C. elegans* can sense light, which initiates the process of negative phototaxis. As a result, exposure to lethal doses of light are avoided (Ward et al., 2008). Studies

have suggested that this sensory response provides a mechanism for the condition of worms in soil (Edwards et al., 2008). They sense light through a group of photoreceptor cells, some of which respond to light by opening cGMP-sensitive CNG channels. Studies conducted on photoreceptor neuron ASJ have determined that phototransduction in this neuron occurs in ASJ and is mediated by a G protein-mediated process, which requires membrane-associated guanylate cyclases and not cGMP-cleaving phosphodiesterases (PDEs). The data suggests a model, where light signaling in ASJ occurs through transduction of LITE-1 which is mediated through G-protein signaling. This leads to up-regulation of the second messenger cGMP which results into opening of cGMP-sensitive CNG channels and causes stimulation of photoreceptor cells. Thus, a phototransduction cascade in *C. elegans* links the function of a taste receptor to phototransduction (Liu et al., 2010).

1.5.2 Study of regulation of cGMP levels in AWC neurons in *C. elegans*

The nematode *C. elegans* is attracted to various odors, with the help of two head neurons, known as AWC right and AWC left, it can sense and seek out attractive odors, e.g., butanone, isoamyl alcohol (Bargmann et al., 1993). The odor molecules bind to seven transmembrane G-protein coupled receptors, which remain localized to the sensory cilia and hence mediate the chemosensation in AWC (Troemel et al., 1995). The cGMP acts as a secondary messenger in odor signaling in AWC. The receptor guanylyl cyclases DAF-11 and ODR-1, along with cGMP-gated calcium channels, are essential for AWC mediated odortaxis. The protein kinase G, EGL-4, plays an important role in olfactory adaptation of the *C. elegans* AWC sensory neurons (L'Etoile and Bargmann, 2000). Fluctuating levels of cGMP were induced by odor in the adult cilia that play a role in sending the EGL-4 into the AWC nucleus to produce long term adaptation (O'Halloran et al., 2012). The mutations in genes encoding the guanylyl cyclases localized at cilia result in low cGMP, while mutations in cGMP phosphodiesterase block EGL-4 nuclear entry after prolonged exposure to odor. On the other hand, when the cGMP phosphodiesterase PDE3 was over expressed using a heat-inducible promoter in adult worms, significantly higher numbers of worms displayed nuclear-GFP:EGL-4 (O'Halloran et al., 2012). Together, these studies suggest that reducing or increasing the cGMP levels can dynamically modulate the nuclear entry of EGL-4.

1.5.3: The study of human phosphodiesterase PDE10A gene in *C. elegans*

The PDE10A gene exhibits properties of a cAMP PDE and a cAMP inhibited cGMP PDE. The human PDE10A gene is located on chromosome 6q26. Comparison of this gene to those with GAF domains indicate that PDE10A has a different gene organization from PDE5A and PDE6B (Soderling et al., 1999). In comparison to the genome of *C. elegans*, it has an ORF encoding a possible PDE which is expected to be similar with the amino-acid sequences and exon-intron arrangement of this gene which corresponds to PDE10A in humans. Therefore, the human PDE10A gene potentially evolved from a nematode PDE with a GAF domain (Fujishige et al., 2000). The human PDE10A has a 5' upstream sequence of the transcription start site that represents the features of a house keeping gene. From the study of phylogenetic tree analysis, it was observed that the PDE10A gene has a distinct exon-intron arrangement as compared to

other PDEs. Based on the studies with the genome sequencing of the *C. elegans*, there were six probable PDE genes, the *C32E12.2* and the *RO8D7.6* which were predicted to contain a GAF domain in the N-terminus region, and also showed a higher similarity in sequence with the human PDE10A protein and the PDE2A protein (Beavo et al., 1994). The *C32E12.2* gene contains identical axon-intron boundaries to that of the human PDE10A gene, which is suggestive of the close evolution between the human and nematode gene. The *C32E12.2* gene product includes one GAF motif, whereas the human PDE10A gene contains two GAF domains. The PDE10A gene is expected to be derived from an ancestral gene, which is common with the *C32E12.2* gene. The *RO8D7.6* gene in *C. elegans* has been predicted of containing a GAF domain identical to the human PDE10A and PDE2A proteins. In comparison to the *C32E12.2* gene, the *RO8D7.6* gene contains 12 exons, and the DNA region encoding a catalytic domain is un-interrupted by introns. The presence of a PDE10A related gene *C32E12.2* in *C. elegans* suggests the importance of this gene in a lower organism like the nematode. Due to the expression of PDE10A gene in human striatum, the *C32E12.2* gene would be interesting to study. Thus, *C. elegans* might be considered a suitable organism for studying the development of the neuronal system, in terms of comparing the human and nematode PDEs (Fujishige et al., 2000).

1.5.4: Study of human PDE δ and the *C. elegans* ortholog CE δ

The holoenzyme in rod photoreceptor phosphodiesterase (PDE) consists of three subunits termed PDE α , PDE β and PDE γ . A fourth sub-unit PDE δ , co-purifying with bovine PDE was identified and further cloned and expressed (Baehr, 2014). In this study, it was observed that the recombinant protein expressed was solubilized in a similar form to its native protein. Studies carried out on PDE δ indicated that this gene is expressed in other tissues other than the retina. Studies with yeast are suggestive that the human PDE δ interacts with RPGR (which is a GTPase regulator in retinitis pigmentosa) and the GTP binding protein rab, and both are expressed in the large form (Li and Baehr, 1998). In *C. elegans*, PDE α gene presents with the same pattern of axon-intron arrangement showed a similar sequence to that of the PDE δ gene. It was identical in the C-terminus to the retina-specific protein HRG4 which is a homolog of the *C. elegans* gene *unc-119*, expressed in the nematode neurons. Human PDE δ , *ce δ* and HRG4 have similar functions. The bovine PDE δ was previously expressed in insect cells and was reported to be biologically active. The hPDE δ , *CE δ* and HRG4 proteins were expressed as GST-fusion proteins in soluble form and cleaved by thrombin. The PDE activity on these proteins determined that the h-PDE δ was equally active as the recombinant PDE δ expressed in insect cells. The *CE δ* was as active and soluble as compared to the majority of PDE. The HRG4 showed little effect of activity. The protein fractions were also further assayed in a dose-dependent manner. This data confirmed that the protein expressed in nematode has almost the same biological activity as the protein expressed in mammalian photoreceptors.

The C terminus of PDE δ plays an important role in protein folding and activity and required for its cellular location when expressed in tissue culture. Hence truncation mutants were generated 10(M1) and 20(M2) amino acids at the C-terminus., hPDE δ and its truncated mutants were expressed as thioredoxin fusion proteins in *E. coli*. These proteins were also analyzed for PDE

membrane detachment and thio-hPDE δ disrupted PDE membrane partially but showed low activity. Rod PDE is considered to be retina specific and PDE δ is also expressed in retina tissues. To identify distinct proteins from PDE that may interact with PDE δ and CE δ , and indicated similar biochemical properties. The interaction of PDE δ and β subunits indicated that the C-terminus region is important for its interaction. The RPGR peptide at the N-terminus is not isoprenylated and proteins like rhodopsin kinase do not bind to PDE δ , hence the data from these studies suggested that lipid modifications are not essential for the binding (Li and Baehr, 1998).

1.5.5: Study of cGMP signaling in *C. elegans* sensory system

cGMP as second messengers plays an important role in *C. elegans* for regulation of signal transduction with its sensory neurons such as thermosensory, olfactory, gustatory and O₂ sensing neurons (Shidara et al., 2017). Behavioral and genetic studies in *C. elegans* suggest that sensory transduction is mediated by cGMP in many of these neurons, however cAMP is not present in any of these cells (Couto et al., 2013). Analysis of the cGMP signaling in the nematode O₂ sensor to visualize PDE1, PDE2 and PKG cGMP indicated that the *C. elegans* PDE1 and PDE2 are orthologs of mammalian Ca²⁺ stimulated PDE1 and cGMP stimulated PDE2. It is now accepted that PDE1 and PDE2 can form a negative feedback loop regulating each other. Rise in cGMP results in stimulation of PKG and PDE2, and further causes reduction and increase in cGMP (Hofmann et al., 2009). The mechanism which controls the rise in Ca²⁺ also controls a Ca²⁺ dependent negative feedback loop which inhibits accumulation of cGMP, including PDE1 activation (Persson et al., 2009). Negative-cGMP responses do not exist in mutants defective in cGMP gated channel subunits and responses O₂-evoked cGMP. It is known that cGMP dynamics can differ in distinct compartments of the PQR neuron, the cGMP levels in the PQR can fall while Ca²⁺ levels rise, and a rise in O₂ can trigger a rapid increase in cGMP, which is sustained when O₂ is high, but falls when O₂ decreases (Busch et al., 2012). In PDE2 disruption, a rise in O₂ can cause a fall, instead of a rise, in cGMP in PQR neurons. Hence, the role of PKG and PDE2 is to control the rise in cGMP following a rapid increase in O₂ to prevent excessive Ca²⁺ dependent negative feedback (Couto et al., 2013).

1.5.6: Role of cGMP dependent thermotransduction in the *C. elegans* thermotaxis

Nematodes have specialized thermoreceptor neurons to detect internal temperature. A slight change in temperature is sufficient enough for activation of neurons through the process of sensory thermotransduction (Kimura et al., 2004). There are two distinct behaviors in the thermal pattern in *C. elegans*: 1) Negative thermotaxis represents a dominant behavior during when the ambient temperature exceeds the growth temperature. 2) Isothermal tracking, a process in the nematode, is when the worm reaches a thermal zone within 2°C of the cultivation temperature. It is a strategy in which the nematode adapts to the curvature of its propulsive undulations in response to the temperature changes measured at its head (Wang et al., 2013; Luo et al., 2006). AFD, AWC, and ASI are bipolar thermoreceptor neurons, which are involved in the thermal pattern. The study focuses on AFD neurons, and five genes that are important in thermotransduction by AFD. *Tax-4* and *tax-2* genes encode the β subunits located in the CNG ion

channel, whereas *gcy-8*, *gcy-18* and *gcy-23*, which encode receptor guanylate cyclases (rGCs) and are exclusive in AFD neurons. The *tax-2* and *tax-4* genes are involved in thermoreceptor currents in AFD (Inada et al., 2006). There are six PDE genes present in the *C. elegans* genome: PDE1, PDE2, PDE3, PDE4, PDE5 and PDE6, of which PDE1, PDE2, PDE3 and PDE5 play a role in phototransduction in the UV receptors of *C. elegans* (Liu et al., 2010). Furthermore, it is also known that, PDE2 has been identified as an essential element involved in the thermotransduction cascade in AFD (Wang et al., 2013). PDE activity helps to regulate mechanisms with the thermoreceptor currents (ThRCs), and thus PDE activity is essential for AFD transduction. Between the PDE1 and PDE2 genes expressed in AFD, the PDE2 is essential for temperature response. The function of AFD are dependent on a signaling network, which involves guanylate cyclases and a cGMP-gated ion channel (Clark et al., 2006; Wasserman et al., 2011). Mutation in the PDE2 gene has been known to prolong ThRCs in AFD. In addition, the role of neuronal calcium sensor-1 (NCS-1), a calcium binding protein which is associated with guanylate cyclase-activating proteins (GCAPs), in regulation of the membrane current in AFD was examined. In terms of PDE2 mutants, loss of NCS-1 caused prolongation in ThRCs and thus increased their threshold. Loss of PDE2 had no effects on currents activated with voltage. However, increase in the voltage-activated outward currents were detected with loss of NCS-1. Hence, the signaling network involving GCY-8, PDE2 and NCS-1 proteins regulate the mechanism with ThRCs, thus controlling the intracellular cGMP levels regulated by temperature (Wang et al., 2013).

1.6 PDE3 in *C. elegans*, an overview

Earlier studies carried out in the Manganiello laboratory at the NHLBI/NIH by (Samidurai et al., 2011, unpublished data) began to characterize the *C. elegans* cyclic nucleotide phosphodiesterase 3 (CEPDE3), which is known to be a homolog of the mammalian PDE3 family. In contrast to the mammalian PDE3 gene family, which is comprised of two distinct, but highly related, genes that generate two isoforms PDE3A and PDE3B, a single nematode PDE3 gene is present on *C. elegans* chromosome II, spanning about 20.2 kb, and encodes at least two different PDE3 isoforms. The CEPDE3 long form (LF) consists of 11 exons and codes for a 63.5 kDa protein; the short form (SF) has 8 exons and codes for a 54.2 kDa protein (refer to Fig. 1.7). Both CEPDE3 isoforms have the characteristics of mammalian PDE *Pfam* and phosphodiesterase domains. Both CEPDE3 isoforms also have the HD metal binding motif, which is unique for the PDE superfamily. There are several putative kinase phosphorylation sites around the HD domain in both CEPDE3-SF and LF (Samidurai et al., 2016, unpublished data) (see Fig.1.8).

Although multiple sequence homology alignment of CEPDE3 with that of the human PDE family indicate that *C. elegans* PDE3 is close to mammalian PDE3, the overall sequences of the catalytic domains of mammalian PDE3 and CEPDE3 are quite different. CEPDE3 lacks the unique 44 insert found in the catalytic domains of mammalian PDE3 isoforms. CEPDE3-LF and SF isoforms show an overall 97% homology between each other and 100% homology among their catalytic domains, and they are not analogous to mammalian PDE3A and PDE3B isoforms. Despite these differences, preliminary studies described in this thesis indicate that CEPDE3 LF and SF hydrolyze cAMP with high affinity, and are markedly inhibited by cilostamide, which is a specific inhibitor of the PDE3 family. These findings suggest that a detailed comparison of the catalytic pockets of

CEPDE3 isoforms and mammalian PDE3 isoforms will allow identification of the critical structural determinants of the PDE3 catalytic domain, and could provide useful information that would aid in developing clinically relevant PDE3 inhibitors. In this thesis, I investigated the *CEPDE3* gene by subcloning its two isoforms into the expression vector pGEX-6P1. I studied recombinant protein expression of the CEPDE3 short and long isoforms, as well as purification, and enzyme kinetics in order to characterize the properties of the CEPDE3 isoforms, and further plan to crystallize the proteins in collaboration with Dr. Heng Ming Ke at the University of North Carolina.

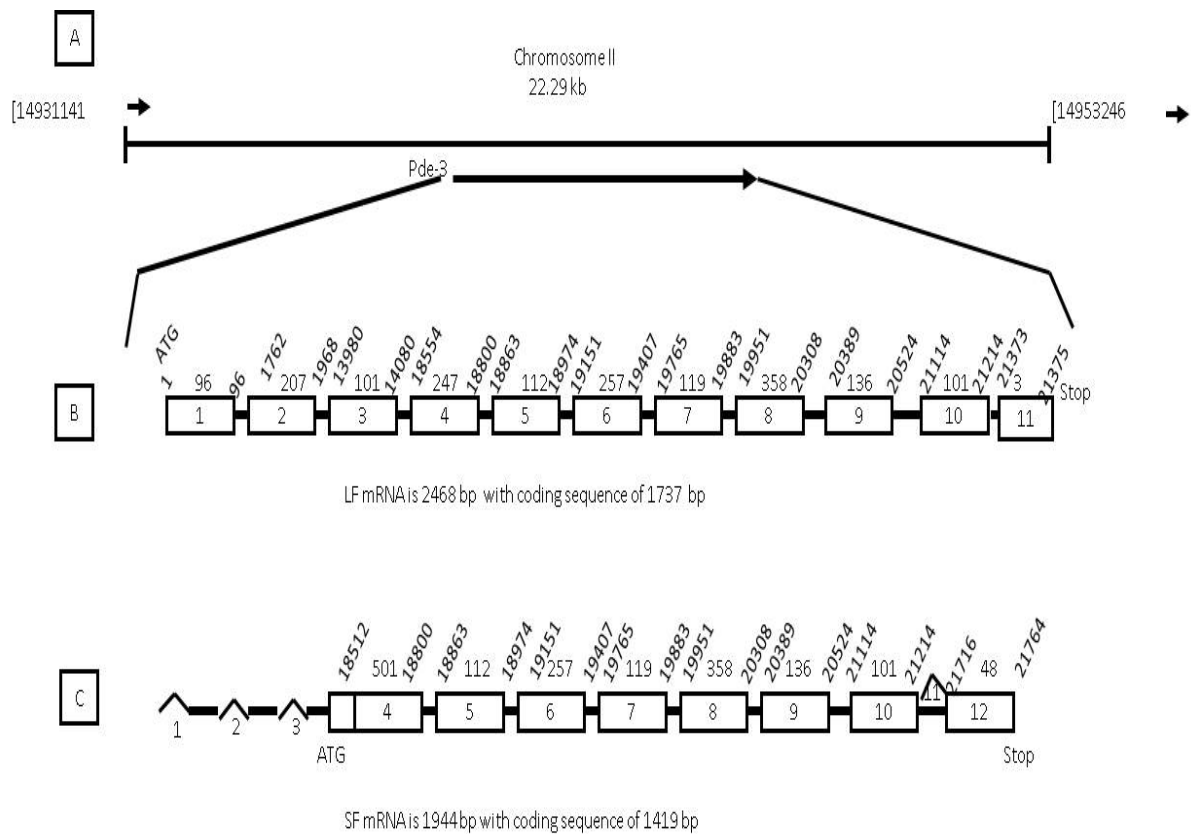


Figure 1.7: Diagrammatic representation of the structural organization of the *C. elegans* PDE3 (CEPDE3) gene

Location of the CEPDE3 gene and the two isoforms: long and short isoform. (A) Location of CEPDE3 genes on chromosome II represented by the (bold line) with the NCBI accession No: NC-003280.8. (B, C) Coding exon, intron boundaries in the long and short isoform, respectively. Exons are represented by rectangle boxes and introns are the connecting lines. The number on top of the box denotes the length of each exon. Start and end region of each exon with the slanting numbers. CEPDE3-LF (B) consists of 11 exons and CEPDE3-SF (C) differs from CEPDE3-LF both at N-terminus and C-terminus regions, in that SF lacks the first 3 exons and has alternative 4th and 12th exons (Samidurai. A et al., unpublished data on studies of CEPDE3 isoforms in insect cells).

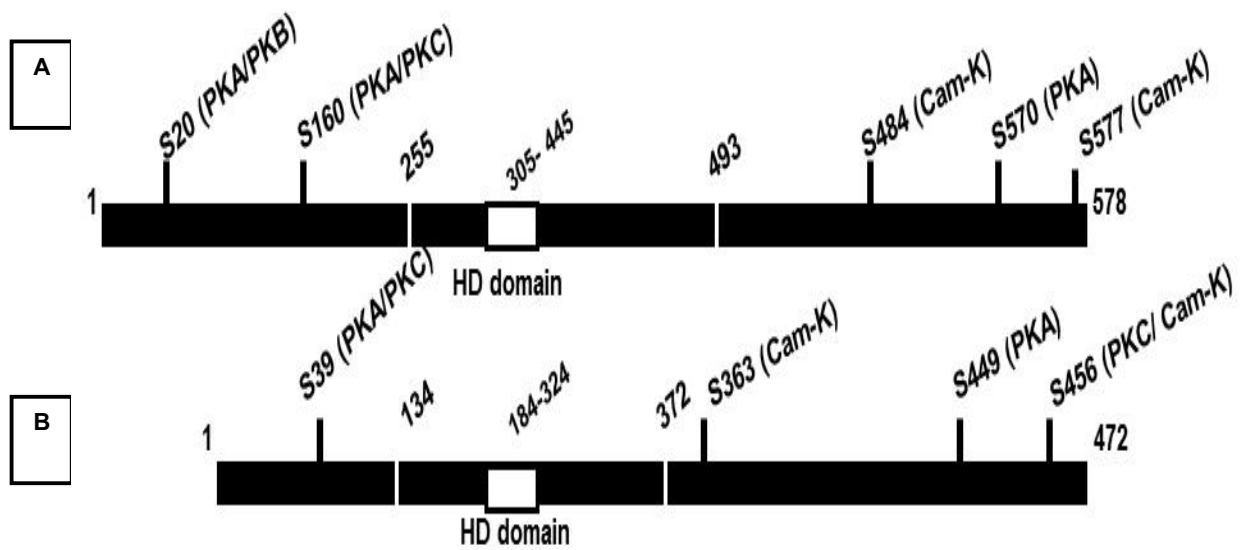


Figure 1.8: Diagrammatic representation of the HD domain present in *CEPDE3* gene.

The HD domain found in the catalytic region of *CEPDE3* is indicated by boxes marked in white. Putative phosphorylation sites present in *CEPDE3-LF* (A) and *CEPDE3-SF* (B) for PKA, PKB, PKC, and Cam-K are indicated Image reference (Samidurai et al. 2016, unpublished data).

Chapter 2

Chapter 2: General Materials and Methods

2.1: Experimental design

The study of *C. elegans* Phosphodiesterase 3 (CEPDE3) subcloning, expression, purification, and characterization was divided into two stages. The first stage involved subcloning experiments with CEPDE3 isoforms, short form (SF) and long form (LF), using vector pGEX-6P1 to further express, extract and detect proteins by western immunoblotting. The isoforms were expressed in *E. coli* and purified by using GST purification columns. The second stage of this study was to optimize conditions for solubility and scale up expression to purify a large scale of CEPDE3 proteins based on optimizing conditions using the batch method with glutathione sepharose 4B, including cleavage of GST-tag with enzyme PreScission Protease. Purified proteins were subjected to an enzyme kinetics study and PDE3 enzyme activity was detected. The isoforms were also characterized based on substrate affinities using cAMP and cGMP. Further concentration of purified proteins for crystallization of CEPDE3 isoforms is ongoing in collaboration with Dr. Hengming Ke at the University of North Carolina.

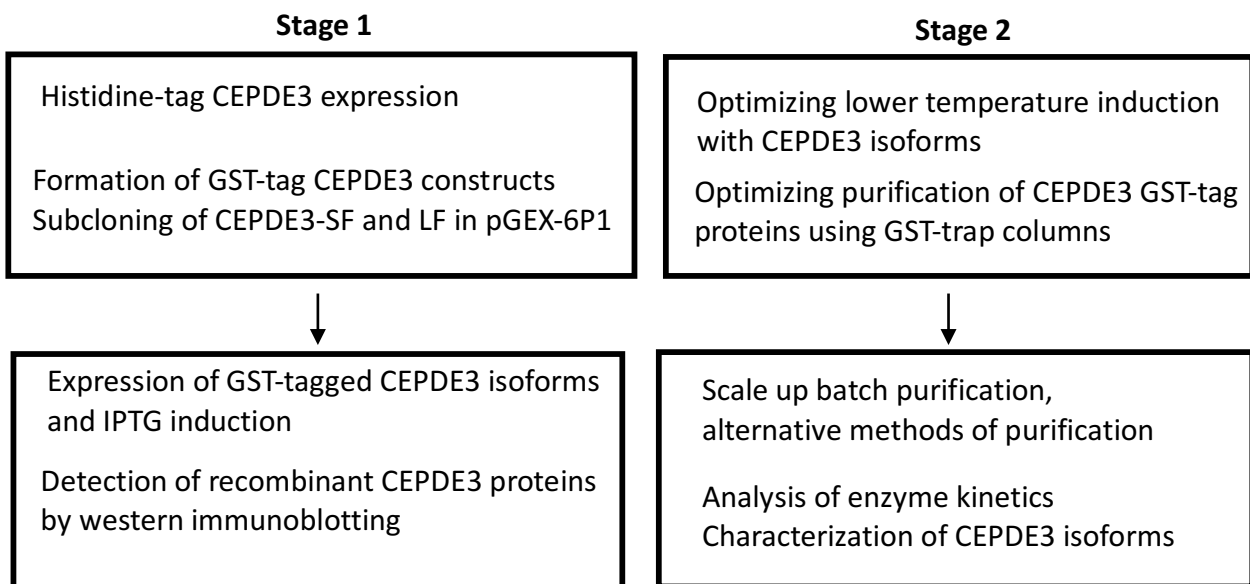


Figure 2.1: Experimental design for the study of CEPDE3 isoforms

Flowchart representing experimental design of CEPDE3-SF and LF isoforms purification and characterization. Stage 1 and 2 involved subcloning, GST CEPDE3 expression, purification and enzyme kinetics.

2.2: General Materials

General laboratory glassware, plasticware, chemicals solvents and reagents were obtained from various companies, Roche, Invitrogen, Sigma-Aldrich, Gold-Bio unless otherwise stated. All bacterial cell culture ware, Falcon tubes, reagents, plates were already sterile and used directly. Health and safety procedures were respected where hazardous substances and biological material was used. Experiments involving the use of hazardous chemicals and radioactive materials used in this study were carried following the health and safety measures for storage and disposal as per the standard protocols and guidelines set by the National, Heart, Lung and Blood Institute (NHLBI) and National Institutes of Health (NIH).

Materials used in individual experiments are listed below

2.2.1: PCR experiment

Advantage GC cDNA PCR kit, PCR tubes. Molecular grade water, purified plasmids of CEPDE3-SF and LF.

2.2.2: Subcloning experiment

A) Plasmids: CEPDE3-LF and SF in pET-21D expression vector were stored as glycerol stocks or CEPDE3-SF and LF mini prep purified DNA. pGEX-6P1 vector DNA was obtained from GE Healthcare.

B) Plasmid Purification kits

QIAPREP-miniprep kit, catalog no: (27106), High speed plasmid midi kit, catalog no: (12643) and Qia quick-gel extraction kit, catalog no: (28704) were used for plasmid isolation and gel purifying experiments.

C) Ethanol precipitation: 100% ethanol, distilled water (DW), 3 M sodium acetate.

D) Restriction enzymes: *EcoRI*, *NotI* (Roche, NEB), Molecular grade water.

E) Agarose gel electrophoresis: Agarose SEAKEM, TAE buffer 1X AccuGENE Lonza, Safe stain-Biotium, 6X DNA loading gel, DNA marker from NEB.

F) Ligation and bacterial transformation

DNA Ligation kits 2.1 from TAKARA, catalog no: (6022), BL21 strain of competent cells from New England Biolabs catalog no: (C2530H). Mix and go competent cells, catalog no: (T3007, Zymogen), Rosetta Gami strain, Lennox L Broth LB ampicillin 50 µg/ml and 100 µg/ml plates, kanamycin 50 µg/ml and 100 µg/ml plates, SOC medium (Quality Biologicals).

2.2.3: CEPDE3 expression and cell lysis

Lennox broth (LB) agar liquid medium, antibiotic-ampicillin stock solution. Glycerol (> 99%), (catalog no: T9284). Triton X-100 (catalog no: 12850883, Sigma-Aldrich). Isopropyl-1-thio- β -D-galactopyranoside (IPTG) (Gold bio Inc.).

A) Cell lysis using French Press

10X PBS pH 7.4, 5 M NaCl, 20 mM Tris-HCl buffer pH 7.4, protease inhibitor cocktail tablets (Roche).

2.2.4: Protein purification

A) Affinity purification of GST fusion proteins

GST spin trap columns (catalog no 28952359, GE Healthcare).

Lysis buffer: 1X PBS, 400 mM NaCl, 5% glycerol, 50 mM Tris-HCl, supernatant containing expressed target fusion protein. Glutathione sepharose 4B resin (catalog no 17-0756-01, GE Healthcare), Triton X-100 (Invitrogen).

B) Protein assay

Bradford protein assay kit (Thermofisher Scientific), Coomassie gel stain and Quick Stain (Expedeon).

C) Proteolytic cleavage to remove GST affinity tag

Affinity-purified fusion proteins of CEPDE3-LF and CEPDE3-SF

Vector-specific enzyme PreScission Protease (GE Healthcare, catalog no: 27-0843-01).

Lysis buffer: PBS pH 6.2, Triton X-100, protease inhibitor tablets.

D) Ultracentrifuge

Beckman Coulter ultracentrifuge glass tubes (5 ml), mini rotor Beckman Coulter ultracentrifuge.

2.2.5: PDE3 enzyme assay

All chemicals and reagents used in the preparation of buffers were obtained from Sigma Aldrich, Quality Biologicals.

Radioactive Isotope ^3H was obtained from Sigma Aldrich

Columns: Poly-Prep chromatography columns catalog no (731-1550) were obtained from Bio-Rad. QAE-sephadex A-25 was obtained from Seakem.

Ecoscint XR scintillation gel and dispensing pump was obtained from National Diagnostics.

2.2.5.1 Cell samples

CEPDE3-LF and SF bacterial soluble lysate and purified protein samples were used. CEPDE3-SF and LF Flag-tag lysates expressed in insect cells were provided generously by Dr. Faiyaz Ahmad (Staff Scientist at the NHLBI laboratory) and used in PDE3 enzyme kinetics experiments with cAMP and cGMP hydrolysis, and to determine IC_{50} .

2.2.5.2: Equipment

Gene Amp PCR system 9700 (Applied Biosystems). Electrophoresis chamber for SDS-PAGE gels (Bio-Rad). Electrophoresis cell and electrophoresis chamber for agarose gel (Embitec).

Power supply, gel casting tray and combs. Eppendorf thermomixer, vortex (Daigger). Table top centrifuge, mineral light lamp (UVP Bioimaging Systems). Bacterial shaker incubator, low-temperature incubator, orbital shaker (Bellco). Sonicator, dounce and pestle. French Press Microfluidizer by (Microfluidic), model no: M110P.

2.3: General methods

2.3.1: Preparation of plasmid DNA

Plasmid DNA was extracted using the QIA prep mini, midi and maxi kit as per the instruction manual provided in the kit. For miniprep, 1 to 5 ml bacterial culture was used to harvest cells. For maxi prep, 50 to 150 ml medium was used to pellet bacterial cells. DNA was eluted with 50 to 100 μ l volume for mini prep and 500 μ l for maxi prep. The concentration of DNA was determined by nanospec and further analyzed by restriction double digest on an agarose gel.

2.3.1.1: Experiment 1: PCR with CEPDE3-LF and SF

PCR master mix for both LF and SF was prepared and mixed in the order shown below in Table 2.1. LF and SF cDNA was added in duplicates of 10 tubes. 0.6 μ g of LF and 1.2 μ g SF concentration were used per tube. For a negative control, distilled water was used in place of DNA. 24 μ l of the master mix was added to each tube. The plasmid DNA mixture was vortexed and placed in the PCR machine, then programmed to run overnight (refer to Table 2.2) with final overnight cooling at 16°C. The following day, samples were analyzed on agarose gels.

Table 2.1: PCR Mastermix reaction

The mastermix reaction to perform PCR for both CEPDE3-LF and SF isoforms was prepared as listed in the table below and prepared in 10 tubes each, including a negative control with no DNA.

1	Molecular grade water	132 μ l
2	5x GC melt	60 μ l
3	5x Rxn buffer	60 μ l
4	50x dNTPs	6 μ l
5	10 μ M Forward Primer	12 μ l
6	10 μ M Reverse Primer	12 μ l
7	50x GC advantage taq polymerase	6 μ l

Table 2.2: PCR program cycle for CEPDE3 amplification

PCR was performed with the Gene amp PCR systems 9700, the program was set for overnight incubation according to the cycles and the settings listed in the table. PCR reactions were carried out for both CEPDE3 isoforms. The conditions listed in the table were based on the programs available on the Gene amp system, except an additional step for cooling was introduced at 16°C for cooling when samples were to be left overnight

1 st Hold	3 Temp 30 cycles	Cycle 2	Cycle 3	2 Hold	16°C cooling
94.0	94.0	63.0	68.0	10:00 minutes	Overnight
5.00 minutes	0:45 seconds	0.45 seconds	4.00 minutes		
Denaturation	Denaturation	Annealing	Extension		

2.3.1.2: Experiment 2: ethanol precipitation

Method: This method of purifying DNA was carried out for subcloning of CEPDE3-LF plasmid DNA, 160 μ l of DW was added, along with 40 μ l of acetic acid and 1000 μ l of cold ethanol 100%, to make a total volume of 1440 μ l. This reaction mix was stored at -30°C. The following day, samples were taken out of the freezer, thawed, and centrifuged at 14,000 rpm at 4°C for 30 minutes. By centrifuging the samples DNA was precipitated in the form of pellet at the bottom and supernatant was carefully drained. 600 μ l of 70% ethanol (200 proof ethyl alcohol) was added and tubes were centrifuged again at 14,000 rpm for 30 minutes at 4°C. After confirming the presence of a pellet at the bottom of the tube, supernatant was discarded and the centrifuge and wash step were repeated one more time. Supernatant was discarded and the pellet was dissolved in 150 μ l of water, by gently tapping.

2.4: TOPO cloning reaction

CEPDE3-LF TOPO cloning reaction was performed based on the protocol provided with Zero TOPO blunt kit from Invitrogen, the following table explains the reaction designed.

Table 2.3: TOPO cloning reaction preparation.

TOPO cloning reaction mix was prepared based on the instructions provided with the kit and all reagents were added as listed in the table below.

Reagent	Volume
LF PCR product	0.5-4 μ l
Salt solution	1 μ l
Water	Add to a total volume of 5 μ l
PCR-II blunt TOPO	1 μ l

For optimizing the PCR reaction, PCR samples of six different CEPDE3-LF clones (A1, A2, B1, B2, C1, C2) were used in two concentrations of 20 and 50 ng each of cDNA to perform six individual reactions.

2.5: Subcloning experimental method

2.5.1: Restriction double digest of CEPDE3-LF and SF

In order to subclone the isoforms into pGEX-6P1, CEPDE3-LF or SF plasmids were mixed in microcentrifuge tube with 2 μ l each of restriction enzymes *EcoRI* and *NotI*, 3 μ l of restriction buffer and 15 μ l of DW to make a total volume of 30 μ l. All reagents were mixed together and incubated for 3 hours at 37°C. The pGEX-6P1 vector was digested in the same manner, and all digested samples were analyzed on an agarose gel.

2.5.2: Agarose gel electrophoresis

Preparing the agarose gel

To prepare a 1.2 % gel, 0.6 g of agarose powder was added to a 500 ml flask and 50 ml 1X TAE buffer was added. The mixture was heated in a microwave until the agarose was dissolved and the solution appeared clear. The melted agarose solution was poured into a casting tray and was allowed to cool until firm and solid.

Loading and running the gel: The DNA samples was mixed with the loading dye in 1:1 proportion and loaded on the agarose gel. 5 μ l of DNA ladder standard was added to the 1st well and 10-15 μ l of the samples were loaded into the adjacent wells. The gel was run at 100 volts for 90 minutes.

Gel staining

The gel was carefully removed using gloves from the casting tray and placed into the staining dish wrapped with a cling film. Biotium safe stain mix was added (1:5000). The gel stained for at least

20-25 minutes. Following the staining, the gel was removed from the staining solution, placed on a tray, and viewed under the UV light quickly.

2.5.3: Gel extraction of DNA fragments for cloning

After double digested samples of CEPDE3 isoforms and pGEX-6P1 bands were observed at the predicted length and appropriate size. DNA fragments from insert and vector were carefully excised under UV light. The bands were excised from the agarose gel with a clean, sharp scalpel, and extra agarose was removed, then gel purified using the standard protocol from QIAGEN gel extraction kit. The excised DNA bands were weighed in a tube, and each gel slice was dissolved in 3 volumes of buffer QG (provided in the kit). After purification, samples were eluted using 30 μ l of DW. DNA yield was measured using a nanospec.

2.5.3.1: Ligation for CEPDE3-LF and SF

Ligation reaction was set in two different concentrations (labelled A and B) for both CEPDE3-LF and SF using TAKARA-2.1 DNA ligation kit.

CEPDE3-SF: Reaction A was prepared in 10 μ l volume adding 6 μ l CEPDE3-SF DNA, 2 μ l pGEX-6P1 DNA, 1 μ l of buffer and 1 μ l of the ligase. Reaction B had 7 μ l CEPDE3-SF DNA and 1 μ l pGEX-6P1 DNA in 1 μ l of buffer and ligase each.

CEPDE3-LF: Reaction A was carried out using 4 μ l of CEPDE3-LF DNA and 2 μ l pGEX-6P1 DNA added to 1 μ l each of buffer, ligase and DW. Reaction B was carried out using 5 μ l of CEPDE3-LF and 2 μ l of pGEX-6P1 in 1 μ l each of buffer, ligase and DW.

All four reactions were set to incubate overnight at 16°C. 1 μ l of solution III (transformation enhancer) provided with the ligation kit was added to each of the ligation mix to improve transformation efficiency prior to plating the mixture.

2.5.4: Bacterial transformation

2.5.4.1: Experimental method 1

Bacterial transformation was carried out using DH5 α competent cells (Invitrogen). Tubes of competent cells were thawed on ice. 1-5 μ l (1-10 ng) of DNA was added to the cells and mixed gently by avoiding pipetting. For the pUC19 control, 2.5 μ l of 250 ng of DNA was added to the cells and mixed gently. Tubes were incubated on ice for 30 minutes, then heat shock was performed for exactly 20 seconds in a 42°C water bath without shaking. Tubes were placed on ice for 2 minutes. 950 μ l of pre-warmed SOC medium was added to each of the tube. Tubes were then incubated at 37°C for 1 hour, with shaking at 225 rpm. 20 to 200 μ l from each transformation mix was spread on pre-warmed selective plates (LB with 100 μ g/ml ampicillin) in two different concentrations of 100 and 200 μ l each. The remaining transformation reaction was stored at +4°C for additional cells to be plated the next day if colonies were not present.

2.5.4.2: Experimental method 2

This method of transformation was performed using Zymogen competent cells, hence this method required no heat-shock process. Incubated ligation mix was placed on ice. DH5 α competent cells obtained from Zymogen were used in this experiment. 2 vials containing 100 μ l of competent cells were divided into 4 tubes with 50 μ l cells each. 5 μ l of the ligation mix from reaction A and B for both CEPDE3-LF and CEPDE3-SF (as mentioned in section 2.5.4.1) was added to the cells and incubated on ice for 5 minutes. 500 μ l of the SOC medium was added to each of the tubes, and the transformation mix was incubated for 1 hour at 37°C, with shaking at 225 rpm. Meanwhile, ampicillin plates (50 μ g/ml) were pre-warmed at room temperature. After incubation, 100 μ l of each transformation mix was spread on 4 LB plates. The remaining transformation mix was centrifuged at high speed (10,000xg for 5 minutes) and most of the supernatant decanted. The pellet was gently resuspended in the remaining supernatant. This mixture was applied to 4 additional plates. All plates were incubated overnight at 37°C.

2.5.4.3: Experimental method for inoculation of colonies in liquid culture

After single colonies were observed on the plates, following overnight incubation, each of the single colonies were picked and used to inoculate 5 ml of liquid LB medium with ampicillin in a 15 ml conical tube. The culture was incubated overnight at 37°C with shaking at 225 rpm. The following day, bacterial cell culture was pelleted by centrifugation at 10,000xg for 15 minutes at 4°C. QIAGEN mini prep kit was used to isolate plasmid, by following the standard protocol provided with the kit. Plasmids were further analyzed by restriction digests using *EcoRI* and *NotI*.

2.6: CEPDE3-LF and SF expression

2.6.1: Cell-lysis using sonication

Positive clones obtained from new constructs of CEPDE3-SF and LF with pGEX-6P1 were expressed and cell-lysis was performed. CEPDE3-LF pre-culture was grown overnight at 37°C with shaking at 225 rpm. The following day, the culture was diluted in 15 ml and cells were induced with IPTG at 37°C for 2 hours with shaking. Cells were then pelleted and resuspended in Tris-HCl buffer pH 6.2 to perform cell-lysis. Cells were lysed using sonication. The sonicator was set at the speed of duty cycle 5, with 1 second interval, which was repeated for 10 cycles. During sonication, the cells were kept on ice. Total lysate was then centrifuged at 10,000xg for 15 minutes and fractionated into the soluble supernatant and insoluble cell fraction, which were collected separately. The insoluble cell-pellet was resuspended in 4 ml of Tris-HCl buffer pH 6.2 with protease inhibitor tablets, 0.1% Triton X-100 and lysosome. This suspension was sonicated briefly and incubated in a warm water bath at 37°C, followed by centrifugation at 10,000xg for 5 minutes. The soluble supernatant sample was then collected in a tube.

2.6.2: Recombinant CEPDE3 expression experiments (cold-shock process)

Glycerol stocks were prepared from confirmed positive clones of both SF and LF plasmids as described in section (2.5.5.3). Overnight pre-culture was grown at 37°C in LB broth, with ampicillin and shaking at 225 rpm. The following day, ~ 1 ml of pre-culture was added to pre-warmed 250 ml LB broth, with 100 µg/ml ampicillin. OD was monitored every hour at 600 nm until the OD 0.4 to 0.5 was reached. Flasks were then transferred to the 4°C cold room and placed on a gently shaking platform. The bacterial culture was monitored hourly until an OD of 0.6 was obtained. Cells were then induced with 1 mM IPTG and flasks were transferred to a 25°C incubator for overnight induction, with shaking at 225 rpm. The following day, cells were harvested by centrifugation at 10,000xg rpm. Cell-pellets were washed with 1xPBS, and resuspended in 1X PBS, then transferred to new conicals and re-centrifuged at 10,000xg for 15 minutes. Finally, bacterial cell-pellets were resuspended in lysis buffer (PBS and Tris-HCl based), prepared as described below (section 2.6.3) and cell-lysis was performed using a French press (described in section 2.6.4).

2.6.3: Cell-lysis buffer optimization

Lysis buffers used for cell lysis of CEPDE3-LF and SF bacterial cell pellets were prepared by optimizing conditions based on pH levels. These buffers were prepared following the protocol for protein expression and cell-lysis mentioned in the handbook for GST fusion proteins (by GE Healthcare) for high yield and purity of GST-tagged isoforms. Tris-HCl and PBS buffers were prepared as two buffers, each with pH 6.2 or pH 7.4, and were labelled accordingly.

Buffer 1: 20 mM PBS, 400 mM NaCl, 5% glycerol, pH 6.2

Buffer 2: 50 mM Tris-HCl, 400 mM NaCl, 5% glycerol, pH 6.2

Buffer 3: 20 mM PBS, 400 mM NaCl, 5% glycerol, pH 7.4

Buffer 4: 50 mM Tris-HCl, 400 mM NaCl, 5% glycerol, pH 7.4

2.6.4: Bacterial cell-lysis with French press

Bacterial cell-pellets were resuspended in cold lysis buffer with protease inhibitor tablets. Cells were gently mixed and dissolved in the buffer to form a total cell-lysate. The French press equipment was started 5-10 minutes prior to cell-lysis. The cylinder was washed once with distilled water and then with the lysis buffer. The tray beneath the tubes was filled with ice, so when the resuspended cells undergo cell-lysis under high pressure, they remain cold to avoid protein degradation. 50 ml of cell-lysate, and the same amount of extra buffer, was added depending on viscosity of the cell mixture. The French press was operated at a pressure of 19,000 PSI. The lysate was collected through a tube and passed through the cylinder again. While performing this procedure, care was taken so no air bubbles entered the cylinder, as this slows down the process. The lysate was passed through the cylinder 3-4 times and the final cell-lysate was collected in a tube. The lysate was kept on ice at all times. It was further subjected to

centrifugation at 10,000xg for 15 minutes, and fractionated into soluble and insoluble fractions in separate tubes. The insoluble cell-pellet was resuspended in 1x PBS, vortexed and washed, then re-centrifuged at 10,000xg for 15 minutes. The resulting pellet was suspended in an equal amount of lysis buffer, equivalent to the soluble protein fraction, and briefly sonicated. Aliquots of all protein fractions were taken at all steps and analyzed with Coomassie gel staining and western blot.

2.6.5: Separation of proteins by SDS-PAGE

2.6.5.1: Western blot analysis

Western blot is a commonly used technique to detect and measure relative amounts of a given protein. Protein samples at a concentration range from 1-2 µg/ml were mixed with 2x Laemmli sample buffer (Bio-Rad-USA) and heated to 99°C for 2 minutes, and then placed on ice. The samples were then centrifuged at 14,000 rpm for 5 minutes before loading onto a SDS-PAGE gel. 5-15 µl of sample were loaded onto a pre-cast 4-20% SDS-PAGE gel (Bio-Rad). 4 µl of Precision Plus Protein Western (Bio-Rad) biotinylated molecular size markers were loaded onto the SDS-PAGE gel as a standard for molecular weight. The gels were then run at 100 V for 1.5-2 hours in 1X Tris-HCl-glycine SDS-PAGE running buffer (Bio-Rad). Proteins were visualized by two separate gels; one underwent Coomassie staining using instant blue stain (Expedeon, USA) and one underwent transfer for western blotting. In the transfer process, the second gel was carefully placed on a sheet of nitrocellulose that was pre-soaked in 20% cold methanol and then sandwiched between two sheets of blotting paper (Invitrogen, USA), before placing it in a western transfer cassette (Bio-Rad). The cassette was then inserted into a mini-protean electrophoresis tank (Bio-Rad) and electrophoresis was performed using 1X Tris-HCl-glycine buffer (Bio-Rad) containing 20% methanol at 220 amps for 2.5 hours. For western detection, the blot was pre-incubated with a blocking solution of 1X PBS containing 5% skimmed milk powder. Primary and secondary antibody sources, dilutions and incubation periods are shown in Table 2.5 below. After each antibody incubation, the blots were washed 3 times, for 5 minutes each, with 1X PBS and 0.01% Tween-20. To detect the molecular markers, StrepTactin-HRP conjugate was added during incubation with secondary antibodies at a dilution of 1:2500. Detection of HRP conjugates was detected by using supersignal West Femto or Pico chemiluminescent substrate (Thermo Scientific). The chemiluminescent signal on the blots was detected using the Fuji film intelligent dark box.

Table 2.4 Primary and secondary antibodies used in the CEPDE3 study.

The table shows the primary and secondary antibodies used in detection of CEPDE3 proteins with western immunoblotting and are listed with their source, dilution and incubation times. Some of these antibodies were generated in the Manganiello lab and some of them were commercial.

Primary Antibody	Source	Dilution	Incubation time
Rabbit-anti-SF PDE3-Nterm	Manganiello laboratory	1:2000	O/N at 4° C
Rabbit-anti-SF PDE3-Cterm	Manganiello laboratory	1:2000	O/N at 4° C
Rabbit-anti-LF PDE3-Nterm	Manganiello laboratory	1:2000	O/N at 4° C
Rabbit-anti-LF PDE3-Cterm	Manganiello laboratory	1:2000	O/N at 4° C
Goat-anti-GST	GE Life Science	1:3333	O/N at 4° C
Secondary Antibody			
Donkey-anti-Rabbit-HRP	Promega	1:2500	1.5 hours at RT
Donkey-anti-Goat-HRP	Promega	1:2500	1.5 hours at RT

2.7: Protein purification using GST-spin trap columns

2.7.1: GST-spin trap columns

GST-spin trap columns were used for small scale experiments. The initial purification using GST spin trap column was performed by using CEPDE3-LF soluble sample. The column was inverted gently. After centrifuged in a table-top centrifuge, at the speed of 100xg for 30 seconds, the storage buffer was removed. The columns were equilibrated by 600 µl binding buffer (PBS buffer pH 6.2, 2% Triton X-100 or Tris-HCl buffer pH 6.2, 2% Triton X-100, depending on the lysis buffer used) and centrifuged at 100xg for 30 seconds.

The LF protein sample was passed through the column several times and the column was gently inverted to mix. Following application, the column was centrifuged for 30 seconds at 100xg, flow-through collected and beads were washed 3X with 600 µl of binding buffer. Elution buffer was prepared using 10 mM reduced glutathione mixed with binding buffer. 200 µl of elution buffer was added to the column and column was sealed and incubated for 1 hour at 4° C. Post incubation, eluate was collected by centrifuging for 30 seconds at 100xg, and elution step was repeated one more time. The spin column was then washed 3x with binding buffer. Following washing, a small amount of beads (20 µl) present at the base of the column were carefully pipetted out, mixed with equal amount of sample buffer, boiled at 99°C for 2 minutes, and centrifuged for 5 minutes at 500xg. Sample buffer eluate was then carefully loaded onto a SDS-PAGE gel. In addition, all purification fractions were loaded onto the same gel for western immunoblotting. Proteins were detected using anti-GST antibody as a primary antibody and anti-goat HRP as a secondary antibody.

2.7.2: Batch method using GST-spin trap columns

Experimental design: This experiment was designed using a batch method with GST-spin trap column. 100 ml overnight culture was grown at 37°C, with shaking at 225 rpm, followed by IPTG induction for 2 hours at 37°C. LF pellets were obtained by centrifugation and bacterial cell-pellets were resuspended in Tris-HCl buffer pH 6.2, with protease inhibitors. The cells were lysed using sonication, 1 second intervals, 10 x 10 cycles.

Preparation of beads: Based on the batch method, beads from the GST spin trap columns were gently taken out by careful pipetting and transferred into an Eppendorf tube. Storage buffer was removed by centrifuging them at 100xg for 5 minutes. Beads were washed and equilibrated with binding buffer. Beads were resuspended in 50 µl of buffer to perform purification with Tris-HCl buffer pH 6.2, 50 µl of binding buffer was added to the beads to prepare 50% slurry, and thus determine the optimal conditions for purification of proteins.

Sample incubation: 1.5 ml of soluble supernatant extracted and homogenized from cell-lysis was incubated with a 50 µl of the glutathione sepharose beads slurry from the spin column. Instead of passing the supernatant over the columns several times, beads were incubated for 3-4 hours with gentle shaking in the cold room (4°C). Following incubation, beads were centrifuged and flow-through collected, beads were washed with binding buffer (Tris-HCl buffer pH 6.2, 0.1% Triton X-100 and protease inhibitors) three times. LF protein was eluted using 20 mM reduced glutathione. 20 µl of beads from the column were mixed with an equal amount of sample buffer and boiled at 99°C, and centrifuged for 5 minutes at 10,000xg. This step was carried out to determine the amount of proteins still bound to the beads after elution. All purification samples were analyzed by SDS-PAGE and western immunoblotting analysis. Proteins were detected using anti-GST primary antibody and anti-goat HRP secondary antibody.

2.7.3: Protein purification with batch method using glutathione sepharose 4B

This method was designed based on the soluble supernatant obtained from French Press and using glutathione sepharose 4B resin. Glutathione sepharose 4B resin was used and 50% slurry was prepared as described above in section 2.7.2. 1.33 ml of glutathione sepharose beads were centrifuged at 500xg to remove storage buffer and were resuspended in 1 ml cold PBS 1X to prepare a 50% slurry.

Preparation of protein samples: Supernatant from CEPDE3-LF and SF extracted using French press was centrifuged at 10,000xg for 15 minutes, to remove any cell debris. Since the supernatant was thick and viscous, it was diluted 4x times to reduce viscosity. 10 mM DTT to final concentration in 10 ml volume was added to the diluted supernatant before mixing with the washed beads. Proteins were added to the washed beads for overnight incubation at 4°C with gentle rotation. Following day, flow-through was collected by centrifuge at 500xg for 5 minutes. The beads were washed with 1xPBS and 10 mM DTT 4x and 2x with 20 mM Tris-HCl, pH 8. The beads were then subjected to on-column cleavage.

2.7.3.1: PreScission protease enzymatic cleavage

2.7.3.1.1: Preparation of cleavage buffer

Cleavage buffer was prepared freshly prior to digestion. Depending on the volume of beads and culture, buffer was prepared. For 10 ml culture with 1.33 ml slurry of beads, a 12 ml buffer was prepared using the following components: 50 mM Tris HCl, pH 7, 300 mM NaCl, 1 mM EDTA, 1 mM DTT, and 0.1% Triton X-100, buffer was then chilled at 4°C prior to use.

2.7.3.1.2: On-column cleavage of fusion proteins

The fusion protein-bound matrix was washed with 10 bed volumes of cleavage buffer at 5°C and residual buffer removed. 1 mg/ml protein requires 10 units of the enzyme. Accordingly, for each ml of washed glutathione sepharose bed volume, 40µl (80 units) of PreScission protease was added to 960 µl of cleavage buffer. The PreScission protease containing buffer was added to the fusion protein-bound glutathione sepharose beads and gently resuspended. The beads were incubated at 4°C overnight. Eluate was collected by centrifuging the beads at 500xg for 5 minutes at 4°C. An aliquot of beads followed by 1st incubation was taken and mixed with equal amount of sample buffer. The elution step was then repeated. Fusion proteins bound beads were washed with freshly prepared 10 bed volumes of cleavage buffer prior to incubation with enzyme for the second time. With the second incubation, 30 µl (60 units) of PreScission protease enzyme was added to 970 µl of buffer and incubated for 4-6 hours at 4°C with gentle rotation. Eluate was collected by centrifugation and all fractions of purification were analyzed with coomassie stain and western immunoblotting.

2.8: Homogenization of CEPDE3-LF and SF using ultracentrifuge

This method was based on fractionating proteins with increased speed using an ultracentrifuge. Bacterial cell culture of CEPDE3-LF and SF was grown at 37°C and cells were expressed using the cold-shock therapy and lysed using the French press. Cell-pellets were resuspended in cold lysis buffer PBS, pH 6.2 and protease inhibitor cocktail tablets were added (1 tablet/10 ml cell-lysate mixture). Total cell-lysate was fractionated by centrifuging at 10,000xg for 15 minutes and soluble supernatant was collected. 15 ml of CEPDE3-LF and SF soluble supernatant was further fractionated by ultracentrifugation in the 5ml of Beckman centrifuge tubes with 2.5 ml of supernatant in each of the tubes. Centrifuge speed was set at 100,000xg for 30 minutes and the supernatant removed. Cell-pellets collected at the bottom of the tubes were gently transferred into a conical tube and resuspended with ~ 14 ml of Tris-HCl buffer, pH 7 with 0.1 % Triton X-100, and protease inhibitor tablets, then gently homogenized using homogenizer. The cell-pellet mixture was further briefly sonicated in 2-3 intervals at duty cycle 30. The homogenized mixture was incubated at 4°C with gentle rotation for ~ 4 hours. Following incubation, samples were centrifuged at 20,000xg for 15 minutes. Soluble supernatant was collected and insoluble cell-pellet was resuspended in equal amount of Tris-HCl buffer, pH 7 adjusting to the same volume of the 1st supernatant obtained after ultracentrifugation. All samples were analyzed for protein

concentration by gel staining and western immunoblotting. The flow-chart below explains the various stages of the protein fractionation.

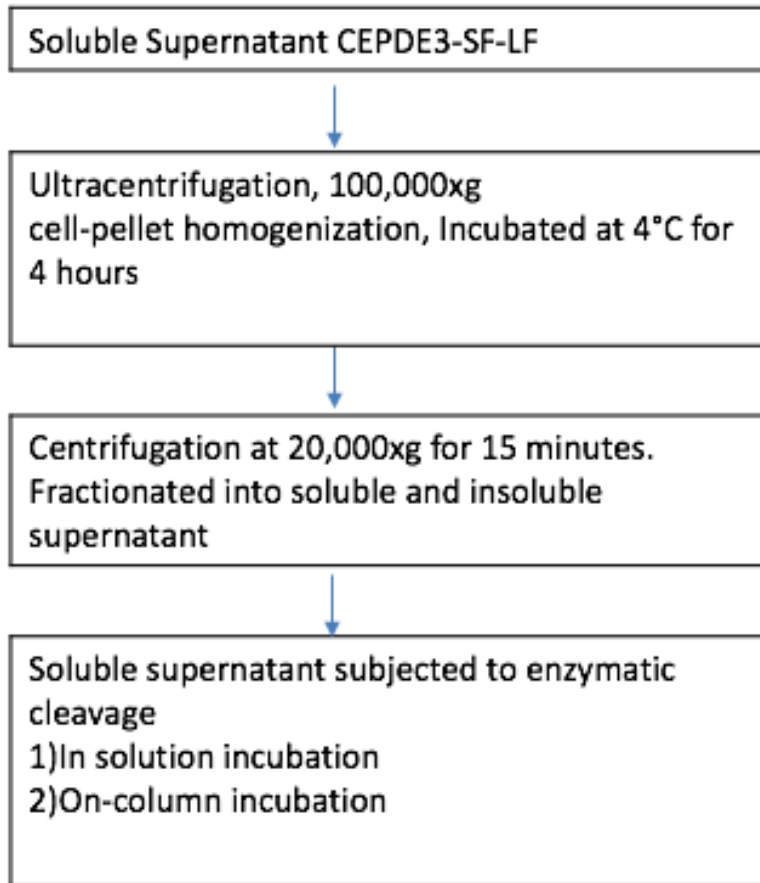


Figure. 2.2: Protein fractionation by ultracentrifugation

Soluble protein was subjected to ultracentrifugation following homogenization and further fractionated into soluble and insoluble fractions. Soluble proteins were then subjected to on-column and direct cleavage using PreScission protease.

2.8.1: Experimental protocol for enzymatic cleavage

Soluble supernatant obtained from 100,000xg ultracentrifugation was subjected to enzymatic cleavage using PreScission protease. This was carried out using two methods 1) direct cleavage with the enzyme and 2) on-column cleavage method. Methods described in detail below.

2.8.1.1: Direct incubation with PreScission Protease

750 µl of CEPDE3-SF soluble protein obtained from experiments described in (section 2.8) from ultracentrifuge was dialyzed using a dialysis cassette at 4°C. At the end of dialysis, the soluble protein was incubated with 60 units (30 µl) of PreScission protease enzyme overnight at 4°C with gentle shaking on rotator. Following incubation with enzyme, 250 µl of glutathione sepharose 4B beads were aliquoted and centrifuged at 500xg for 5 minutes, washed and resuspended in binding to prepare a 50% slurry. The protein mixture with enzyme was incubated with glutathione sepharose 4B slurry at 4°C for 3-4 hours with rotation. At the end of incubation, the protein mixture was centrifuged for 5 minutes at 500xg and eluate collected. Beads were washed 2X with 1 ml of Tris-HCl buffer pH 7 and centrifuged at 4°C, washes collected separately. (50 µl) aliquot was taken, beads were analyzed with sample buffer. All purification fractions were analyzed on gel.

2.8.1.2: Batch method incubation with PreScission Protease

250 µl of glutathione sepharose 4B beads were taken and subjected to wash and incubation using Tris-HCl buffer pH 7 and a 50% slurry was prepared. 1 ml of CEPDE3-LF solubilized protein, obtained from experiments described in section 2.8, was applied to the washed beads and 10 mM DTT was added and incubated overnight at 4°C overnight with gentle shaking. At the end of incubation, the flow-through was collected by centrifugation at 500xg for 5 minutes.

Wash steps: Beads were washed 2X with 1 ml cold 1xPBS with 10 mM DTT and 2X with 20 mM Tris-HCl pH 7, washes were collected separately.

Preparation of cleavage buffer

Cleavage buffer was prepared using 50 mM Tris-HCl pH7, 300 mM NaCl, and 1 mM DTT. Beads were washed with 1 ml of cleavage buffer. In 250 µl of cleavage buffer, 20 units (10 µl) of PreScission protease enzyme and beads were incubated at 4°C for 3-4 hours with gentle shaking. At the end of incubation, beads were centrifuged at 500xg for 5 minutes and eluate collected, beads were analyzed with sample buffer. All fractions from purification were analyzed on SDS-PAGE gel for western blotting and coomassie gel stain.

2.9: Ion exchange chromatography

Cell lysis was carried out using 20 g CEPDE3-LF cell-pellets with Tris-HCl buffer pH 7 using French press at 19,000 PSI, 100 ml lysate was obtained. 10 ml supernatant used (4x dilution with lysis buffer) in purification with DEAE sepharose beads. 5 ml DEAE sepharose beads were pipetted in 50 ml conical tube, centrifuged at 1000xg for 5 minutes, storage buffer was decanted, beads were washed with 3 bed volumes of Tris-HCl buffer, pH 7 and centrifuged at 1000xg for 5 minutes. The diluted supernatant with protease inhibitor tablets was added to beads, three tubes with 10 ml (diluted supernatant) in each and 5 ml beads were used in each of these tubes for overnight incubation at 4°C with gentle shaking. The following day, beads were centrifuged at 500xg for 5

minutes and flow-through collected. The beads were washed with 3 bed volume of Tris-HCl buffer, pH 7 and centrifuged at 100xg for 5 minutes; the wash step was repeated 3X.

Elution: Three separate elution buffers: 1) 20 mM Tris-HCl, 100 mM NaCl, pH 6.2) 20 mM Tris-HCl, 300 mM NaCl, pH 6.5, 3) 20 mM Tris-HCl, 500 mM NaCl, pH 7 were prepared and incubated with the beads in three tubes each for 30 minutes at 4°C. At the end of incubation, beads were centrifuged at 1000xg for 5 minutes and eluate collected. Samples were analysed by western immunoblotting.

2.10: CEPDE3 enzyme activity assay

2.10.1: Preparation of QAE Sephadex-A-25 columns

Binding capacity: 1ml of A-25 wet gel has a total ion binding capacity of 500 μ mol or 3-3.5 μ M/mg/dry gel. 10 g of QAE sephadex A-25 gels were swollen in 500 ml distilled water for 2-3 hours. After the gels were swollen completely, floating gels and excess of water were taken off. Swollen gels were resuspended in equal amount of water. 1 ml of 50% suspension of gel and water was pipetted into the polyprep chromatography columns. 1 ml of A-25 gel suspension was pipetted into the columns and bottom closure was removed. Prior to use columns were washed.

Column wash

Once the columns were packed with the QAE sephadex, they had to be washed in the following order as listed in the box below, prior to start of the assay.

10 ml 1 M HCl
10 ml 0.5 M HCl
4x-10 ml H ₂ O

2.10.2.2: Preparation of buffers for enzyme assay

Enzyme assay reaction mix was prepared based on several buffers using various components. It was critical that each buffer was prepared carefully based on concentration and pH, and stored at the appropriate temperatures. Accordingly, all buffers were prepared prior and stored.

Table 2.5: Preparation of assay buffer (2X stock)

Assay buffer was used as a primary buffer in setting up a reaction mix for the enzyme assay. Final concentration of the buffer was (50 mM Hepes, 0.1 mM EGTA, and 8.3 mM MgCl₂).

Reagents	Volume (ml)
0.15 M Hepes/0.3 mM EGTA	134
1 M MgCl ₂	3.35
H ₂ O	62.65

Table 2.6: Preparation of stop solution

Stop solution was used to stop the enzyme hydrolysis reaction after addition of substrate. Final concentration for cAMP was 10 mM, 5 mM AMP.

Reagents	Volume (ml)
4x stock (40 mM cAMP+20 mM 5'-AMP)	10
10 ml 1 M HCl	10
20 ml H ₂ O	20

Table 2.7: Preparation of snake venom

Snake venom (Crotalus atrox) contains nucleotidase and hence was used for hydrolysis of cAMP. Final concentration of the venom in the assay was (0.18 mg/assay/100 µl).

Reagents	Volume
Crotalus Atrox (rattle snake venom)	375 mg
0.5 M Tris-HCl, pH 8.0	40 ml
H ₂ O	160 ml

Table 2.8: Preparation of neutralizing solution

Neutralizing solution was prepared by using the base NaOH and was used in the reaction mixture after addition of venom.

Reagents	Volume (ml)
0.5 M Tris-HCl, pH 8.0	20
1 M NaOH	10
H ₂ O	10

Table 2.9: Preparation of ³H-cAMP assay substrate

³H-cAMP substrate was used for hydrolysis of cAMP; it was prepared using 30 μM of cold cAMP. In a PDE3 enzyme reaction the ³H-cAMP was degraded to ³H-5'AMP by PDE in the sample and was proportional to the amount of PDE present in a given sample. Substrate and products are exchanged on the QAE anion exchange column. cAMP binds to the resin and adenosine passes directly into the scintillation vial ³H-cAMP volume was adjusted to make final counts of 20-35,000 cpm/100 μl as substrate for assay and stored at -30°C.

Constituents	Volume (ml)	Final Concentration
0.1 M HEPES, 0.2 mM EGTA, pH 7.4	15	50 mM HEPES, 0.1 mM EGTA
1 M MgCl ₂	0.25	8.3 mM
³ H-cAMP in 0.05 N HCl	0.025	< 0.01 mCi
30 μM (cold) cAMP	0.3	0.3 μM (0.1 μM in assay)
DW	14.42	-
Total	30	-

2.10.3: Preparation of reaction mix

Table 2.10: Preparation of a standard reaction mix in the PDE enzyme assay

CEPDE3 enzyme assay template used for preparation of reaction mix that was prepared using reagents and radiolabelled ³H-cAMP substrate with a concentration of < 0.01 mCi in the order listed in the table. All components were added to a 1.5 ml eppendorf tube and incubation time and temperatures followed to set the reaction.

Samples	1	2	3	4	5	6	Total	Blank
Assay buffer 2x	100 µl	100 µl	100 µl	100 µl	100 µl	100 µl	5 ml	100 µl
Enzyme	10 µl	10 µl	10 µl	20 µl	20 µl	20 µl	5 ml	DW
Cilostamide	DMSO	DMSO	6 µl	DMSO	DMSO	6 µl	5 ml	DW
Incubate 30°C	3 min	3 min	3 min	6 min	6 min	6 min	5 ml	
DW	84 µl	84 µl	88 µl	65 µl	74 µl	74 µl	5 ml	100 µl
Substrate	100 µl	100 µl	100 µl	100 µl	100 µl	100 µl	100 µl	100 µl
Incubate 30°C 10 minutes								
Neutralization solution	100 µl	100 µl	100 µl	100 µl	100 µl	100 µl	5 ml	100 µl
Stop solution	100 µl	100 µl	100 µl	100 µl	100 µl	100 µl	5 ml	100 µl
Vortex								
Venom	100 µl	100 µl	100 µl	100 µl	100 µl	100 µl	5 ml	100 µl
Incubate 37°C 30 minutes								
Reaction mix	600 µl	600 µl	600 µl	600 µl	600 µl	600 µl	600 µl	600 µl

The reaction mix was prepared as listed in Table 2.10. A set of three tubes (two duplicates and one tube with inhibitor) were prepared for each concentration of enzyme used. Equal amount of DMSO was added in duplicates in place of inhibitor. DW was added to the tube with blank. The samples with 20 µl of enzyme were incubated with longer incubation time for 6 minutes and the ones with 10 µl enzyme was incubated for 3 minutes after adding the PDE3 inhibitor cilostamide. Before loading the samples, columns were prepared with the wash steps, as mentioned in the previous steps. A total of 600 µl of reaction mix was prepared in Eppendorf tubes. 500 µl of the reaction mix was loaded on to the columns in to the vials. All samples were eluted with 5 ml of DW and 10 ml of ready gel was added in all the samples including the blank. At the end of the assay, a vial for total count was prepared which contained 100 µl substrate, with 5 ml of DW and 5 ml scintillation gel. All the scintillation vials containing eluates were read on the scintillation counter. Assay time was optimized depending on the incubation with inhibitor cilostamide. Accordingly, incubation time of the enzyme with inhibitor was adjusted from 5-10 minutes. Activity of different PDEs was determined by performing the assay with and without a specific inhibitor and calculating the difference in time.

2.10.4: PDE assay calculations

The assay reaction contained 300 μl x 0.1 μM cold cAMP = 30 pmol. The fraction of ^3H -cAMP that was degraded in t minutes was calculated as (sample cpm-blank)/max.

Consequently,

PDE activity in the assay tube = 30 pmol x (cpm-blank)/Max x (t) = pmol hydrolyzed/min.

Each calculation was adjusted for total volume of reaction mixture by multiplying with a factor of 1.2, because only 500 μl out of a total volume of 600 μl was loaded onto the column. Accordingly, CEPDE enzyme assay calculations were made using the below equation:

PDE3 activity in the assay tube for 10 min = 30 pmol x (cpm-blank)-(cilostamide-blank)/Max = pmol hydrolyzed/min.

2.10.4.1: Enzyme kinetic calculations

The Michaelis-Menten equation explains the relation of the concentration of substrate to the rate of reaction of an enzyme:

Michaelis-Menten Equation: $V = V_{\text{max}}[S]/K_m + [S]$

This equation is based on two considerations, K_m and V_{max} . V_{max} is the maximum velocity, the maximum rate that the PDE3 enzyme reaction occurs or goes to completion. K_m is the Michaelis constant and is the concentration of the substrate that is required for a reaction to occur at $\frac{1}{2} V_{\text{max}}$. Based on the Michaelis-Menten equation, V is the reaction rate (velocity) at a substrate concentration $[S]$. Since $K_m = [S]$ at $\frac{1}{2} V_{\text{max}}$, K_m and substrate concentration have the same unit; hence they are related. Based on the experimental data from the hydrolysis of cAMP and cGMP, the K_m and V_{max} values were calculated using the Lineweaver-Burk method.

2.10.4.2: The Lineweaver-Burk method

In biochemistry studies, the Lineweaver-Burk plot was developed by Hans Lineweaver and Dean Burk, and graphically represents the Lineweaver-Burk equation of enzyme kinetics. The Lineweaver-Burk plot is the double reciprocal of the Michaelis-Menten equation:

$$1/V = 1/V_{\text{max}} + K_m/V_{\text{max}} \times 1/[S]$$

The Lineweaver-Burk plot was used to determine the K_m and V_{max} . The Y-intercept of the graph is equivalent to the inverse of V_{max} , and the X-intercept of the graph is equal to $-1/K_m$. On the graph, we plot the substrate concentration ($[S]$) against the velocity (V). Plotting V against $[S]$ or $1/V$ against $1/[S]$, with substrate concentration values on the X axis and the velocity on the Y axis. When we plot $1/V$ against $1/[S]$, the Y intercept is $1/V_{\text{max}}$, the X intercept is $1/K_m$, and the slope = K_m/V_{max} .

CEPDE3-SF and CEPDE3-LF samples were used to measure the hydrolysis of the substrates cGMP and cAMP by plotting substrate concentration against velocity ($[S]/V$) and using the double reciprocal plots of $1/[\text{substrate}]$ against $1/\text{velocity}$ ($1/[S]/1/V$). Based on the graph equation of each plot, K_m and V_{max} were calculated.

Chapter 3

Chapter 3: Cloning of CEPDE3-SF and CEPDE3-LF into pGEX-6P1

3.1: Introduction

3.1.1: Traditional cloning

Cloning is a fundamental technique used in molecular biology to construct new recombinant DNA molecules. One such application of this method is to create constructs for high level gene expression in *E. coli*. In the traditional procedure, an insert is either amplified by PCR and restriction digested, or released by restriction digestion and purified from a parent vector. The fragments of the insert to be cloned are then combined with a vector digested with the same enzymes and recombined using DNA ligase. The ligation product of the mixture is further introduced into a transformation system such as competent *E. coli* cells, and transformants are identified by selecting an appropriate genetic marker. Transformants are then analysed and DNA is subjected to restriction endonuclease mapping to detect if the desired recombinant DNA molecule was created (Struhl, 2001).

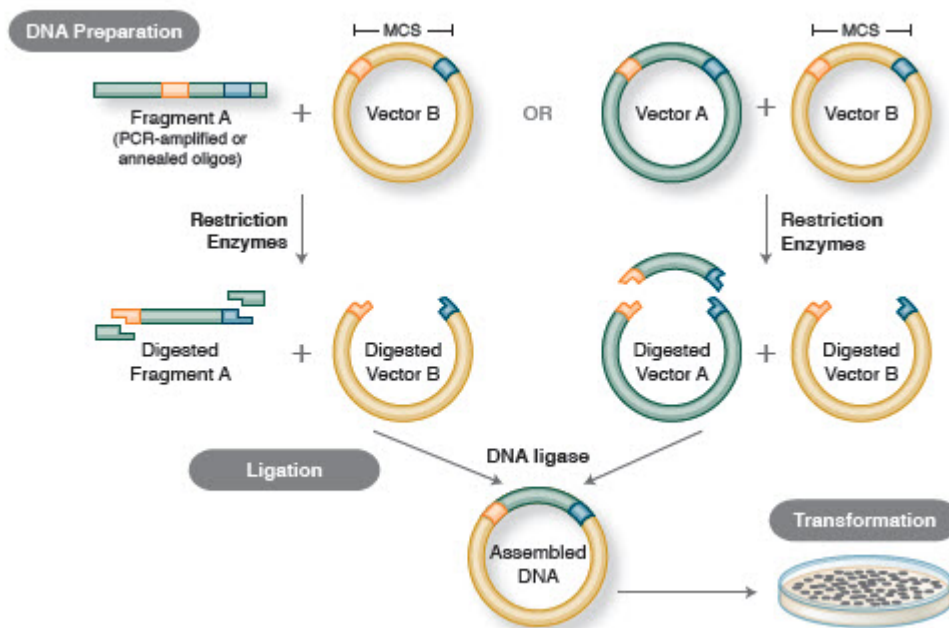


Figure 3.1: Subcloning process of a gene

Diagrammatic representation of the subcloning workflow and various steps involved in recombination cloning process to form a DNA molecule. Image reference: (<https://www.neb.com/tools-and-resources/feature-articles/foundations-of-molecular-cloning-past-present-and-future>).

3.1.2: Alternative methods of cloning

The naturally existing restriction sites situated on each side of the region to be cloned are not always compatible. In PCR cloning, the restriction sites can be engineered into PCR primers to create restriction sites on either side of the DNA (Carson et al., 2012). In the restriction enzyme ligation method, there are limitations with which enzyme restriction sites can be chosen, depending on the sequence and the efficiency of restriction enzymes (www.GetSynbio.com). When inserting one plasmid into another, it is not often clearly known how the foreign DNA becomes associated with the recipient plasmid. Junction-fragment libraries (collection of genomic DNA) are generated by chromosome jumping. This collection of libraries enable us to assess large areas of genome and overcome the large distance in common cloning techniques. this stretch of DNA can be deleted by biochemical manipulations in the cloning techniques (Yegnasubramanian, 2013). The main concern was to avoid formation of non-circularized fragments. Using restrictions enzymes for partial and complete digestion is an alternative commonly used in cloning technique (Rohan et al., 1990). Recombination cloning technology overcomes many of the limitations of using restriction sites and ligation. It also enables access to a wide range of vectors through the use of “gateway” cloning, where the recombination sites are present in a range of related vectors that allow inserts to be swapped from one vector to another by recombination (‘Addgene: Plasmid Cloning by PCR (with Protocols).

3.1.3: Plasmids for high level expression and purification of protein in *E. coli*

The components of the expression plasmids commonly used are a combination of replicons, promoters, selection markers, multiple cloning sites, and fusion tag sequences, as well as strategies to remove the tags once they are added. Plasmids contain an origin of replicon with one origin of replication and the cis-control elements associated with it. The replicon controls copy number. High plasmid number results in more yield of recombinant protein, as the cell contains many expression units. However, a high plasmid can also impart a metabolic burden on the cell machinery, and this could cause decrease in the bacterial growth rate. For expression of recombinant proteins, a strong promoter is essential. The promoter has to be induced by chemical means, isopropyl-beta-D-thiogalactopyranoside (IPTG) is used to regulate transcription of the *lac* operon and induces gene expression (Khow and Suntrarachun, 2012). Both cloning and expression vectors can be used as molecular tools for gene expression.

3.1.4: Cloning by recombination

TOPO cloning technology (Thermo Fisher Scientific) is one of the more widely used methods of cloning due to its rapid process, easy to use and effective method (Matsumura, 2015). The characteristic feature of TOPO cloning process is the enzyme DNA topoisomerase I, which has a dual function both of a restriction enzyme and a ligase, and can cleave and rejoin DNA during replication.

3.1.4.1: TOPO cloning method: Function of Topoisomerase I

The topoisomerase I used in TOPO cloning technology originates from the Vaccinia virus, this enzyme directly binds to duplex strand of DNA and breaks the phosphodiester backbone at a specific site after the sequence 5'-CCCTT-3' (Shuman et al., 1991). The energy used to break the phosphodiester backbone is generated by the covalent bond formation between the 3' phosphate of strand post cleavage and a tyrosyl residue (Tyr-274) from the protein. The Topoisomerase can rejoin the DNA strand with the same bond which was cleaved originally or religate to form an acceptor DNA molecule and thus form a recombinant DNA molecule, the reaction goes to reverse and the topoisomerase is released (Geng et al., 2006).

How TOPO[®] Cloning Works

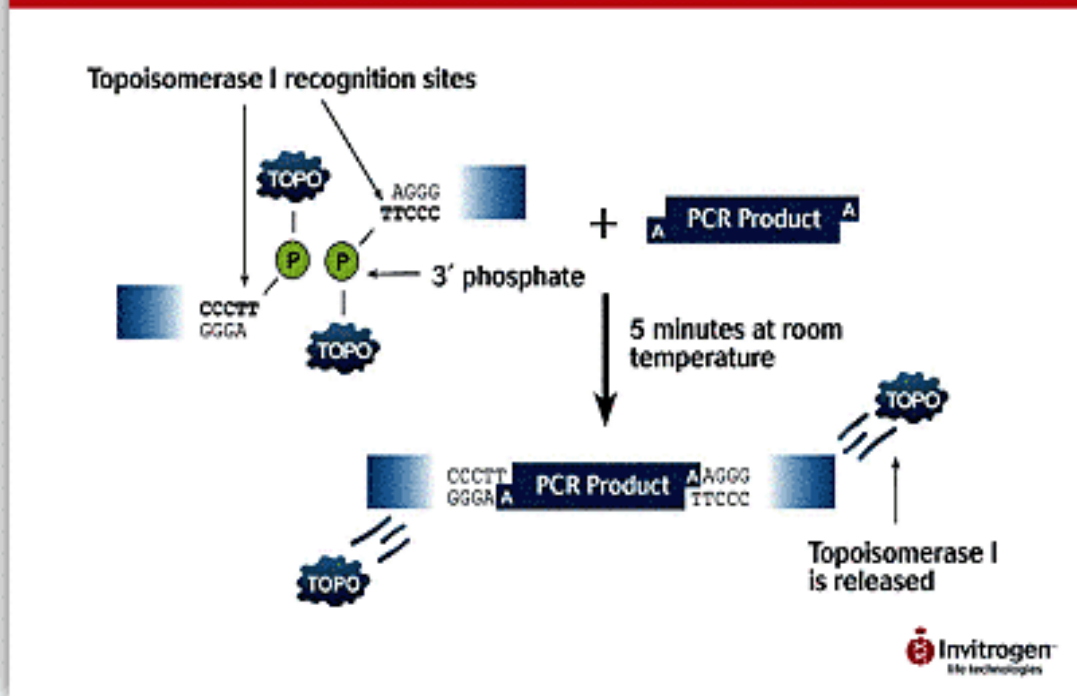


Figure 3.2: Diagrammatic representation of an overview of a standard TOPO cloning process.

TOPO blunt vector functions as a linearized vector. Due to the terminal transferase activity of Taq polymerase, it adds a single (A) to the 3' end of the PCR products. The vector contains single, 3'overhanging deoxythymidine (T) residues, thus the PCR products can ligate with the vector. This ligation reaction is known to occur rapidly at room temperature. Following ligation, the TOPO plasmids can be used to transform the competent cells provided with the kit (image adapted from www.thermofisher.com).

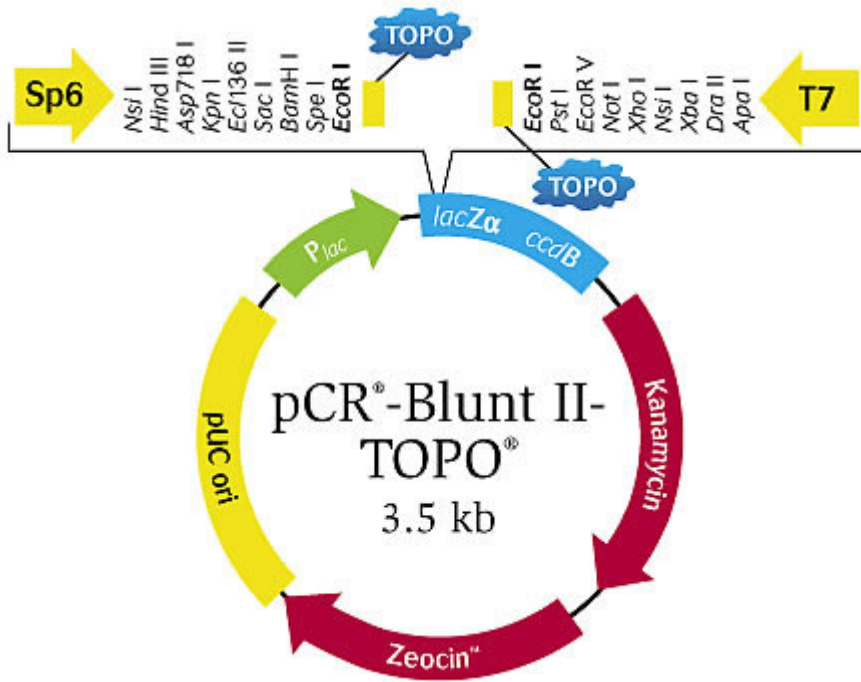


Figure 3.3: Diagram featuring TOPO blunt vector map with the multiple cloning site region

The vector plasmid map shows a 3.5 kb plasmid vector containing a kanamycin resistant gene, the Sp6 and T7 primer/promoter sites at the 5' and 3' end, respectively shows the restriction sites flanked across both the sides of the promoter region (www.thermofisher.com).

3.1.4.2: Gateway cloning

Gateway cloning is based on a recombination cloning method. It offers an advantage over other cloning, a piece of DNA is moved from one plasmid into another plasmid via a single recombination reaction. This DNA transfer makes the process simple and reduces the time involved with restriction enzyme cloning. To approach this method, the DNA to be cloned must have specific restriction recombination sites. This process requires to first clone the desired DNA fragment into a donor plasmid, followed by this reaction the DNA fragment can then be cloned into any compatible Gateway destination vector. Thus, a gene of interest can be cloned in one step by restriction enzyme digestion and subsequently into a donor plasmid and bacterial recombination to move it easily into suitable plasmids as per requirements, that also make it easy to carry out many molecular biology techniques. For example, fusing it with different tags like GST and MBP, and introducing it into various promoters and backbone vectors with different selection cassettes. TOPO cloning was considered an alternative approach for long-form following PCR. The idea of considering TOPO cloning was based on many of its advantages. These polymerases have extensive 3' to 5' exonuclease activity and do not leave 3'-A overhangs. TOPO cloning involves cloning of blunt end PCR-products into an expression vector in the presence of Topoisomerase.

This process also gives the flexibility to sequence positive clones to assure the plasmids are free of any mutations before proceeding with their subcloning into another vector (Addgene Choosing a Molecular Cloning Technique protocol). The vector designed for TOPO cloning has a single strand of GTGG overhangs at one end and a blunt end at other end. The overhang combines with the DNA and anneals to the CACC sequence which is placed in the primer. The addition of Topoisomerase I mediates the ligation reaction (Invitrogen TOPO Blunt-End for Subcloning protocol). Directional TOPO cloning enables the cloning of blunt-end PCR-products into any expression vector in a single orientation. PCR-product of LF insert was successfully subcloned into TOPO-vector.

3.1.5: Gene synthesis

Gene synthesis also known as artificial gene synthesis is a method which involves the chemical synthesis of a DNA sequence that represents a single or multiple genes. This process enables to efficiently produce long stretches of natural and non-natural nucleic acid sequences which provides a broad platform for limitations of biological experiments (Sequeira et al., 2016). It differs from molecular cloning and polymerase chain reaction, where the process does not have to begin with pre-existing DNA sequences, hence a completely synthetic double stranded DNA with no limits in the nucleotide sequence or size is essential. Sequences that are difficult to isolate from natural sources can be routinely generated. The process of gene synthesis also allows the possibility to develop genes containing modified nucleotides (Hughes et al., 2011).

3.1.5.1: Applications of Gene synthesis

Commonly used application is the technique of codon optimization that offers an extensive platform for engineering of genes that enable heterologous gene expression in a variety of host organisms. It is a process by which an amino acid sequence is rendered as a DNA sequence with codon usage suitable to a given organism (Angov et al., 2011). To begin, an amino acid sequence can be reverse-translated using highly utilized codons for an expression host (Hughes et al., 2011). The translational efficiency is enhanced by optimizing codon usage as per the requirement in a particular host organism (Lanza et al., 2014). The codon optimization technique gives the ability to design and synthesize custom DNA sequences of increasing length and complexity. A standard molecular biology laboratory can routinely synthesize DNA sequences up to 2 kb within a week using just a thermocycler, DNA polymerases, and commercially synthesized oligonucleotides.

3.1.5.2: Importance of codon optimization

There are several reasons that optimization of the codon is used, every species has differences in the codon usage, which is often considered the major factor affecting gene synthesis levels (Wang et al., 2012).

- a) Due to redundant nature of genetic code composition, gene sequences can be redesigned in a way to replace a set of rare codons with the preferred codon, to enhance translational efficiency and modify the translation elongation rates.
- b) Synonymous codon changes may affect protein conformation and stability, the sites of post-translational modifications can be altered and affect protein cellular function and thus have impact on gene expression levels without altering the amino acid sequence (Mauro et al., 2011).
- c) The 5' mRNA secondary structure affects the translational efficiency, hence synonymous codon substitution at this region can have greater impact on the gene expression level (Angov et al., 2011).

3.1.6: Background of CEPDE3 initial constructs

Studies conducted on CEPDE3 isoforms in the Manganiello laboratory (by Samidurai et al.) were performed with amplified fragments of CEPDE3-SF and LF cloned into the baculovirus expression vector containing a Flag-tag epitope at its C-terminus and expressed using Sf21 cells. Producing a large amount of Flag-tag proteins using the insect-cells was challenging with possible issues related to protein folding. In addition, expression using insect cells took a longer duration of time, ~ 2 weeks, than *E. coli*. Hence it was not a suitable method for expressing and purifying a large amount of mg/ml protein required for crystallization studies. Considering the challenges, a bacterial expression system using *E. coli* was considered to be a suitable alternative in the CEPDE3 gene study.

3.2: Aims

The aims of this chapter were to

Subclone *CEPDE3* gene into expression vector, this was achieved by

- Performing PCR for amplification of the *CEPDE3* gene for subcloning
- TOPO-cloning of CEPDE3-LF isoform
- Codon optimization for CEPDE3-SF isoform
- Subcloning of CEPDE3-SF and LF inserts into pGEX-6P1 expression vector

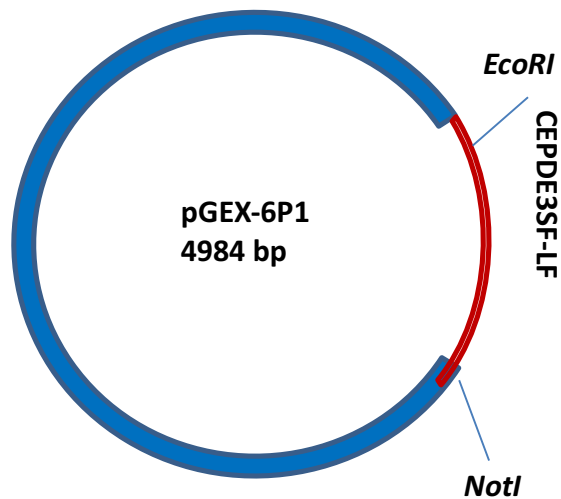


Figure 3.4: Diagram featuring a subcloning vector map of the recombinant *CEPDE3* gene

CEPDE3-SF and *LF* inserts subcloned into the *pGEX-6P1* vector. *EcoRI* and *NotI* are the two common restriction sites identified within the insert and destination vector. The predicted insert size for *CEPDE3-SF* is ~1.7 kb and *CEPDE3-LF* is ~1.9 kb. *pGEX-6P1* vector has a size of ~4.9 kb.

3.3: Results

3.3.1: Experimental design for subcloning of CEPDE3-SF and LF into pGEX-6P1

The initial studies with CEPDE3 constructs in pET21-D vector resulted in low CEPDE3 expression and PDE activity. Several attempts in improving the His-tag protein expressions failed. Hence some control experiment with autosomal recessive hypercholesterolemia (ARH) a GST-tag protein generously provided by (NHLBI staff scientist, Dr. Jiro Kato) was expressed in *E. coli* and inducible by IPTG. Based on the high expression of GST-tag proteins, it was decided to form new CEPDE3 constructs using pGEX-6P1. After analysing gene sequences of CEPDE3 and pET-21D vector, further subcloning studies were planned in order to form new constructs of CEPDE3-LF and SF using the N-terminal GST-tag vector pGEX-6P1. It was decided to re-amplify the existing cDNA constructs of *CEPDE3* gene from the initial pET-21D vector, which involved excising the gene of interest and subcloning into the destination vector. *EcoRI* and *NotI* were determined to be suitable restriction sites for both insert and vector for the insertion of CEPDE3-SF and LF into pGEX-6P1. Long and short-form plasmids subjected to restriction double digests (refer to Chapter 2, section 2.5). DH5 α cells were used for a transformation reaction.

Bacterial transformants were subjected to restriction double digests and agarose gel analysis of the clones indicated that insert plasmids did not show the correct size of both inserts (CEPDE3-SF~ 1.7 kb and CEPDE3-LF~ 1.9 kb) and pGEX-6P1 (~ 4.5 kb) vector (Fig. 3.5 and 3.6).

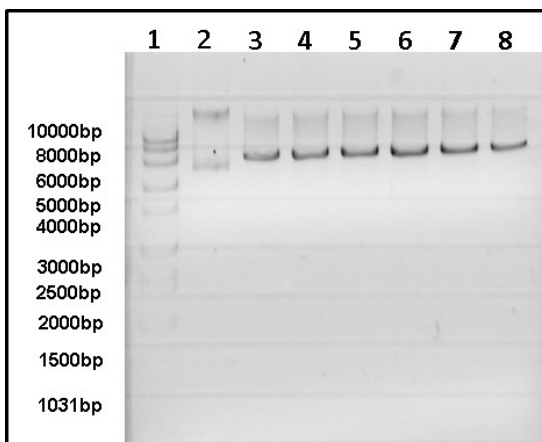


Figure 3.5: Subcloning with CEPDE3-LF and pGEX-6P1

Agarose gel analysis subjected to restriction double digests using *EcoRI* and *NotI*. Lane 1: MW marker, lane 2 contains control undigested plasmid, lanes 3-8 contain plasmid DNA extracted from each single colony of the transformants.

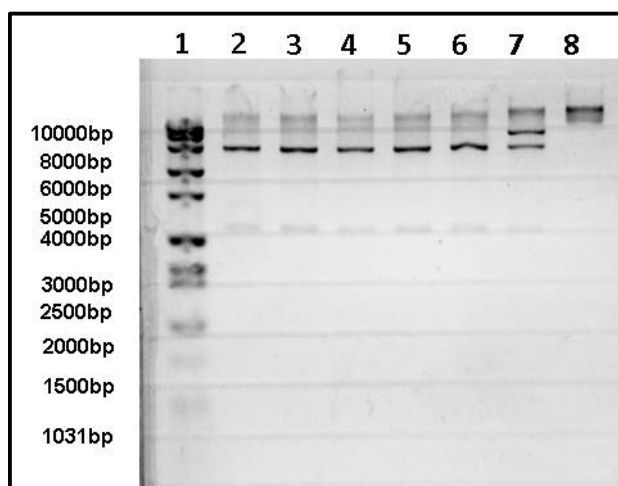


Figure 3.6: Subcloning with CEPDE3-SF and pGEX-6P1

Agarose gel analysis of restriction double digests of CEPDE3-SF and pGEX-6P1 by EcoRI and NotI to determine subcloning of the insert into the vector. Lane1: marker, lanes 2-7 are plasmids from single colonies, lane 8 contain undigested plasmid as a control.

Further subcloning experiments were attempted based on the same protocol with alterations in using a range of competent cells from a derivative of BL21 and TOP-10 competent cells, also a different ligation kit from Roche was used. However, transformation analysis confirmed only digested pGEX-6P1 vector DNA bands and no CEPDE3-SF and LF insert bands were observed.

Troubleshooting measures were taken to purify new plasmid stocks of pGEX-6P1 and used in subcloning of CEPDE3 inserts. Unfortunately, the experimental data did not show any positive insert or vector bands, and thus indicating that this subcloning reaction using the old constructs was not successful. Based on the experimental data it was decided to perform analysis on the gene sequences of the inserts.

3.3.2: Sequence analysis of isoforms and improved primer design

Original constructs of CEPDE3-LF and SF in pET-21D vector designed by (Samidurai et al. 2008 unpublished data) were analysed. It was observed that the previously designed primers for CEPDE3-SF and LF constructs had no stop codon, in order to facilitate the extension of a C-terminus His-tag located after the insert at the MCS region in the pET 21D vector sequence. The vector sequence of pGEX-6P1 was also analysed, and the common restriction sites, *EcoRI* and *NotI* were found to be compatible with CEPDE3 sequences and pGEX-6P1. As the GST-tag is located at the N-terminus, no frame shift was required at the *EcoRI* restriction site in pGEX-6P1 in order to keep the sequence in frame. However, the primers previously designed for pET21D vector added two nucleotides before the ATG start codon. To avoid frame-shift mutations, two

primers were designed for each of the isoforms, based on the common restriction sites, to amplify both sequences. See Fig. 3.7, below, for CEPDE3-SF and LF isoforms primer designs.

1) CEPDE3LF-EcoRI

5'- TAG AAT TCA CCA TGT CTG ATG GGC ATA TGC -3'

2) CEPDE3LF-NotI

5'- TAG CGG CCG CTC ACT GAC TAA GAT CCG AG -3'

3) CEPDE3SF-EcoRI

5'- TAG AAT TCA CCA TGA ACT CCA AGG TTT TTA AAT C -3'

4) CEPDE3SF-NotI

5'- TAG CGG CCG CTC AGA CAT ATT CCT CTT CGG C -3'

Figure 3.7: Primers designed for CEPDE3-SF and LF

Primers were designed for PCR reaction based on the two common restriction sites, EcoRI and NotI, identified in both CEPDE3 long and short inserts and pGEX-6P1 vector.

3.3.3: PCR amplification of CEPDE3-SF and LF using new primers

PCR (polymerase chain reaction) cloning is a common technique that allows any nucleic acid sequence to be amplified in cycles, and generates a large number of copies of it. More importantly, it allows researchers to design primers to match the DNA-segment to be copied (Kubista et al., 2006). PCR experiments were designed for both CEPDE3-SF and LF isoforms. Accordingly, both plasmids were purified using miniprep QIAGEN kits following the standard protocol in the kit. Both CEPDE3 plasmids showed a high concentration of DNA, CEPDE3-LF: 331.6 ng/ μ l and CEPDE3-SF had a concentration of 618 ng/ μ l. A detailed protocol of the PCR master mix preparation is listed in Chapter 2 (section 2.3.1.2). PCR experiments were performed using increasing concentrations of DNA. CEPDE3-LF and SF plasmids were run on a 1.2% agarose gel. Insert band sizes of both CEPDE3-SF and LF did not correspond to predicted size of 1.9 kb for LF or 1.7 kb for CEPDE3-SF. The same experimental samples were further loaded on an e-gel and the run time extended to 30 minutes, thus a total of 90 minutes run time determined the right size of the CEPDE3-SF and LF plasmid length (see Fig. 3.8). Both plasmid inserts corresponded to the predicted size, CEPDE3-LF \sim 1.9 kb and CEPDE3-SF \sim 1.7 kb.

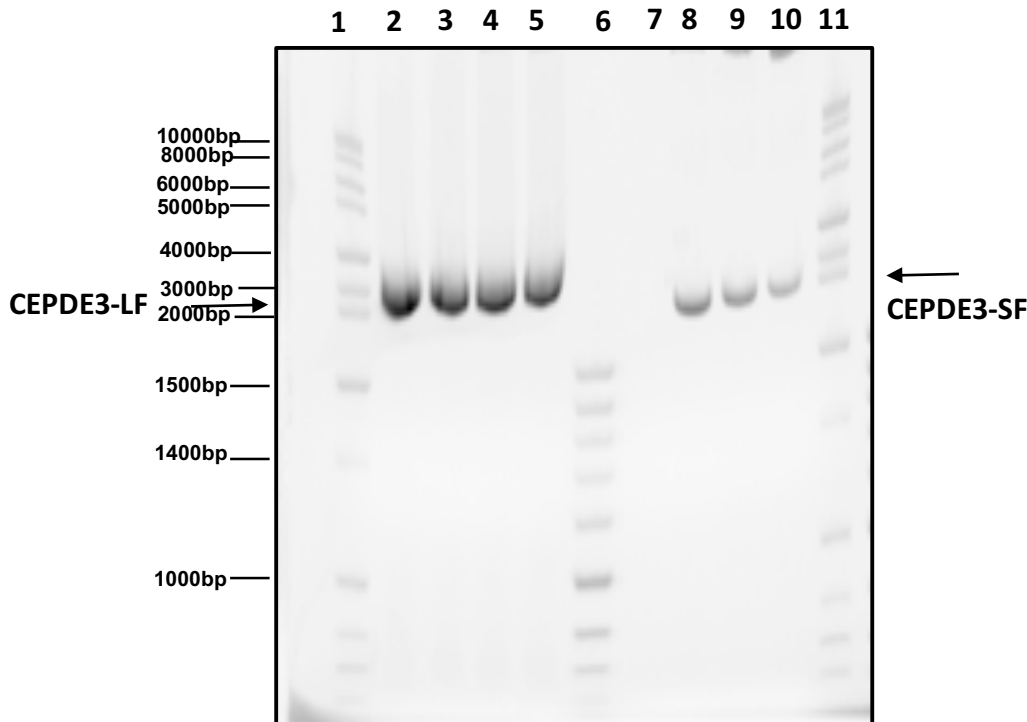


Figure 3.8: Analysis of PCR samples of CEPDE3 LF and SF amplification run on an e-gel

PCR samples of CEPDE3-LF and CEPDE3-SF were analysed on e-gel with a run time of 90 minutes. Lanes 1, 6 and 11 contain MW marker, lanes 2, 3, 4 and 5 contain LF PCR samples with increasing concentrations of LF DNA. LF plasmids were loaded in the following order, lane 2: 0.3 μ g, lane 3: 0.6 μ g, lane 4: 0.9 μ g, and lane 4: 1.2 μ g. Lanes 8-10 contains SF samples of DNA. The SF plasmids were loaded in the following order, lane 8: 2.4 μ g, lane 9: 1.8 μ g, and lane 10: 1.2 μ g of DNA.

With successful PCR reactions, it was decided to continue subcloning of LF by TOPO cloning. As an alternative, the CEPDE3-SF was synthesized as a full length gene. Subsequently both the isoforms were subcloned into the pGEX-6P1 vector.

Another PCR experiment with LF was performed based on the same protocol used in the 1st experiment described in section 3.3.3. CEPDE3-LF was reamplified from the cDNA clone and analysed on agarose gel. PCR products were loaded in several duplicates, 0.6 µg of LF DNA in each well, along with a positive control of cDNA and a negative control (with no DNA). All PCR inserts were closely matched the predicted size of CEPDE3-LF (1.9 kb) (band indicated by the arrow). Some contamination was observed in the cDNA clones, non-specific bands were observed between 4000-5000 bp and the PCR product was gel purified (see Fig. 3.10).

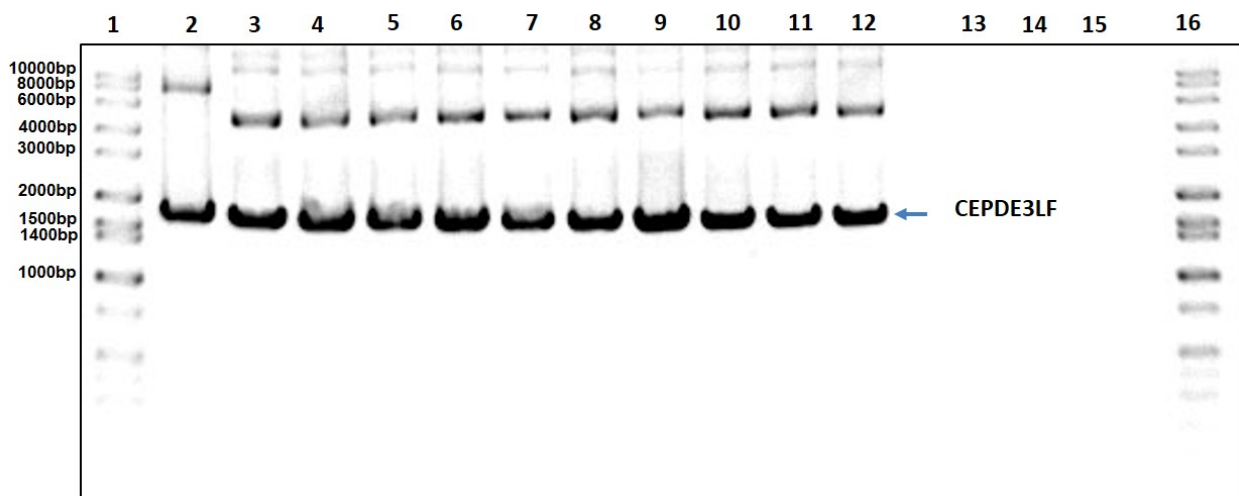


Figure 3.9: Amplification of CEPDE3-LF fragments by PCR

CEPDE3-LF was amplified and analysed on a 2% agarose gel. Lanes 1 and 16 contain MW marker, lane 2 contains a positive control of CEPDE3-LF insert, lanes 3 to 12 contain LF PCR samples, lanes 13-15 contain samples with no DNA added as a negative control.

All PCR inserts corresponded to the expected size of ~ 1.9kb for CEPDE3-LF. For further steps, PCR amplified product of CEPDE3-LF were gel purified using a QIAGEN gel purification kit following the standard protocol (refer to Chapter 2, section 2). In addition, 66 µg DNA in 200 µl was loaded on 0.8% agarose gel (Fig. 3.10). Extra care was taken as to not expose the bands for a long time to UV and excise the band accurately, so as to avoid the extra agarose on gel and thus prevent contaminants in the purified sample of DNA.

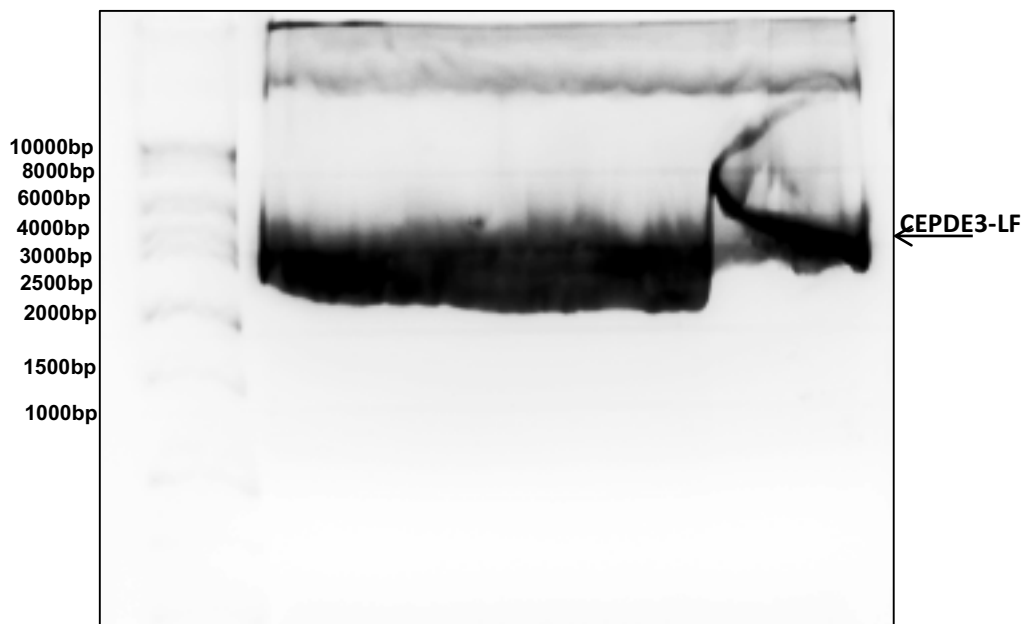


Figure 3.10: Agarose gel analysis of the resultant CEPDE3-LF PCR amplified product

PCR product of CEPDE3-LF was analysed on agarose gel and this product was further gel purified, insert band was excised and extracted from the gel using QIAGEN gel extraction kit and used in the ligation reaction with pGEX-6P1.

3.3.4: TOPO cloning and analysis

TOPO cloning reactions were performed following the standard protocol provided with the TOPO cloning kit (Invitrogen, USA). Three PCR samples of CEPDE3-LF were used with varying concentrations and each sample was used to prepare a reaction mix using concentrations of 20 ng and 50 ng each (refer to Chapter 2, section 2.4). One shot competent cells provided with the kit were used for transformation. Agar plates with 50 µg/ml kanamycin were used for selection and 100 µl of bacterial cells were spread on the plate, then set to incubate overnight at 37°C. Transformants from the CEPDE3-LF subcloning reaction were grown and plasmids extracted. Six colonies were picked from each of the plates and used to inoculate liquid culture LB broth containing kanamycin (50 µg/ml). Plasmids were isolated with QIAGEN mini prep kits following the standard protocol. DNA was eluted using 50 µl of elution buffer for all six samples analysed using nanospec for DNA concentrations. The following concentrations were recorded for each colony: A1: 296.4 ng/µl, A2: 225.7 ng/µl, B1: 282 ng/µl, B2: 114 ng/µl, C1: 30.2 ng/µl, and C2: 212 ng/µl. All six plasmid sample preparations from TOPO plasmid preps were subjected to restriction digestion using enzymes *EcoRI* and *NotI*. Digested samples were analysed on an agarose gel along with a positive control of CEPDE3-LF and an uncut sample (Fig. 3.10). The clones, A1, A2 and B2, showed bands with insert and vector corresponding to ~3.5 kb (top band) for the TOPO vector

and ~1.9 kb (lower band) for CEPDE3-LF, hence the plasmids with the correct insert-vector size were considered true positive clones with the predicted insert size (see Fig. 3.11) and were confirmed by sequencing.

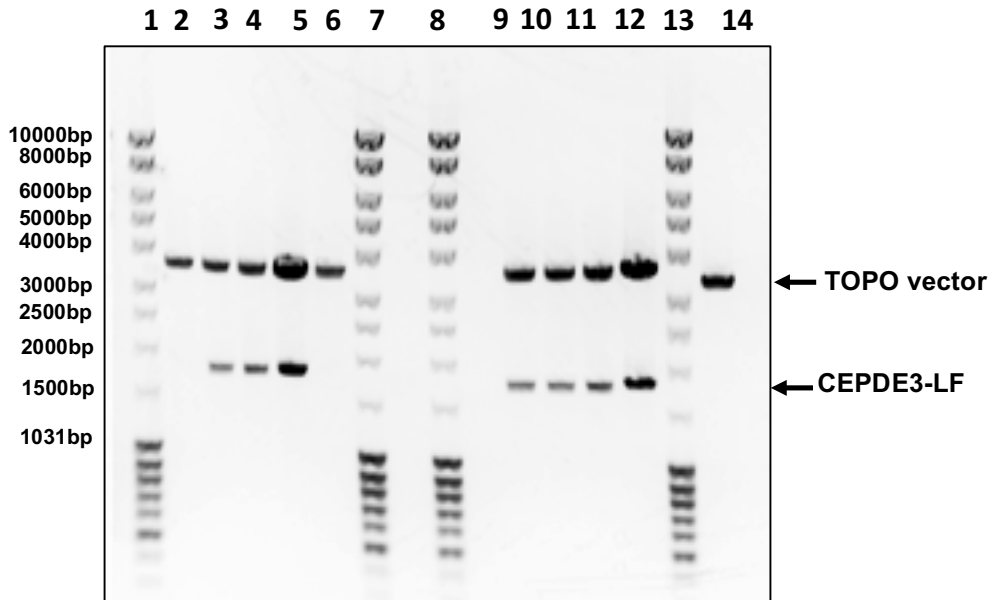


Figure 3.11: Restriction analysis of recombinant TOPO cloning in CEPDE3-LF.

Transformants from TOPO cloning reaction in CEPDE3-LF were analyzed on agarose gels. Single colonies from the TOPO cloning were grown and plasmids were extracted and further digested with NotI and EcoRI, then separated on a 1.2% agarose gel. Lanes 1, 7, 8 and 13 contain DNA ladder marker. Lanes 2 and 6 contain enzyme digested empty vector as a control. CEPDE3-LF-TOPO clones double digested with enzyme were loaded in the following lanes: Lanes 3-5 contains digested plasmids from A1. Lane 5: A2, and lanes 9-12 contain clones from B1, B2, C1 and C2.

3.3.5: Subcloning of CEPDE3-LF into pGEX-6P1

CEPDE3-LF plasmid extracted from LF TOPO construct was further subcloned into pGEX-6P1. Transformation was carried out using zymo competent cells. These cells are designed for a quick step transformation which eliminates the heat-shock step. Confirmed positive clones from CEPDE3-LF plasmids subcloned in TOPO cloning vector were amplified and plasmids were isolated using Maxi-prep. LF plasmid cDNA determined a yield of 776 ng/μl. Simultaneously some pGEX-6P1 vector plasmid was double digested using the restriction enzymes *EcoRI* and *NotI* to analyse its length. A ligation reaction for CEPDE3-LF and pGEX-6P1 was incubated overnight at 16°C. The following day, the ligation mix was directly transformed using Zymo mix and go competent cells without the need of a heat-shock step hence the ligation mix was directly added to the

competent cells and transformants were plated (refer to Chapter 2, section 2.5.4.2 and 2.5.4.3). After overnight incubation, several single colonies were observed, single colonies used to inoculate LB medium with ampicillin. Positive clones were confirmed by single or double restriction digests using the restriction enzymes *EcoRI*, *NotI* and *EcoRI+NotI*. Samples were analysed on a 0.8% agarose gel. Double digested samples showed the correct size bands with the CEPDE3-LF insert (1.9 kb) and pGEX-6P1 vector (~4.9 kb) (Fig. 3.12).

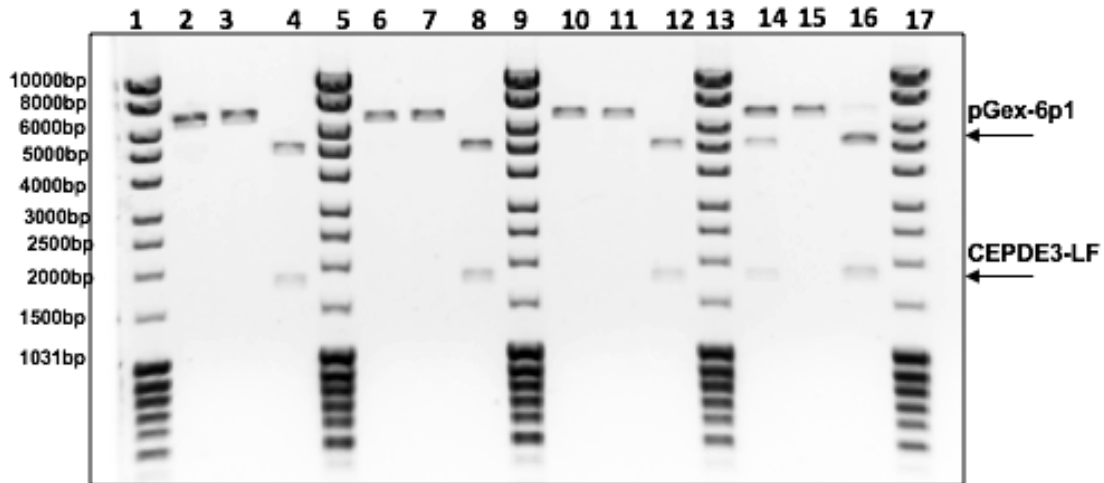


Figure 3.12: Subcloning analysis of CEPDE3-LF and pGEX-6P1 expression vector

CEPDE3-LF fragments from *TOPO* cloning vector ligated into *pGEX-6P1* vector. After *E. coli* transformation, cloned vector DNA was purified using *QIAGEN* mini prep kit and digested by *EcoRI* and *NotI*. Digested DNA fragments were separated using 1.2% agarose gel. Lanes 1, 5, 9, 13 and 17 contain DNA ladder marker. Lanes 2, 6, 10 and 14 contain *EcoRI* digested plasmids, lanes 3, 7, 11 and 15 contain *NotI* digested plasmid. Lanes 4, 8, 12 and 16 contain *EcoRI* and *NotI* double digested plasmid of *CEPDE3-LF pGEX-6P1*.

3.3.6: *CEPDE3-SF* gene synthesis

CEPDE3-SF isoform was gene synthesized to perform codon optimization. Having the process of gene synthesis done commercially obviates the need of PCR. Hence a gene can be directly subcloned into the desired vector. The *CEPDE3-SF* isoform was subjected to codon optimization with an aim to enhance levels of protein expression and solubility in *E. coli*. Short-form (*CEPDE3-SF*) codon optimization was performed at Integrated DNA Technologies (IDT). A protocol for codon optimization performed at IDT is explained in the steps in the following section.

3.3.7: Cloning by gene synthesis

Gene synthesis of the selected cDNA sequence was processed at IDT. The following link gives the website used for gene synthesis: <http://eu.idtdna.com/pages/products/genes/custom-gene-synthesis>

The system can also test for complexities and screen for potential restriction site problems, and provides a warning message if any problems are detected. Detecting the sequence complexity thus allows small changes to be made to the sequence if necessary. To be able to clone CEPDE3-SF into pGEX-6P1, *EcoRI* and *NotI* sequences were engineered at the ends of the CEPDE3-SF sequence. To begin with the codon optimization process, a single sequence of the *CEPDE3-SF* gene was entered (<http://www.ebi.ac.uk/Tools/msa/clustalw2/>).

The input page at IDT is shown in Fig. 3.13. The open reading frame is shown with *EcoRI* and *NotI* as two restriction enzymes that were unique and considered compatible with CEPDE3-SF. In the next step, the ORF sequences were accordingly used by IDT to perform codon optimization. The top 5 codon optimized sequences generated were then checked to see if there were any new *EcoRI* and *NotI* sites generated, to avoid adding cut sites internally.

Enter a Single Sequence

Gene Name
PDE3

Sequence
5' Restriction Site **EcoRI** Sequence Size 1419

```

801 TATTTTAGCC ACCGATCTGA AACAGCATT CGAGATTATT ATGACGTTA CTGAGCGTCT GACTGAGATC GATGTGCAGG
881 TGGAAACTGA TCGTCTGCTG ATIGGCARAT TGCTGATTAA AATGGCAGAT ATCAACTCTC CAACAAAACC GTACGGCCTG
961 CATCGCCAGT GGACAGATCG TATTTGGGAA GAATTTTATG AGCAAGGTGA TGATGAACGC CGTTCGCGGT TACCTATCAC
1041 GCCTTACATG GATCGCGGTG ATGCGCAGGT GGCTAAACTG CAGGATTCTT TTATCGCACA CGTGTCTCTG CCACTCGCAA
1121 CCGCGATGAA CGAATGCGGC TTACTGCCTA TTTTACCGGG CCTGGATACT AGTGAGCTCA TCATCAATAT GGAACATAAC
1201 CATCGTAAGT GGAAGAACA GATCGAACTG GAAAACGGAG GCTCTTATGA AGCACAGATC ACCTGCAATG GTGGAACAGC
1281 AGTCAATGGC GTGATTGAAG AAGAGAGCGC CAGTACTAGT GATAGCCCGG ATCCTCGTCC CGATTACCA CTGGACAGCG
1361 ACCTGTCACA GGTGCCAIII ACAATCTGCT GCTCTATTGC CGAGGAAGAA TACGTCTGA

```

Sequences may be entered in the following Nucleic Acid formats: DNA Bases(A,C,G,T), FASTA or GenBank 3' Restriction Site **NotI**

5' UTR N/A N/A 3'UTR

5' Restriction Site **GAATTC** **GCGGCCGC** 3' Restriction Site

Notes

[Perform Codon Optimization](#)

Figure 3.13 Diagrammatic representation for gene synthesis of the *CEPDE3-SF*

The above diagram represents the screen shot of the IDT input page of the *CEPDE3-SF* gene sequence used to perform codon optimization. Using the IDT tool, a desired gene sequence is entered and further subjected to codon optimization.

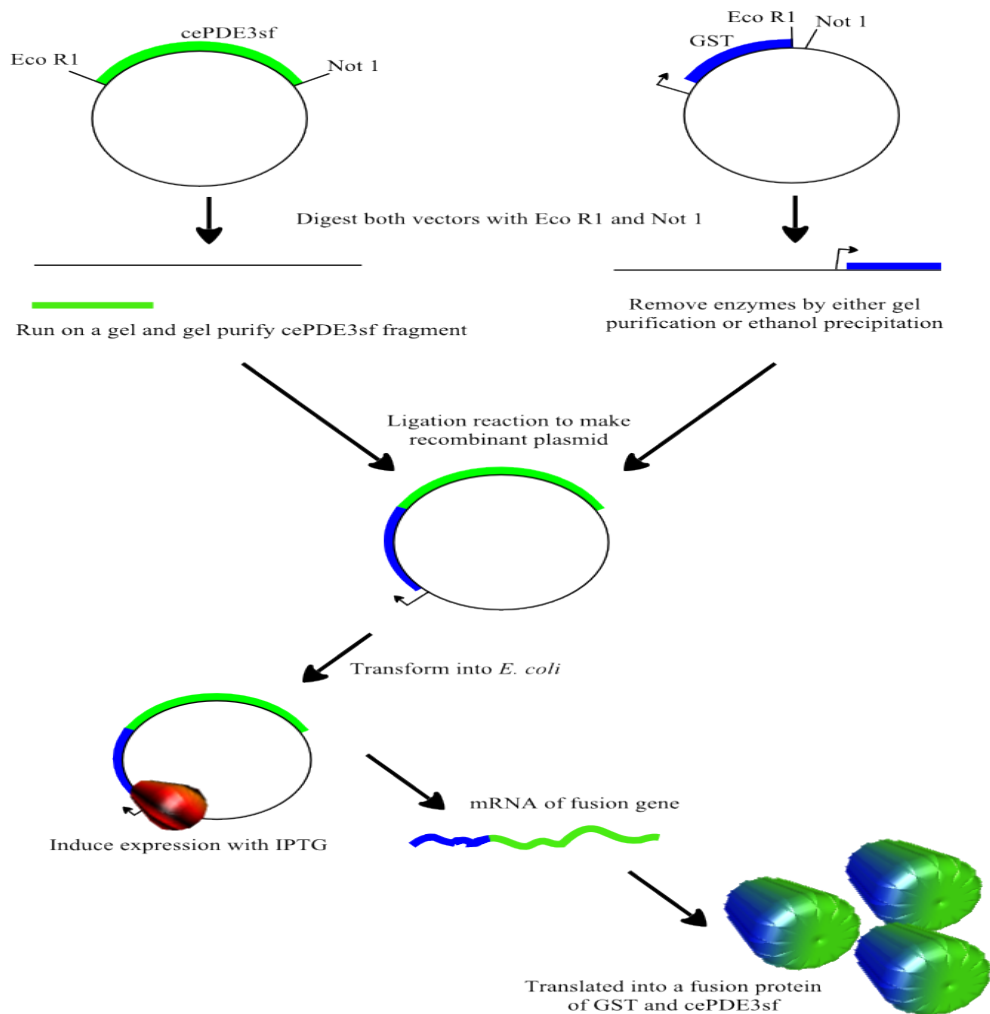


Figure 3.14: Workflow for cloning of codon optimized *CEPDE3-SF* gene in GST-tagged pGEX-6P1 Restriction digestion of *CEPDE3-SF* and GST-tagged vector by *EcoRI* and *NotI* is followed by gel purification of the insert and vector, and ligation to make a recombinant plasmid, which is transformed into *E. coli* and protein expression is induced with IPTG.

3.3.8: Subcloning of CEPDE3-SF with pGEX-6P1

Codon-optimized plasmid of CEPDE3-SF in pIDT vector was subjected to restriction digestion using *EcoRI* and *NotI* and transformed using zymogen competent bacterial cells. Amplified insert and vector plasmids were analysed by restriction double digests (Fig. 3.15). CEPDE3-SF and pIDT had bands corresponding to their predicted sizes of 1.7 kp (CEPDE3-SF) and 3.5 kb (pIDT vector). pGEX-6P1 corresponded to ~4.5 kb.

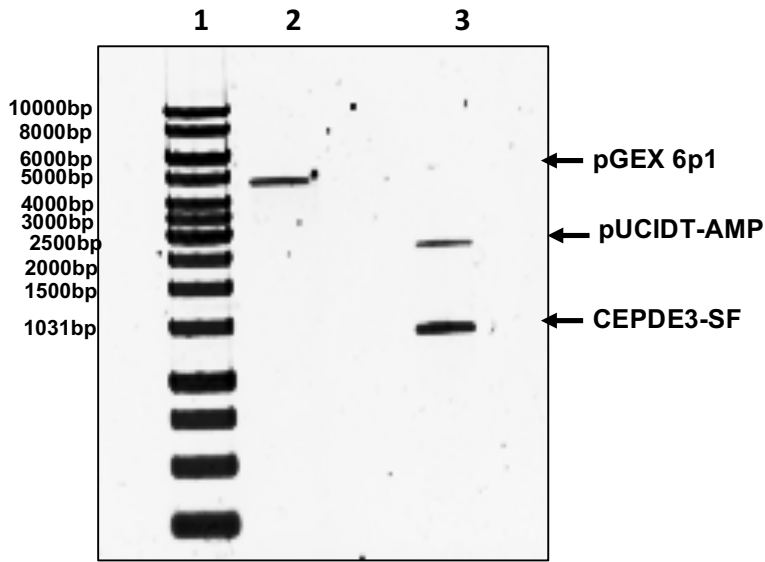


Figure 3.15: Agarose gel analysis of pGEX-6P1 and codon optimized CEPDE3-SF plasmid in pIDT vector

CEPDE3-SF plasmid and *pGEX-6P1* subjected to double digestion using restriction enzymes *EcoRI* and *NotI*. Lane 1: MW marker, lane 2: *pGEX-6P1* plasmid, and lane 3: *CEPDE3-SF* plasmid in IDT vector.

3.3.9: Subcloning of CEPDE3-SF into pGEX-6P1

The bands corresponding to linearized pGEX-6P1 and digested CEPDE3-SF (see Fig. 3.15) were excised from the agarose gel under UV light and gel purified. Next, a ligation of CEPDE3-SF into pGEX-6P1 was performed using the TAKARA (version 2.1) ligation kit, following the ligation protocol (refer to Chapter 2, section 2.5.3.1). Bacterial transformation was carried out using Zymo competent cells, (refer to Chapter 2, section 2.5.4.2) transformed cells were spread at different inoculant size (50, 100, 200 μ l) onto LB plates with ampicillin and incubated at 37°C overnight. Single colonies were used to inoculate LB medium with ampicillin. Plasmids were isolated from the bacterial cultures with a QIAGEN miniprep kit and clones were subjected to further analysis by restriction enzyme digests using *EcoRI* and *NotI*. Samples were then run on a 0.8% agarose gel to confirm positive clones (Fig. 3.16). A number of successful recombinant clones were identified and verified by DNA sequencing. These clones showed an upper band size at \sim 5 kb, the expected size for pGEX-6P1, and lower insert band size at \sim 1.7 kb, the predicted size for CEPDE3-SF. CEPDE3-SF plasmids were further confirmed as positive clones by gene sequencing analysis.

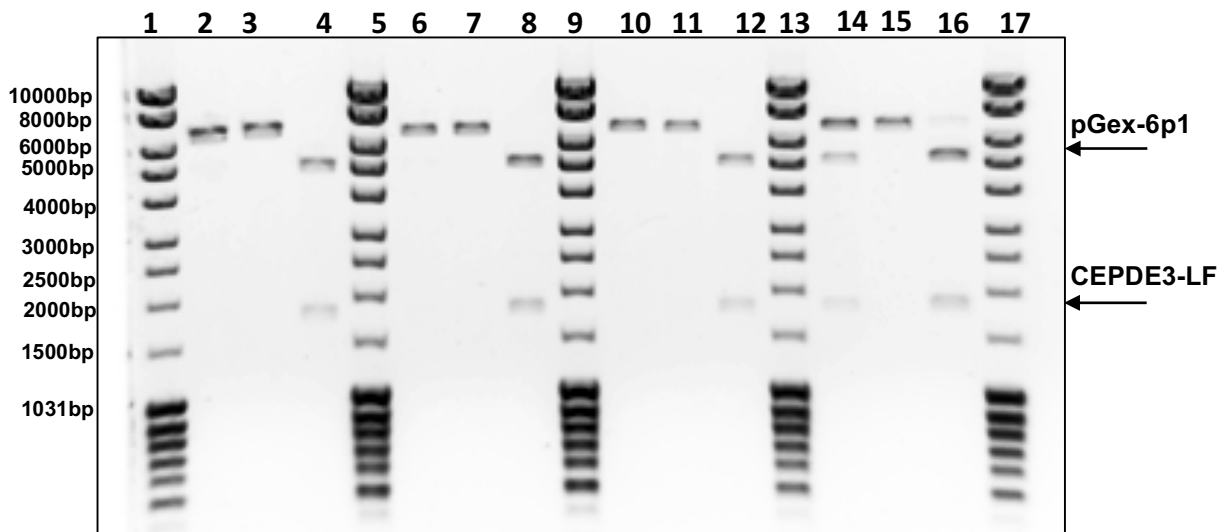


Figure 3.16: Agarose gel analysis of codon optimized CEPDE3-SF and pGEX-6P1

Transformants from CEPDE3-SF and pGEX-6P1 subcloning were subjected to restriction double digests using restriction enzymes *EcoRI* and *NotI*. Lanes 1 and 12 contain markers. Lanes 2-11 contain clones of CEPDE3-SF pGEX-6P1 vector from each single colony.

3.4 Discussion

3.4.1: Overview

Subcloning technique is commonly used to create a recombinant DNA molecule, in theory it is a simple and straightforward technique which utilizes a wide range of restriction endonucleases and other enzymes, including ligases, essential to insert one piece of DNA into a vector expression plasmid. However, traditional ligation dependent cloning can also be hampered due to several reasons including a lack of appropriate restriction sites, errors in enzymatic reaction, effects for inefficient transformation into *E. coli*. Failure in subcloning, often leads to repetition of the entire process multiple times, either following the same protocol or making alterations, which can be time consuming with limited success. Careful selection of reagents and restriction sites, as well as using new effective techniques with advancements in technology are some of the options to yield efficient results from subcloning (Matsumura, 2015). The subcloning study in *CEPDE3* gene was based on creating new constructs of the *CEPDE3* isoforms from the originally existing constructs in the pET-21D vector. The initial method based on traditional cloning did not yield desired results. Hence, the alternative approach was considered, which involved designing new PCR primers for both the *CEPDE3* isoforms and performing PCR experiments. Followed by PCR, it was decided to study each of the isoforms using different approaches. The long isoform (*CEPDE3*-LF) PCR product was subcloned into the TOPO vector by directional cloning and subsequently subcloned into pGEX-6P1 for further study. For *CEPDE3*-SF, codon optimization technique was used. Reports have suggested the use of codon optimization techniques enhances the expression and solubility levels to a great extent in proteins (Gustafsson et al., 2012). With the design of new tools and technology, the initiation and elongation of translation can be adapted. As a result, gene designing studies can be used to modify protein production and regulatory functions can be controlled (Dragosits et al., 2012). Codon optimization for *CEPDE3*-SF was performed at IDT technologies and subsequently *CEPDE3*-SF was subcloned into the pGEX-6P1 expression vector. Confirmation of positive clones using the restriction enzymes *EcoRI* and *NotI* showed bands at the estimated length of the *CEPDE3* isoform insert and pGEX-6P1 vector. Thus, the *CEPDE3* isoforms were successfully subcloned into pGEX-6P1. Both isoforms were confirmed by gene sequencing analysis.

3.4.2: Initial subcloning of *CEPDE3* isoforms

Traditional subcloning depends on several factors. Initially, it was not clear why using traditional subcloning with restriction enzymes did not produce the desired results with the *CEPDE3* isoforms. However, as discussed earlier, the His-tag *CEPDE3* constructs were subcloned in pET21D vector (see section 3.3.2), and the original sequence of the *CEPDE3* gene was designed to facilitate the extension of a C-terminus His-tag. This sequence change may have contributed to the limited success with the initial subcloning experiments that were based on traditional cloning to insert the *CEPDE3* gene in the pGEX-6P1 vector with a N-terminal GST-tag.

The efficiency of subcloning experiments can often be improved to achieve the desired results, and avoid repetition, by following simple procedures which can be monitored and are easy to trouble shoot at every step (Yegnasubramanian, 2013). Some common factors affecting subcloning and the traditional cloning method, are discussed in detail below. Subcloning of a gene requires several strategic decisions. It requires the designing of new constructs, which begins with choosing the desired cloning vector, depending on the nature of study to be carried out. While it is critical that the experimental settings are designed in a way to minimize other background events, to gain more efficiency in the subcloning reaction, errors may affect transformation. When considering background errors in a subcloning reaction, it primarily begins with examining the preparation of plasmid, and the purity of enzymes (Struhl, 2001).

3.4.3: Parameters in traditional cloning

Purifying plasmids is a primary and critical step in a cloning procedure that needs to be carefully assessed, as impurities in the plasmid DNA can alter the subcloning reaction. Using the QIAGEN extraction kits for plasmid preparation in CEPDE3 was efficient, as no additional steps outside the standard protocol were required to purify the cDNA inserts. Preparing higher volumes of *E. coli* culture is more efficient in extraction and purification of large amount of cDNA. Based on these parameters, the CEPDE3 plasmids were purified from a culture of 1 litre *E. coli*. Studies performed on agarose gel electrophoresis identified that cloning errors are reduced to a great extent by DNA-analysis on agarose gels and gel purification (Kevin Struhl, 2001).

Gel purification has to be carried out carefully under UV light. This technique requires selective removal of the desired insert with precision, as the extra agarose from the gel may cause contamination. In addition, long exposure of the gel under UV-light may also reduce transformation efficiency of the DNA. Hence, practicing efficient and quick gel purification techniques are essential when carrying out the isolation of the desired fragment. Otherwise, undesired ligation products may be generated (Dugaiczuk et al., 1975). After the initial unsuccessful attempts with traditional cloning in CEPDE3, ethanol precipitation and phenol-chloroform extraction methods were carried out as alternative extra step to purify DNA. Another reason for inefficient subcloning can also be the presence of solvents with a high concentration of salts, introduced in some of the gel extraction protocols. High salt is known to cause inhibition of T4 ligase DNA (Jana and Deb, 2005).

3.4.3.1: Troubleshooting in PCR experiments

The initial PCR reactions performed on CEPDE3 isoforms did not yield the desired insert fragments of expected length. Based on these results, some trouble shooting was done and protocols were assessed carefully to make changes. Some considerations that should be considered before setting up a PCR-experiment to amplify a gene or insert to be used for subcloning include: 1) The nature of insert and 2) Conditions of the PCR reaction. DNA concentration, reagents for buffers, and annealing temperature adjustments due to GC content in the templates or primers are essential (Bornhorst et al., 2004). Primer design is important in

relation to the nucleotide composition at the 3' end of the sequence, to avoid mispriming. The primer size, nucleotide constituents of the PCR product, and structure of the PCR template around the primer annealing sites are all important to consider (Cobb and Clarkson, 1994).

Preparation of the PCR-master mix should be carefully performed so that the PCR-templates are not degraded before the start of reaction. The presence of exonucleases can cause the degradation of nucleotide overhangs, and result in reduced efficiency of cloning. However, if stored carefully at the appropriate temperature, some PCR-products can result in successful cloning even after long storage times at 4°C. Careful preparation of plasmid and avoiding contamination during the setup of the master mix reaction is also critical for successful reactions. The PCR-program used (as listed in Chapter 2, Table 2.2) was optimal for CEPDE3 isoforms. CEPDE3-LF PCR samples were also run on an e-gel to optimize the run time. Extending the run time for further 45 minutes helped obtain the desired results. Following PCR, the two different approaches were adapted for both CEPDE3 isoforms. The long-form was cloned using the TOPO blunt vector in a recombination reaction, and then further subcloned into its destination expression vector.

3.4.3.2: Analysis of restriction enzymes

Assessment of restriction endonucleases have to be carefully selected based on the design of the gene sequence. If the target gene or DNA-molecule does not have the appropriate restriction sites, PCR-primers can be designed to incorporate the suitable restriction sites at either end of it, to enable restriction digestion and ligation into a particular destination vector. By adding the restriction sites via PCR during amplification of a gene, any target gene can be inserted into a desired vector (Lebedenko et al., 1991). With the CEPDE3 isoforms, a new set of primers were designed prior performing PCR, based on the two restriction sites (*EcoRI* and *NotI*) with two sets of primers for each. In TOPO cloning, is essential to use a restriction endonucleases that generate complimentary blunt ends at the terminal end of the PCR-product. This strategy only requires one restriction enzyme, but can lead to insertion of the molecule in either direction. Therefore, orientation of the DNA-molecule needs to be confirmed after ligation. Overall, every step of restriction digests and ligation reactions can take some length of time, and requires close monitoring to result in success. Even if a restriction enzymes function efficiently, there may be some small parts of DNA molecules which could cause contamination. Another common error in subcloning is the incomplete digestion of the plasmid DNA by restriction endonuclease. It is possible to reduce this error, but it may be difficult to completely eliminate it.

3.4.3.3: Ligation

The ligation reaction is a critical step in the subcloning process and requires efficiency. Inefficient ligation can result, when undesired molecules are combined with the vector and insert. There are many different reasons why this can occur, including an incorrect concentration of the desired insert, the ligation product can be insoluble, or the ligase may have lost its efficiency due to repeated handling, freeze-thaws, or long term storage at -20°C. In addition, the purified DNA

molecules may contain impurities, or the enzymatic reaction could possibly have a low pH. The ligation reaction is significantly lower if the pH is less than pH 6, therefore dissolving the DNA in 1 M Tris-HCl (pH 7) is also suggested (Evans et al., 1998). In addition, there is also the chance that the vector or insert will self-ligate; one end of a molecule can join to the other end of the same molecule, or to another molecule, resulting in vector-to-vector or insert-to-insert joining. This reaction results into a circular plasmid and undesirable *E. coli* transformants, and is generally resolved by using two restriction endonucleases to generate incompatible ends (Niumsup and Wuthiekanun, 2002). The correct proportion of the insert to vector ratio in the ligation is also essential for a successful reaction. Another factor to consider is the concentration of DNA, which can also affect the ligation reaction. A low concentration may result in intramolecular ligation with a double stranded DNA molecule. At the same time, a higher concentration of DNA can result in intermolecular ligation. In addition, multiple vector and inserts can be assembled to form a long concatemer (Damak and Bullock, 1993).

3.4.4: Alternative methods of cloning for CEPDE3 isoforms

Codon optimization of CEPDE3-SF

The short isoform CEPDE3-SF-construct was codon optimized at IDT. The idea to carry out codon optimization with CEPDE3-SF was to improve the expression levels of CEPDE3-SF so as to codon optimize a particular DNA sequence by changing its codon to match the most prevalent tRNAs. In doing so, it enables the protein to undergo efficient translation and may enhance expression. Protein expression level can vary with all tRNAs among different species, as not all tRNAs are expressed in the same way and at similar levels across different species. This arrangement of codon optimization can be adjusted depending on the cell and tissue type in each species. For example, if specific information regarding protein expression is in *E. coli*, it is best to consider the parameters for bacterial protein expression. Also the new gene can be synthesized in a way that restriction sites are not introduced in the altered gene sequence. Altering the gene sequence by using the technique of gene synthesis (codon optimization) can also improve gene expression level considerably. The usage of codon bias generally reflects a balance between mutation and natural selection, that leads to optimal translational efficiency (Angov, 2011).

The approach of codon usage bias and its impact on gene expression levels has been discussed in various studies (Gustafsson et al., 2012; Burgess-Brown et al., 2008; Angov, 2011). There are some codons in the genetic code which are redundant. Simultaneously, there are mutations in the genetic code that can alter levels of protein expression to a great extent. These mutations can also bring changes in structural properties of proteins (e.g., protein conformation), affect post-translational modifications, and protein functions depending on the role of the amino acid it encodes or the type of mutation. For example, if a nonsense mutation occurs, it can change an amino acid to a stop codon, which can lead to premature termination of the translation process, enzymatic signaling, etc. Introducing synonymous mutations, does not alter the encoded amino acids in a way that changes the nature of a protein. Hence, sequences are designed in a way that its amino acid sequence is slightly changed, and thus favors efficient soluble protein expression due to enhanced translation (Zhou et al., 2004; Baca and Hol, 2000). The short isoform of CEPDE3

was successfully codon optimized, the insert size of ~ 1.7 kb was confirmed by agarose gel analysis (refer to Fig 3.15).

TOPO cloning of CEPDE3-LF

In contrast to traditional cloning, ligation independent cloning offers a wide range of rapid techniques which excludes the ligation process. For example, TOPO cloning is an efficient method of directly inserting a gene of interest into a destination vector where it can then be shuttled into an expression vector (Stevenson et al., 2013). The CEPDE3-LF PCR product was successfully cloned using the TOPO-blunt vector and the desired insert was obtained (see section 3.3.4. and Fig 3.11).

3.4.4.2: Subcloning of CEPDE3 isoforms in to pGEX-6P1

CEPDE3 constructs of TOPO cloned long-form and codon optimized short-form were subcloned into the expression vector pGEX-6P1. In this subcloning reaction, bacterial transformation was carried out using Zymogen competent cells. The step of heat shock was eliminated, as these cells are made chemically competent and do not require the heat shock procedure. These cells are known to produce $> 10^8$ DNA transformations (Zymoresearch.com). During the process of bacterial transformation with CEPDE3 isoforms in pGEX-6P1, an alternative technique of processing the transformation mix was carried out apart from the standard process. A small amount of the transformation mix was spread on plates directly, while the remaining amount was concentrated by centrifugation and supernatant taken out and stored separately. The concentrated cell-pellet of bacteria formed was resuspended in a small amount of the supernatant post centrifugation and the mixture was spread on a plate. The number of colonies formed in the direct transformation versus the cell-pellet mixture transformation varied. The standard direct plating resulted in fewer colonies, while a dense pattern of colonies was observed in the cell-pellet method. This method increased the number of bacteria plated, by spinning down the cells into a pellet, and increased the chance of transformed colonies growing efficiently.

3.4.4.1: Summary

The initial cloning techniques did not show the desired results in the CEPDE3 subcloning study. While the traditional cloning requires monitoring at every step and a careful selection of reagents and enzymes, it can be time consuming and involve complex steps. With the use of polymerase chain reaction increasingly widespread, a range of ligation independent techniques for cloning complex PCR products of recombinant clones are available (Aslanidis and de Jong, 1990). As these techniques are comparatively faster than a traditional cloning reaction, results can be achieved efficiently. Therefore, the two CEPDE3 isoforms were studied based on two different techniques. The CEPDE3-LF was studied using TOPO cloning and the CEPDE3-SF was codon optimized. Both CEPDE3 isoforms were successfully subcloned into pGEX-6P1 vector and sequence verified.

Chapter 4

Chapter 4: Protein expression of the *C. elegans* CEPDE3-SF and CEPDE3-LF isoforms

4.1: Introduction

4.1.1: The use of *E. coli* as a host organism for protein production

Microorganisms are considered ideal hosts for recombinant production of proteins as they can be grown at a high density, to facilitate high level protein synthesis. A wide range of expression systems are also available for expression in cell cultures of mammals, plants or insects and in some cases transgenic animals. Several factors require consideration while choosing the appropriate system for expression such as protein solubility, functionality, importance of post-translational modifications, speed of production, and yield (Demain and Vaishnav, 2009). The use of *E. coli* for heterologous expression of proteins has the advantage that it has fast growth kinetics. In optimal growth conditions, doubling times for *E. coli* can be as little as 20 minutes (Rosano and Ceccarelli, 2014). The bacteria is also well characterized genetically, and the availability of a range of cloning vectors and mutant host strains makes *E. coli* a favorable host for producing recombinant proteins rapidly with a high yield (Sivashanmugam et al., 2009). The *E. coli* physiology and metabolism is well understood and it is a common expression host to produce recombinant proteins, due to its relative ease of manipulation and inexpensive culture costs. Finally, the time-span required for generation of recombinant protein is also relatively short compared to other systems.

In *E. coli*, the purification of milligram quantities of protein can be achieved in a relatively short time. Simply shaking flask cultures in an incubator can produce many tens of milligrams of a heterologous protein per liter of a culture, without the use of fermentation technology. High density cell culture methods are also designed to produce a recombinant protein using rich growth medium for cultivation (Rosano and Ceccarelli, 2014). However, there are certain limitations with *E. coli*. Despite high expression and rapid growth rate, misfolding of proteins can result in insoluble protein aggregates called inclusion bodies. Some expression problems are also caused by weak promoters, poor translation initiation or the existence of rare codons (Angov, 2011). In addition, *E. coli* have limitations with glycosylation, phosphorylation and acetylation in comparison to other hosts such as insect cells, yeast and mammalian expression systems.

4.1.2: Advantages and disadvantages of *E. coli* for recombinant protein expression

Table 4.1: Advantages and disadvantages in an *E. coli* expression system

The table below lists some of the common advantages and disadvantages of using *E. coli* in recombinant protein expression. Though it is a rapid process with fast growth kinetics, it also has the limitation that recombinant proteins produced can form protein aggregates, or have structure and functional changes.

Advantages	Disadvantages
Rapid growth and expression	Post-translational modifications; glycosylation
High yield	Sometimes insoluble; inclusion bodies
Easy to culture and genome manipulation	Disulfide bonds, difficult to express
Cost-effective	Proteins with endotoxin
Easy labelling for structural studies	Acetate formation results in cell toxicity

4.1.2.1: Choosing the appropriate *E. coli* host

There are a wide variety of *E. coli* mutant strains characterized, that have been used in recombinant DNA. However, *E. coli* host strains have been specifically designed to aid expression of heterologous proteins (Daegelen et al., 2009). The BL21 strains are commonly used, and an important feature of these strains is that they are deficient in *OmpT* and *lon* proteases. *OmpT* is an outer membrane endoprotease that readily cleaves T7 RNA polymerase (Burgess-Brown et al., 2008). *lon* is an inner membrane enzyme, that is ATP-dependent and rapidly degrades misfolded and recombinant proteins. *OmpT* cleaves synthetic substrates in between dibasic residues with high substrate efficiency. The cleavage of sequences containing dibasic residues is known to have an important role for inactivating the proteolysis of bacterial transmembrane proteins and the degradation of recombinant proteins expressed in *E. coli* (Quick and Wright, 2002). Since *OmpT* is a membrane protein, it fractionates with the insoluble proteins fractions and copurifies with the protein aggregates present in the form of inclusion bodies of the protein. It is also known to remain resistant to high temperatures and denaturing conditions (McCarter et al., 2004). Deletion of both these proteases in *E. coli* has resulted in increased expression and stability of recombinant proteins.

Meanwhile, BL21 star DE3 cells have a mutation in the *rna* gene, which encodes RNase E, an enzyme that degrades mRNA within the cell. This mutation reduces levels of endogenous RNases, limits enzyme activity, and mRNA degradation, and thus imparts mRNA stability. Therefore, the mutation supports basal level gene expression of vectors. Hence, there is an increase in the mRNA transcripts, which results in an increase in protein yield (Kennell, 2002). *BL21 trxB*, *Origami*, and *Rosetta-gami* strains have mutations in thioredoxin reductase (*trxB*) or glutathione reductase (*gor*) genes. These strains are useful when expressing proteins with multiple disulfide bonds, which tend to be difficult to express without aggregates forming. In addition, they allow

the formation of cytosolic disulfide bonds, and help in the protein solubility, and thus enhance expression levels of disulfide containing proteins (Fathi-Roudsari et al., 2016).

Table 4.2: Characteristic features of *E. coli*

The important features of E. coli strains to consider when choosing a host for recombinant protein expression are listed below in the table.

Features of ideal expression strains:	
endA	does not degrade DNA
hsd	does not restrict unmethylated DNA
lon	lacks intracellular protease
ompT	lacks outer membrane protease
pLysS	inhibits T7 RNA polymerase
tonA	resistant to T1 phage

4.1.2.2: Affinity Tags

Affinity tags commonly known as fusion tags are used in the formation of a construct for expression in *E. coli* to improve recombinant protein expression. There is a wide choice of affinity tags available and tags often enhance recombinant protein expression and can increase protein solubility and facilitate folding, thus aid in further purification (Hammarstrom et al., 2005). Without altering the function and structure of a protein, tags can be placed on either side of the N- or C-terminus. Several affinity tags have been developed and can be classified depending on their properties and the targeted protein. There are affinity tags which use peptides or fusion partners to bind to small molecules ligands, which are linked to a solid support. For example, glutathione S-transferase (GST) binds to glutathione attached to resin, and hexahistidine (His-tag) binds to immobilized metals (Lichty et al., 2004). The choice of using particular tags depends on protein requirement and function. In *E. coli*, some of the most common solubility enhancing tags are (MBP) maltose-binding protein (Kapust et al., 2002), N-utilization substance A (NusA), (Davis et al., 1999), and glutathione S-transferase (GST) (Harper and Speicher, 2011). If large quantities of proteins are required of partially purified material, in a cost-effective way, GST and His tags are suitable (Bucher et al., 2002). A comparison of various affinity tags that influence protein expression level and solubility placed the tags in the following order MBP> NusA> GST> His-tag (Lichty et al., 2005). Using a His-tag as N-terminal fusion partner showed less solubility, but a GST-tag improved the rate of solubility (Lichty et al., 2005). The CEPDE3 isoforms were initially subcloned with the His-tag located at the C-terminus of the *CEPDE3* gene sequences.

With the new constructs, the GST-tag was located at the N-terminus, to allow the isoforms to be expressed as GST-tagged constructs.

Glutathione-S-transferase (GST) is derived from *Schistosoma japonicum* and has been used as an affinity fusion partner (26 kDa) for purification of target proteins (Costa et al., 2014). It has a high affinity for glutathione coupled to a sepharose matrix, through reversible binding, and the target proteins can be eluted using mild conditions without denaturation, with the help of reduced glutathione. A common vector used to add a GST-tag to genes is the pGEX series of vectors, which can have a positive impact on protein solubility in *E. coli* (Malhotra, 2009). The *Tac* promoter present in the pGEX-6P1 vector is in the -35 region and the -10 region of the vector, which makes it an highly efficient promoter (De Boer, Comstock, & Vasser, 1983). When RNA polymerase binds these two regions, transcription begins downstream of the promoter. Therefore, it plays an important role in gene expression and can increase the expression level of a target gene when used in recombinant expression system. Proteins produced with GST-tags have been used in several applications including NMR and crystallography (Harper and Speicher, 2011). Therefore, the recombinant GST-tagged CEPDE3 proteins were considered a suitable alternative to increase the expression levels of the CEPDE3 isoforms.

4.2: Aims

This chapter aims:

- To express recombinant CEPDE3-SF and CEPDE3-LF proteins as GST-tagged fusion proteins in a soluble form
- To cleave the GST-tag from CEPDE3 isoforms using PreScission protease enzyme

4.3: Histidine-tag protein expression

Initial protein expression experiments were carried out with constructs of *C. elegans* phosphodiesterase 3 CEPDE3-SF and LF cDNAs in the pET-21D expression vectors and expressed as histidine tagged proteins in *E. coli*. Expression of CEPDE3 isoforms was induced with 1 mM IPTG, CEPDE3-LF and SF cDNAs were grown in liquid LB broth with ampicillin at 37°C overnight at 225 rpm. Bacterial cells were homogenized using 1% Triton X-100 and lysozyme, cells lysed using homogenizer and bacterial cell lysates were further sonicated. Protein fractions were fractionated by centrifugation at 10,000xg for 15 minutes. Solubility of the isoforms was confirmed by western blotting. CEPDE3-LF and CEPDE3-SF isoforms were detected using the CEPDE3 isoform specific N-terminus antibody. For CEPDE3-LF, bands were detected at ~ 58 kDa, which was not close to the predicted size of ~ 63.5 kDa. Protein activity of the soluble forms was determined by assaying for PDE enzymes. An enzyme assay with soluble protein for CEPDE3-SF was performed. Experimental data from western blots, protein assays and activity measurements with CEPDE3-SF and LF preparations determined low protein expression (see Fig. 4.1a and 4.1b).

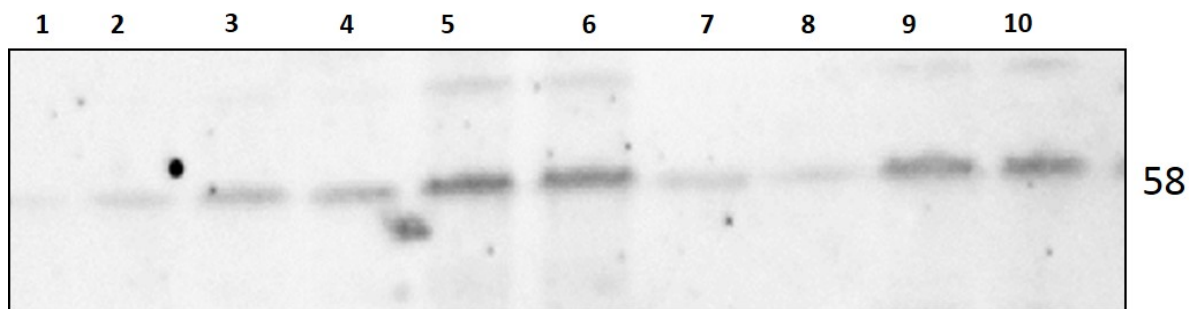


Figure 4.1a: Western blot analysis of His-tag CEPDE3-LF isoform

CEPDE3-LF expressed as His-tag proteins were detected by western immunoblotting. Lane 1 contains marker, lanes 2-4 contains bacterial lysate derived from harvesting cells and was fractionated by centrifugation and resulted in an insoluble cell-pellet and supernatant. The cell-pellet (lanes 5 and 6) was subjected to homogenization and thus fractionated into insoluble and soluble protein fractions. Lanes 7-8 contains soluble supernatant fractions and lanes 9-10 contain insoluble protein fractions. Proteins were detected by a long-form specific N-terminus antibody.

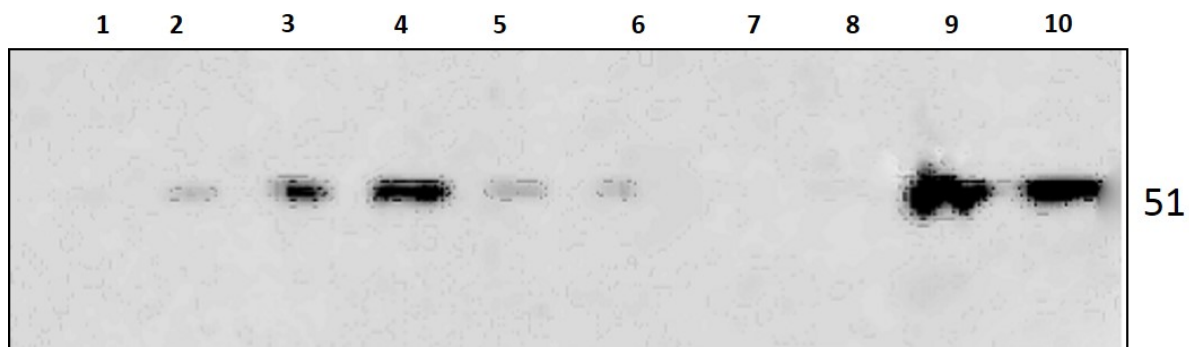


Figure 4.1b: Western blot analysis of His-tag CEPDE3-SF isoform

CEPDE3-SF proteins expressed were detected by western immunoblotting. Lane 1 contains marker, lanes 2-4 contains cell-lysate, lanes 5 and 6 contain insoluble cell pellet that was homogenized and fractionated to form soluble and insoluble fractions. Lanes 7-8 contain supernatant fractions and lanes 9-10 contain insoluble protein fractions. Proteins were detected by a short-form specific N-terminus antibody.

Further attempts made in improving levels of protein expression failed, hence it was decided to perform control experiments. An experiment using autosomal recessive hypercholesterolemia (ARH) GST-tagged proteins expressed in *E. coli* (provided by Dr. Jiro Kato Staff Scientist at NHLBI) was performed. *E. coli* transformed cells were induced with IPTG overnight at 37°C and some cells were grown in the absence of IPTG (Fig. 4.2). Anti-GST antibody was used as a primary antibody and anti-goat HRP was used as a secondary antibody. The IPTG induction increased expression of ARH protein, which showed distinct dark bands from lane 2 to lane 5. Below these dark bands were also several bands detected at lower molecular weight, including a GST band detected at 26 kD. Meanwhile, lanes 6 to 9 had faint bands from protein samples grown in the

absence of IPTG. Therefore, GST-tagged ARH protein expression was significantly induced by IPTG.

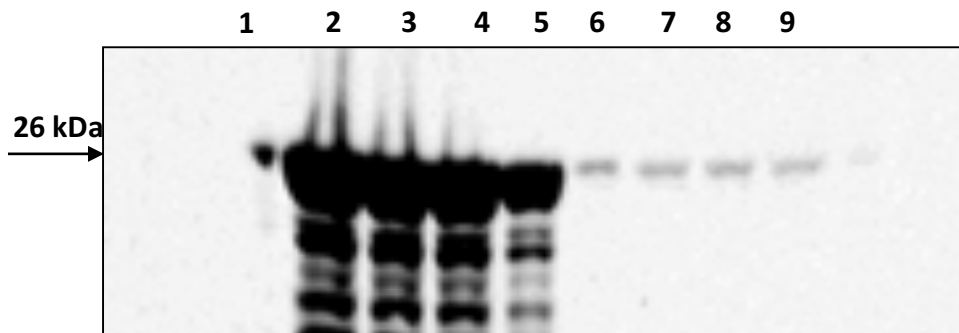


Figure 4.2: Western blot analysis to detect expression of ARH protein

A control experiment using GST-tagged ARH proteins induced by IPTG along with non-induced bacteria were grown at 37°C. Samples were loaded on the gel as follows, lane 1 contains marker, lanes 2-5 contain IPTG induced ARH protein, lanes 6-9 contain ARH protein fractions grown as a control, with no IPTG. Blot was incubated with anti-GST primary antibody.

Based on the experimental analysis from GST-ARH expression, it was decided to form new constructs of CEPDE3 isoforms using pGEX-6P1 GST-tag vector to aid recombinant protein expression and extract soluble proteins. CEPDE3 sequence analysis was confirmed and the pGEX-6P1 vector was considered suitable for further studies. The parameters of this study is discussed in detail in the following sections.

4.3.1: Expression of CEPDE3-SF and LF GST-tagged protein expression

Initially, protein expression experiments with constructs of CEPDE3-LF and SF proteins in pGEX-6P1 were carried out on a small scale to optimize culture growing conditions, and thus to determine favorable conditions for expression. Experiments were performed based on a screening optimization protocol (Handbook of GST Gene Fusion System, G.E. Healthcare) for GST-tagged proteins using Tris-HCl and PBS based buffers (refer to Chapter 2, section 2.6.3 for preparation of buffers). CEPDE3-LF cells were grown in a 5 ml culture at 37°C and induced by IPTG at 37°C, overnight. For cell-lysis, 1 ml pellets of short form and long form were lysed with Tris-HCl and PBS buffers to determine optimal conditions. Each of these pellets were lysed with 1 ml of plain PBS 1X, buffer 1 (PBS pH 6.2), buffer 2 (Tris-HCl pH 6.2), buffer 3 (PBS pH 7.4) and buffer 4 (Tris-HCl pH 7.4), with protease inhibitors. 100 µl of 1mg/ml lysozyme was added with 2% Triton X-100 to each of the pellets. Thereafter, pellets were sonicated with the pattern of 1 sec x 10 times in the interval of 3 cycles. Followed by sonication, all pellets were incubated at 37°C for 30 minutes. Lysed cells were further centrifuged at a maximum speed for 5 minutes at 4°C and fractionated into soluble supernatant and insoluble pellets, which were collected separately.

CEPDE3-LF soluble fractions were loaded on a SDS-PAGE gel in the amount of 15-20 µg and the insoluble fractions were loaded in the range of 5-10 µg. The CEPDE3-LF was detected using an

anti-GST primary antibody and anti-goat HRP secondary antibody (Fig 4.3). Experimental results suggested that using 1XPBS for protein cell-lysis was not optimal, in comparison to PBS or Tris-HCl based buffers in the range of pH 6.2 and pH 7.4. Therefore, PBS buffer pH 6.2 was considered optimum buffer for cell-lysis for further experiments in the CEPDE3 expression study.

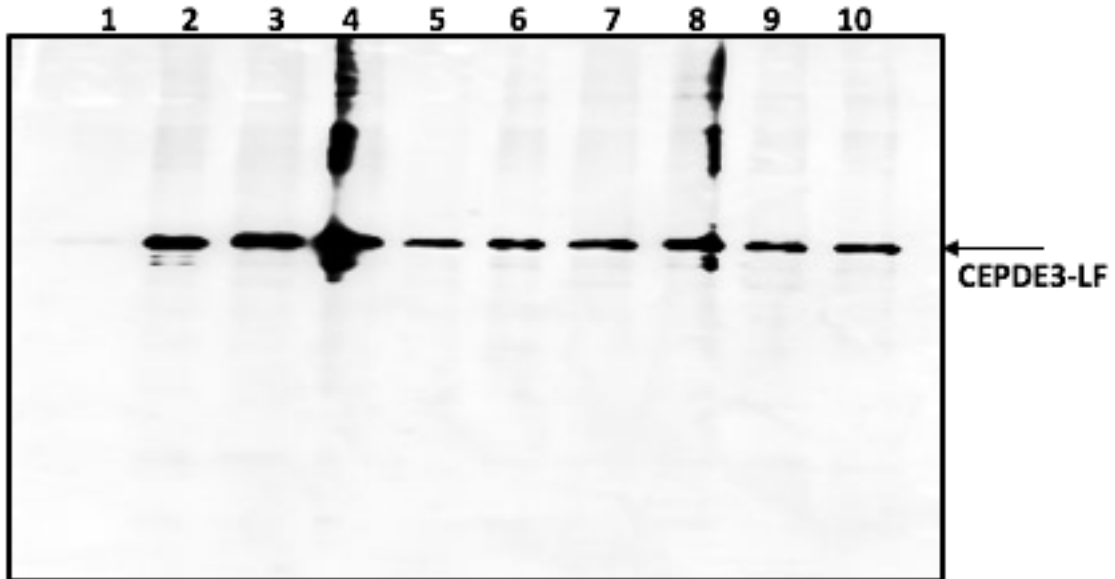


Figure 4.3: Western blot analysis for buffer optimization study

CEPDE3-LF protein cell-lysis fractions were lysed to optimize conditions using range of cell-lysis buffers. Lane 1 contains marker, lanes 2 and 3 contain soluble supernatant and insoluble cell-pellet fractions lysed with PBS. Lanes 4 and 5 contain supernatant and insoluble pellet lysed using PBS buffer pH 6.2. Lanes 5 and 6 contain supernatant and insoluble pellet lysed using Tris-HCl buffer pH 6.2. Lanes 7 and 8 contain supernatant and insoluble pellet lysed using PBS buffer pH 7.4. Lanes 9 and 10 contain supernatant and insoluble pellet fractions lysed using Tris-HCl buffer pH 7.4.

4.3.2: Specificity of antibodies for expressed GST-tagged SF and LF proteins

The Manganiello laboratory developed CEPDE3-SF and CEPDE3-LF specific polyclonal primary antibodies in rabbit for both the N and C terminus regions of the CEPDE3 isoforms, as well as a common antibody that recognizes both isoforms. To confirm specificity of each isoform, these antibodies were tested using protein expression studies. Total cell lysates of both GST-tagged CEPDE3-SF and CEPDE3-LF expressed in bacteria were loaded in duplicates on a SDS-PAGE gel in the amount of ~20 µg per well. Flag-tagged CEPDE3-SF (~4 µg) and Flag-tagged CEPDE3-LF (~2.5 µg) expressed in insect cells were loaded as controls. The Flag-tagged control samples were provided by Dr. Faiyazd Ahmad, a Staff Scientist at NHLBI-NIH.

As seen in Figure 4.4, SF and LF lysates were analysed by western blots that were incubated with anti-GST-tag antibody. Both CEPDE3 isoforms were detected by the anti-GST antibody and showed bands at the predicted sizes of ~ 90 kDa (CEPDE3-LF) and ~ 80 kDa (CEPDE3-SF). The lower molecular bands detected below the CEPDE3-LF samples at ~ 26 kDa are GST alone. To test the specificity of the CEPDE3-SF antibodies made by the lab, blots were also incubated with the CEPDE3-SF C-terminus antibody that detected only short form specific proteins at ~ 90 kDa (Fig. 4.5). Some protein degradation also appears with double bands that were observed at ~ 50 kDa. In addition, N terminus specific antibodies for CEPDE3-SF were tested (Fig. 4.6). The CEPDE3-SF N-terminus antibody was specific and detected only SF protein bands. However, there were lower molecular weight bands detected at 26 kDa in the lanes where CEPDE3-LF samples were loaded, which appeared to be GST bands.

To test the specificity of the CEPDE3-LF antibodies, a blot was incubated with CEPDE3-LF C-terminus antibodies (Fig. 4.7) which detected specific bands in lanes that contained CEPDE3-LF protein only. In addition, CEPDE3 proteins were incubated with N-terminus antibodies for CEPDE3-LF (Figure 4.8), which only detected the CEPDE3-LF proteins. Meanwhile, a common antibody to both isoforms, recognized both CEPDE3-SF (~ 84 kDa) and CEPDE3-LF (~ 90 kDa) proteins (Fig. 4.9). In addition, there were bands detected at ~ 40 kDa, below both CEPDE3 proteins, which may be degradation products detected by the common antibody. In summary, experimental data demonstrated that both CEPDE3 isoforms were detected as GST-tagged proteins by anti-GST antibody (Fig. 4.4), and each of the CEPDE3-SF and LF N- and C-terminus antibodies recognized their specific isoforms, while the common antibody detected both isoforms (Fig. 4.5-4.9).

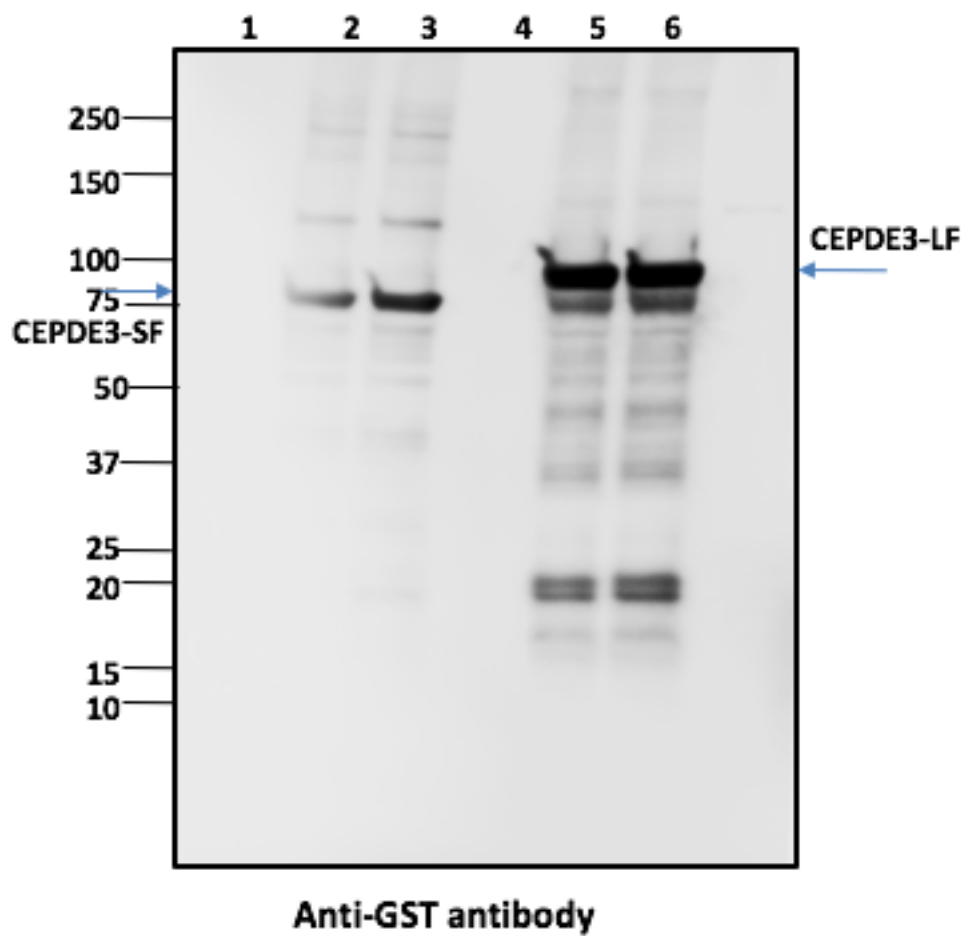


Figure 4.4: Detection of CEPDE3 proteins using anti-GST antibody

GST-tagged CEPDE3-SF and LF proteins expression lysates were loaded in duplicate. Lane 1 contains MW marker. Lanes 2-3 contain duplicates of SF cell-lysates. Lanes 5 and 6 contain CEPDE3-LF lysates. GST-tagged lysates were detected with anti-GST antibody.

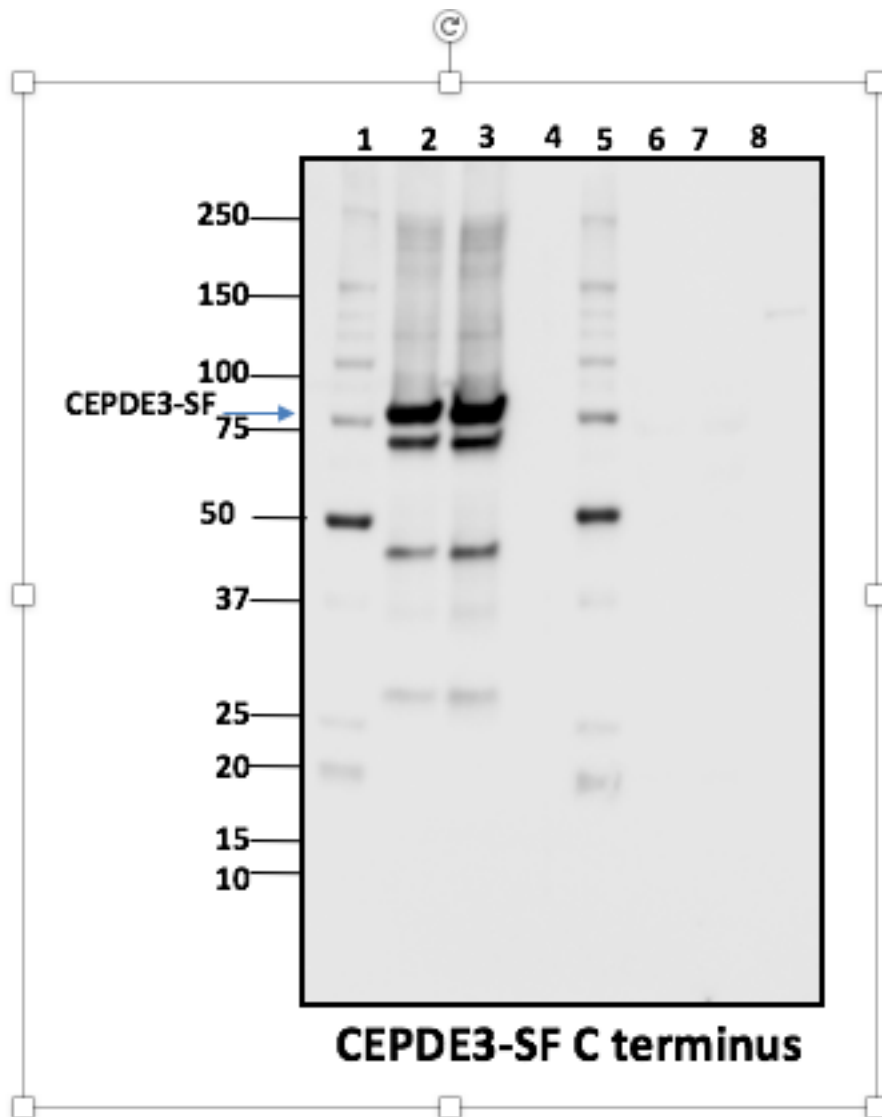


Figure 4.5: Western blot analysis to detect specificity of CEPDE3-SF C-terminus antibody

CEPDE3 protein expression fractions of *CEPDE3-SF* and *LF* isoforms were loaded to detect specificity of the short-form C-terminus antibody. Lanes 1 and 4 contain MW marker. Lanes 2 and 3 contain duplicates of *CEPDE3-SF* lysates, lane 5: *CEPDE3-SF* Flag-tag control, lanes 6 and 7: duplicates of *CEPDE3-LF* lysates, lane 8: *CEPDE3-LF* Flag-tag control.

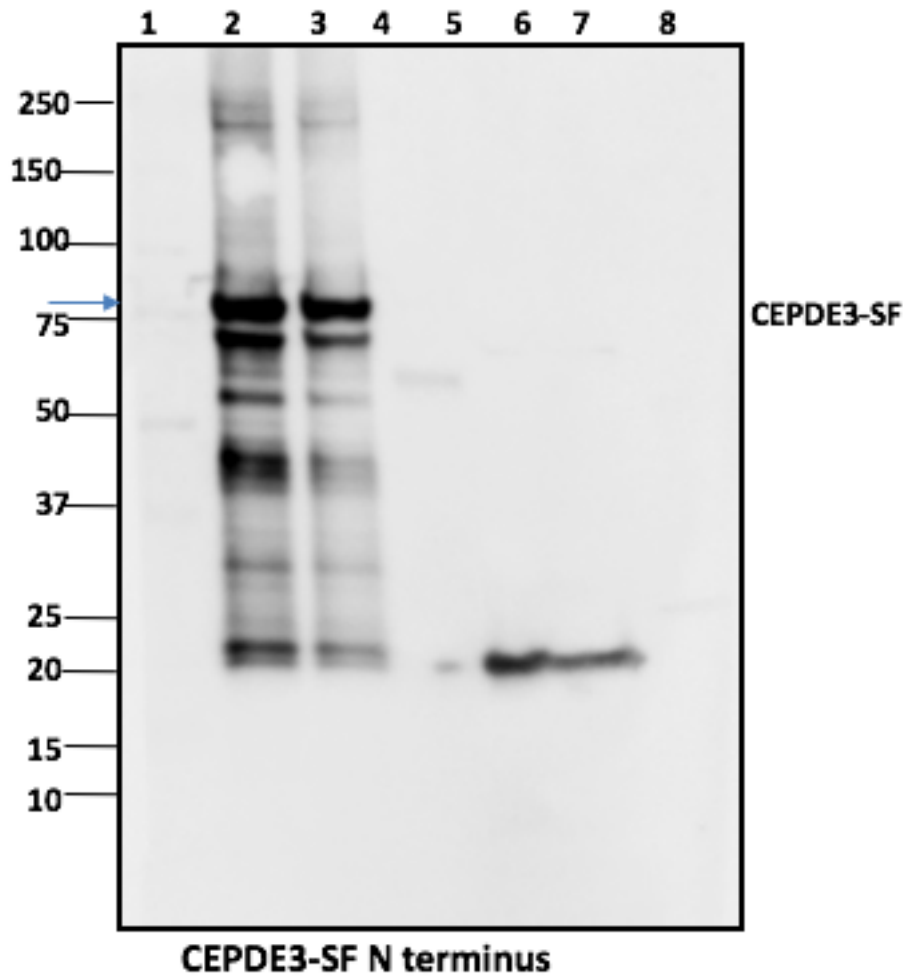


Figure 4.6: Western blot analysis to detect specificity of antibody with CEPDE3-SF N-terminus
Protein expression fractions of CEPDE3-SF and LF isoforms were loaded to detect specificity of CEPDE3-SF N-terminus antibody. Lanes 1 and 4 contain MW marker, lanes 2 and 3 contain duplicates of CEPDE3-SF lysates, lane 4: CEPDE3-SF, Flag-tag control, lanes 6 and 7: duplicates of CEPDE3-LF lysates, lane 8: CEPDE3-LF Flag-tag control.

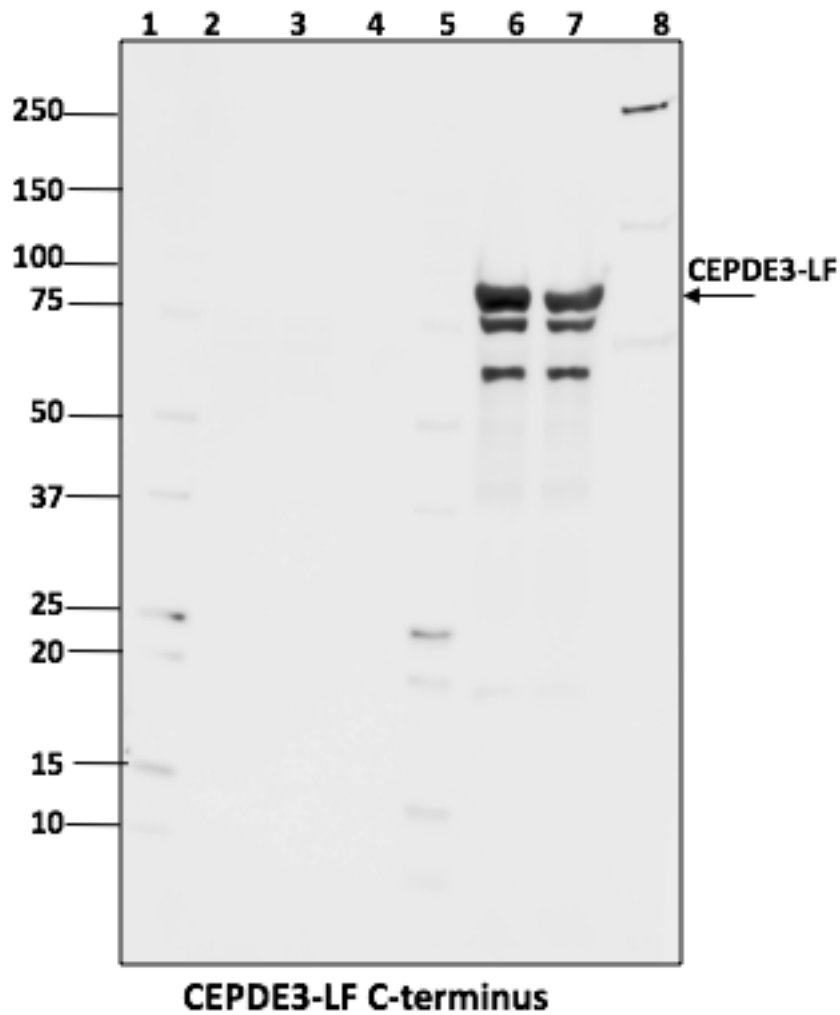


Figure 4.7: Western blot analysis to detect specificity of antibodies using CEPDE3-LF C-terminus antibody

CEPDE3 protein expression lysates of *CEPDE3-SF* and *LF* isoforms to detect specificity of *CEPDE3-LF* C-terminus antibody. *CEPDE3* proteins were loaded in duplicates, lane 1 contains MW marker. Lanes 2 and 3 contain duplicates of *CEPDE3-SF* lysates, lane 4: *CEPDE3-SF* Flag-tag control, lanes 6 and 7 contain duplicates of *CEPDE3-LF* lysates, lane 8: *CEPDE3-LF* Flag-tag control.

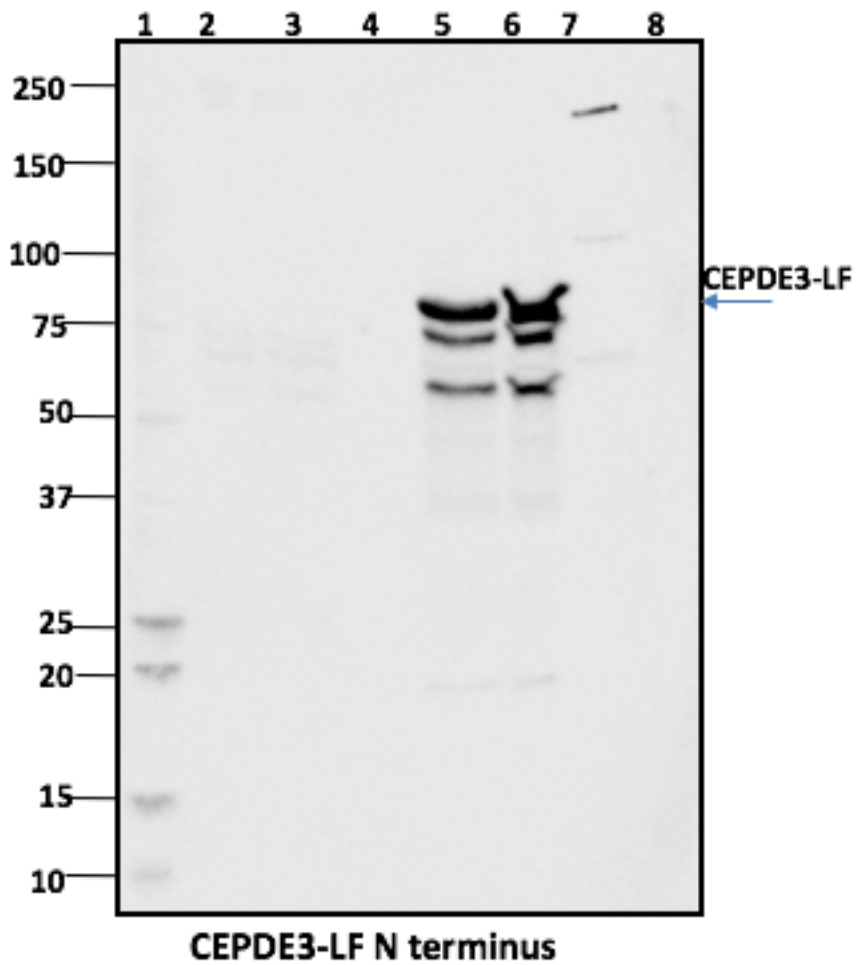


Figure 4.8: Western blot analysis to detect specificity of long-form N-terminus antibodies

CEPDE3 protein lysates fractions of SF and LF isoforms were loaded to detect specificity of CEPDE3-LF N-terminus antibody. CEPDE3 lysates were loaded in duplicates, lanes 1 and 4 contain MW marker. Lanes 2 and 3 contain duplicates of CEPDE3-SF lysates, lane 4: CEPDE3-SF Flag-tag control, lanes 6 and 7: duplicates of CEPDE3-LF lysates, lane 8: CEPDE3-LF, Flag-tag control.

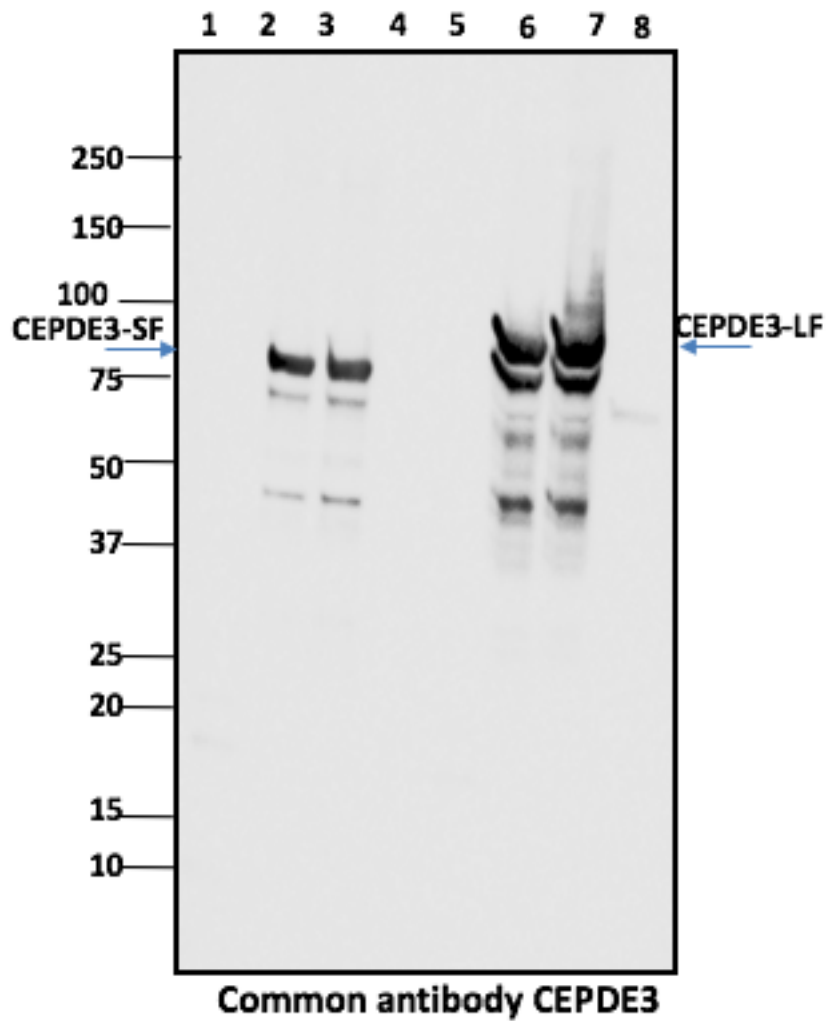


Figure 4.9: Western blot analysis to detect specificity of common antibody to both CEPDE3-SF and LF isoforms.

CEPDE3 protein expression lysates of CEPDE3-SF and LF isoforms were loaded to detect specificity of CEPDE3 common antibody. CEPDE3, lane 1 contains marker, lanes 2 and 3 contain duplicates of CEPDE3-SF lysates, lane 4: CEPDE3-SF Flag-tag control, lanes 6 and 7: duplicates CEPDE3-LF lysates, Lane 8: CEPDE3-LF Flag-tag control.

4.3.3: Optimizing culture conditions

Initial protein expression experiments of CEPDE3-LF GST tagged construct were performed on a small scale, growing overnight 50 ml cultures at 37°C induced by 1 mM IPTG. Cells were lysed using a French press at the speed of 19,000 PSI in the interval of two cycles (for a detailed protocol refer to Chapter 2, section 2.6.4). The CEPDE3-LF was detected using an antibody to the N-terminus of the CEPDE3-LF protein. As seen in Fig. 4.10, lane 2 contains the original cell-lysate derived from *E. coli* which was subjected to homogenization and fractionated into soluble and insoluble fractions. Lane 3 contains the soluble fraction with faint bands, lane 4 contains the insoluble fraction with dark bands. Lanes 2 and 3 also showed bands at 20-25 kDa, which are the bands for GST protein of ~ 26 kDa. Western blot data indicated that most of the protein still remained in the insoluble form as aggregates.

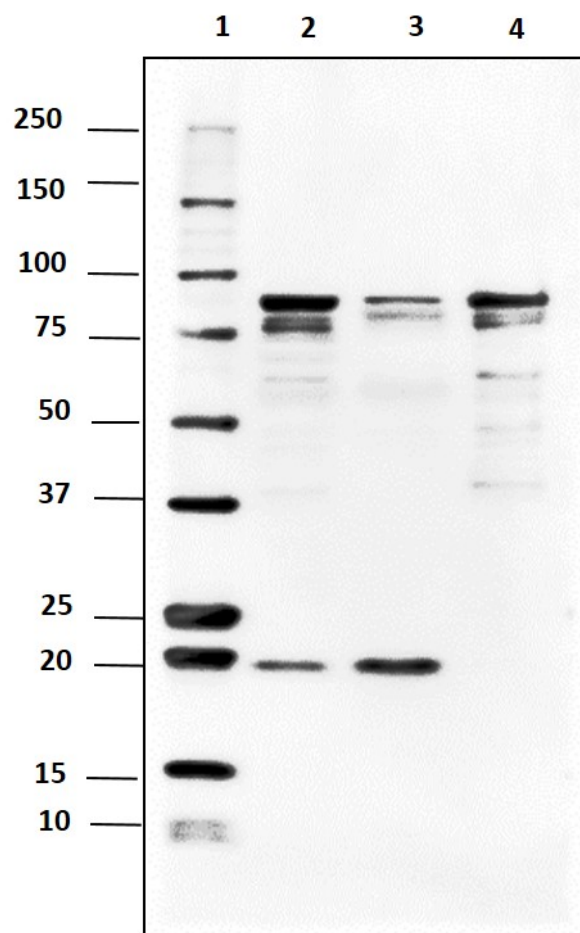


Figure 4.10: Western blot analysis of CEPDE3-LF protein expression

CEPDE3-LF protein expression at 37°C were lysed using a French press and isoforms detected using the long-form N-terminus specific antibody. Lane 1 contains marker, lane 2 contains total cell-lysate, lane 3 contains soluble supernatant, and lane 4 contains insoluble cell pellet.

CEPDE3 gene expression experiment was repeated, but instead of an overnight induction, the time was limited to 4 hours at 37°C. Protein was loaded in the range of 15-30 µg on two SDS PAGE gels for coomassie (Fig. 4.11A) and western blot (Fig. 4.11B). Both the gels included Flag-tagged CEPDE3-LF insect cell lysate as a control. However, the control shows three bands. The predicted size of CEPDE3-LF without a GST tag is ~ 63.5 kDa. Hence, the lowest band seen in the control sample in lane 6 is the true CEPDE3-LF band at ~ 63.5 kDa. Based on their size, the upper two bands may be dimers or other multimers of the Flag-tag control protein. Experimental data from the induction study demonstrated that once again, a significant amount of protein was observed in the insoluble fraction.

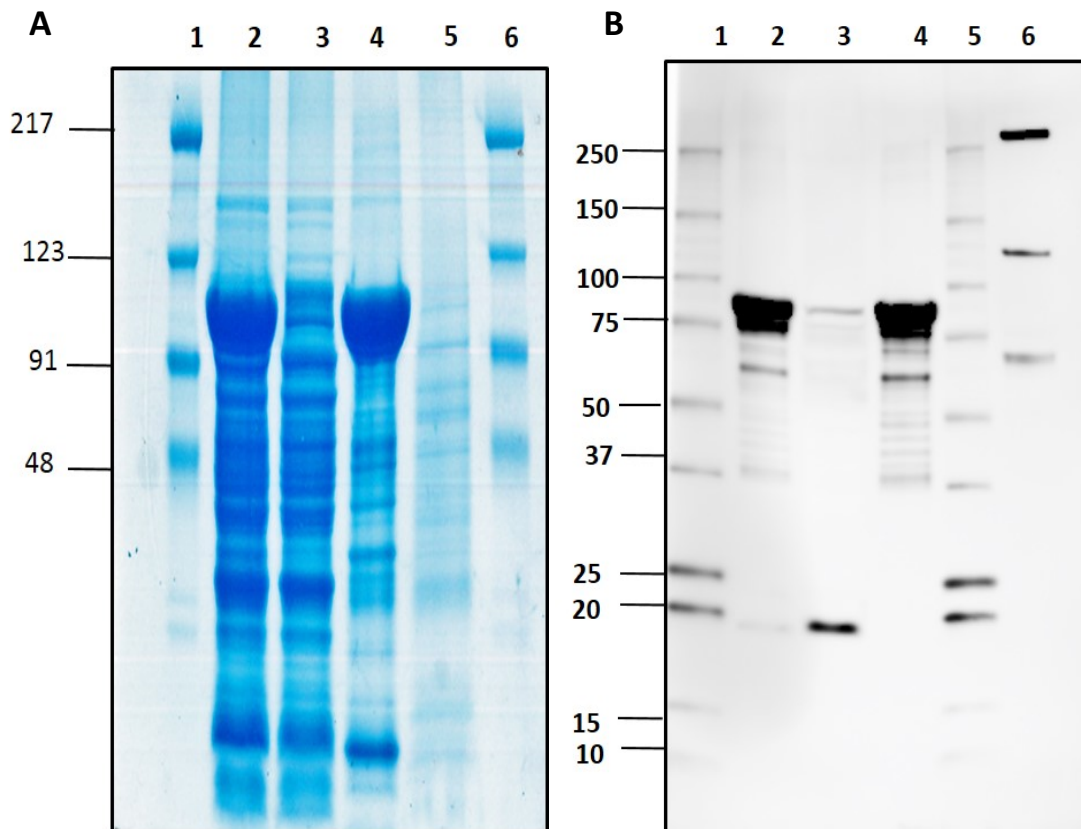


Figure 4.11: CEPDE3-LF protein expression at 37°C.

CEPDE3-LF isoform expression fractions induced at 37°C and analysed on two gels. Panel A, coomassie gel expression fractions loaded as follows: lanes 1 and 5 contain MW marker, lane 2 contains total lysate, lane 3 contains supernatant, and lane 4 contains insoluble cell-pellet, lane 5 contains LF Flag-tag control. Panel B, western blotting samples loaded in the following order, lanes 1 and 6 contain MW marker, lane 2 contains total lysate, lane 3 contains supernatant, and lane 4 contains insoluble cell-pellet, lane 5 contains LF Flag-tag expressed in insect cell as control

4.3.4: Effect of cold-shock therapy on CEPDE3-LF

CEPDE3-LF isoforms were grown overnight at 37°C as per the regular induction protocol described in the previous section (4.3.3). Bacterial culture was placed in the incubator with shaking at 37°C until cells reached OD 0.4. Thereafter, there were some changes made in the expression and induction protocol. At this point, the CEPDE3-LF culture flasks were transferred to 4°C in a cold room setting and placed on a rotating platform with gentle shaking. The shift in temperature from 37°C to 4°C enabled the cells to grow at a slow rate, in contrast to the rapid growth that occurred at 37°C, thus exposing the cells to a “cold shock”. OD was monitored at hour intervals. Thus, shifting the cells to 4°C was meant to prolong the incubation time at the cold temperature, so that the proteins had longer to fold correctly. After measuring the OD at regular intervals, it was observed that cells took at least 5-6 hours to reach an OD of ~ 0.5-0.6 in the cold room temperature. Thereafter, each flask was divided into two 250 ml cultures each. 1 mM IPTG was added to one of the flasks. An equal amount of plain LB medium was added to the other flask as a negative control. Both the culture flasks were incubated overnight at 25°C, with 225 rpm shaking. Following induction, cells were harvested the next day using the standard protocol and cell lysis was performed by French press (Chapter 2, section 2.6.4). All proteins were fractionated into insoluble and soluble fractions, obtained from each of the cell cultures, and were assayed for protein concentration, then analyzed by SDS-PAGE gel. Between 15-40 µg from all protein fractions was loaded on both gels and blots were incubated with antibodies (Fig. 4.12a) or stained with coomassie (Fig.4.12b). All the gels were loaded in the same pattern with the fraction induced with IPTG on the left and fractions of cells without IPTG on right. Lanes containing samples from induced proteins (lanes 2-4) showed large, distinct bands at ~ 90 kDa, the predicted size of CEPDE3-LF with a GST-tag, in comparison to the samples from lanes 5-7, which were uninduced samples with no IPTG induction. This experimental data indicated that CEPDE3-LF proteins were greatly induced by IPTG. In addition, due to the effect of cold-shock on CEPDE3-LF induction, a significant amount of protein was extracted in the soluble form.

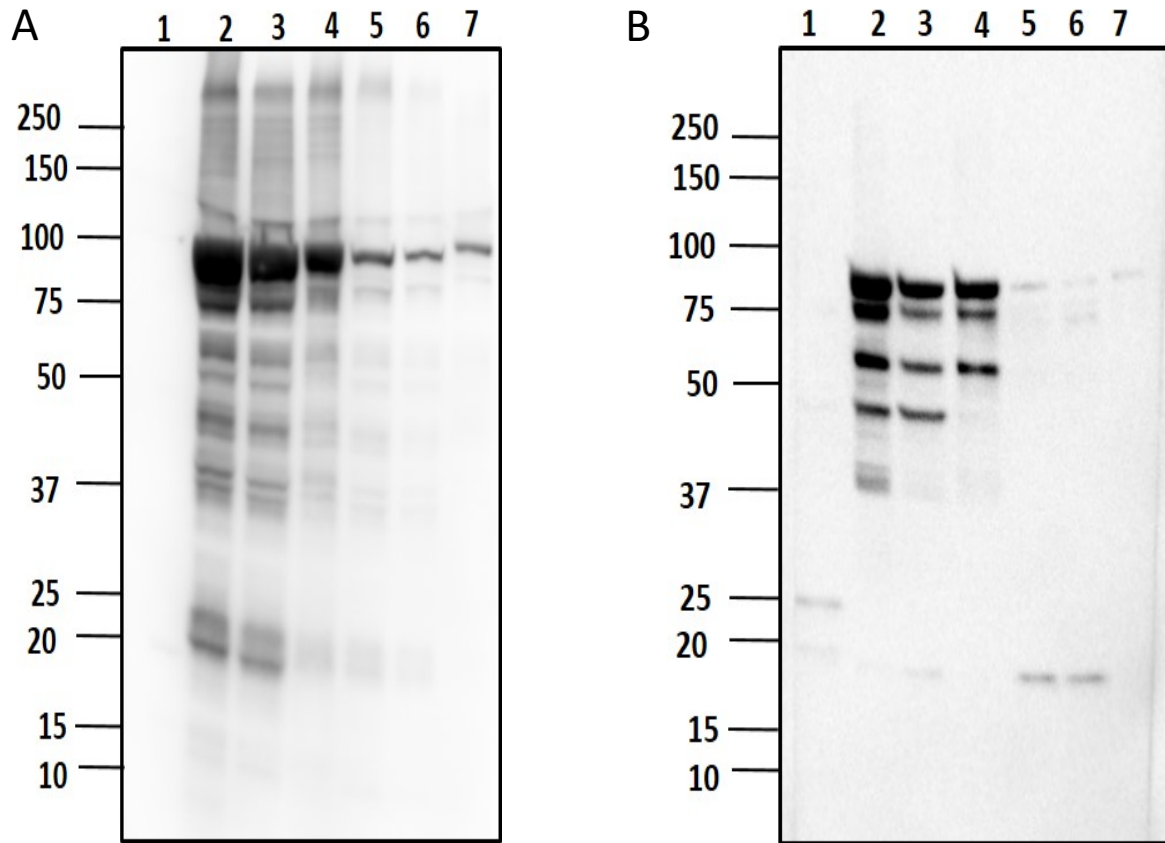


Figure 4.12a: Western blot analysis of lower temperature expression

CEPDE3-LF isoforms were expressed and induced at a lower temperature of 25°C. Protein fractions were loaded in the following order in both the blots, lane 1: marker, lane 2: total cell lysate, lane 3: soluble protein, lane 4: insoluble cell-pellet. Lanes 5-7 contain cell-lysate, supernatant and insoluble cell-pellet grown in the absence of IPTG. Blot A was incubated with anti-GST antibody and blot B was incubated with CEPDE3-LF N-terminus antibody.

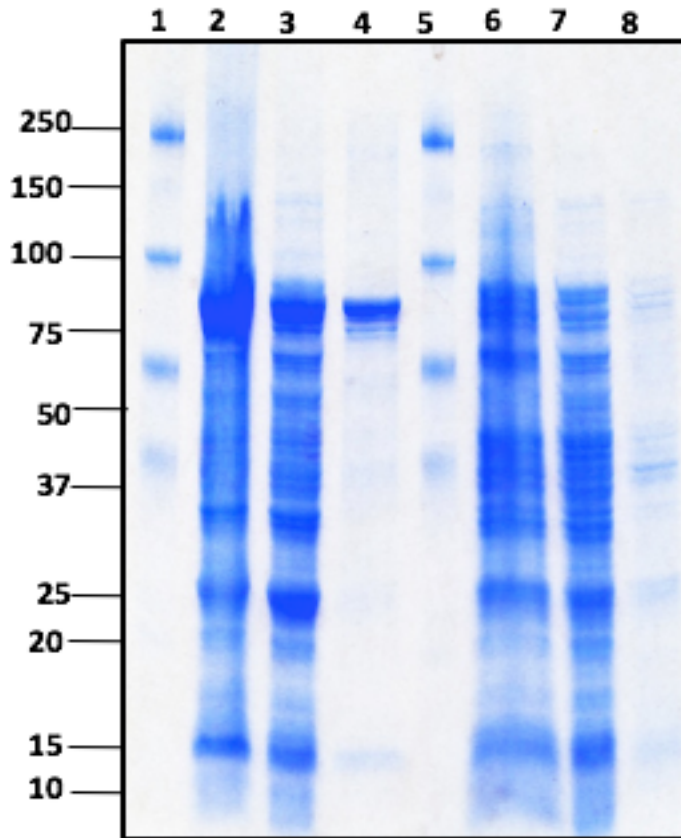


Figure 4.12b: Protein analysis at lower temperature

CEPDE3-LF isoforms were expressed and induced at lower temperature of 25°C. Protein fractions were loaded in the following order, lane 1: MW marker, lane 2: total cell lysate, lane 3: soluble protein, lane 4: insoluble cell-pellet. Lanes 6-8 contains cell-lysate, supernatant and insoluble cell-pellet grown in absence of IPTG.

Based on lower temperature induction, further optimization studies were carried out, using a range of IPTG concentrations and temperatures to induce CEPDE3 proteins. For comparison, a 100 ml culture was induced with 1 mM IPTG overnight at 37°C alongside two individual CEPDE3-LF cultures of 50 ml grown using the cold-shock therapy. Bacterial cells were grown at 37°C, with shaking at 225 rpm, until an OD of 0.4 was obtained. The two bacterial cell-culture flasks were taken out of the incubator and further placed in the cold room (4°C), with gentle shaking, until a > 0.5 OD. Cells in both flasks were induced with 0.5 mM or 1 mM IPTG concentrations, respectively, and subjected to lower temperature induction at 25°C overnight. Cell lysis was performed using the French press and PBS based buffer pH 6.2 was used. The total cell-lysate was fractionated into soluble and insoluble protein by centrifugation. Protein fractions obtained from individual culture was subjected to protein assay and further analyzed by western

immunoblotting. Cells induced at lower temperature, with 0.2 mM and 1 mM IPTG, showed an increase in protein expression and solubility. In contrast, protein fractions induced at 37°C also showed good expression. However, a significant amount of protein was also present in the insoluble form. Thus, experimental data demonstrated that a lower temperature with cold shock increased the protein solubility levels, as compared to induction carried out at 37°C.

Table 4.3: Effect of lower temperature on protein expression and solubility

CEPDE3 proteins were expressed and induced at a range of temperatures from 20, 25 and 37°C to determine the expression and solubility with proteins. The table summarizes the study of effects of time and range of temperatures on total % solubility in CEPDE3 proteins carried out using a range of temperatures with 8 hours and overnight induction.

Protein fractions	Culture conditions	Protein mg/ml	~% solubility
Lysate	1L-37°C-8h	3.8	
Supernatant soluble	1L-37°C-8h	1.4	45
Cell pellet insoluble	1L-37°C-8h	0.9	
Lysate	1L-25°C-ON	3.5	
Supernatant soluble	1L-25°C-ON	2.7	75
Cell pellet insoluble	1L-25°C-ON	0.5	
Lysate	1L-25°C-ON	3.7	
Supernatant Soluble	1L-25°C-ON	2.6	84
Cell pellet insoluble	1L-25°C-ON	0.6	
Lysate	1L-20°C-ON	3.2	
Supernatant soluble	1L-20°C-ON	2.9	81
Cell pellet soluble	1L-20°C-ON	0.8	

4.3.5: Large-scale protein expression in CEPDE3-LF

Following an optimization study for protein solubility, using cold-shock therapy with CEPDE3-LF at low temperature (in the range of 20 and 25°C) induction, further experiments were repeated to confirm if the results obtained were reproducible for protein solubility in the supernatant fraction. Accordingly, experiments were planned to scale up protein expression studies to produce large quantities of mg/ml protein. Based on the protocol used with small scale study, large scale culture studies were planned with the help of a facility within the Department of Biochemistry at NHLBI-NIH. A 5-liter culture was grown and induced at 20°C with 1 mM IPTG induction and the French-press was used for cell-lysis, similar to the method used in small-scale preparations. From the bacterial cell pellets obtained, ~ 30 grams of CEPDE3-LF cell pellets were resuspended in 150 ml of cell lysis buffer with protease inhibitor tablets. Approximately 200 ml of total cell lysate was obtained after cell lysis with the French-press method and further fractionated into soluble and insoluble fractions. All protein fractions were analyzed for protein concentration and western-immunoblotting. A 200 ml lysate was obtained and fractionated into 180 ml of soluble supernatant and the remaining insoluble cell pellet was resuspended in an equal amount of buffer to the soluble fraction. Fig. 4.13a shows western blot image of protein fractions incubated with anti-GST as primary antibody (panel A) and an anti-goat HRP as the secondary antibody. The fractions from lane 3 and 4 were samples from soluble and insoluble protein fractions. The soluble fraction showed distinct bands. There were also some bands of lower molecular weight seen in the soluble samples. GST bands appeared at ~26 kDa. Fig. 4.13b shows a western blot incubated with CEPDE3-LF N-terminus (panel B) and CEPDE3-LF-C terminus (panel C) isoform specific antibodies. A similar pattern of bands was seen in both of the blots incubated with N- and C-terminus antibodies, with bands of lower molecular weight from non-specific proteins or degradation detected in the cell-lysate and soluble fractions. Protein samples were loaded in the amount of ~ 15-25 µg in all three fractions. This experimental data determined that scaling up the protein expression produced reproducible data, with proteins recovered in the soluble fractions, when a large scale expression study was carried out.

A

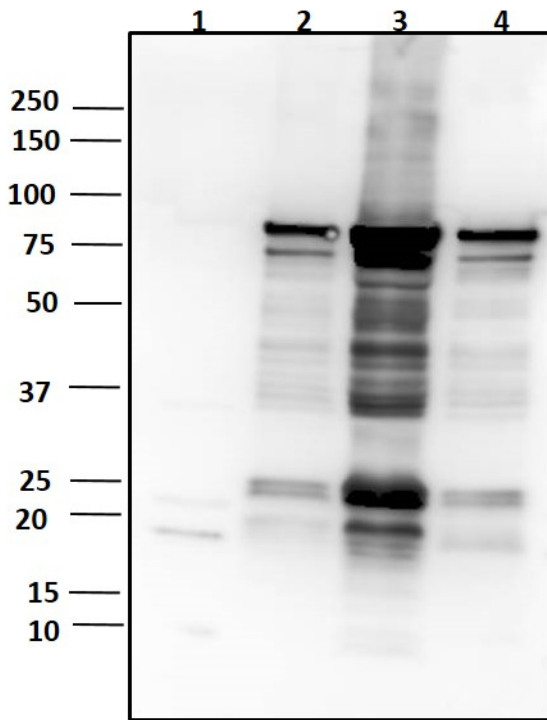


Figure 4.13a: Western blot analysis of CEPDE3-LF protein expression

Protein fractions were induced with a large scale culture of ~ 5 ml at 20°C using 1 mM IPTG overnight. Blot incubated with anti-GST primary antibody and anti-goat secondary antibody. Lane 1: contains MW marker, lane 2: total cell-lysate, lane 3: soluble supernatant, lane 4: insoluble cell-pellet.

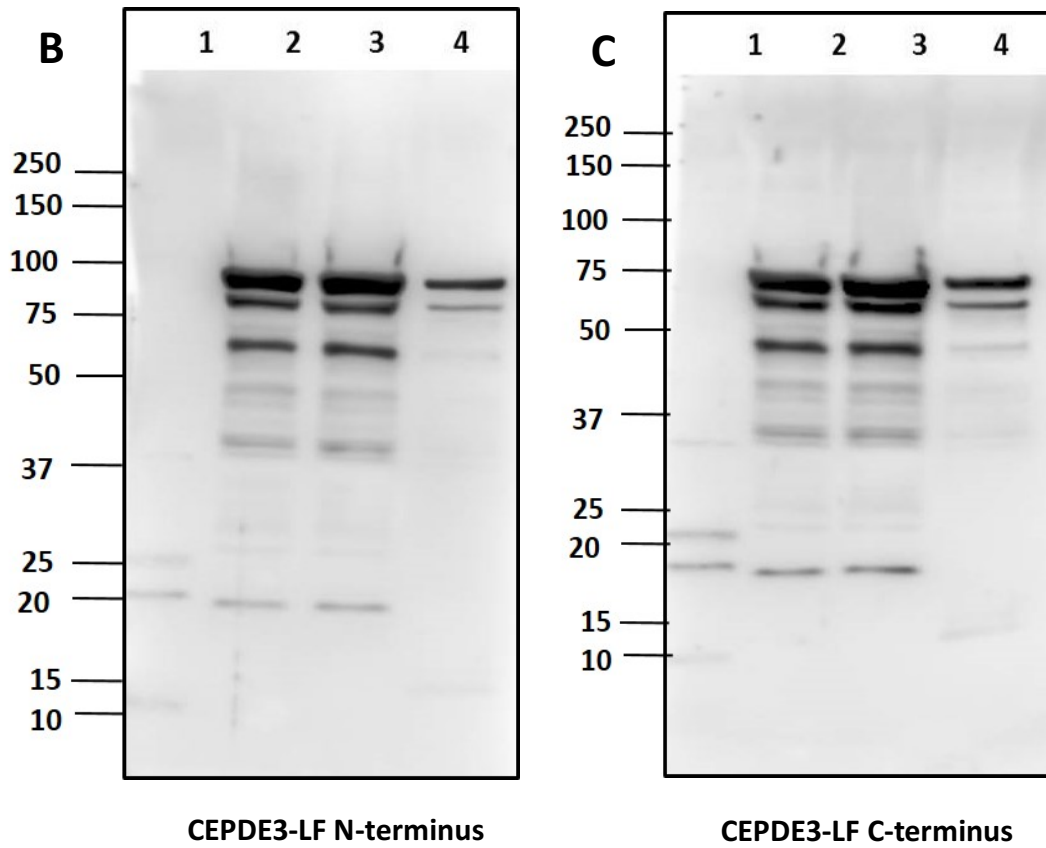


Figure 4.13b: Western blot analysis of CEPDE3-LF protein expression

Protein expression fractions induced with 1 mM IPTG overnight at 20°C were detected using CEPDE3-LF N- and C-terminus antibody. Protein fractions loaded on both gels as follows, lane 1 contains MW marker, lane 2 contains cell-lysate, lane 3 contains soluble supernatant, lane 4 contains cell-pellet. Blot in panel A incubated with CEPDE3-LF N-terminus antibody and blot in panel B incubated with CEPDE3-LF C-terminus antibody.

4.3.6: CEPDE3-SF expression

Initial CEPDE3-SF protein expression experiments were carried out using the same protocol designed for protein expression in CEPDE3-LF. The cold shock protocol of extended incubation time in the cold room (at 4° C) was applied and OD was monitored at regular intervals of 1 hour. The cultures were induced with 1 mM IPTG and further incubated at lower temperatures of 20 and 25°C. Cell harvesting and cell lysis steps were performed using the PBS pH 6.2 buffer for cell-lysis and homogenized using the French press equipment at 19,000 PSI. Protein fractions obtained from both cultures induced at 20 and 25°C were analyzed by SDS-PAGE. Protein fractions were loaded in the range of 8-12 µg. Fig. 4.14 shows the resulting western blot image for CEPDE3-SF expression at 20°C samples (lanes 2-4) and 25°C (lanes 6-8). Expression from both 20°C and 25°C induction showed a significant amount of protein in insoluble fractions (lanes 2, 4, 6 and 8) and soluble fractions (lanes 3 and 7). In addition, bands below ~ 90 kDa were present, which may due to some protein degradation. However, these bands do not appear to the same extend in the soluble fractions (as seen in lane 3 and 7). The CEPDE3-SF Flag-tag control expressed in insect cells was detected by a band at ~ 55 kDa, which is the predicted size for CEPDE3-SF protein without the GST-tag (lane 9).

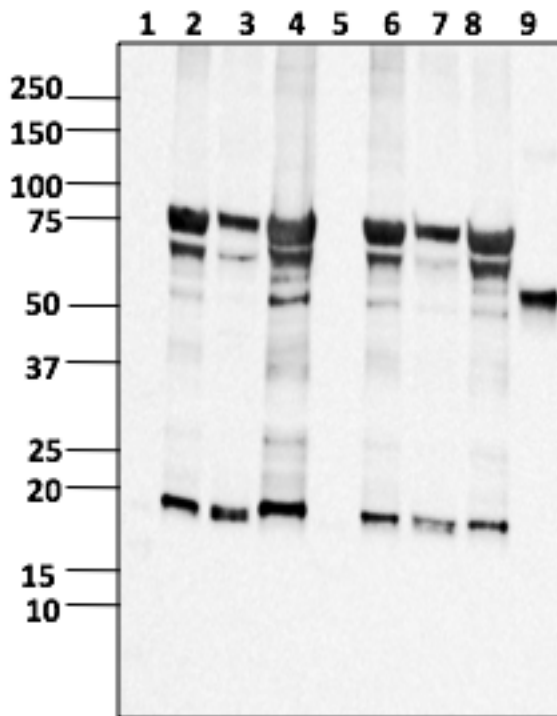


Figure 4.14: Western blot analysis from the CEPDE3-SF protein expression at 20°C and 25°C.

CEPDE3-SF protein fractions were induced at 20°C and 25°C. Protein expression fractions loaded as follows: Lane 1 and 5 contains marker, lanes 2-4 contain protein fractions from 20°C induction, lane 2: cell-lysate, lane3: soluble supernatant, lane 4: insoluble cell-pellet. Lanes 6-8 contain protein fractions from 25°C, lane 6: total cell-lysate, lane7: soluble supernatant, lane8: insoluble cell-pellet, and lane 9: CEPDE3-SF Flag-tag protein expressed in insect cells as a control. Blot was incubated using CEPDE3-SF N-terminus antibody.

4.3.7: CEPDE3-SF expression in comparison to CEPDE3-LF

Expression studies with CEPDE3-SF had low solubility, hence it was decided to analyse the pattern of expression and induction in both CEPDE3 isoforms, to assess solubility level of both isoforms at the same time. Hence the long-form (CEPDE3-LF) cells were grown at the same time and under the same conditions as CEPDE3-SF proteins. Both cultures were grown at 37°C until OD > 0.5. Thereafter, the CEPDE3-SF and LF culture flasks were transferred to cold room at 4°C, the extended incubation time in the cold room at 4°C was monitored at regular intervals of 1 hour. The CEPDE3-LF culture obtained an OD of ~ 0.5, in < 5 hours. However, the CEPDE3-SF cultures took a longer duration to obtain an OD of 0.5 at 4°C, ~ 8 hours. This difference in growth may be one of the factors that affected the previous experiment (section 4.3.6), where the solubility was low, as the required time for the SF cells to grow until OD of ~ 0.5 was > 5 hours.

Accordingly, in this experiment, the long-form culture was induced with 1 mM IPTG at the end of 5 hours and CEPDE3-SF culture was induced at the end of 8 hours. Flasks were transferred for overnight induction at 20°C. In addition, the induction time for the cultures was prolonged further for 1-2 hours (~16 hours in total). Cells were harvested and lysed using PBS buffer pH 6.2 and cell lysis performed using French Press. Cells were fractionated and centrifuged to form soluble and insoluble fractions. All protein fractions were loaded on gel for analysis, along with a Flag-tag control protein (see Fig. 4.15). Western blot was incubated with anti-GST antibody (with panel A) and incubated with CEPDE3-SF N-terminus antibody (panel B). Both blots had protein samples loaded in small amounts, ~15 µg in the cell-lysate and supernatant fractions. Panel B contains an additional lane with 5 µg CEPDE3-SF Flag-tag control (lane 5) for CEPDE3-SF protein expression. Experimental data demonstrated that the soluble fractions showed an increase in solubility, with most of the proteins expressed in a soluble form and very little protein detected in the insoluble form. Blots incubated with anti-GST antibody for short-form detected all fraction bands at the predicted size for CEPDE3-SF of ~ 75 kDa. By extending the incubation time and prolonging induction time, the CEPDE3-SF cultures showed a higher protein yield and recovered protein in the soluble form.

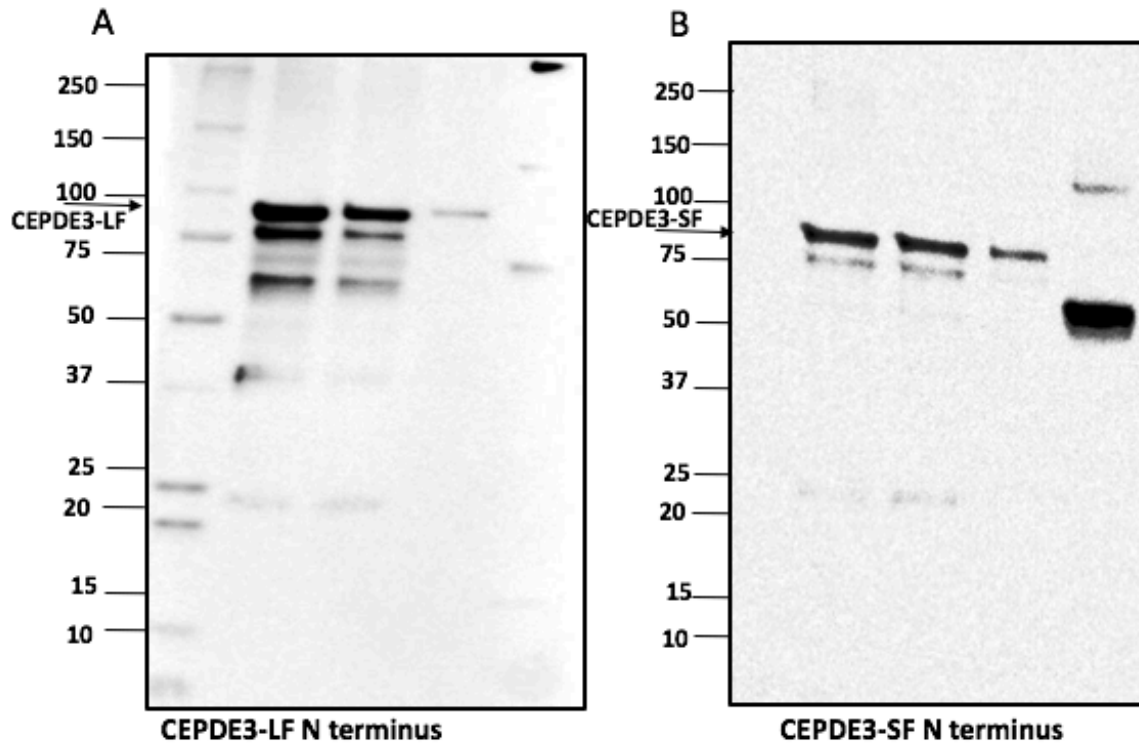


Figure 4.15: Protein expression of CEPDE3-LF and SF at 20°C

CEPDE3 LF and SF protein expression fractions induced at lower temperature. Panel A, CEPDE3-LF protein expression fractions, lane 1: MW marker, lane 2: cell lysate, lane3: soluble supernatant, lane 4: insoluble cell-pellet, lane 5: CEPDE3-LF, Flag-tag proteins expressed in insect cells loaded as control. CEPDE3-LF blot was incubated with CEPDE3-LF N-terminus antibody. Panel B, lane 1: MW marker, lane 2: cell lysate, lane3: soluble supernatant, lane 4: insoluble cell-pellet, lane 5: CEPDE3-SF, Flag-tag proteins expressed in insect cells loaded as control. CEPDE3-SF blot was incubated with CEPDE3-SF N-terminus antibody.

4.4: Discussion

4.4.1: Overview

Constructs of *CEPDE3* gene were redesigned from the existing Histidine-tag constructs in pET-21D vector to form GST-tagged constructs. These constructs were expressed as recombinant proteins to be further purified using the GST-fusion system. In this section, I will discuss the challenges in protein expression and several measures that were taken to overcome insolubility and expression issues with the CEPDE3 isoforms. There have been vast amount of resources and information available in the area of *E. coli* recombinant protein expression. Several strategies have been proposed for improving protein expression and solubility. Some of the common strategies are simple based on altering culture conditions to address challenges in protein expression studies. Depending on the amount and nature of proteins required, a careful screening study can help produce recombinant soluble proteins without the formation of aggregates (Sørensen and Mortensen, 2005; Harper and Speicher, 2011). The expression of CEPDE3 isoforms with His-tag had low yield and solubility. Purification techniques using immobilized affinity chromatography (IMAC) were attempted but resulted into low binding. Hence the GST-tag fusion system was considered as an alternative to express recombinant protein with higher yield and improved solubility for further studies to be carried out. Strategies based on altering culture conditions, including lower incubation and induction temperature (e.g. techniques of cold shock therapy), and modifications in cell-lysis methods, were used to establish optimal recombinant protein expression and solubility.

4.4.2: Background on CEPDE3 isoforms

Studies on CEPDE3 recombinant protein expression was carried out earlier using SF21 expression host system at the Manganiello laboratory by Samidurai et al. (2008-2011). The insect cell host mediates a high expression of recombinant protein, however, the insect cells have limitations due to higher cost, maintenance, and longer duration of time ~ 2 weeks for protein synthesis (Gecchele et al., 2015). In studies with CEPDE3 isoforms, these limitations were observed in terms of protein folding and limitations for producing a (mg/ml) quantity of protein required for crystallization. Hence, the use of *E. coli* was considered a more suitable alternative. In earlier *E. coli* expression with CEPDE3 isoforms, constructs of CEPDE3-SF and LF were subcloned into pET expression vector and expressed as His-tagged proteins. The goal was to express a large amount of protein in the host organism *E. coli*, and then purify it in a recombinant form to study the biochemical properties of PDE. His-tags have been reported to have high-level of protein expression (Costa et al., 2014) and are also considered to be efficient in protein solubility. However, the protein solubility may be dependent on the size of the protein (Tsunoda et al., 2005). Our CEPDE3 His-tag constructs had a low protein yield, poor solubility, and low enzyme activity. Indeed, others have also reported reduced solubility and increased level of aggregation with His-tag recombinant proteins (Majorek et al., 2014). Further attempts in improving protein expression and solubility based on parameters with temperature, cell-lysis, and induction were attempted. Using competent cells, like BL21-DE3 and Rosetta-gami, was one method tried to increase the expression level. However, our attempts to improve CEPDE3 protein expression levels with these strains failed.

Given the nature of proteins, proteins can behave differently when combined with fusion tags. (Esposito and Chatterjee, 2006). As discussed earlier in section 4.1.2.2, GST-protein expression experiments were carried out, and a test with ARH-GST protein expression study was performed to observe the GST expression. Based on the experimental analysis from the high induction of ARH-GST constructs, it was decided to form new gene constructs of the CEPDE3 isoforms using the pGEX-6P1 vector with the GST fusion partner located at the N-terminus. The pGEX series of vector from the glutathione S-transferase (GST) fusion is designed for high level inducible expression of a gene with the GST-tag. Initial protein expression results with GST-tagged proteins showed improved levels of expression, as compared to the old constructs with His-tagged proteins, but had limited protein solubility. As discussed previously in Chapter 3, sequence analysis of the old His-tag constructs of CEPDE3 isoforms showed that CEPDE3 inserts were modified to aid the His-tag protein expression. This modification may have been one possible reason the initial protein expression and solubility of the CEPDE3 constructs were not successful after they were initially subcloned into the pGEX-6P1 vector. Several optimizing studies were performed to overcome the challenges with protein solubility and are discussed in further detail in the following sections.

4.4.3: Common factors influencing protein solubility

4.4.3.1: Protein solubility

Protein expression levels showed a significant increase with CEPDE3 constructs in GST-tag vector as compared to the His-tag protein expression. Producing proteins in mg/ml with GST-tag constructs was efficient. It was critical to extract CEPDE3 proteins in soluble form, to purify them for further studies. However, a significant amount of proteins existed in aggregates in the form of inclusion bodies. Factors like growth temperature, concentration of inducer (IPTG), host strain, protein size and toxicity are some of the factors which may have an impact on the expression and or solubility of the protein. In addition, structural and catalytic properties of a protein are dependent on the amino acid sequence, which determines the protein's biochemical properties e.g. protein folding, stability of the protein, and hydrophobicity. Based on the literature, there are disadvantages to using GST as a solubility and affinity tag, as it depends on the protein oligomeric state. GST contains four solvent exposed cysteines, which can cause a significant amount of oxidative aggregation, making it a poor choice for tagging oligomeric target proteins (Harper and Speicher, 2008).

To establish efficient recombinant protein production, there has to be a well-suited correlation between the protein expression, protein solubility and purification of the proteins (Esposito and Chatterjee, 2006.). The initial protein expression study on CEPDE3 isoforms was designed on a small scale with proteins induced at 37° C, however a large amount of protein formed insoluble aggregates. There are several measures suggested for the extraction of proteins in soluble form, including changes in cell-lysis methods, addition of reagents to dissolve inclusion bodies, altering culture and growth conditions (e.g. lowering temperature for culture growth), lowering induction

temperature, optimizing IPTG concentration and using *E. coli* strains which favor protein expression (Kataeva et al., 2005).

4.4.3.2: Effect of temperature on protein expression

In the GST fusion system, the GST protein accumulates in the cytoplasm. In theory, due to the large size of the GST-tag, one can expect the solubility of the GST moiety would promote solubility to its fusion partner (Harper and Speicher, 2011). However, while performing experiments, it was not clear which proteins fractions will remain soluble and which ones will form aggregates as occlusion bodies. The recombinant heterologous protein expression can occur in different locations, such as the cytoplasm and the periplasm. Proteins occurring in cytoplasm may show a high yield, however they could be growing as insoluble aggregates. Hence, several studies support the idea that introducing optimal growth conditions with temperature and culture media changes can improve solubility (Khow & Suntrarachun, 2012; Ford et al., 1991).

4.4.3.2.1: Effect of cold shock on CEPDE3 solubility

Modifying the culture conditions, such as lowering temperature and optimizing induction times is a preferred option in comparison to extracting proteins using strong denaturants, which may cause extracted protein to unfold. Therefore, optimization studies were planned with a lowered temperature during incubation and induction times. Based on these parameters, modifications were made in the techniques of CEPDE3 protein overexpression, with an aim to increase the exposure of the cells to lower temperature. A shift in temperature from 37°C to 4°C at the beginning of the exponential phase may allow the growth rate to occur at a slow rate, thus enabling the protein to fold under stable conditions, unlike the growth at higher temperature. In addition, the shift from a higher temperature to a considerably lower temperature, such as ~ 10°C, is known to induce bacterial cold shock proteins (CSPs) in *E. coli*. These proteins are essential for the bacteria to continue its growth during the shift of temperatures (Ferrer et al., 2003). Cold shock proteins are also known to be involved in translation and are homogeneous with other prokaryotic organisms. They have identical sequences and share a common domain with the eukaryotic Y-box proteins, that play a role in activating transcription in cells (Jones and Inouye, 1994). Furthermore, lower temperature growth leads to an increased number of chaperones in *E. coli*. and, simultaneously, reduces protein degradation (Khow and Suntrarachun, 2012). Finally, a shift in temperature may result in increased membrane insertion, and in turn, may increase the number of chaperones associated with the CEPDE3 isoforms (Gordon et al., 2008; Chen et al., 2003).

In theory, increased levels of chaperones are important in the production of protein at lower temperatures (Qing et al., 2004, Ferrer et al., 2003). As discussed above, lower temperature induction may induce Csp proteins that enhance translation. The reduction in temperature may also be helpful to slow the rate of protein production, which could relieve the some of the metabolic burden on the cell-machinery. In addition, an increase in growth time at lower temperature can be helpful in recovering solubility (Hammarström et al., 2002; Harper and

Speicher, 2011; Dormiani et al., 2007). Thus, a common approach in improving recombinant protein expression and solubility in *E. coli* generally involves optimizing culture conditions and lowering temperature.

4.4.3.2.2: Effect of IPTG on protein expression

IPTG induces gene expression by binding to the *lac* repressor, causing its removal from the *lac* operon and activating the T7 promoter in the pGEX vector. For the expression of certain proteins, it may be important to slowly induce the promoter with a low concentration of IPTG, while with others a high concentration of IPTG may be required for transcription of the expression plasmid to occur (Sadeghi et al., 2011). Control studies carried out in absence of IPTG showed very little induction, therefore the CEPDE3 isoforms were induced with 1 mM IPTG. In addition, induction was carried out both at 37°C and 25°C. In comparison to induction at 37°C, 25°C induction improved protein solubility (refer to Table 4.3). The induction carried out at 37°C showed a solubility of 58%, while the inductions carried out at 25°C resulted in > 80-90% solubility. Thus, IPTG induction of the cells at low temperatures increased the expression of proteins in the soluble form.

4.4.4: Summary

Experimental data with CEPDE3 long and short form protein expression demonstrated that CEPDE3 proteins expressed as GST-tagged proteins were detected by anti-GST antibody, as well as the CEPDE3 N- and C-terminus isoform specific antibodies. Each isoform was only detected by its respective antibodies and the common antibody recognized both isoforms. Hence, it is reported that there was no cross-reactivity between the antibodies for the different isoforms. The principle objective of this study was to set a standard for overexpression of soluble GST-tagged CEPDE3 isoforms in *E. coli*. Based on the objective, the incubation of bacterial culture in the cold room, implementing 'cold-shock' therapy had a significant impact on recovering the soluble form of the protein. The optimal growth temperature for IPTG induction in CEPDE3 isoforms in *E. coli* was 25°C and the optimum IPTG concentration was determined to be 1 mM, with an overnight induction time. It was also observed that there was a good correlation between the small and large scale expression studies for both isoforms, in such a manner that both could be produced in milligram quantities. The experimental data was reproducible and could be performed in a range from 50 ml culture up to 1-liter culture and higher. Most importantly, this study identified the optimal induction time and temperature necessary for the CEPDE3 isoforms to be overexpressed as GST-tagged recombinant proteins in a soluble form.

Chapter 5

Chapter 5: Protein purification for *C. elegans* PDE3 isoforms

5.1: Introduction

5.1.1: Chromatography techniques

Chromatography is a quantitative analytical process by which compounds are separated from one another by selectively binding molecules and compounds to various matrices, separation occurs under the influence of a mobile phase over a stationary phase. Recombinant proteins are overexpressed and subsequently purified to determine the biochemical properties of a given protein. A strong purification system, such as chromatography, is essential to carry out purification of the recombinant proteins. In a standard chromatography, substances, like protein lysate, dissolved in a liquid or mobile phase containing a mixture of proteins are passed through a stationary phase containing specialized molecules. The medium of the stationary phase is selected by its nature and capacity to purify the desired substances from the other impurities and contaminants present in the mobile phase (Walls and Loughran, 2011).



Figure 5.1: Diagrammatic representation of general chromatography

Analyte is a protein mixture applied to a column to separate and analyze its individual components. The column consists of the matrix; it is the stationary phase or adsorbent that stays fixed inside the column. The separation of the various components of the analyte is based on their differential affinities to the stationary and mobile phase and results in differential separation of the components. The higher the adsorption to the stationary phase, the more slowly the molecule passes through the column. Molecules with higher solubility in the mobile phase will move faster through the column. Bound components are released using an appropriate solvent as purified components and are collected in the form of eluate.

5.1.2: Types of Chromatography

There are different chromatography methods based on chromatography techniques, including affinity chromatography, ion exchange chromatography and hydrophobic interaction chromatography, which are based on the binding and eluting principle. Each of these techniques requires specific elution conditions. Size exclusion chromatography is based on diffusion, it does not require any specific elution conditions, and molecules are separated based on their size.

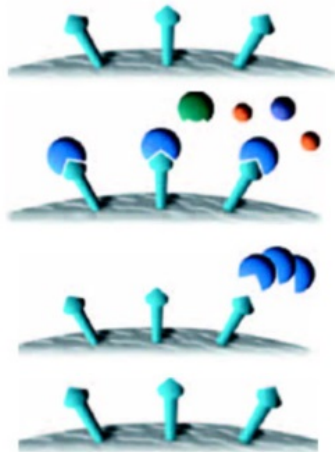
Ion exchange (IEX) chromatography is commonly used in purification of biological materials. It is based on two types of exchanges; cations and anions. In cation exchange, the stationary phase (or matrix) contains a negative charge, whereas in anion exchange the resin contains a positive charge. This principle works very specifically with the charge and pH of buffers. When a charged protein mixture is passed through the stationary phase, it passes through the resin and will not

elute from the column until elution (salt) buffer of a certain ionic strength and pH is passed through the column, which favors its elution. Hence, this method of separation is very selective, as it requires a careful determination of the pH required for all buffers used in the incubation and elution step with accurate pH.

5.1.3: Affinity Chromatography

Affinity chromatography is one of the most commonly used techniques in chromatography for purification of a specific molecule or a complex mixture containing a group of molecules. This technique enables rapid protein purification on the basis of biological function and protein structure. The aim of affinity chromatography is to recover the target solute from a complex mixture of molecules in a single step elution (Ling et al., 2014). In this technique, proteins are separated based on a reversible interaction between a protein and a specific ligand, which is coupled to a chromatography matrix. Affinity chromatography method applies selective purification for a molecule from a mixture of complex proteins, with a specific biological interaction between two molecules. This is a reversible process that occurs through a biphasic interaction with one of the molecules (the ligand), which is usually attached to a stationary gel matrix, whereas the other molecule (target protein) is in a mobile phase with a heterogeneous group of molecules (e.g. protein mixture in a soluble form or cell-lysate). Thus, helps purify proteins in a fast, single step, and the technique can be applied to purifying large scales of protein, from a hundred to thousand-fold times. Usually the starting material used is a supernatant mixture derived from cell lysate (Harper and Speicher, 2008). The stationary phase can then be removed from the mixture. The final process to achieve purified protein involves several washing steps and elution, which results in recovery of highly purified protein depending on the efficacy of the technique and nature of protein (Mercado-Pimentel et al., 2002).

Key stages in an affinity purification:



1. Affinity medium is equilibrated in binding buffer
2. Adsorption of target and elution of unbound material
3. Elute bound target(s) by changing conditions
4. Re-equilibration

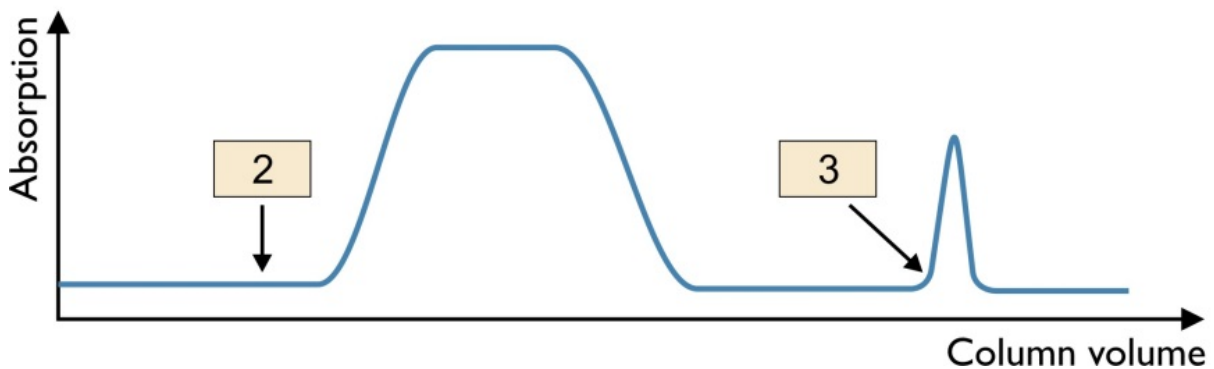


Figure 5.2: Overview of the workflow in an affinity chromatography process through different phases

In an affinity chromatography process, the molecules in the sample with a matching binding site can bind to the specific ligand molecules bound to the matrix. Other non-specific molecules are washed off. By altering the composition of the liquid phase, the protein of interest can be isolated as pure protein. The lower graph shows the phases in elution (Image reference: www.gelifesciences.com).

In addition, the affinity chromatography technique for the selection of ligand is based on few criterias: 1) the ability to retain binding affinity for the specific protein of interest and 2) the unbound material comes out through wash. Thus, the binding between the ligand and target molecule must be reversible, in order to allow the target molecules to be detached from the ligand in its active form. An example of a standard biological interactions used commonly in affinity chromatography is that of an enzyme and a substrate. The most common use of affinity chromatography is purifying recombinant proteins. This technique has high affinity for the protein of interest and, hence, offers high selectivity for protein purification (Urh et al., 2009).

Batch and column steps

Column chromatography is the main method used for solid phase binding involved in purification. The matrix is packed onto a column and the starting material is passed through the column for the initial binding phase, binds to the column matrix, washed with a wash buffer, eluted with an elution buffer applied to the column, and collected as an eluate. These steps are carried out under ambient pressure conditions. Alternatively, a batch method of purification can be utilized, in which the starting material is added to the solid phase in a separate Eppendorf tube, mixing and removing the liquid phase by centrifuging, collecting the flow-through, washing several times and centrifuging, then adding elution buffer and re-centrifuging to isolate the eluate.

5.1.3.1: Effect of affinity tags on protein purification

Fusion proteins, peptide sequences, and affinity tags have become highly desirable tools for purifying recombinant proteins using affinity chromatography. The affinity tags have several benefits to facilitate the purification of the target proteins, and make recombinant proteins easy to detect (Terpe, 2003; Waugh, 2011). They allow high throughput analysis in purification studies. Genetically designed fusion tags can be introduced to proteins to facilitate protein purification. It is also recommended, in theory, to introduce one or two different tags, as every tag comes with a different function (Waugh, 2005). In addition to making purification feasible, affinity tags can increase solubility and or enhance protein expression. However, tags are not restricted with these functions, they have been known to enhance the structural and functional properties of a protein, e.g. post translational modifications. The location of the tags can also have an impact on protein folding or expression. N-terminus tags are known to have a high impact on the protein expression and enhance solubility (Hartz et al., 1991). Fusion tags placed at the N-terminus are effective, provided the mRNA can still initiate the translation process. There can be problems, where the secondary structures in mRNA interferes with the ribosome binding (Hartz et al., 1991). Sometimes, sequence determinants located at the N- or C-terminus regions can also play a role with degradation of protein, hence introducing the fusion tags can prevent degradation of recombinant protein, although no clear mechanism has been shown (Flynn et al., 2003). As discussed earlier in Chapter 4, *E. coli* protein expression has challenges with protein insoluble aggregates. Commonly used affinity tags include hexahistidine tags which bind to immobilized metal ion (for example, Zn^{2+} or Ni^{2+}). In the Glutathione S-transferase system, the GST fusion protein binds to glutathione sepharose resin (Smith et al., 1995). Affinity tags can affect protein solubility and some tags have been engineered as solubility enhancing tags, however the underlying mechanism is not clear.

The GST fusion system is based on three major components, the pGEX series of plasmid vectors, the components involved in purification of GST proteins for chromatography, and, finally, the site-specific proteases designed for cleavage of the GST moiety (GST fusion protein purification handbook). As discussed earlier, the concept of GST-tagged proteins is based on the affinity of GST to the glutathione ligand coupled to a matrix. However, since this binding is reversible and the GST proteins can be eluted, this mechanism does not alter the nature and structure of the desired protein. In addition, elution of these recombinant proteins does not involve complex

procedures; they can be eluted using mild elution techniques, such as salts and buffers (Lichty et al., 2005). or with cleavage of tags, the technique utilized in this thesis.

5.2: Aims

This chapter aims:

- To purify GST-tagged CEPDE3 proteins, CEPDE3-LF (long-form), CEPDE3-SF (short-form) based on affinity chromatography, using the GST fusion system (glutathione sepharose 4b)
- Enzymatic cleavage of the GST-tag using site-specific protease (PreScission protease)

5.3: Results

5.3.1: Purification of CEPDE3 LF and SF

Purification experiments with CEPDE3 proteins were designed initially on a small scale for CEPDE3-LF using a culture volume (0.5-1 ml) with GST-spin trap columns to screen optimum conditions. Further experiments were planned, increasing the culture volume to ~ 10 ml, and using the batch method with glutathione sepharose 4B resins to screen for optimal purification conditions. Enzymatic cleavage with the enzyme PreScission Protease was performed to remove the GST-tag. The flow-chart below explains the purification strategy applied for the outcome of purified CEPDE3-LF and SF proteins.

5.3.2: Experimental outcome for CEPDE3 LF and SF protein purification

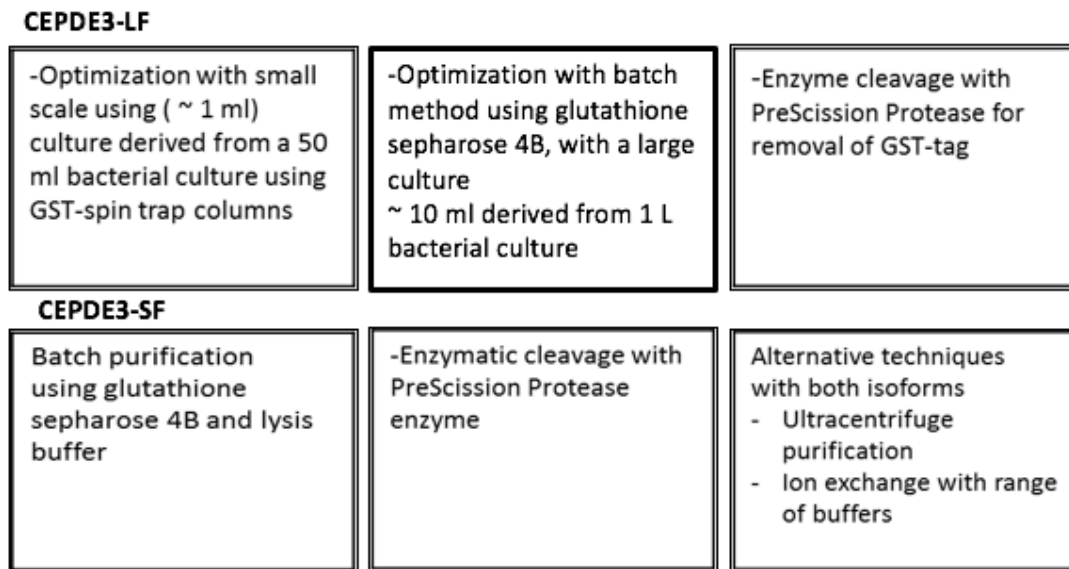


Figure 5.3: Chart of the purification study representing the experimental outcome

The various stages in a protein purification study with CEPDE3 isoforms carried out using small and large scale culture volumes to screen optimizing conditions and using alternative purification techniques with an aim to increase protein yield and purity.

5.3.3: CEPDE3-LF purification

5.3.3.1: CEPDE3-LF purification with GST-spin trap columns

Initial purification for long-form protein was designed based with a small volume ~ 600 µl and using a PBS buffer pH 6.2 and Tris-HCl buffer pH 6.2 in two individual tubes to compare purification (refer to Chapter 2, materials and methods section 2.7.1). Protein mixture was passed several times through the column.

Elution of beads with sample buffer: Proteins were eluted using elution buffer containing 10 mM reduced glutathione. All fractions were analyzed to determine the amount of protein purified. A small aliquot of the beads was taken out from the GST-spin trap column slurry and applied to equal amount of sample buffer to detect the protein present on the glutathione beads.

Results: The eluted samples in lane 5 and 13 (circled) were proteins eluted with glutathione in PBS and Tris-HCl buffers, respectively (Fig. 5.4). The bands from beads fractions post elution as seen in lane 7 and lane 15 showed dark distinct bands, which indicated elution was not efficient enough to elute all the proteins from the beads, a significant amount of protein was present in

the beads. Using anti-GST antibody, the eluted CEPDE3-LF showed bands above 75 kDa, the predicted size of GST-tagged CEPDE3-LF.

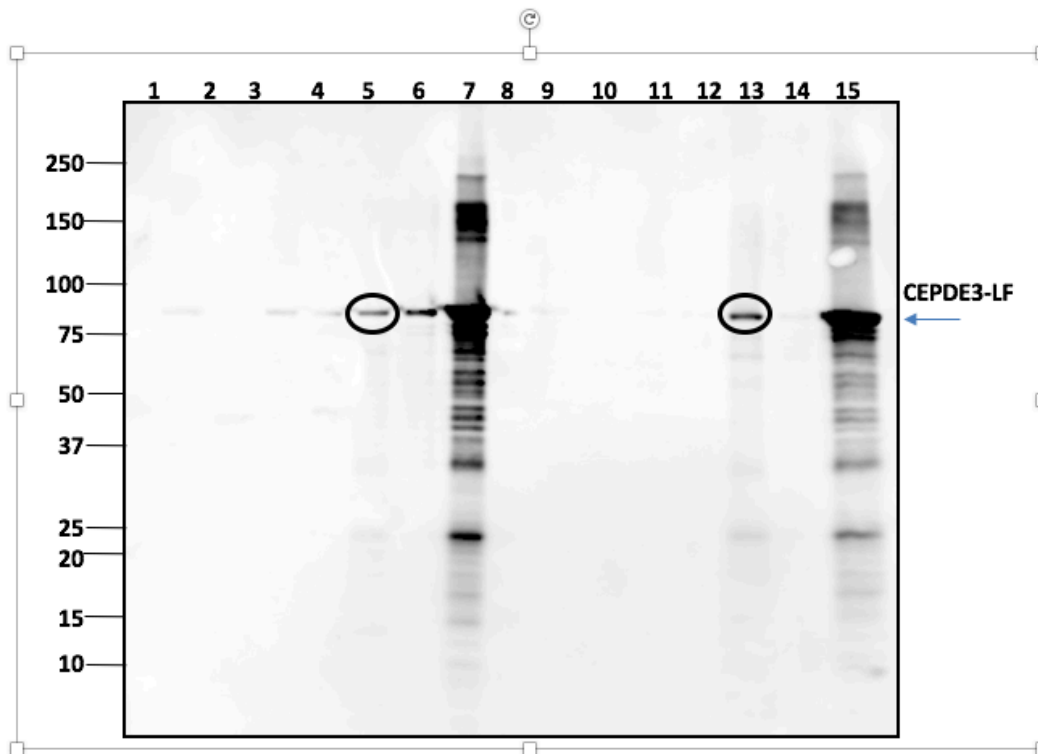


Figure 5.4: Western blot analysis of GST-spin traps purification with CEPDE3-LF proteins

CEPDE3-LF soluble supernatant were purified on a small scale using the GST-spin trap columns. Protein purification fractions were loaded on a gel to detect by western immunoblotting. On the left, lanes 1-7 are purification fraction samples, purified using buffer 1 (PBS pH 6.2), lane 1: supernatant, lane 2: wash 1, lane 3: flow-through lane 4: wash 2, Lane 5: eluate, lane 6: wash 3, lane 7: beads post elution, lane 8: MW marker. Lanes 9-15 are samples purified using Tris-HCl buffer. Lane 9: soluble supernatant, lane 10: wash1, lane 11: flow-through samples, lane 12: wash 2, lane 13: eluate, lane 14: wash 3, and lane 15: beads after elution. Eluate bands are indicated by circle in both buffer samples.

Experimental data from Fig. 5.4 demonstrated that using PBS and Tris-HCl based buffers detected proteins at the predicted size of long-form, however, elution using elution buffer containing 20 mM reduced glutathione was not effective as protein remained bound to the beads, hence further optimization in the protocol to establish efficient purification was essential.

5.3.3.2: CEPDE3-LF purification using batch method derived from GST-spin trap columns

Based on experimental analysis described in section, 5.3.3.1, further attempts were made to improve purification using GST-spin trap. It was decided to use a batch method of purification using the spin column with CEPDE3-LF proteins. Accordingly, two changes were made in the protocol. 1) Beads were taken out from a GST-spin trap column and transferred into a microcentrifuge tube subjected to wash and equilibration to prepare a 50% slurry. 2) Glutathione beads were incubated with the protein mixture for 3-4 hours with gentle shaking at 4°C, to increase the contact time of proteins with beads (for detailed protocol, refer to Chapter 2, section 2.7.2). Resultant western blot of the purification fractions is seen in Fig. 5.5. This method of batch purification did not help, as protein came out with flow-through and did not bind to the beads. Hence, increasing the incubation time did not produce desired results and thus further optimization was required for successful purification.

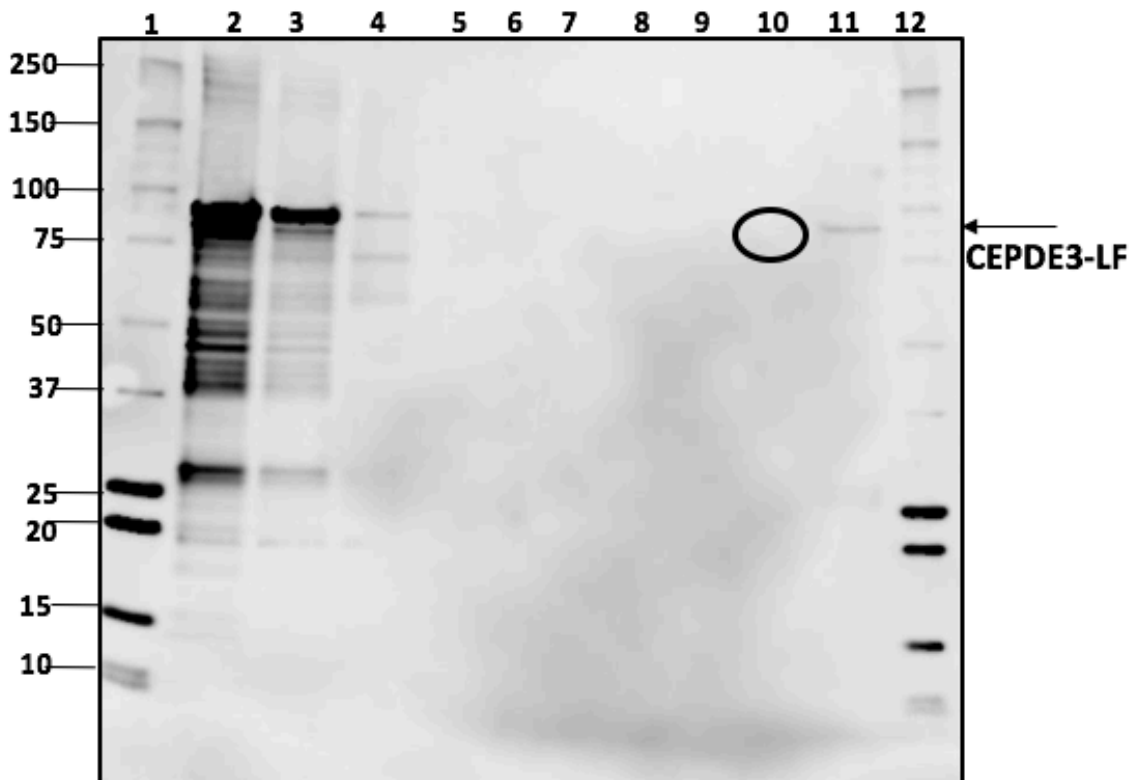


Figure 5.5: Western blot analysis of purification samples from CEPDE3-LF based on batch method

CEPDE3-LF proteins were purified using batch method with GST-spin trap columns by taking out resin in an eppendorf tube. Protein fractions loaded on gel to detect by western immunoblotting. Lanes 1 and 12 contain marker. Lane 2: protein supernatant, lane 3: flow-through, lanes 4-9 contain wash fractions, lane 10: expected eluate band circled, and lane 11: beads post elution. Proteins were detected using anti-GST antibody.

5.3.4: CEPDE3-LF purification experiments using Tris-HCl and PBS buffers

5.3.4.1: Experimental method

This experiment was designed focusing on cell-lysis preparation, cell-lysis experiments with CEPDE3-LF were carried out optimizing with a range of cell-lysis buffers based on the protocol recommended by (GST fusion protein purification handbook, G.E. Healthcare).

Accordingly, PBS buffer 6.2 and Tris-HCl buffer pH 7.4 (refer to Chapter 2, section 2.6.3 for buffer preparation) were each used for lysing bacterial cells, which were grown and induced by IPTG at 37°C. Additionally, 2% Triton X-100 and lysozyme were used in cell-lysis and then further sonicated. Protein mixture was fractionated at 10,000xg for 15 minutes as supernatant and insoluble cell-pellet.

Glutathione sepharose 4B beads were prepared by equilibrating with PBS or Tris-HCl buffer in two individual tubes each to compare the efficiency with buffers in purification. Bacterial soluble supernatant was incubated with individual beads in each tube at 4°C. Following incubation, columns were washed with respective buffers 3-4 times, collecting washes separately.

Proteins were eluted using 20 mM reduced glutathione by passing the elution buffer several times over the columns, and incubating the beads with buffer for 5 minutes on a rotator, at room temperature. Beads were centrifuged at 500xg for 5 minutes at 4° C and eluates were collected separately into two tubes. A small portion of the beads from each tube were analyzed with sample buffer. All samples were analyzed for western immunoblotting and proteins detected using anti-GST antibody (Fig. 5.6).

Purification fractions from both PBS and Tris-HCl buffer method did not yield the desired results as no bands were observed with the eluates obtained from both buffers and protein came out in the flow-through fractions hence binding was poor and proteins were not eluted (Fig. 5.6). Therefore, at this point, it was important to determine the binding properties with glutathione sepharose beads.

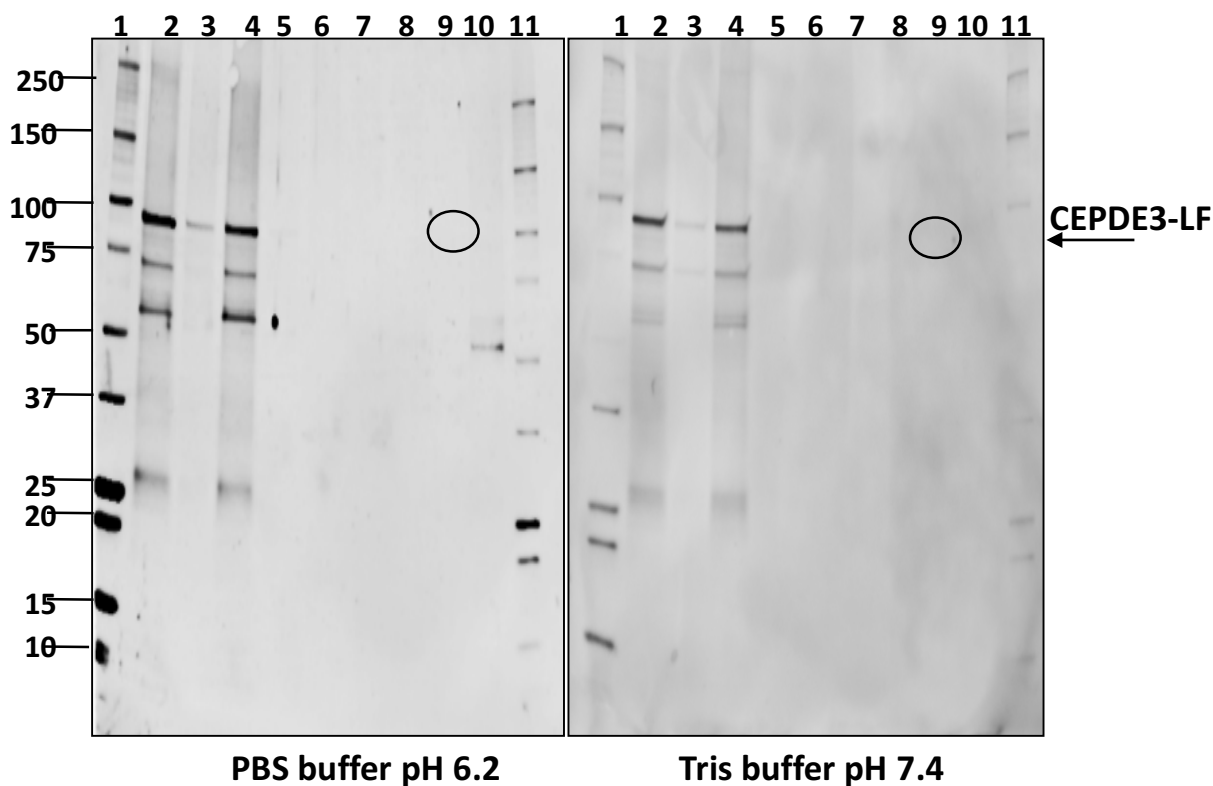


Figure 5.6: Screening of buffer for optimization in purification

Analysis from CEPDE3-LF batch purification screening with PBS and Tris-HCl buffers. The left panel A shows PBS buffer pH 6.2 and right panel B shows purification fractions using Tris-HCl buffer pH 7.4. Lanes 1 and 11 in both blots contain MW marker, and purification fractions loaded in the same order, Lane 2: contains soluble supernatant, lane 3 contains wash, lane 4 contains flow-through1, lanes 5-8 contain wash fractions, lane 9 contains eluate (location of expected band is circled in both blots), and lane 10 contains beads after elution.

5.3.5: GST control experiment

Based on the experimental data analysis derived from purification using GST-spin trap columns and optimizing buffer conditions, it was decided to perform some control experiments to investigate the binding capacity of GST proteins to glutathione sepharose 4B resin obtained from (G.E. Healthcare). Accordingly, it was decided to perform purification experiments using a pure GST-tag (26 kDa) protein incubating with glutathione sepharose 4B at various time intervals to determine binding conditions.

GST-protein incubation: This method was performed to optimize binding capacity of the beads, hence no elution step using elution buffer was performed. GST-tag fusion protein provided by (Dr. Jiro Kato NHLBI Staff Scientist) was expressed using *E. coli* and cell lysates were incubated with the glutathione sepharose 4B resin at 4 °C, for a range of time intervals including 2, 4, 6, 8 hours and overnight with gentle shaking. Post-incubation with beads, beads were centrifuged at 500xg for 5 minutes and flow-through was collected at respective time intervals. The individual beads were washed 3-4 times with PBS binding buffer. An aliquot of the protein bound beads were applied to equal amount of sample buffer. Accordingly, flow-through and respective bead samples obtained from various time intervals were loaded onto the gel and analyzed by western immunoblotting. Proteins were detected using primary anti-GST antibody and secondary anti-goat HRP antibody.

Experimental data detected strong bands from flow-through and beads fractions from all samples of various time intervals). However, bands representing flow-through from 8 hours (lane 8) and overnight incubation (lane 10) showed bands with less intensity which indicated that protein was not coming out in flow-through, and hence bound to the beads with increasing incubation time, and thus binding was efficient. Hence, increasing incubation time, particularly 8 hours and overnight incubations, increased binding efficiency of the GST protein bands (Fig. 5.7).

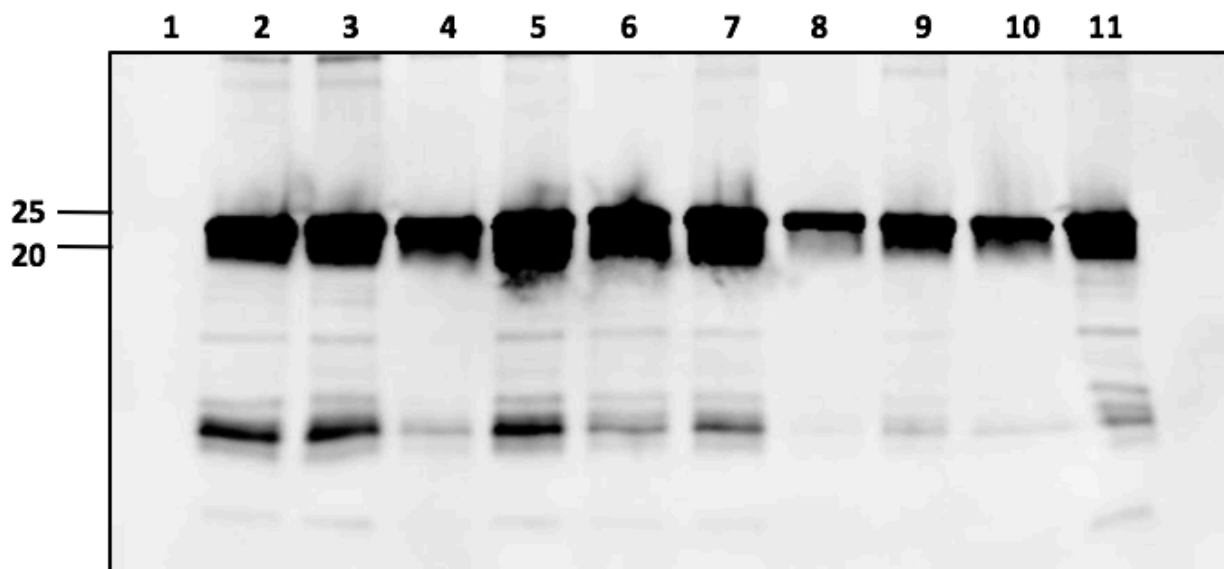


Figure 5.7: Optimization study using GST-fusion protein

GST fusion protein was incubated with glutathione sepharose beads and flow-through and beads were collected at time intervals from 2, 4, 6, 8 hours and overnight incubation respectively, samples were loaded on gel as seen above. Lane 1 contains marker, lanes 2 to 11 contain flow-through and beads samples from (2, 4, 6, 8 hours and overnight incubation) with flow-through loaded in the left lane (lanes 2, 4, 6, 8, and 10) and beads loaded in the right lane (lanes 3, 5, 7, 9, and 11).

5.3.6: Scaling-up of CEPDE3-LF batch purification

Further purification experiments with CEPDE3-LF were designed to improve binding efficiency with glutathione sepharose 4B resin and simultaneously were also aimed to purify a large amount of protein through screening optimal conditions based on the batch method. The binding capacity of glutathione resin is > 5 mg GST per ml of the chromatography medium. A revised protocol was designed for further purification experiments to increase binding efficiency and improve the yield of purified protein.

Cell lysis: A 1-liter culture was induced with 1 mM IPTG at temperature of 25°C overnight. Cell-lysis was performed using a French Press and cells fractionated by centrifuging at 10,000xg for 15 minutes, and 80 ml of soluble supernatant was obtained, 2ml of the soluble supernatant was taken out and used for purification. There were few changes made in this protocol as listed:

1) The soluble supernatant fraction extracted using French Press was diluted by ~5 fold to reduce viscosity. 2) Freshly prepared 10 mM DTT was added to the soluble supernatant to improve the binding efficiency, for detailed protocol (refer to Chapter 2, section 2.7.3.1). 3) The elution was performed using an on-column cleavage method with PreScission Protease enzyme and eluted protein was concentrated by precipitation by 20% TCA.

Results: Protein fractions from purification were analyzed on coomassie gel and western blot detected with CEPDE3-LF N terminal. Bands from eluate with TCA precipitation indicated dark bands, close to predicted size of CEPDE3-LF (~ 63.5 kDa) (see Fig. 5.8). Though protein was still coming out in flow-through. However, the binding efficiency was increased, as compared to the previous experimental data discussed in Fig. 5.4 to 5.6. Experimental data demonstrated that the revised purification protocol based on cell-lysis method using French Press, addition of 10 mM DTT and further reducing viscosity of the soluble protein helped increased the binding capacity of the proteins in the batch purification method with glutathione sepharose 4B. Elution using on-column cleavage with PreScission protease was considered an effective method than elution using reduced glutathione. Instead of competitive displacement it effectively cleaves the protein and releases the purified protein from the column, the size was determined to be close to the estimated size of CEPDE3-LF, as the band size was shifted from ~ 90 kDa to ~ 63.5 kDa after cleavage of GST-tag.

Based on this conclusion, further experiments with CEPDE3-LF were repeated, however it was aimed to perform elution by eliminating the TCA precipitation method. The purifications experiments were further designed by introducing extra wash steps (refer to Chapter 2, 2.7.3 for a detailed protocol). Experimental data demonstrated that the results from purification with the revised protocol were reproducible, and on-column cleavage was performed eliminating TCA precipitation. Western blotting (Fig. 5.9A) and coomassie staining (Fig. 5.9B), showed proteins from elution 1 and elution 2 post cleavage. The size of CEPDE3-LF after cleavage with enzyme corresponded to correct size of the long-form (~ 63.5 kDa).

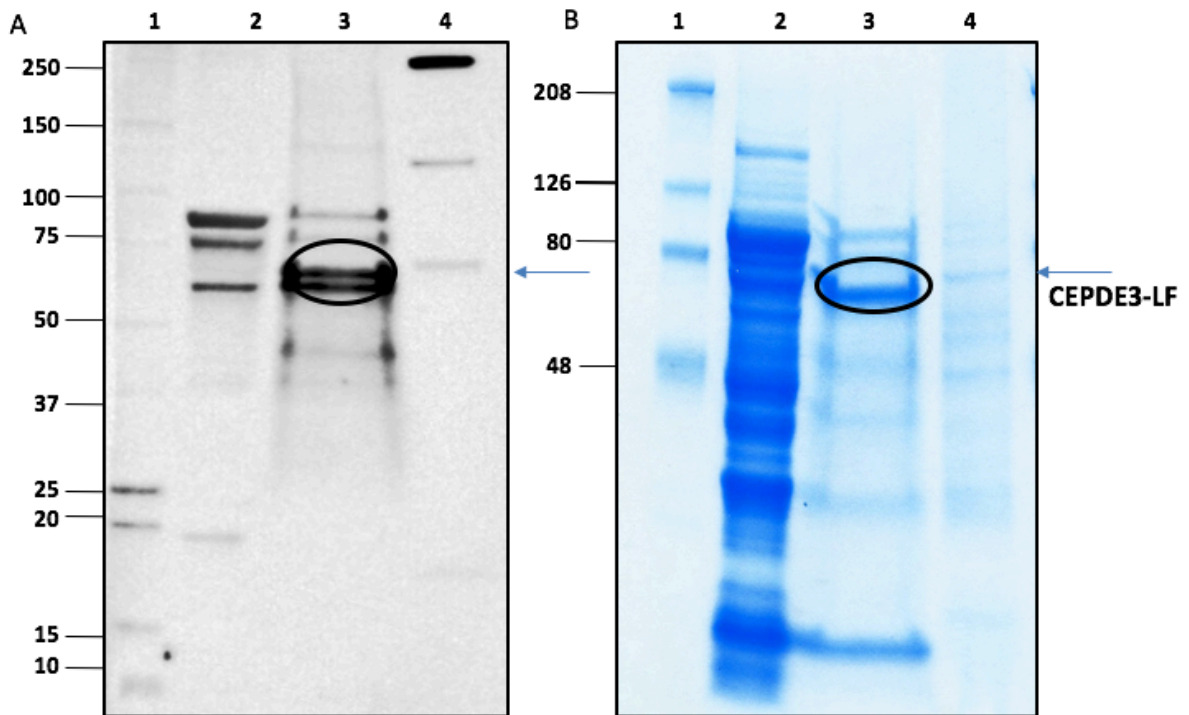


Figure 5.8: Western blot analysis of CEPDE3-LF purification with on-column cleavage using PreScission Protease enzyme

CEPDE3-LF soluble supernatant was purified using glutathione sepharose 4B with batch method, elution was performed using on-column cleavage by PreScission Protease and eluate precipitated with TCA. Panel A, western blot incubated with CEPDE3LF N-terminus antibody. Panel B, coomassie stain. Lane 1 in both the gels contain MW marker, lane 2: contains flow-through, lane 3: eluate fraction, lane 4: contains CEPDE3-LF Flag-tag protein extracted from insect cells loaded as a control.

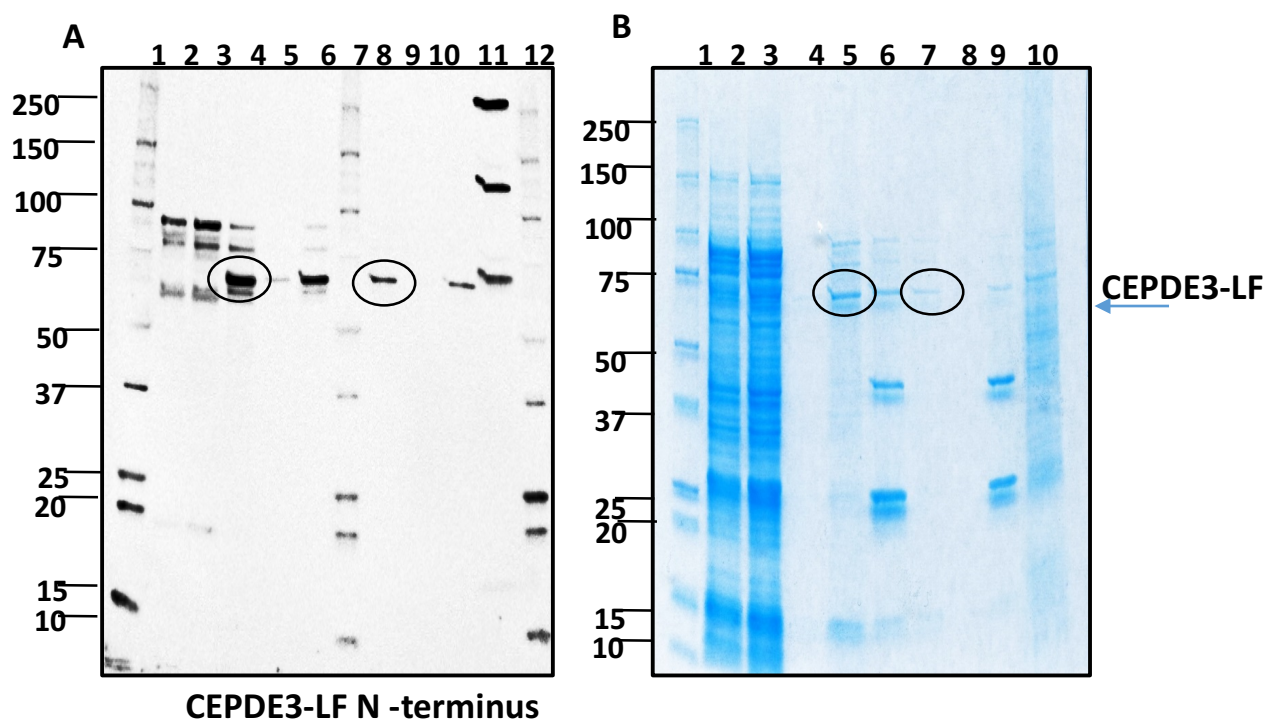


Figure 5.9: CEPDE3-LF protein purification using glutathione sepharose 4B

CEPDE3-LF batch purification fractions were analyzed on gel. Panel A: western blot, samples loaded as follows, lanes 1, 7 and 11 contain MW marker, lane 2: supernatant, lane 3: flow-through, lane 4: LF eluate1 (circled) post enzymatic cleavage. Lane 5: cleavage wash, lane 6: beads post elution. Lane 8: eluate 2 (circled), lane 9: cleavage wash 2, lane 10: beads post elution 2, lane 11, CEPDE3-LF control.

Panel B: coomassie gel, lane 1, marker, lane 2, supernatant, lane 3 flowthrough, lane 4: cleavage wash1, lane 5: eluate1 (circled), lane 6: cleavage wash, lane 7: elution 2 (circled), lane 8: cleavage wash, lane 9: beads post elution 2, lane 10: contains CEPDE3-LF, Flag-tag control. Western blot incubated with CEPDE3-LF N-terminus antibody.

5.3.6.1 Optimization study for effective enzyme cleavage

To determine the efficacy of on-column enzymatic cleavage, an optimization study was performed with LF bound protein beads. A batch method with on-column cleavage optimization was carried out to determine the effective time required for on-column cleavage with CEPDE3-LF. 75 μ l of the LF bound beads from purification of LF proteins were incubated with 10 units of Precision protease enzyme at 4°C. To optimize conditions, sample aliquots were taken out at the time intervals of 1, 2, 4, and 8 hours, as well as overnight incubation. These sample aliquots were analyzed by western blot and coomassie gel. Proteins were detected using CEPDE3-LF N-terminus antibody, bands post enzymatic cleavage from 1, 2, 4, 8 hours or overnight samples represent band size that correspond to \sim 63.5 kDa, the predicted size of CEPDE3-LF. Bands detected from various time incubation determined similar band intensity post cleavage with the

PreScission Protease enzyme. However, 6 or 8 hours and overnight time for incubation were considered as optimum.

Note 1: As a control protein cell-lysates expressed in insect cells (Flag-tag) were loaded, to estimate the protein size, however the bands from control CEPDE3-LF showed three bands. It was not clear why that band pattern was observed, but the lower band was considered the true band. It corresponded to the bacterial CEPDE3-LF protein predicted size (Fig. 5.8-5.10). Similarly, the CEPDE3-LF cleaved protein without the GST tag showed bands that were ~ 63.5 kDa, the predicted size of CEPDE3-LF without the GST tag.

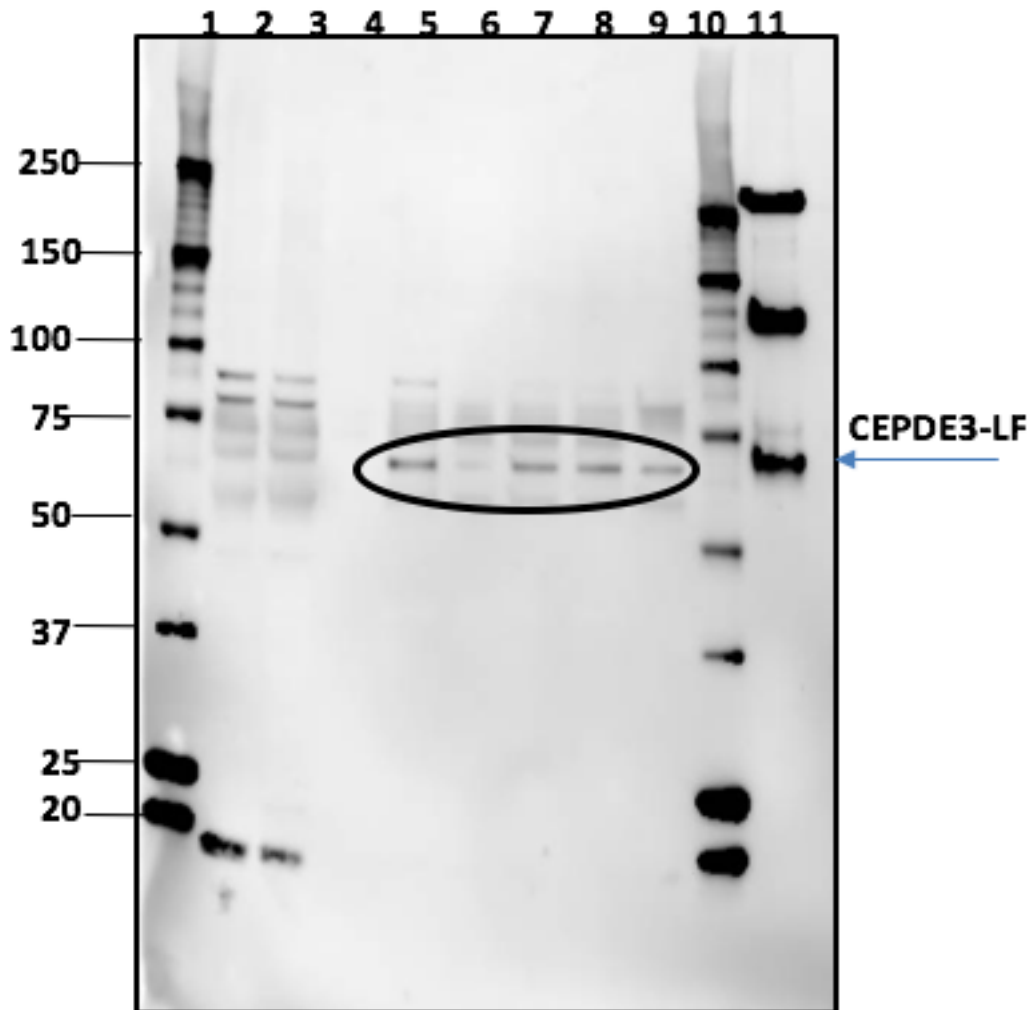


Figure 5.10: Optimization of enzymatic cleavage of CEPDE3-LF purified protein using enzyme Precision protease.

CEPDE3-LF purified proteins were screened for optimization of time required for on-column cleavage conditions at several time intervals ranging from 1, 2, 4, 8 hours and overnight incubation. Samples taken out post-cleavage at these time intervals were loaded on to the gel as follows, lanes 1 and 10 contain marker, lane 2 contains LF supernatant, lane 3 contains eluate before cleavage, lanes 4 was blank, and lanes 5-9 contain samples from 1, 2, 4, 8 hours and overnight incubation. Lane 11 contains samples of CEPDE3-LF derived from insect cells, as a control.

5.3.7: Measures for improved binding efficiency of CEPDE3-LF with batch method

The amount of purified protein obtained from a 1-liter bacterial culture of long-form protein expressed in *E. coli* resulted in a yield of ~ 1.7 mg/ml, which further produced a purified protein of ~ 0.4 mg/ml in 200 µl of volume. Though the purification results obtained were effective in terms of cleavage of GST-tag, few non-specific bands were observed in the purified protein fractions, also the protein yield was comparatively low as required in mg/ml amount for crystallization. Thus, a clean purified protein band with a high yield was required for further experiments. Several optimizing techniques were screened to increase the protein yield and binding capacity, the following sections describe the techniques used.

5.3.7.1: Pre-incubation of glutathione sepharose 4B with BL21 culture

Prior to incubation with CEPDE3 proteins, glutathione sepharose 4B beads were incubated with *E. coli* expressed in BL21 culture. This procedure was carried out, in an attempt, to limit non-specific binding to the glutathione beads. Hence, this step was introduced, with a possibility that it may reduce the background bands of lower molecular weight proteins, and thus may further increase the binding capacity of CEPDE3 proteins to glutathione sepharose 4B and help in obtaining a pure band. Based on these parameters, it was decided to pre-incubate the glutathione sepharose beads with BL21 competent cell-culture, which could possibly block non-specific *E. coli* protein and help in obtaining clear eluate bands. Glutathione sepharose slurry was incubated prior with lysed BL21 bacterial culture at 4°C overnight on a rotator, this protocol was carried out in the same pattern based on batch protocol experiments used in CEPDE3-LF. Following incubation with BL21 cells, beads were washed 4X with PBS buffer and 2X with 200 mM Tris-HCl pH 8, the washed beads were re-incubated with CEPDE3-LF protein lysate at 4°C overnight and the batch purification protocol was repeated (as described in Chapter 2, section 2.7.3). Proteins bound to beads were eluted with on-column cleavage using the enzyme PreScission protease. See Fig. 5.11 for western blot image. Eluate bands detected from this method were very faint as compared to the on-column cleavage with CEPDE3-LF standard protocol (refer to Fig. 5.9). Thus, experimental results determined that prior incubation of glutathione sepharose beads with BL21 culture decreased the binding efficiency of CEPDE3 proteins and hence the yield of protein was even lower as compared to the eluate samples from previous purification experiment (as seen in Fig. 5.9). Hence, this technique was not considered a suitable method.

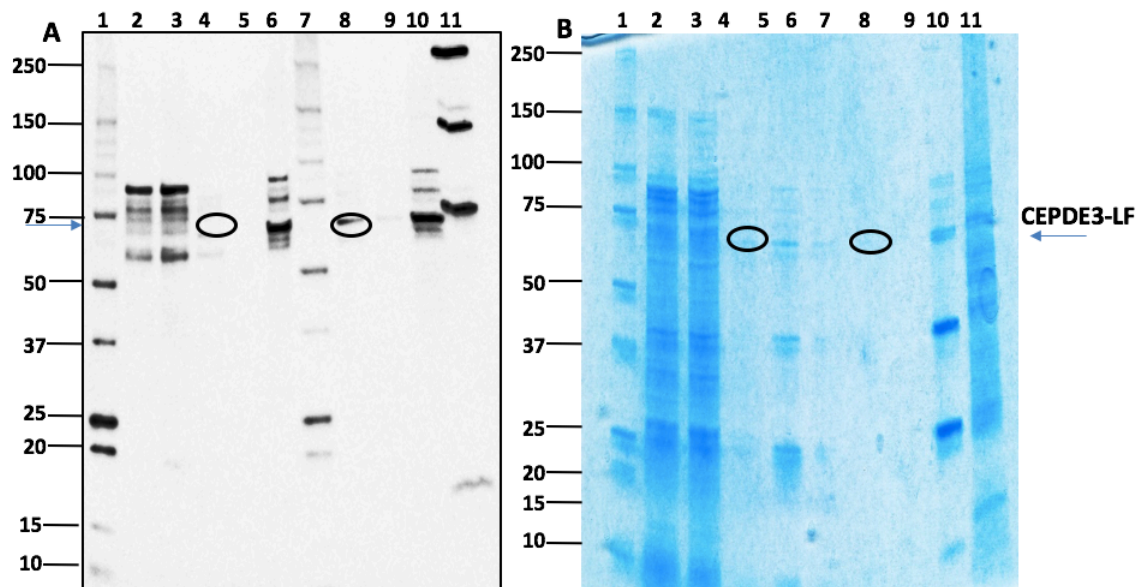


Figure 5.11: Protein purification of CEPDE3-LF using pre-incubated glutathione sepharose with BL21 cells

Western blot analysis and coomassie stain gel of the CEPDE3-LF purification fractions from glutathione sepharose 4B with prior incubation to BL21 cells. Lanes 1 and 7 in both gels contain MW marker and samples loaded in the same order, lane 2: soluble supernatant, lane 3: flow-through, lane 4: eluate1, lane 5: wash1, lane 6: bead 1, lane 8: eluate 2, lane 9: wash 2, lane 10: bead2, and lane 11: CEPDE3-LF Flag-tag control.

5.3.7.2: Regeneration of Glutathione Sepharose 4B

In affinity chromatography method, the biochemical mixtures are separated based on specific biological interactions. The glutathione resin is developed for single step purification method. The glutathione beads can be regenerated, however the binding efficiency may be reduced. Regenerating glutathione sepharose 4B is a process in which beads are subjected to wash steps based on a high and low pH buffer and then re-used in further purification of proteins. The experiment based on regeneration of glutathione sepharose 4B was aimed to improve purity of the CEPDE3 proteins. Regenerated beads contain several preexisting non-specific lower molecular weight proteins bound along with the target protein. Incubating protein mixture with the regenerated beads may allow the lower molecular weight proteins to covalently bind to the glutathione sepharose 4B beads, and thus may block the lower molecular weight protein. Based on these parameters, the technique may be helpful in reducing the non-specific background that appeared in purification experiments, and thus improve purity with CEPDE3 proteins.

Experimental method: The pre-used LF-bound glutathione sepharose 4b beads (~1.2 ml) were incubated with (10 mM reduced glutathione buffer, pH8) for overnight incubation at 4°C on a rocking platform, the following day, beads were centrifuged at 500xg for 5 minutes and eluate collected. A high pH buffer with (0.1 M Tris-HCl, 0.5 M NaCl, pH 8.5) and low pH buffer (0.1 M sodium acetate, 0.5 M NaCl, pH 4.5) were prepared. Beads were washed with 3 bed volumes of

high pH buffer, following the resin was washed with 3 bed volumes of 1XPBS. Beads were then washed alternatively with low pH buffer. Equilibration of resin was carried out by washing with 3-5 bed volumes of cold 1XPBS. Following the regeneration procedure, CEPDE3-LF samples with 10 mM DTT were incubated and thereby following the batch method purification as explained in (section 5.3.6). All fractions were analyzed by western blotting (Fig. 5.12). Experimental data demonstrated that regeneration of beads did not improve binding efficiency of glutathione sepharose 4B with CEPDE3-LF proteins as the yield of protein was low.

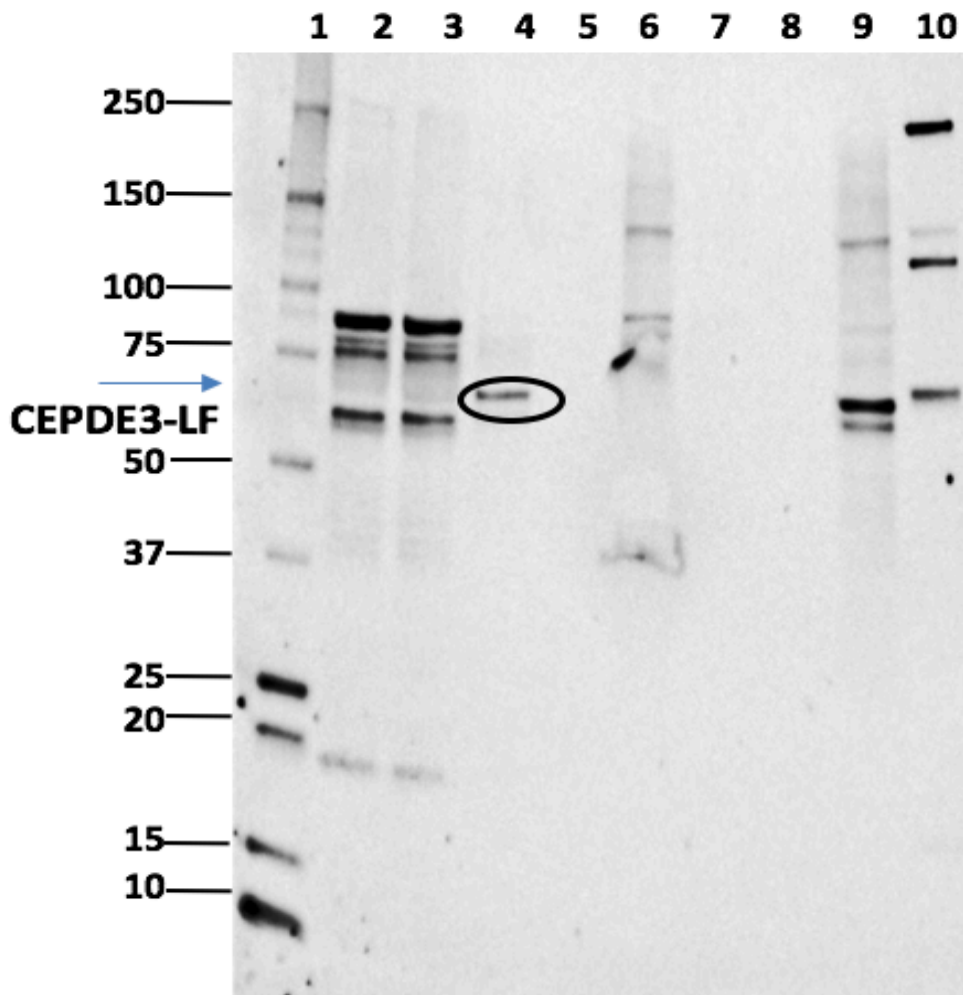


Figure 5.12: Analysis of CEPDE3-LF protein purification by using regeneration technique

CEPDE3-LF proteins purified using glutathione sepharose 4B, which was regenerated to reduce the non-specific binding of lower molecular weight proteins. Lane 1 contains marker, lane 2 contains supernatant, and lane 3 contains flow-through. Lane 4 contains eluate1, indicated by the circled band. Lane 5 contains wash 1. Lane 6 contains bead. Lane 7 contains eluate 2. Lane 8 contains wash2, and Lane 9 contains bead 2. Lane 10 contains CEPDE3-LF Flag-tag control expressed in insect cells.

5.3.7.3: Protein fractionation using ultracentrifuge technique

5.3.7.3.1: CEPDE3-LF studies

Gentle fractionation techniques have been used to separate the cell components, while preserving the functions. If carefully selected, the disruption procedures such as fractionating proteins using an ultracentrifuge can help recover the organelles in a protein intact, depending on the homogenizing conditions (i.e., buffers, pH range). Cell fractionation methods have been used after the commercial development of the ultracentrifuge in 1940, allowing proteins to be separated based on their size and density (Alberts et al., 2002). Cell fractions derived from this process can be impure, but centrifugation can be repeated several times until a clear fraction is obtained. CEPDE3 purification on a large scale, to improve yield in a cost-efficient manner was important, hence ultracentrifugation was considered as an alternative measure to obtain clean protein bands. In addition, performing enzymatic cleavage on a clear soluble protein fractionated from ultracentrifugation maybe more effective than a on-column cleavage performed using batch method purification.

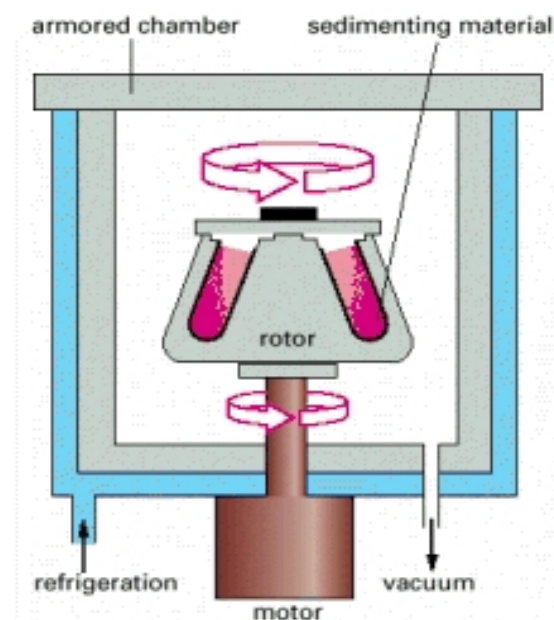


Figure 5.13: Diagrammatic representation of a preparative ultracentrifuge

The samples to be processed are placed into the tubes which are inserted in to the ring of cylindrical holes in a metal rotor. When the rotor moves rapidly at high centrifugal forces it allows particles to sediment. The vacuum causes less friction and in turn prevents heating of the rotor and allows the refrigeration system to maintain the temperature throughout the processing at 4°C.

CEPDE3 cell-fractions were centrifuged in an order of increasing speed. Soluble supernatant lysed with French press was extracted by centrifuging at 10,000xg, the supernatant fraction was then subjected to ultracentrifugation at the speed of 100,000xg. Cell-pellets obtained after centrifugation were further homogenized using 0.1% Triton X-100. (For a detailed protocol refer to Chapter 2, section 2.8).

Results

All purification fractions fractionated using ultracentrifuge were loaded on gel to analyze the amount of protein present in individual fractions by western blot and coomassie gel stain (Fig. 5.14). Panel A and B have purification fractions loaded in the same pattern. Lane 1 in both blots contain MW marker, lane 2 is the supernatant starting fraction derived from French press, lane 3 contains supernatant post centrifugation at 100,000xg, lane 4 contains cell-pellet which was homogenized and centrifuged to obtain soluble protein. Lane 5 in both the gels shows the band circled containing soluble supernatant, which was obtained after homogenizing the cell-pellet. Lane 6 contains insoluble cell-pellet. Some lower molecular non-specific proteins weight bands were observed in the protein fractions at ~15 kDa (Fig 5.14, panel A western blot). 3 $\mu\text{g}/\mu\text{l}$ of protein was obtained in the soluble fractions after homogenization from a cell-pellet of ~ 3.75 μg obtained from a starting material of ~ 4.5 $\mu\text{g}/\mu\text{l}$. (Final volume of all fractions was as listed in the flow-chart in Chapter 2, section 2.8). Experimental data obtained from ultracentrifugation helped increase the purity of proteins, and the yield of the soluble fraction was increased. CEPDE3 soluble protein obtained from 100,000xg pellet recovered 80-90% in the soluble form, and the protein bands were relatively clean, with fewer non-specific protein bands (as seen in Fig. 5.14). The soluble supernatant of 13 ml obtained in the final step was used for enzymatic cleavage (described in section 5.3.7.3.2).

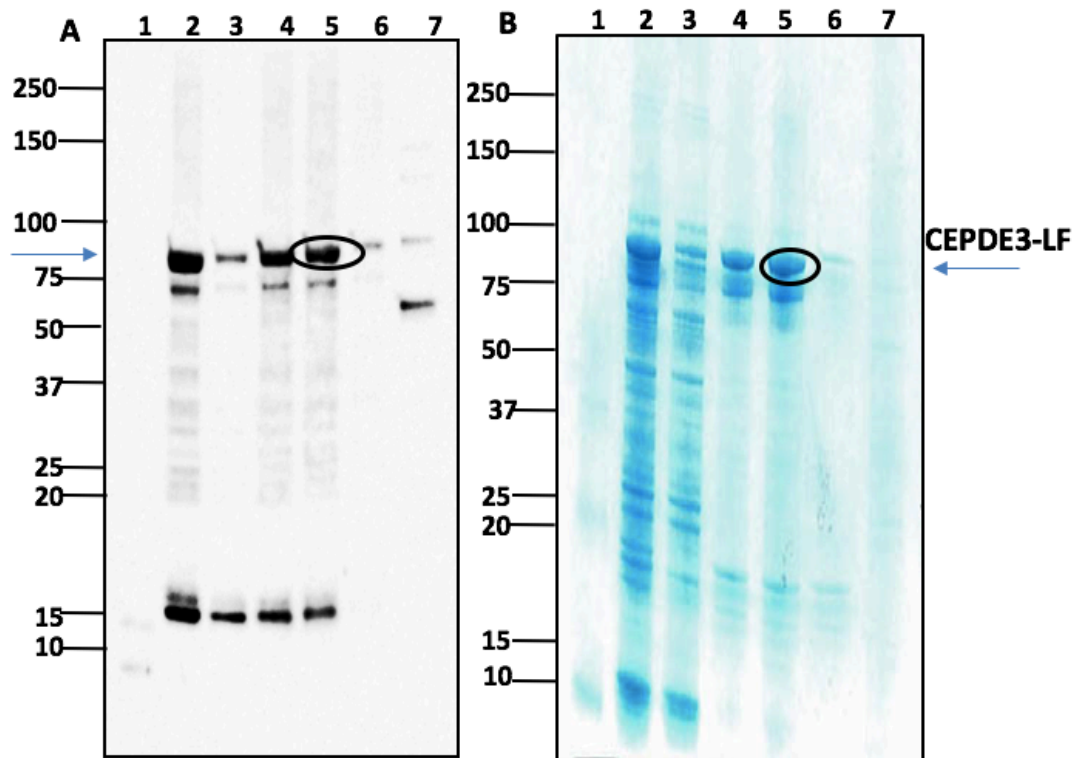


Figure 5.14: Analysis of CEPDE3-LF purification fractions by ultracentrifugation

CEPD3-LF soluble samples were fractionated using ultracentrifugation and all protein fractions loaded on to gel. Panel A, proteins were detected by western blot incubated with CEPDE3 N-terminus antibody. Panel B, coomassie staining. Samples were loaded in the same order. Lane 1: MW marker, lane 2: soluble supernatant, lane 3: supernatant fraction derived after 100,000xg centrifugation, lane 4: cell-pellet obtained post centrifugation, lane 5: contains soluble supernatant obtained from cell pellet, and lane 6: insoluble supernatant after centrifugation.

5.3.7.3.2: Enzymatic cleavage of soluble samples of CEPDE3-LF and SF using PreScission Protease enzyme

The soluble protein derived from fractionation by centrifugation using ultracentrifugation as (described in section 5.3.7.3.1) was subjected to enzymatic cleavage using PreScission Protease. (Detailed protocol listed in Chapter 2, section 2.8.1).

1) **Method 1:** Based on the batch method, a small amount (750 μ l) of CEPDE3-LF soluble protein was incubated with glutathione sepharose 4B, with overnight incubation and following wash, an on-column enzymatic cleavage using PreScission Protease enzyme performed.

2) **Method 2:** This method was based on in solution cleavage with the soluble CEPDE3-LF protein incubation with PreScission Protease enzyme and further incubating with glutathione sepharose 4B resin.

Performing enzymatic cleavage in two different methods was carried out to investigate the efficiency of each technique for optimizing the suitable conditions, in terms of purity of the desired protein, and also for the amount of enzyme to be used with the cleavage process.

Results

Method 1: All purification fractions from the direct method were analyzed on SDS-PAGE gel with western blotting (Fig. 5.15, left panel) or coomassie staining (Fig. 5.15, right panel), eluate fraction shows a band close to molecular weight, the predicted size of CEPDE3-LF (~ 63.5 kDa). The protein yield was ~ 0.7 μ g/ μ l, however other non-specific bands of lower molecular weight were detected after enzyme cleavage. As a polishing step, it was decided to incubate the purified eluate fraction obtained from direct incubation method with glutathione sepharose 4B for 2-3 hours at 4°C and centrifuge at 500xg for 5 minutes. However, additional incubation of eluate with glutathione sepharose 4B did not help as a polishing step to clear the non-specific bands and obtain purified CEPDE3-LF protein.

Method 2:

As seen in Fig. 5.16, the resultant western blot and coomassie gels from batch method of purification using on-column cleavage did not show any bands with eluate, also binding was not very efficient. Hence this method was ineffective to perform enzymatic cleavage.

Experimental data from CEPDE3-LF purification determined that PreScission Protease was effective in enzymatic cleavage performed in solution, however there were lower protein bands detected in the purified sample. Hence attempts made to obtain a pure protein band on the gel were not successful. Further methods were evaluated based on other techniques as discussed in the section below (section 5.3.8).

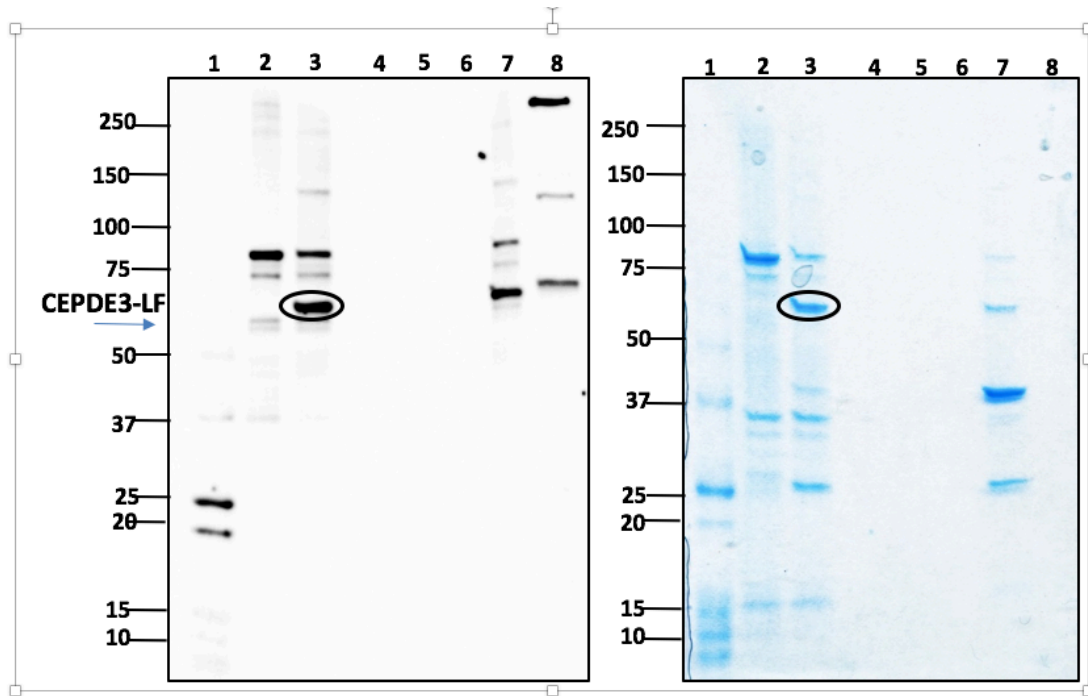


Figure 5.15: Analysis of enzymatic cleavage samples from PreScission protease using direct enzyme incubation

Soluble supernatant samples obtained as discussed (see Fig. 5.13) were subjected to enzymatic cleavage and protein fractions detected with western blot (panel A) and coomassie gel stain (panel B). Lane 1 in both gels contain MW marker. Lane 2 contains soluble supernatant, lane 3: eluate, and lanes 4-6 contain wash fractions, lane 7: beads post elution, and lane 8: CEPDE3-LF Flag-tag control. Western blot incubated with CEPDE3-LF N-terminus antibody.

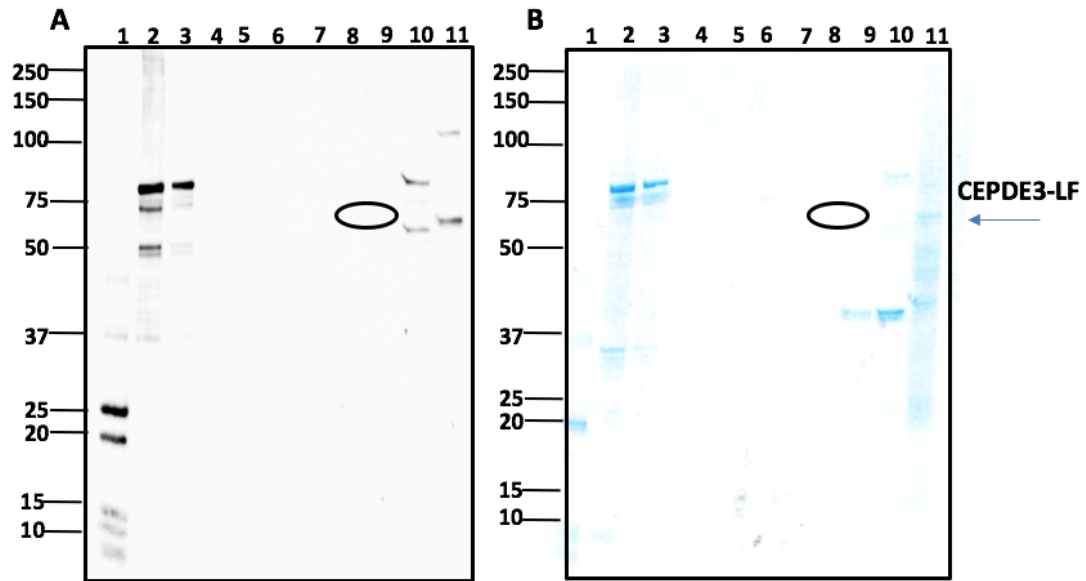


Figure 5.16: Enzymatic cleavage using batch method

Analysis of enzymatic column cleavage with PreScission protease using CEPDE3-LF purification fractions from batch incubation method. Lane 1 contains marker, lane 2: supernatant, lane 3: flow-through, lanes 4-8 contain wash fractions, lane 9: eluate, lane 10: beads post elution, and lane 11: contains LF CEPDE3 Flag-tag control derived from insect cells. No eluate bands were obtained from this method of enzyme cleavage.

5.3.8: Ion exchange chromatography

The principle of ion exchange chromatography (IEX) is based on the specificity of buffers, hence the buffer pH is very critical in determining the optimal conditions for purifying proteins using this technique. DEAE sepharose was used in this study to perform purification. Sephadex ion exchangers are produced by introducing a functional group onto sephadex, which is a cross-linked dextran matrix, these groups get attached to the glucose units in the matrix by stable ether linkages. Diethyl-(2-hydroxy-propyl) aminoethyl is the functional group and chloride is the counter ion. Due to its hydrophilic nature, sephadex shows very low nonspecific adsorption and is insoluble in all solvents, hence it is suitable as a base for an ion exchange matrix (Rossomando, 1990).

In an effort to increase the efficiency of purified protein and remove nonspecific bands, ion exchange chromatography using DEAE sepharose beads was used. Experiments were based on the same purification protocol that was applied in affinity chromatography (refer to section 5.3.6). A 10 ml of CEPDE3-LF supernatant, derived from 200 ml of cell-lysate, was diluted 4-5x with Tris-HCl buffer pH7.4 and incubated with 5 ml of prewashed DEAE sepharose beads slurry. Proteins were eluted using three different concentrations elution buffer: 1) 20 mM Tris, 100 mM NaCl, 2) 20 mM Tris, 300 mM NaCl, 3) 20 mM Tris, 500 mM NaCl. Protein bound beads were incubated with each of the elution buffers separately. (For a detailed protocol on ion exchange chromatography using the range of elution buffers, refer to Chapter 2, section 2.8).

Post incubation, aliquots of the beads were taken in three individual tubes. Eluate was collected by centrifugation. All purification fractions were loaded on SDS-PAGE gels and analyzed by western blot (Fig. 5.17, panel A) and coomassie gel (Fig. 5.17, panel B). However, in lanes 5 and 6 no eluate bands were seen. Adding NaCl in increasing concentrations did not help in elution of the protein, and thus no effect in increasing protein yield. Lanes 6-8 were the protein eluates obtained using increasing concentration of salt buffers, hence further optimization was required with the DEAE sepharose method.

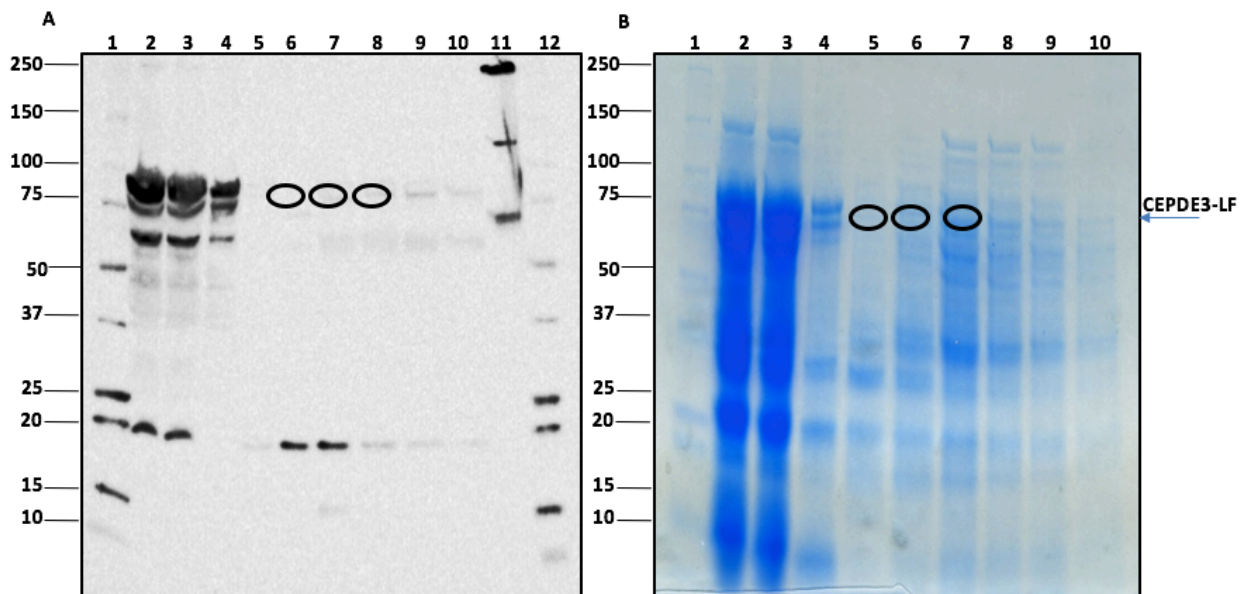


Figure 5.17: CEPDE3-LF purification using ion exchange chromatography with DEAE sepharose resin.

CEPDE3-LF proteins were purified using DEAE sepharose beads with the batch method. All protein fractions were loaded on two gels for western blot (panel A) or coomassie (panel B). Lanes 1 and 12 contain MW marker, lane 2: LF supernatant, lane 3: flow-through, lanes 4 and 5 contain wash fractions. Lanes 6-8 contain eluate fractions from elution using 100, 300 and 500 mM NaCl concentration. Expected eluates are circled and indicated by an arrow. Lanes 9-10: contain bead fractions from 100 and 300 mM fractions post elution, lane 11 contains CEPDE3-LF Flag-tag insect cells control. Western blot incubated with CEPDE3-LF N-terminus antibody. Panel B, protein purification fractions loaded in the same order as panel A, except there was only one wash fraction loaded in lane 4, and there is no additional MW marker, hence there are only 10 lanes.

5.3.8.1: Optimization conditions for protein purification with range of pH buffers using IEX

These experiments were carried out with CEPDE3 proteins to optimize conditions with ion exchange chromatography. Hence, it was decided to use Tris-HCl buffers with a range of pH from pH 6 to 7 as binding and wash buffers. Based on the batch protocol (described in section 5.3.8). DEAE sepharose beads of 1 ml volume were pre-incubated with soluble CEPDE3-LF supernatant (3x diluted) in 15 ml volume. 5 ml of each of the soluble supernatant were incubated with beads resuspended with respective buffers of pH 6, pH 6.5, and pH 7. Elution was carried out using elution buffer (20 mM Tris-HCl, 500 mM NaCl) with pH adjusted to 6, 6.5 and 7 for each of the incubation reaction set in three different tubes. Beads were incubated with elution buffer at 4°C for 5 minutes and centrifuged, with the three eluates collected separately. Samples were analyzed on a SDS-PAGE gel (Fig. 5.18). Western immunoblotting and coomassie staining did not show clear eluate bands from the three eluates of varying pH, as seen in panel A and B below (estimated eluates circled). Thus, experimental data indicated that the binding was poor in this

method of purification, and it was not considered a suitable method for purifying CEPDE3 isoforms.

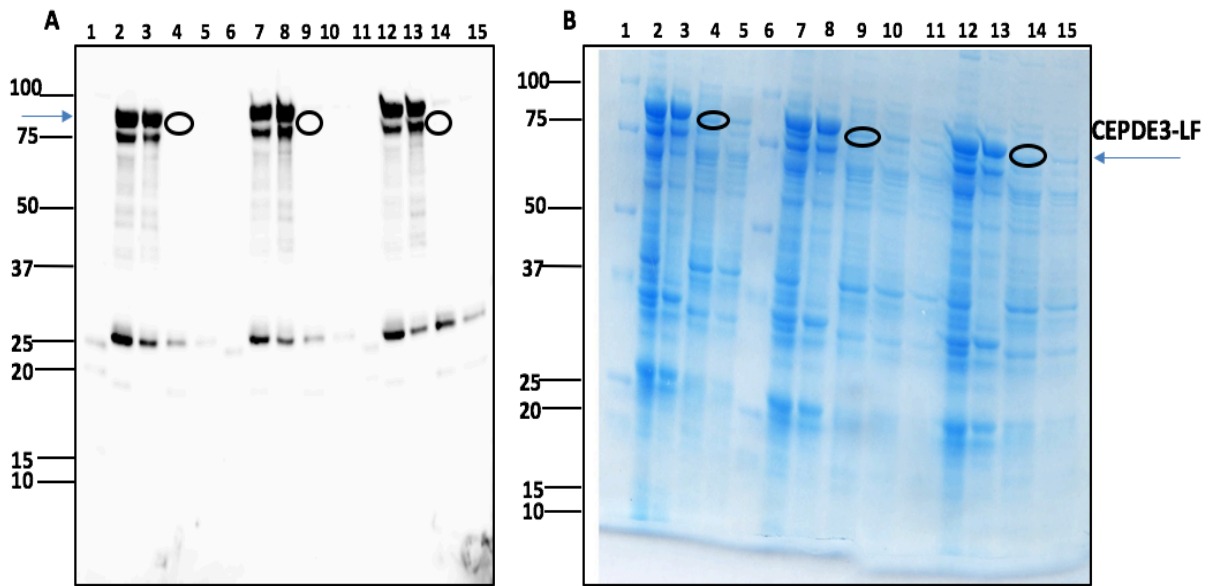


Figure 5.18: optimization with DEAE sepharose purification using various buffers

Analysis of purification samples of CEPDE3-LF using DEAE sepharose, loaded on gel for western blot (panel A) and coomassie staining (panel B). Gels contain the protein fractions in the following order: Lanes 1, 6 and 11 contain marker. Lanes 2-5 contain supernatant, flow-through, eluate and beads samples with buffer pH6. Lanes 7-10 contain supernatant, flow-through, eluate and beads incubated with buffer pH 6.5. Lanes 12-15 contain supernatant, flow-through, eluate and beads post elution incubated with buffer pH 7. The fractions marked in circles is where CEPDE3-LF eluate fractions should be. The actual protein size indicated by the arrow. Western blot was incubated with CEPDE3-LF N-terminus antibody.

5.3.9: CEPDE3-SF purification experiments

5.3. 9.1: Batch purification with CEPDE3-SF using glutathione sepharose 4B

CEPDE3-SF protein purification experiments were designed based on the same protocol used for purification experiments with CEPDE3-LF (as listed in section 5.3.6). A 10 ml supernatant derived from an 80 ml lysate extracted from 1-liter bacterial culture was used in this experiment. SF protein supernatant diluted (2.5x) using PBS buffer pH 6.2. All fractions from purification were analyzed by western blotting and coomassie gel stain. CEPDE3-SF proteins were detected using anti-GST (panel A) and CEPDE3-SF N-terminus (panel B). Bands circled in western blots (see Fig. 5.19a) and coomassie gel (Fig 5.19b) were the eluate bands obtained.

Experimental data from CEPDE3-SF purification using glutathione sepharose 4B demonstrated effective on-column enzymatic cleavage with PreScission protease. The purified protein were ~ 54.8 kDa, the predicted size of CEPDE3-SF. Eluate bands were detected on coomassie gel at lower molecular weight. A soluble supernatant of ~ 1.7 mg/ml of 10 ml used for purification produced an (eluate1 obtained from elution 1) fraction of ~ 0.7 mg/ml and (eluate obtained from eluate 2) showed recovery of 0.33 mg/ml. Protein yield was comparatively low, hence further optimization using other techniques were also tried in CEPDE3-SF purification as described in the next section (5.3.9.2).

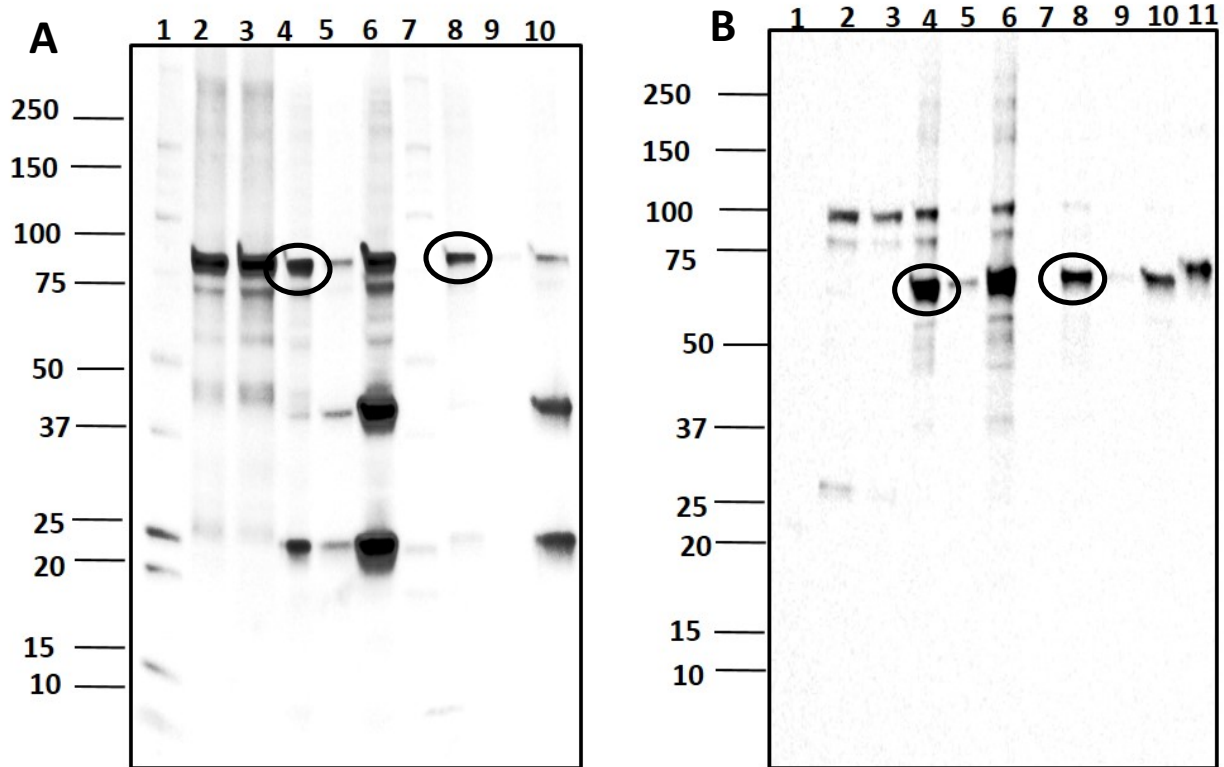


Figure 5.19a: Analysis of CEPDE3-SF purification using glutathione sepharose 4B by batch method.

CEPDE3-SF purification using glutathione sepharose 4B. Protein fractions detected by western immunoblotting. Both blots contain samples in the same order. Lanes 1 and 7 contain marker, lane 2: supernatant, lane 3: flow-through, lane 4: eluate1 indicated by circled band, lane 5: wash 1, lane 6: bead1 post elution, lane 8: eluate2 indicated by circled band, lane 9: wash2, lane 10: bead2 post elution. Blot in panel B contains an additional lane 11 with CEPDE3-SF Flag-tag control sample from insect cells. Blot from panel A incubated with anti-GST antibody, and blot from panel B incubated with CEPDE3-SF N-terminus antibody.

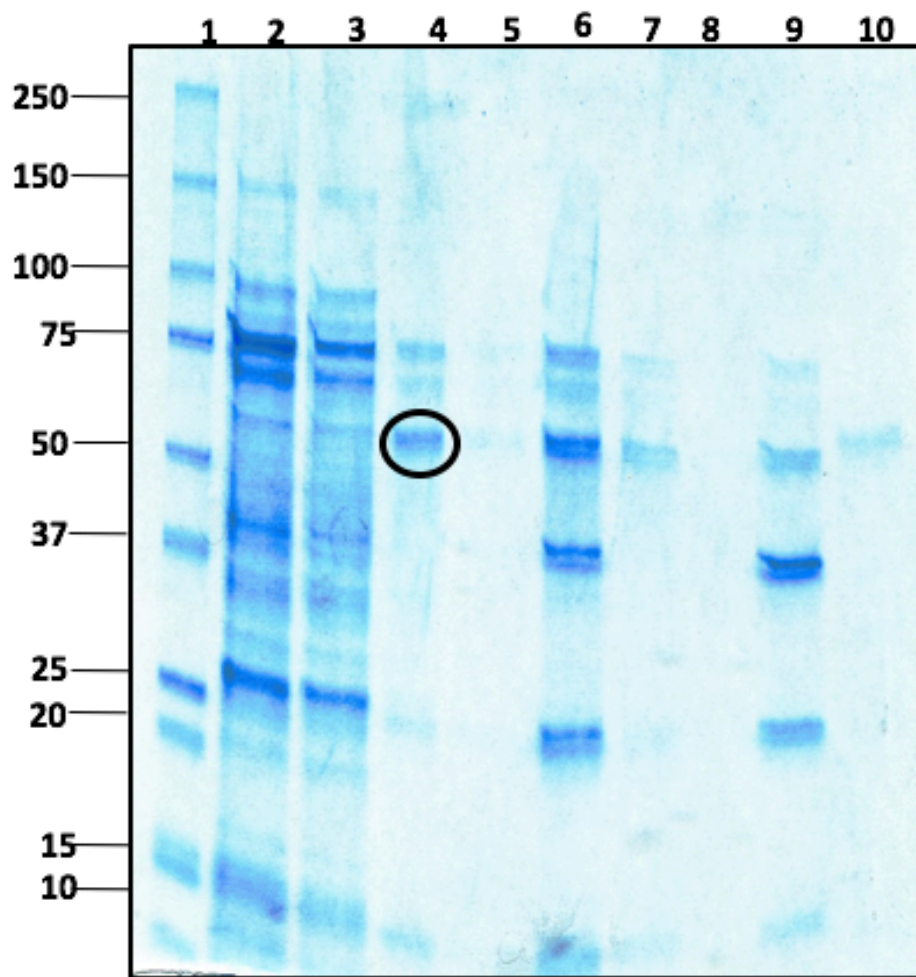


Figure 5.19b: Analysis of CEPDE3-SF purification fractions on a coomassie gel

CEPDE3-SF purification fractions by batch method using glutathione sepharose 4B were analyzed by coomassie gel staining. Lane 1 contains marker, lane 2: SF soluble supernatant lane 3: flow-through, lane 4: eluate1 (circled band), lane 5: wash 1, lane 6: bead1, lane 7: eluate 2 (circled band), lane 8: wash 2, lane 9: bead 2. Lane 10 contains CEPDE3-SF Flag-tag control from insect cells.

5.3.9.2: CEPDE3-SF purification using ultracentrifugation

Experiments with CEPDE3-SF were designed on the same protocol used for CEPDE3-LF purification with ultracentrifuge as described in earlier section (5.3.7.3). Purification fractions using ultracentrifugation were detected using western blots and coomassie images (Fig. 5.20). Results derived from fractionation using ultracentrifuge with CEPDE3-SF were similar to the CEPDE3-LF proteins, a significant amount of the soluble protein was recovered from the cell-pellet post fractionation at 100,000xg. The soluble supernatant indicated clear bands. A starting material of 1.48 mg/ml in 15 ml volume resulted into a 0.6 mg/ml of soluble protein in ~ 14 ml of volume.

5.3.9.3: Enzymatic cleavage

Enzymatic cleavage was performed based on the same method used with long-form, as previously described (section 5.3.7.3.2). Resultant image from direct incubation method (Fig. 5.21, panel A western blot and panel B coomassie staining gel). The eluate band was close to predicted size of short-form ~58 kDa. However, eluate bands post enzymatic cleavage with Precission protease showed other non-specific bands of lower molecular weight. For batch incubation method (refer to Fig. 5.22), no eluate bands were detected with this technique and binding was low.

Experimental data from CEPDE3-SF enzymatic cleavage demonstrated that enzyme cleavage was effective in solution, however eluate bands did not have a clean band and clear background, as desired. Hence, batch incubation technique with CEPDE3-SF proteins post ultracentrifugation was not considered a suitable technique for cleavage of GST-tag. Overall, the experiments with ultracentrifugation resulted in efficient recovery of soluble fractions with clean bands. However, post enzymatic cleavage bands were not pure. Therefore, the technique using ultracentrifuge for purification in the CEPDE3-SF proteins was not considered a suitable method to purify large amount of proteins.

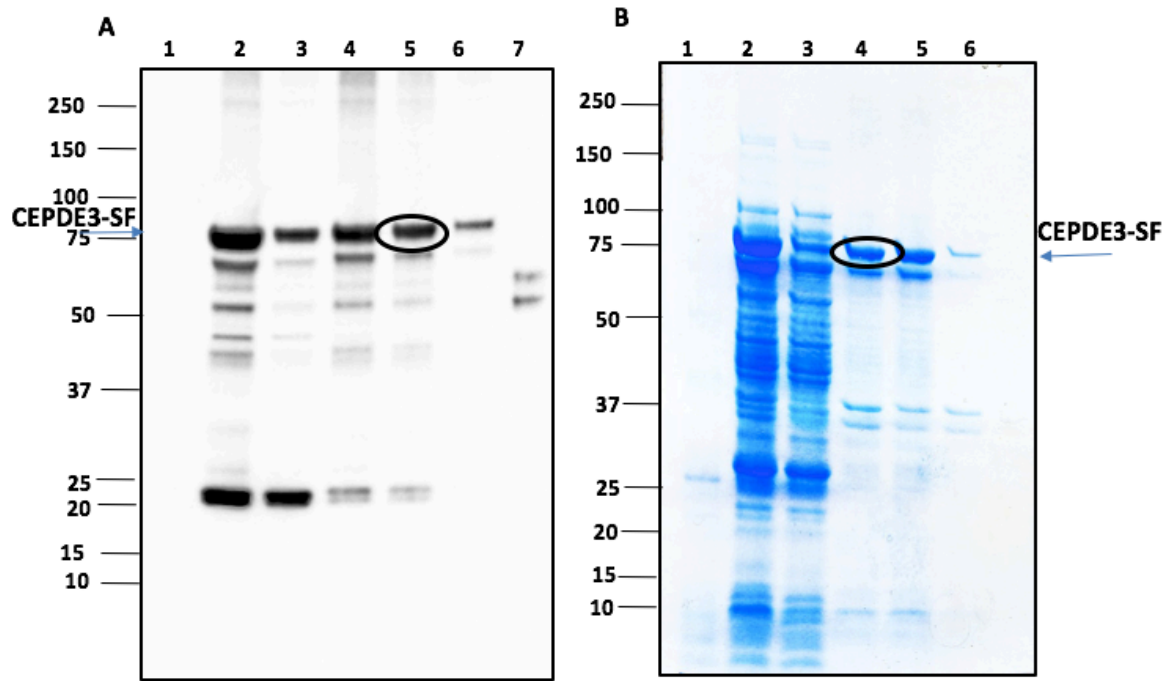


Figure 5.20: Analysis of CEPDE3-SF purification fractionations by ultracentrifugation

Analysis of CEPDE3-LF purification fractions using ultracentrifugation detected by western blot Panel A, incubated with CEPD3-SF N-terminus antibody. Panel B, coomassie staining. Samples were loaded in the same order in Panel A and B. Lane1: MW marker, lane 2: supernatant from 10,000xg, lane3: supernatant post ultracentrifugation, lane 5: cell-pellet homogenized, lane 6: soluble supernatant, indicated by circled band. Panel A contains an additional lane 7, CEPDE3-SF Flag tag control.

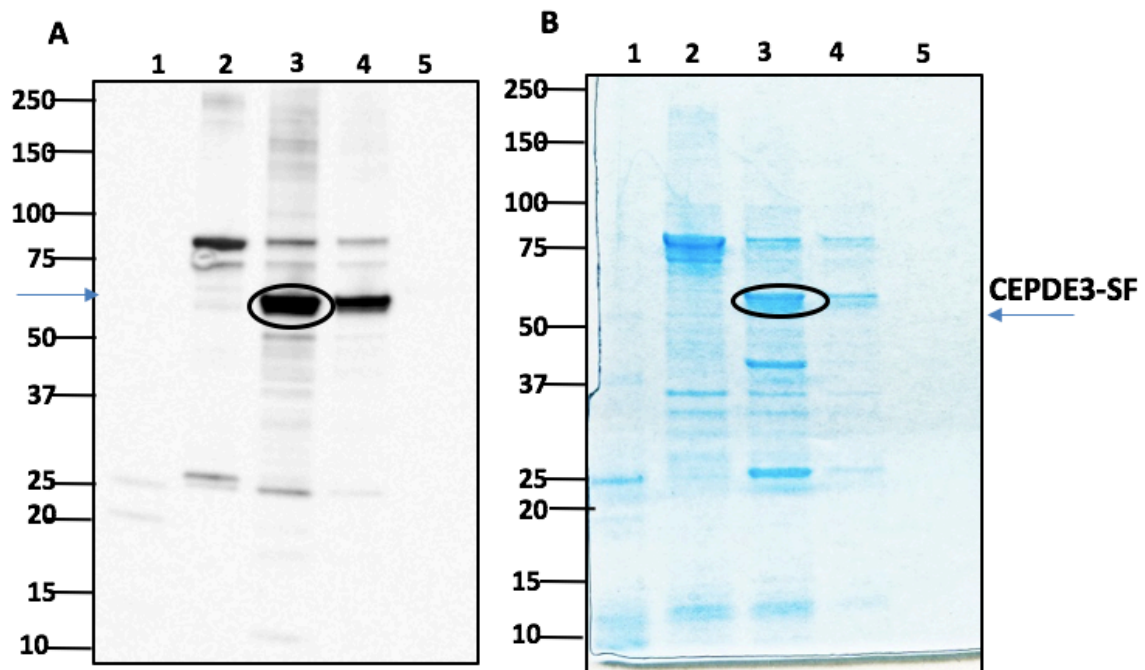


Figure 5.21: Analysis of enzymatic cleavage samples from PreScission protease using direct enzyme incubation

Soluble supernatant of CEPDE3-SF derived from ultracentrifugation was subjected to enzymatic cleavage in solution and incubated with glutathione sepharose beads. Panel A: western blot and Panel B: coomassie gel stains. Lane 1 in both gels contain MW marker, lane 2: soluble supernatant, lane 3: eluate post enzyme cleavage, and lane 4 contains sample of beads post enzyme cleavage. Western blot incubated with CEPDE3-SF N-terminus antibody.

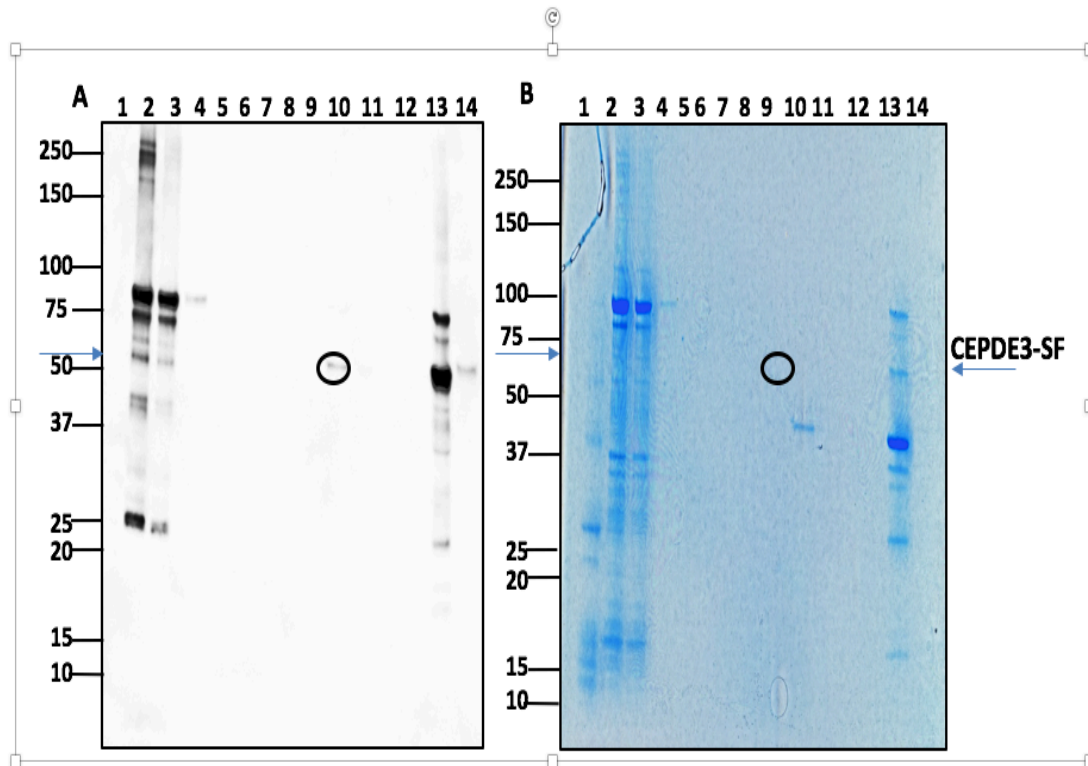


Figure 5.22: Analysis of enzymatic cleavage samples from PreScission protease using batch method

CEPDE3-SF purification soluble fractions extracted using ultracentrifugewas subjected to on-colum enzyme cleavage using glutathione sepharose 4B. Panel A western blot and Panel B coomassie gel stain. Lane 1 contains marker, lane 2: supernatant, lane 3: flow-through, lanes 4-8 contain wash fractions before elution, lane 9 contains eluate, indicated by circled bands, lanes 10-12 contains wash fractions post elution, lane 13 contains beads after elution, and lane 14 contains CEPDE3-SF Flag-tag control.

5.3.10: Summary from protein purification experiments with CEPDE3-LF and SF isoforms

Batch purification of CEPDE3-LF and SF isoforms using affinity chromatography with glutathione sepharose 4B significantly improved binding efficiency with additional changes made in the protocol by adding 10 mM DTT with protein incubation, using French-press for cell-lysis and, reducing viscosity of the bacterial supernatant. Proteins were more effectively eluted through on-column enzyme cleavage using PreScission protease than using an elution buffer containing reduced glutathione. Overall, the purification results were significantly improved, however it was important to produce pure proteins with higher yield in an mg/ml quantity for further crystallization studies. Based on these parameters, several conditions were screened with the long-form to increase binding efficiency and purity. However, neither regeneration of glutathione sepharose 4B or preclearing the beads by incubation with BL21 competent cell lysate, improved binding efficiency of the CEPDE3 proteins to glutathione resin. Ion exchange chromatography was also attempted, but failed to improve the yield. Therefore, additional fractionation by high-speed ultracentrifugation was applied, and this measure resulted in a clear soluble supernatant which gave a clean protein band on a SDS-PAGE gel. However, the protein fraction when subjected to enzymatic cleavage resulted in multiple bands at lower molecular weights. An additional polishing step (incubating with glutathione sepharose 4B) failed to give the desired purity.

Experimental analysis from various protein purification techniques for both CEPDE3-SF and LF isoforms demonstrated that the most effective method for purifying the GST-tagged isoforms was affinity chromatography based on batch method in a small scale. Therefore, batch purification method was continued with glutathione sepharose 4B and on-column cleavage. As an effective measure, batch purification experiments were performed in multiple batches using eppendorf tubes (1.5 ml) as an alternative to performing large scale purification with (10-15 ml) soluble protein supernatant. Small scale purification allowed effective enzyme cleavage with a limited amount of PreScission protease enzyme (10 units), in comparison to the large amount of enzyme (~300 units) required for large batch experiments. Several fractions of eluted protein were collected together, dialyzed using a dialysis cassette and concentrated. This concentrated protein (~3 mg/ml) was further analyzed on native gels (Fig 5.23) and SDS-PAGE (Fig. 5.24) for comparison.

Native gels use non-denaturing gel electrophoresis; the gels are run in the absence of SDS. Therefore, protein separation is dependent on both the protein charge and its hydrodynamic interactions. Native gels are sensitive to any factors that affect the protein conformation and protein charge, hence they are a valuable tool to detect protein changes due to degradation, unfolded oligomers and protein aggregates. Native gels also allow the physical size of the folded complex to remain intact, and hence helps to analyze the biomolecular structure of protein complexes. The purity of the CEPDE3 isoforms was analyzed by examining the nondenatured CEPDE3 protein on native gels (Fig. 5.23), in order to determine the number of bands and to evaluate its efficiency for further studies of crystallization. Both SF and LF had a single band visible. MW markers did not appear either because of the staining intensity of the cathode buffer

or the poor quality of the marker. Further studies of crystallization with the isoforms will be carried out by Dr. Hengming Ke's laboratory at University of North Carolina.

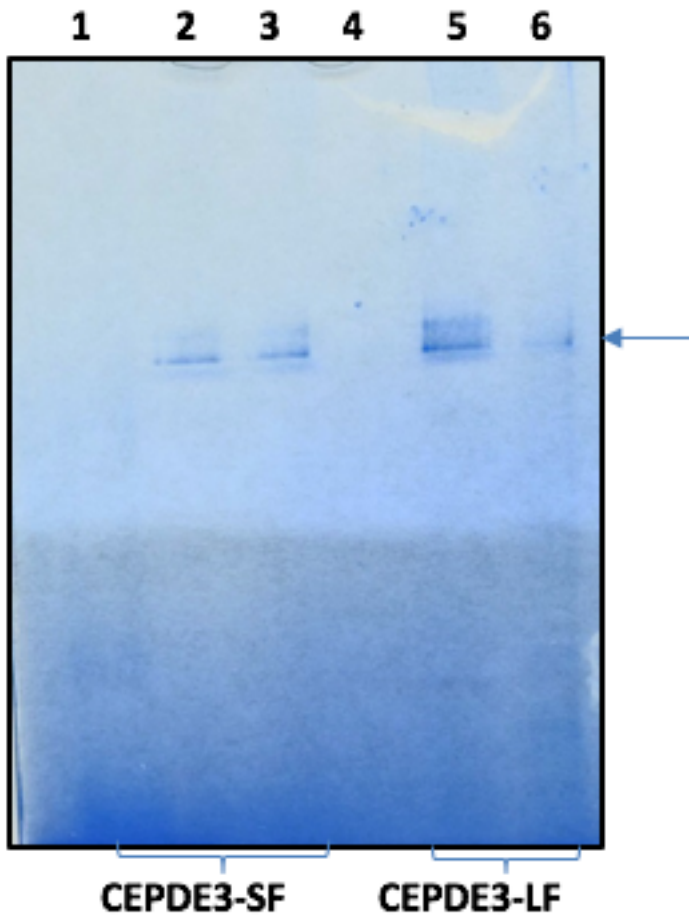


Figure 5.23: Analysis of purified CEPDE3 proteins on native gel

Purified CEPDE3-SF and LF fractions were analyzed on native gels. Duplicates of purified protein samples were loaded with LF and SF each to analyze the purity. Lane 1 contains MW marker, lanes 2 and 3 contain CEPDE3-SF samples in duplicate, lane 4 contained no sample, and lanes 5 and 6 contain CEPDE3-LF samples.

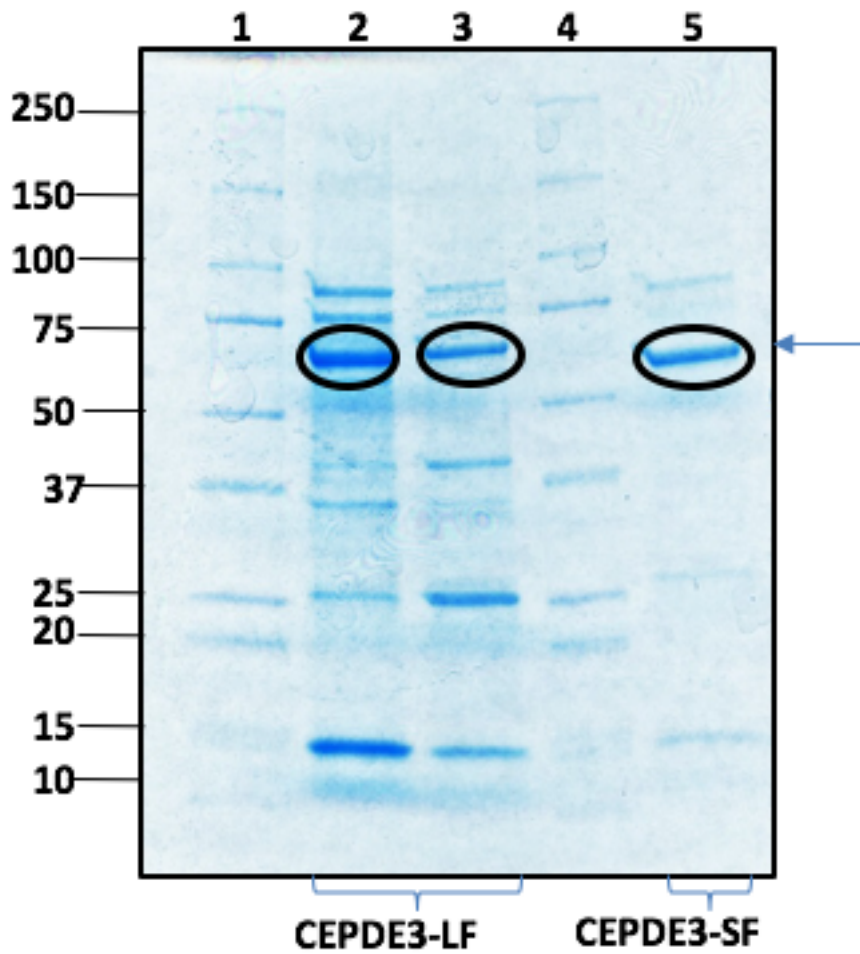


Figure 5.24: Analysis of purified CEPDE3 proteins by coomassie staining

Concentrated purified protein samples of CEPDE3-SF and LF using amicon centrifugal tube were analyzed by coomassie gel staining. Lane 1 and 4 contain marker. Lanes 2 and 3 contain CEPDE3-LF protein from two separate purification preparations. Bands correspond to ~63.5 kDa, the predicted size of LF, and lane 5 contains CEPDE3-SF, band size corresponds to ~58 kDa the predicted size of SF.

5.4: Discussion

5.4.1: Affinity Purification

Overview: CEPDE3 purification study was carried out using the technique of affinity chromatography. In the initial phase, Histidine-tagged constructs of CEPDE3 isoforms were purified using IMAC, this purification resulted into limited success, due to no binding of CEPDE3 to the resin, in addition, low levels of protein expression and solubility were observed with His-tag CEPDE3. As an alternative measure, new constructs of CEPDE3 isoforms were designed to be overexpressed as GST-fusion proteins to facilitate purification of both CEPDE3 long and short isoforms. Accordingly, soluble protein fractions were purified using glutathione sepharose 4B resin using a batch method. On-column cleavage was effective to cleave the GST-tag to release the protein from the beads. To increase protein yield and level of purity, an optimizing study was performed to screen various techniques in improving the binding capacity of the recombinant CEPDE3 proteins.

In general, affinity chromatography for purifying proteins is usually designed before the proteins are characterized, or the nature of the protein is known. Therefore, it is critical to evaluate the most favorable conditions for protein purification (Mercado-Pimentel et al., 2002). Screening procedures for testing the optimal conditions with a small scale protein culture is often helpful in determining the most suitable conditions to produce a large scale of recombinant proteins. The importance of using fusion-tags in purification studies was discussed earlier in Chapter 4, (section 4.1.2.2). Affinity-tags allow a relatively simple technique to purify proteins from a crude bacterial lysate. Using affinity-tags enables researchers to produce a large amount of proteins in mg/ml amounts and purify them, without requiring multiple techniques for further removal of nucleic acids or other cellular debris. Hence, in this thesis study the CEPDE3 isoforms were subcloned into a GST-tag pGEX-6P1 vector to facilitate purification study of CEPDE3 isoforms.

5.4.2: Challenges with protein purification

Earlier, the His-tag CEPDE3 purification study of CEPDE3 isoforms using immobilized metal affinity chromatography (IMAC) was attempted. The concept of purifying proteins based on IMAC involves the interactions between the metal ions Zn^{2+} , Ni^{2+} , and Co^{2+} used for rapid purification of proteins in *E. coli*. The CEPDE3-SF and LF His-tag proteins were purified, using Ni^{2+} and Co^{2+} columns, which resulted in poor or no binding of the His-tagged proteins. However, His-tag protein purification studies have known to be successful in various expression systems, including bacteria (Bornhorst et al., 2004). In my studies with CEPDE3 His-tag constructs, experimental data demonstrated that CEPDE3 isoforms resulted in poor expression with limited solubility. With failed attempts in purifying the His-tagged proteins, a high expression system combined with an affinity tag was essential to aid further purification. Accordingly, the GST-fusion was considered suitable for purifying the CEPDE3 isoforms. It has also been indicated in literature that the GST fusion system has had an impact on high level protein expression and purification (Terpe, 2003; Harper and Speicher, 2008).

5.4.3: GST fusion system

In the study with CEPDE3 isoforms, the glutathione S-transferase (GST) gene fusion system was chosen to aid IPTG inducible expression of GST-tagged CEPDE3 SF and LF isoforms.

Setting up small scale screening of purification studies allows testing of several conditions for protein purification (Sala and de Marco, 2010). Accordingly, GST-spin trap columns were used to evaluate optimal conditions and binding efficiency in a small volume (250-500 μ l of supernatant). However, the most common challenges faced in protein purification experiments are low solubility and poor binding to resin. The challenges of low expression and solubility were addressed by optimizing expression and induction at lower temperatures and a technique called cold shock increased the solubility of proteins. Purification techniques were also optimized using a range of buffers based on pH and concentration as recommended in the (GST protein purification handbook from G.E. Healthcare).

In the CEPDE3 protein purification study, the batch method was performed by transferring the resin from the column into a tube, due to the small capacity of the columns. A small volume of cell lysate (\sim 600 μ l) with PBS and Tris-HCl based buffers produced a similar protein yield by comparing the two buffer conditions. However, while the binding capacity was improved based on optimizing buffer conditions and incubation time, releasing the proteins from the columns were challenging, since the protein remained bound to the beads. Using increasing concentrations of reduced glutathione did not show any improvement. To analyze the amount of proteins bound to the glutathione sepharose beads, SDS sample buffer was applied to a small aliquot of beads and analyzed on a gel. Gel analysis indicated a fair amount of protein remained bound to the bead resin. Hence, it was critical to consider on-column cleavage with PreScission protease to release protein from the column. Overall, the use of GST-spin trap columns helped in screening optimum binding conditions at lower temperature and determine suitable buffers for purification.

5.4.3.1: Challenges with small scale purification

One of the factors that affect the binding of protein to media is the flow rate. The binding kinetics between the GST fusion protein and the glutathione sepharose are relatively slow, hence it is essential to keep the flow rate low during the application time of protein mixture to the resin, in order to maximize binding capacity (Swaffield and Johnston, 2001). When using the batch method with CEPDE3 isoforms, the samples were incubated with beads by gentle shaking on a rocking platform, for efficient binding. Doing so resulted in longer exposure of the fusion protein to glutathione sepharose 4B resin. Thus, the batch method technique in the cold room (at 4°C), with longer incubation time and slow rotation, was effective in increasing the binding capacity of the proteins to the beads. Another factor to be considered during elution of the bound protein was the time and volume of elution buffer, which can vary with every protein (Frangioni & Neel, 1993; Mercado-Pimentel et al., 2002; GST purification system handbook). Therefore, removal of the protein from the beads, was accomplished by cleavage of the GST tag using PreScission Protease treatment

5.4.3.2: Challenges with binding efficiency in GST-tag proteins

While screening conditions for protein purification studies, it is also important to analyze all fundamental steps from protein expression, cell-lysis and homogenization. The bacterial cell-lysis process is a critical process, hence it is important to ensure that the cells are effectively processed and fractionated, to isolate soluble and insoluble protein. Although this is not a complex process, it may be difficult to assess if a protein is present in the insoluble form, depending on the nature of protein, and its folding may result into an overestimation of the concentration of the soluble form. In addition, large affinity tags can sometimes impart metabolic stress on cell machinery, during high levels of recombinant protein production (Costa et al., 2014).

An efficient way to study and assess the nature of protein is analyzing the various protein expression and purification fractions on an SDS gel, which in turn may also be beneficial to determine, if further optimization techniques are required during cell-lysis to improve extraction. There have been several methods proposed to increase binding efficiency, including the gentle handling of protein samples during cell-lysis, to avoid the denaturing of proteins. CEPDE3 proteins were lysed initially by sonication, and then using the French press technique, the latter technique was effective in increasing the protein extraction into the soluble form, as compared to the sonication technique. In batch method purification, it is also necessary to assess the proportion of proteins and beads, exceeding the column capacity may result in inefficient binding of the protein to the glutathione resin and may decrease the binding efficiency and increase the amount of proteins to occur in the flow-through. In CEPDE3-SF and LF batch method study, this was a common problem and was addressed by preparing a 50% slurry of glutathione sepharose for efficient binding of CEPDE3 proteins.

Addition of up to 10-20 mM DTT is another alternative proposed for effective binding of GST-tagged proteins, DTT can also be added in elution buffer (Harper and Speicher, 2008). Adding DTT may also reduce the risk of oxidation of the free SH-groups located on GST, which may cause aggregation of the target fusion protein and result in low yield of GST protein and may also result in low yield of purified protein (Harper and Speicher, 2011; GST fusion handbook). Addition of 10 mM DTT was added to the CEPDE3 soluble supernatant while attempting the batch method purification study. The experiments with CEPDE3 purification showed an increase in binding capacity of the protein samples. Alternatively, reducing the viscosity of the protein samples is also essential in the purification process as it may interfere with the binding limit to the glutathione resin, if the protein has any cell debris or solid aggregates, hence reducing the viscosity of the soluble protein may help to improve binding of the proteins to the beads. Accordingly, these measures were effectively applied in CEPDE3 isoforms, by centrifuging the bacterial supernatant at 10,000xg and further diluting ~4-5 times to reduce viscosity and followed by addition of 10 mM DTT. These measures were effective in efficient binding of GST-tagged proteins to glutathione sepharose 4B in comparison to the previous studies from GST-spin trap purification as discussed in (Fig. 5.8 and 5.9).

Simultaneously, to investigate the binding capacity of CEPDE3 isoforms to the glutathione sepharose 4B columns, a control experiment was performed to assess the binding capacity of

GST protein (26kDa) to glutathione sepharose. using a range of incubation times from (2, 4, 6, 8 hours and overnight) helped to evaluate the optimal condition and assess if binding increased with increased incubation times at 4°C (Fig. 5.7). Experimental data demonstrated that, binding was efficient at all ranges of time intervals, however longer incubation times showed, effective binding, as less protein was coming out from the beads in the unbound fraction. This experimental analysis helped to estimate the efficient time for incubation using the glutathione sepharose 4B with both CEPDE3 isoforms.

5.4.4: Importance of buffers and pH range in protein purification

A range of salt gradients, from no to low or high salt (NaCl) concentrations, are commonly used to exchange, release bound molecules from the glutathione beads. The pH of the buffers used also play an important role, as the charge of a protein is based on pH. Purification studies suggest that it is important to calculate the pI of the target protein, in order to develop a successful strategy of purification (Harper and Speicher, 2008). The pI is the pH of the protein at which it has no charge. If the protein has an acidic pI, the buffers should be prepared at least one pH unit above the pI of the protein, so that the protein is negatively charged. Anion exchange is suitable for these proteins. In contrast, if the protein has a basic charge, cation exchange is suitable and buffers with pH, one unit below should be suitable to ensure that the protein is positively charged (Duong-Ly and Gabelli, 2014).

Using the tool EXPASY, (<http://ca.expasy.org/tools/protparam.html>). The PI of the CEPDE3 isoforms was calculated, CEPDE3-LF alone would have a pI of 5.9 and CEPDE3-SF had a pI of 5.10. The pI of both the CEPDE3 isoforms were close to each other and in the acidic range. However, introducing the GST-tag with CEPDE3 isoforms may alter the PI range. The GST-tag consists of 26 kDa protein and has an isoelectric point in the pH range of 4-5 (Gronwald and Plaisance, 1998). The protein solubility screening study was performed using a range of buffers at different pH. It was determined that both PBS buffer pH 6.2 and 7.4 were optimum, and increased protein binding. Hence, they were chosen as the optimum cell-lysis and purification buffers for CEPDE3 purification.

5.4.5: PreScission protease cleavage

The PreScission Protease is a fusion protein of the glutathione S-transferase (GST) tag and human rhinovirus (HRV) type 14 3C protease with a size of 46 kDa. The mechanism is not very clear as to why the 14 3C protease evolved from a group of viruses as an enzyme for proteolytic cleavage. Rhino 3 virus has also been fused to MBP and His₆ tag in *E. coli* DsbA. Some recent studies have also reported that the enzyme can be fused to the biotin acceptor peptide (BAP) (Waugh, 2011). The PreScission Protease is known to recognize a subset of sequences which include the core amino acid sequence Leu-Phe-Gln/Gly-Pro, cleaving between the Gln and Gly residues. However, the protease carries the disadvantage of leaving behind a Gly-Pro dipeptide on the N-terminus of the recombinant protein after digestion (Weidner and Dunn, 1991). While affinity tags can retain the structure of the recombinant protein and enhance other biochemical properties, such

as solubility, it can be essential to remove the tag for further characterization of the protein. Furthermore, GST forms a homodimer, and if the oligodimeric state of the protein can affect the properties of the target protein, it is preferable to cleave off the GST-tag (Harper and Speicher, 2011).

Also, the tag may alter the structure of the protein and cause difficulties in determining the crystal structure. In theory, the GST tagged proteins containing a PreScission Protease recognition site that can be cleaved either when it is bound to glutathione sepharose or in solution, when the protein is eluted. In addition, the bound protein can be eluted further using elution buffer and optimizing the suitable elution conditions. Ideally, the GST moiety would remain attached to the column and, thus, the protein would be in a purified form without a tag. The pGEX-series of vector have cleavage enzymes available for the cleavage of GST-tag. In addition to PreScission Protease, other enzymes that can be used are bovine thrombin and bovine Factor Xa. However, in the study with CEPDE3 protein purification, only PreScission protease was used. Substrate recognition and cleavage are mostly dependent on primary structure signals, as well as a combination of secondary and tertiary structure of the protein. Since the protease is fused to GST, it can be cleaved with ease while the protein is bound to the glutathione sepharose. To rule out the possibility of interfering proteases, it is often advisable to use protease deficient (*lon* and *OmpT*) *E. coli* strains. Therefore, the CEPDE3 isoforms were expressed in BL21-DE3, a protease deficient strain of *E. coli*.

.

5.4.6: Study of Large scale purification using batch method

My goal for this thesis was to produce a sufficient amount of purified protein for the crystallization of the CEPDE3 isoforms. While carrying out the experiments with on-column purification, further experiments were attempted to increase the volume of the chromatography media to scale up, and increase the capacity to produce recombinant proteins. Therefore, the batch method was followed, allowing the size of column (or volume of glutathione sepharose used) to be increased proportionately to the amount of protein mixture loaded. In CEPDE3 protein purification, a 1.33 ml volume of glutathione sepharose 4B beads was resuspended in 1 ml of buffer to prepare 50% glutathione slurry, ~ 10 ml of 4x solution of bacterial lysate was applied to this slurry for overnight incubation. The final purity of the protein was estimated by the ratio of the amount of protein loaded on to the glutathione sepharose 4B and thus the amount of soluble protein mixture required to produce the necessary amount of purified protein can vary. However, it is not always straightforward to implement these purification protocols. The amount of protein recovered with a small batch purification method can vary from the large scale purification. Also the optimum conditions may vary depending on the size of protein (Sala and de Marco, 2010). An optimization study based on small scale screening using the GST-spin trap columns demonstrated that protein purification performed in a batch method was effective, however protein yield was low and problems were detected at any of the three steps: 1) binding of the protein to glutathione sepharose, 2) cell-lysis and homogenization, or 3) elution. To overcome these problems simple trouble shooting procedures were designed and tested, as described above in Chapter 5 (section 5.3.6).

Scaling up purification methods primarily involves overexpressing large amounts of recombinant proteins and it can be challenging to large amounts. It is a common issue for the expression of eukaryotic proteins in a soluble form (Mercado-Pimentel et al., 2002) As discussed earlier in Chapter 4 (section 4.4.3) various techniques were applied towards producing a high yield of recombinant proteins. Proteins overexpressed in *E. coli* can be insoluble for a number of reasons, including rapid growth leading to improper folding and insufficient chaperones being present. As an alternative technique to overcome problems with insolubility, the use of ionic and non-ionic substances, such as detergents, have been recommended to solubilize proteins (Frangioni & Neel, 1993; Tao et al., 2010). The use of detergents for extracting soluble protein does not limit the binding of GST to glutathione sepharose or alter the properties of the purified target protein. Modifications in cell-lysis methods using 1% Triton X-100 and lysozyme did not alter protein solubility on CEPDE3 proteins. To deal with protein insolubility, screening expression studies with lower temperature settings, with a range of 15-25°C is ideal (Harper and Speicher, 2011). Accordingly, implementing the lower temperature induction protocol for CEPDE3 resulted in increased solubility.

5.4.7: Alternative approaches for scaling up CEPDE3 protein purification

5.4.7.1: Protein fractionation by ultracentrifugation

Protein fractionation is typically carried out by subjecting bacterial cell lysate to centrifugal forces which may gradually increase. Fractionating the cell lysate, helps to analyze which of the fractions obtained, contain the protein of interest. In an ultracentrifuge, high centrifugal forces (up to 70-100,000xg) were used to separate the protein mixture. Due to the high centrifugal force, the separation of proteins was easier, and dependent on size, as high mass particles move outwards, as compared to smaller ones ("Protein Purification Protocols | Paul Cutler | Springer," 2004). In purifying the CEPDE3 isoforms, we aimed to purify the protein by increasing its purity, and thus increasing its enzyme activity. By subjecting the cells to increasing centrifugal forces gradually, the cells which were denser formed a pellet at lower centrifugal forces, than the less dense material. Applying 100,000xg centrifugal forces, led to the recovery of > 80% of the soluble protein from the insoluble cell-pellet and resulted in a clean band for CEPDE3-LF (Fig 5.14 and 5.15). However, further experiments leading to GST-tag cleavage were challenging, the purified protein band was close to the predicted size of CEPDE3 proteins. The fractionated CEPDE3, post enzymatic cleavage resulted into additional protein bands of lower molecular weight (Fig 5.20 and 5.21) for CEPDE3-SF. It wasn't clear why a clean soluble protein post enzymatic cleavage produced multiple low molecular weight bands. Possibly, they could be *E. coli* bands or an effect of the PreScission protease enzyme. The protease carries the disadvantage of leaving behind a Gly-Pro dipeptide on the N-terminus of the recombinant protein after digestion (Weidner and Dunn, 1991). Based on the experimental analysis, the fractionation method using ultracentrifugation was not considered suitable for increasing the protein yield and purity. Accordingly, further measures with other screening techniques for purification were attempted.

The technique of Ion exchange chromatography based on the principle in which molecules are separated depending on net surface charge via cation and anion exchangers. As discussed earlier in section 5.3.8, both types of IEX consist of highly charged matrix. The anion exchangers attract positively charged molecules and negatively charged molecules associate with cation exchangers. Depending on the pI of the protein, suitable ion exchange columns can be used. As an alternative to glutathione sepharose, DEAE sepharose were used to purify the CEPDE3 isoforms. An important factor considered in this process, is the pH of the buffers used for binding and elution, as this is dependent on the charge of the protein (Duong-Ly and Gabelli, 2014). In purification studies with CEPDE3 isoforms, it was important to determine the efficiency of this chromatography system to purify the isoforms to produce high yield protein, in a cost effective way. Using the DEAE sepharose columns, several buffers were screened to determine optimum conditions. Since the binding of proteins to DEAE sepharose is based on fixed charges, and their elution, or displacement, is also dependent on fixed charges, elution carried out using increasing concentrations of salt did not help. Proteins are sticky in nature, and adhere to surfaces, but adding higher salt for adsorption can lead to precipitation and destroy its activity. Proteins can be concentrated by adsorption to IEX in low salt, and eluted under high salt conditions (Rossomando, 1990). Unfortunately, elution was inefficient with all three buffers. Changing the

buffer pH and switching to a Tris-HCl-bis buffer did not improve elution. Therefore, studies with ion exchange chromatography did not yield efficient results for protein purification, in comparison to the affinity chromatography technique using glutathione sepharose 4B medium, which was effective.

In conclusion, experimental findings derived from optimization study screening from various technique, indicated that the batch method purification with on-column cleavage on a small scale (~1-1.5 ml) was effective, as compared to large scale (10-15 ml) volume. Thus, instead of scaling up technique to produce an increased amount of protein in big batches, an alternative of purifying several fractions on a small scale was considered an effective technique for purification, as only a small amount of enzyme ~20 units (10 μ l) was essential for effective cleavage, which proved cost efficient in carrying out experiments in small batches. After further analysis using native gel electrophoresis, and based on further discussion with the collaborator for further studies (Dr. Hengming Ke at the University of North Carolina), it was determined that the band purity was fine for crystallization. However, the protein concentration was still low after concentrating the pure protein fractions. Hence, other preparations were carried out individually, not combining fractions together, to avoid diluting the concentration of the protein. After purifying these proteins, they were stored at -80°C for future crystallization studies to be carried out by Dr. Ke's lab.

Chapter 6

Chapter 6: Enzyme kinetics of *C. elegans* Phosphodiesterase 3 short form and long form (CEPDE3-SF and LF)

6.1: Introduction

The superfamily of PDE enzymes consists of 21 gene families, each family encoding different isoforms. Further splicing variant and isoforms of each family adds to the complex nature of PDEs (Conti et al., 2014). Cyclic nucleotide PDE enzymes are characterized based on their amino acid sequences, substrate specificities, regulators, endogenous and exogenous locations, and pharmacological properties (Mehats et al., 2002; Manganiello et al., 2013). As cyclic nucleotide phosphodiesterases break the phosphodiester bond in the second messengers cAMP and cGMP, these enzymes play an important role in signal transduction mediated by these second messengers. Thus, the cyclic nucleotide signaling system has an important role in PDE activity and has been extensively studied for many years. In particular, cAMP and cGMP regulate multiple cellular functions. Many of the earlier studies conducted on PDEs demonstrated that these signaling molecules were important for modifying PDE activity (Bender and Beavo, 2006). With the advances made in the study of cyclic nucleotides, and different assays designed for the study of PDE activity, it was clear that every PDE family contained many different isoforms, with each having several biochemical and kinetic properties. This chapter focuses on studying the PDE enzyme activity of the CEPDE3 isoforms, the enzyme inhibition using the PDE3 specific inhibitor cilostamide, and the hydrolysis of cAMP and cGMP based on substrate specificities of CEPDE3 enzymes. Performing these studies enabled us to further characterize the CEPDE3 isoforms based on PDE3 activity in protein fractions versus purified proteins. Using the PDE3 specific inhibitor cilostamide, allowed us to analyze the percentage of inhibition and calculate the IC_{50} of the isoforms. Furthermore, studying hydrolysis based on both the substrates would ideally allow the quantitative analysis of the K_m and V_{max} values of each isoform based on their substrate affinities. This analysis would be helpful in comparing the activity of the CEPDE3 isoforms to that of mammalian PDE3.

6.2: Aims

This chapter aims

- To characterize the CEPDE3 isoforms (CEPDE3-LF and CEPDE3-SF) expressed in *E. coli* by determining their PDE3 activity and IC_{50} values using the PDE3 specific inhibitor cilostamide
- To study the cAMP and cGMP hydrolysis using CEPDE3 proteins expressed in insect cells.

6.3: PDE enzyme assay

An enzyme is very selective to the reaction it catalyzes, and with the substrates with which it interacts. Thus, in an enzyme-catalyzed reaction, the products formed by a given enzyme are also specific, as no byproduct is formed. In PDE enzyme assays, the PDEs catalyze the substrate cAMP. The goal of the PDE enzyme assay was to determine the enzymatic activity of the CEPDE3 isoforms by measuring catalysis of their substrate cAMP. In this assay, ³H-labelled cAMP was degraded to ³H-5'-AMP by PDE in each sample during a specified time. ³H-5'-AMP was then degraded to ³H-adenosine with nucleotidase present in *Crotalus atrox* venom. The nucleotidase hydrolyzed nucleotides only, so it did not affect any remaining cAMP. Substrates and products were then separated on anion exchange columns; cAMP binds to the resin, and adenosine passes through the column directly into a scintillation vial. As a result, the amount of adenosine produced can be measured by scintillation counting and is proportional to both PDE activity in the sample and to a given time.

6.3.1: Earlier studies on PDE3 enzyme activity

Initial enzyme activity studies were performed on cell-lysates derived from cells expressing His-tagged recombinant proteins of CEPDE3-SF and LF as discussed in Chapter 4, section 4.3. His-tagged proteins were induced in presence of IPTG at 37°C. CEPDE3-SF soluble supernatant was assayed for PDE enzyme activity and it showed low enzyme activity; repeating the experiment did not show any change in results. Measures were taken to revise the assay protocol and buffers were carefully assessed for the pH values. Simultaneously, attempts were made to improve protein expression; *E. coli* BL21 competent cells were transformed with CEPDE3-LF and CEPDE3-SF plasmids and protein soluble fractions were assayed for enzyme activity. Flag-tagged mouse PDE3B (MPDE3B) recombinant proteins expressed in insect cells was used as a control against CEPDE3 proteins expressed in *E. coli* (MPDE3B lysate was provided by Dr. Faiyaz Ahmad, a Staff Scientist at NHLBI). The Flag-tagged MPDE3B recombinant protein showed a higher enzyme activity than the His-tagged CEPDE3 proteins. Despite attempts made to optimize the protein expression levels and PDE enzyme assay, there was no improvement in the PDE activity. In an effort to overcome these limitations, new constructs were designed to be expressed as CEPDE3-LF and SF GST-tagged proteins in pGEX-6P1 vector. PDE3 activity of the protein fractions assayed in the initial phase of study are summarized in Table 6.1.

Table 6.1: Summary of PDE activity in protein fractions in the early phase of CEPDE3 study

Protein fractions of cell-lysates expressed using the Histidine-tag were assayed for PDE activity against a control of PDE expressed in mouse.

Protein fractions	PDE activity pmoles/min/mg
His-tag CEPDE3-LF	0.132
His-tag CEPDE3-SF	0.042
Flag-tag MPDE3B	1.689

6.3.2: PDE3 enzyme activity in CEPDE3-LF expressed in bacteria

GST-tagged constructs of CEPDE3-LF proteins were overexpressed and induced by IPTG at lower temperature as discussed in Chapter 4, section 4.3.4. CEPDE3 protein fractions (total cell-lysate, soluble supernatant, and insoluble cell-pellet) were assayed to determine PDE and PDE3 enzyme activity using the PDE3 specific inhibitor cilostamide at 1 μ M concentration (refer to Chapter 2, section 2.10 for a detailed protocol of PDE enzyme assay). Approximately 200 ml of total cell-lysate was fractionated into \sim 180 ml of soluble supernatant and the insoluble cell-pellet was resuspended in cell-lysis buffer equivalent to the volume of the soluble supernatant. Aliquots from these samples were used to assay activity of protein fractions. Duplicates of each sample were compared against a sample with the PDE3 inhibitor cilostamide (see Table 6.2). Each calculation was adjusted according to the amount of enzyme added in each reaction (refer to Chapter 2, section 2.10.4 for calculations).

6.3.3: Experimental results of CEPDE3-LF protein expression in bacteria

The PDE3 enzymatic activity was calculated based on GST-tagged CEPDE3 fractions from *E. coli*, treated with and without inhibitor, using 3 H-labelled cAMP as a substrate. In a volume of 200 ml of total cell-lysate, the total PDE3 activity was 884 pmoles/min and specific activity was 2.2 pmoles/min/mg (see Table 6.2). 180 ml of soluble supernatant fractionated showed a total PDE3 activity of 644 pmoles/min and specific activity of 2.1 pmoles/min/mg. Meanwhile, the insoluble cell-pellet showed a PDE3 activity of 40 pmoles/min and a specific activity of 0.3 pmoles/min/mg. These values indicated that \sim 72 % of soluble protein was extracted from the total cell-lysate with PDE3 present.

Table 6.2: PDE3 enzyme activity in CEPDE3-LF protein expression fractions

CEPDE3-LF protein expression fractions were assayed to determine PDE and PDE3 specific enzyme activity in each protein fraction using the PDE3 specific inhibitor cilostamide.

Fractions	Protein (mg/ml)	Volume (ml)	Total protein (mg)	Total PDE activity (pmol/min)	Specific activity PDE (pmol/min/mg)	Total PDE3 activity (pmol/min)	Specific activity PDE3 (pmol/min/mg)
Lysate	2.01	200	402	1005	2.5	843	2.09
Supernatant	1.7	180	306	765	2.5	644	2.1
Cell-pellet	0.75	180	135	54	0.4	40.5	0.3

6.4: Study of PDE3 activity in purified CEPDE3-LF fractions

Clarified lysate was fractionated and purified by batch purification using glutathione sepharose 4B, as discussed in purification experiments (Chapter 5, section 5.3.6 for long-form and section 5.3.9.1 for short-form). Fractions were assayed to determine PDE3 enzyme activity (see PDE enzyme assay protocol in Chapter 2, section 2.10.3). Fractions of CEPDE3-LF supernatant, unbound, and eluted protein were assayed, using the PDE3 specific inhibitor cilostamide at a concentration of 1 μ M. In a given protein sample, there are several PDEs, including PDE3. Total PDE activity represents the activity of all the PDEs in the crude bacterial cell-lysate used in this assay, while using a PDE3 specific inhibitor inhibits only PDE3 in the sample. Hence in this assay reaction, the number of total PDEs and the number of PDE3 inhibited using the PDE3 inhibitor cilostamide were determined based on the assay calculation formula described in Chapter 2 (section, 2.10.4). The CEPDE3-LF soluble-supernatant had a PDE3 specific activity of 1.84 pmoles/min/mg (see Table 6.3), and the purified protein of CEPDE3-LF (eluate1) showed an PDE3 specific activity of 9.4 pmoles/min/mg). Thus, the purified samples of long-form showed a ~5.10-fold increase in specific activity of PDE3 in the bacterial proteins.

Table 6.3: Analysis of PDE3 enzyme activity in CEPDE3-LF protein purification fractions

CEPDE3-LF protein purification fractions obtained from purifying soluble supernatant with glutathione sepharose 4B using batch method were assayed for PDE and PDE3 activity using PDE3 specific inhibitor cilostamide.

Fractions	Protein mg/ml	Volume (ml)	Total protein (mg)	Total PDE activity (pmol/min)	Specific activity PDE (pmol/min/mg)	Total PDE3 activity (pmol/min)	Specific activity PDE3 (pmol/min/mg)
Supernatant	2.01	10	20.1	58	2.88	37	1.84
Unbound	1.9	9	17.1	37	2.16	24	1.4
Eluted	0.4	1.33	0.53	22	41.5	5	9.4

6.4.1: Study of PDE3 activity in purified CEPDE3-SF fractions

A similar experiment was carried out using protein purification fractions of CEPDE3-SF which were obtained from the experiment discussed in Chapter 5 (section 5.3.9.1). The crude soluble-supernatant used for purification had a PDE3 specific activity of 5.6 pmoles/min/mg., while the purified protein of CEPDE3-SF (eluate1) showed an PDE3 specific activity of 20.66 pmoles/min/mg (see Table 6.4). Thus, purified proteins of CEPDE3-SF had a ~ 3.6-fold enrichment in CEPDE3 specific activity after purification.

Table 6.4: Analysis of purified fractions of CEPDE3-SF for PDE3 activity

CEPDE3-SF protein purification fractions were assayed for PDE and PDE3 activity in the soluble supernatant, unbound fraction and purified eluate.

Fractions	Protein mg/ml	Volume (ml)	Total protein (mg)	Total PDE activity (pmol/min)	Specific activity PDE (pmol/min/mg)	Total PDE3 activity (pmol/min)	Specific activity PDE3 (pmol/min/mg)
Supernatant	1.5	10	15	111	7.4	84	5.6
Unbound	1.06	9	9.54	43	4.5	22	2.30
Eluted	0.11	1.33	0.15	4.35	29	3.1	20.66

CEPDE3 protein fractions were fractionated by ultracentrifugation as discussed earlier in purification of long-form (Chapter 5, section 5.3.7.3.1.) and short form (Chapter 5, section 5.3.9.1). All protein fractions were assayed to determine PDE3 enzyme activity. Table 6.5 below summarizes the enzyme activity in CEPDE3 isoforms. CEPDE3-LF had a ~ 8.8-fold increase in enzyme activity and CEPDE3-SF had a ~ 2.8-fold increase in CEPDE3 enzyme activity with samples fractionated by ultracentrifugation.

Table 6.5 CEPDE3 protein fractions from ultracentrifugation assayed for PDE activity

CEPDE3 isoforms protein fractions isolated by centrifugation were assayed for PDE3 activity.

Protein fractions	CEPDE3-LF	CEPDE3-SF
Cell-lysate	1.8 pmoles/min/mg	10 pmoles/min/mg
Purified protein	16 pmoles/min/mg	28 pmoles/min/mg

6.5: Study of enzyme activity in CEPDE3-LF expressed in insect cells

An initial CEPDE3 study conducted in the Manganiello laboratory was based on the CEPDE3 isoforms subcloned into a baculovirus expression vector and expressed as Flag-tag proteins in insect cells (Samidurai et al., unpublished 2010). Flag-tagged proteins were purified and their enzyme activity was shown to have a > 400-fold increase with purification. However, further studies with Flag-tag constructs had limitations due to the need to produce proteins in mg/ml yields. As discussed earlier, in section 6.3.1, CEPDE3 isoforms expressed as His-tagged proteins had low enzyme activity. Meanwhile, the CEPDE3-LF GST-tagged construct (2.1 pmole/min/mg, Table 6.3) had a ~ 15.9-fold increase in activity compared to the His-tagged construct (0.132 pmole/min/mg, Table 6.1). In addition, the enzyme activity of CEPDE3-LF constructs expressed in insect cells was much higher (1647 pmole/min/mg, Samidurai et al., unpublished). Accordingly, because of high enzyme activity, total lysates of CEPDE3-LF expressed in insect cells was assayed against increasing doses of cilostamide (from 0.01 μ M to 5 μ M) to determine the IC₅₀ value (see Fig. 6.1). There was a 20% inhibition of PDE3 enzyme activity with 0.01 μ M cilostamide, and fractions treated with the highest dose of inhibitor (5 μ M) showed 95% inhibition. The IC₅₀ of cilostamide was observed as ~ 0.1 μ M.

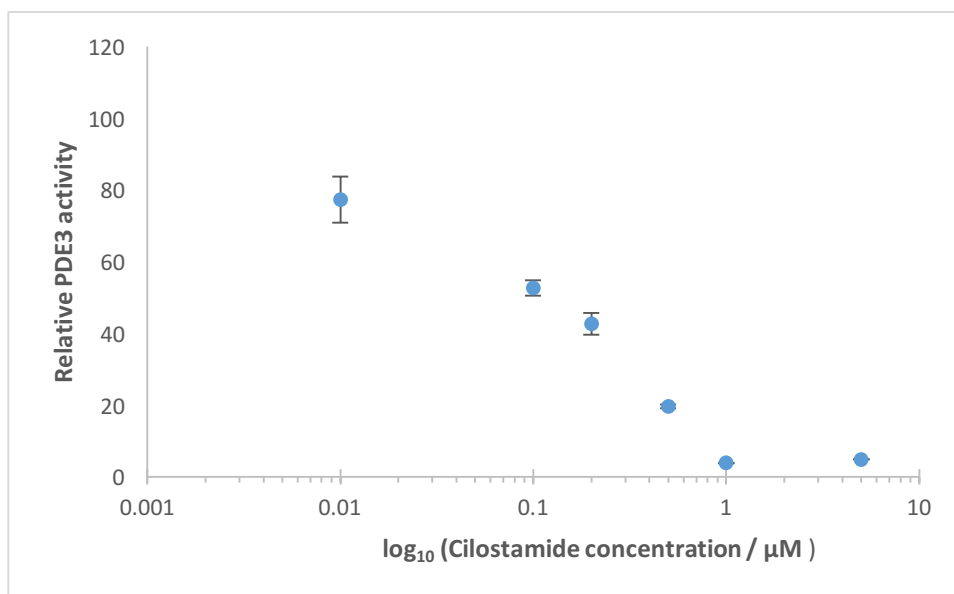


Figure 6.1: Percentage of inhibition of CEPDE3-LF protein expressed in insect cells by cilostamide.

Cell-lysates of CEPDE3-LF isoform expressed in insect cells were assayed to study the effect of increasing doses of cilostamide (from 0.01 to 5 μM). Data points represent means of three repetitions and error bars indicate the standard deviation.

6.5.1: Study of IC₅₀ in CEPDE3-LF proteins expressed in bacteria

CEPDE3-LF fractions of purified protein expressed in bacterial cells were assayed based on the same protocol described in section 6.5 with insect cells. Treatment with 0.01 μM cilostamide resulted in 20% inhibition of CEPDE3-LF activity and treatment with 5 μM cilostamide resulted into 90% inhibition (see Fig 6.2). The observed IC₅₀ of cilostamide against CEPDE3-LF was ~ 0.1 μM.

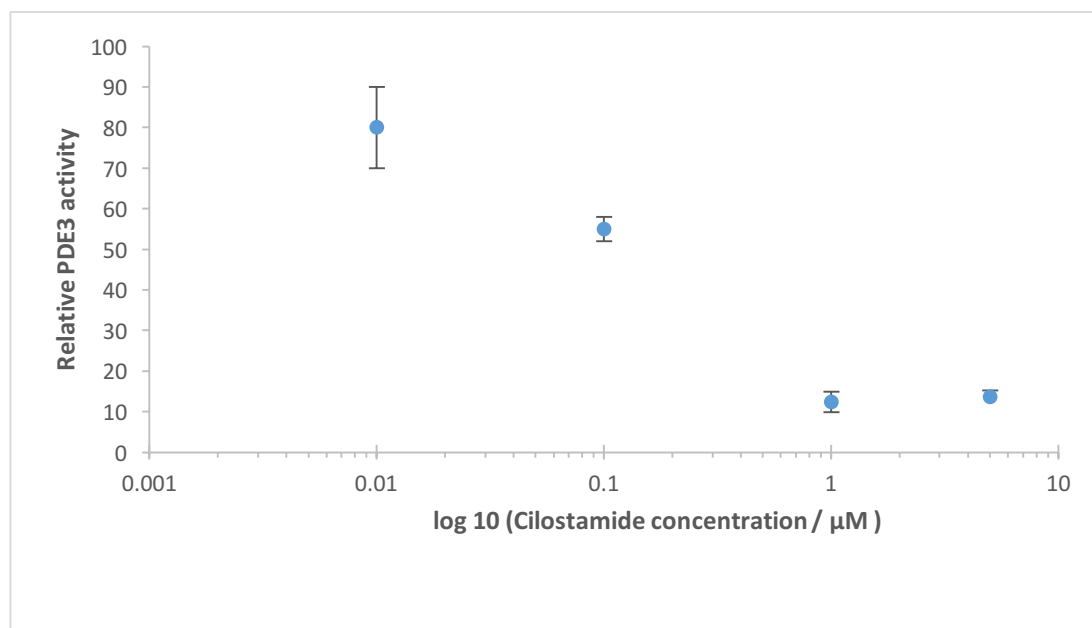


Figure 6.2: Percentage of Inhibition using cilostamide in CEPDE3-LF protein expressed in bacteria.

Cell-lysates of CEPDE3-LF isoform expressed in bacteria were assayed to study enzyme inhibition by increasing doses of cilostamide (from 0.01 to 5 μM). Data points represent means of three repetitions and error bars indicate the standard deviation.

6.5.2: Study of enzyme activity in CEPDE3-SF expressed in insect cells

CEPDE3-SF protein fractions expressed in insect cells were assayed to determine the IC_{50} of cilostamide against the CEPDE3-SF isoform. Experimental data were similar to CEPDE3-LF protein fractions as described in section 6.5. When 0.01 μM cilostamide was added, 10% inhibition was observed, and with 5 μM cilostamide, 95% of inhibition was observed (Fig 6.3). The IC_{50} value of cilostamide against CEPDE3-SF cell-lysate from insect cells was $\sim 0.3 \mu\text{M}$. Thus, this preparation appears to be less sensitive to cilostamide inhibition than CEPDE3-LF described above.

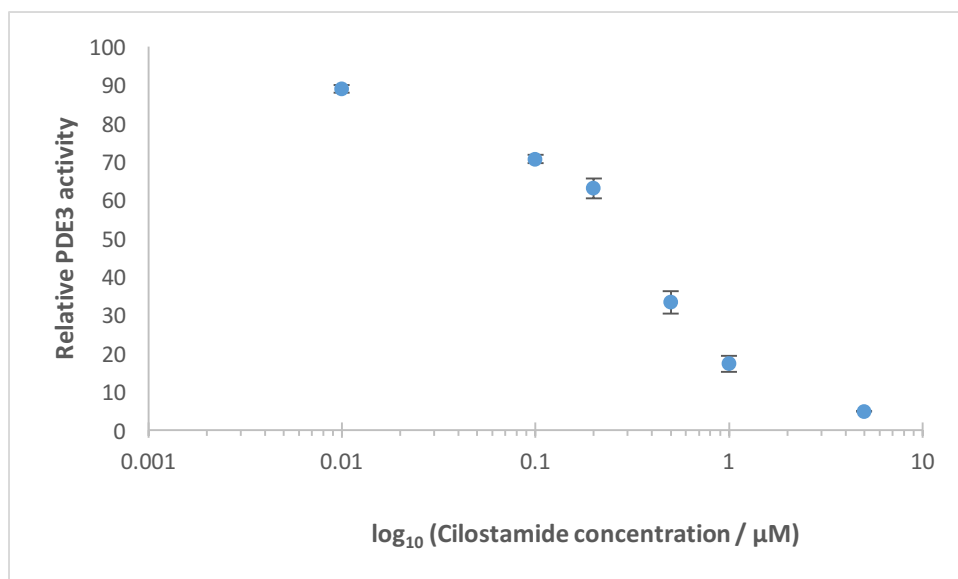


Figure 6.3: Percentage of inhibition using cilostamide in CEPDE3-SF expressed in insect cells
CEPDE3-SF proteins expressed in insect cells were assayed to study the effect of range of doses of cilostamide concentration range from 0.01 to 5 μM and thus determine the IC_{50} values. Data points represent means of three repetitions and error bars indicate the standard deviation.

6.5.3: Effects of dialysis on PDE3 activity

CEPDE3 proteins were purified using a concentration of ~ 10 mM DTT to improve binding efficiency with glutathione sepharose resin. It was not clear if the presence of DTT would affect enzyme activity since it is a reducing agent. Therefore, it was necessary to analyze if removal of DTT by dialysis would increase enzyme activity. Hence, the CEPDE3-LF purified protein samples were dialyzed and further subjected to an enzyme activity assay using the PDE3 specific inhibitor cilostamide. As a control, some undialyzed sample was also assayed. The dialyzed sample showed an increase from 20 to 50 pmoles/min/mg. Hence, a 2.5-fold increase in PDE3 specific activity was observed after dialysis of the purified CPDE3-LF protein (see Table 6.6).

Table 6.6: Effects of dialysis on CEPDE3 enzyme activity

CEPDE3-LF purified protein fractions were subjected to dialysis to determine the effect of DTT added in the purification process. Dialyzed and undialyzed protein samples were assayed to determine enzyme activity using PDE3 inhibitor cilostamide.

Protein Fractions	Protein (mg/ml)	Volume (ml)	Total protein (mg)	Total PDE (pmol/min)	Specific activity PDE (pmol/min/mg)	Total PDE3 (pmol/min)	Specific activity PDE3 (pmol/min/mg)
Eluate (10 mM DTT)	0.30	0.5	0.15	3.5	23.3	3.0	20.0
Eluate dialyzed	0.30	0.5	0.15	10.0	66.7	7.5	50.0

6.6: Study of enzyme kinetics in CEPDE3-LF and SF insect cell lysates**6.6.1: Experimental method**

Since PDE3 enzymes have a dual specificity for both cAMP and cGMP substrate, enzyme kinetics experiments were performed to assay the substrate specificity of CEPDE3. Due to the low enzyme activity of GST-tagged purified protein expressed in bacterial cells, the experiments to study cAMP and cGMP hydrolysis were performed using CEPDE3-SF and LF lysate obtained from insect cells, due to their high enzyme activity.

6.6.1.1: cAMP hydrolysis

In the cAMP hydrolysis experiments, the ³H-cAMP substrate concentration was constant. However, cold cAMP was added in increasing concentrations from 0.1 μM to 4.8 μM (see Table 6.7). In each preparation, the other buffer components were adjusted accordingly. These experiments were used to assay cell lysates from both CEPDE3-SF and CEPDE3-LF isoforms expressed in insect cells for PDE3 activity.

Table 6.7: Preparation of substrate for cAMP hydrolysis

cAMP hydrolysis was performed using constant ^3H -cAMP substrate (< 0.01 mCi) and increasing amounts of cold cAMP. All other components of the buffer were added in (ml) volume to prepare a total volume of 5 ml.

Constituents	1	2	3	4	5	6	7
Concentration cAMP	0.1 μM	0.2 μM	0.4 μM	0.8 μM	1.6 μM	1.2 μM	2.4 μM
Hepes Buffer	2.5	2.5	2.5	2.5	2.5	2.5	2.5
1 M MgCl_2	0.041	0.041	0.041	0.041	0.041	0.041	0.041
30 μM cold cAMP	0.1	0.2	0.4	0.8	1.6	2.4	4.8
^3H cAMP	0.025	0.025	0.025	0.025	0.025	0.025	0.025
DW	2.38	2.34	2.24	2.96	3.36	3.76	4.96
Total	5 ml	5 ml	5 ml	5 ml	5 ml	5 ml	5 ml

6.6.1.2: cAMP hydrolysis with CEPDE3-LF and CEPDE3-SF

6.6.1.2.1: CEPDE3-LF

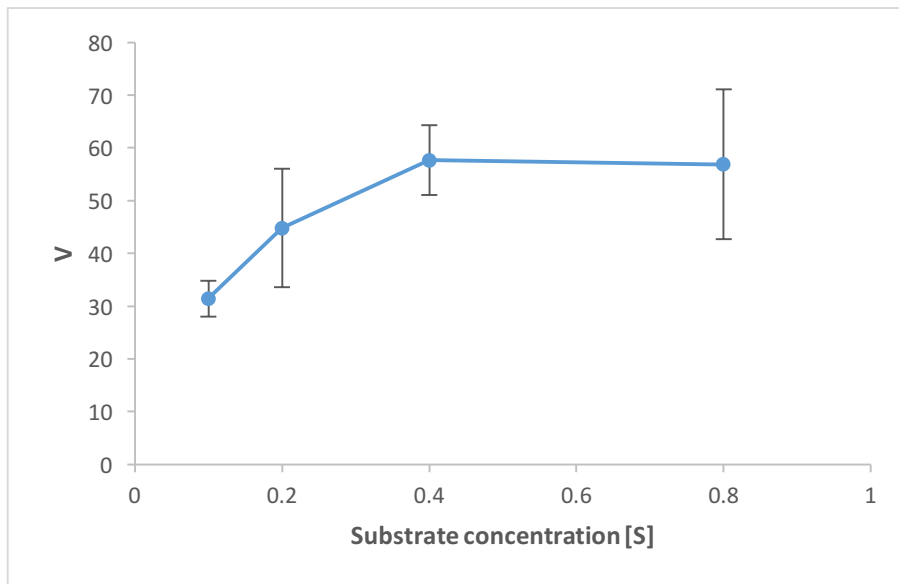
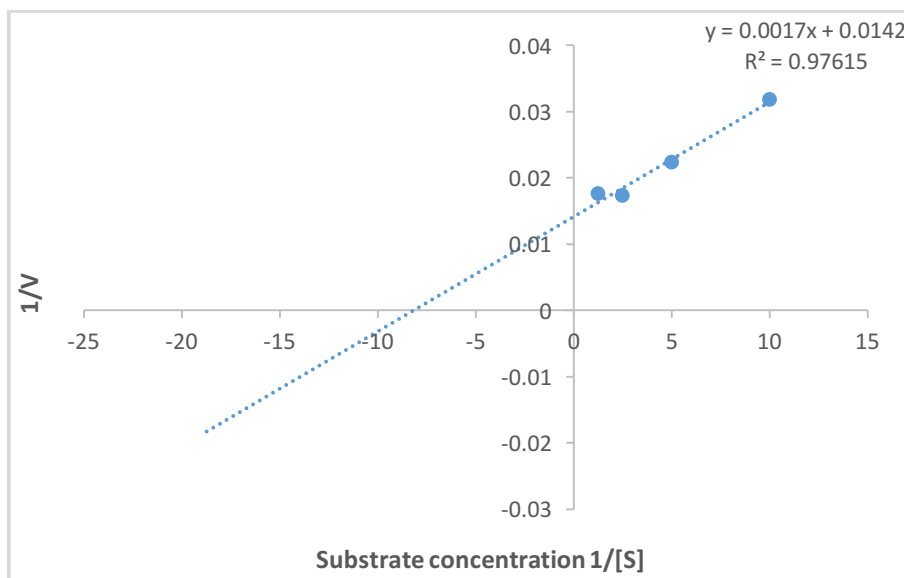
cAMP hydrolysis was performed using CEPDE3-LF lysates expressed in insect cells with substrate concentrations of 0.1, 0.2, 0.4, and 0.8 μM (listed in Table 6.7). The enzyme assays were carried out \sim 5-6 times (experimental data summarized in Table 6.8). Graphs were plotted based on the values of increasing substrate concentrations $[S]$ against V (Fig. 6.4A), and the respective Lineweaver-Burk reciprocal plot based on $1/[S]$ against $1/V$ (Fig. 6.4B). Accordingly, the K_m and V_{max} values were derived based on the graph equation of Figure 6.4B and K_{cat} was also calculated (refer to Chapter 2, section 2.10). The V_{max} for CEPDE3-LF was 70.42 pmoles/min and the K_m was 0.11 μM .

Based on this V_{max} , the K_{cat} was determined. K_{cat} is the first order rate constant, or catalytic constant, when the enzyme is working at its maximum efficiency. $K_{\text{cat}} = V_{\text{max}} (1/\text{initial concentration of enzyme})$. Since the MW of CEPDE3-LF is \sim 63.5 kDa and 17 μg of CEPDE3-LF was used, the initial concentration of enzyme was 267.72 pmoles. Thus, for CEPDE3-LF, $K_{\text{cat}} = 70.42(1/267.72)$. Hence $K_{\text{cat}} = 0.26 \text{ seconds}^{-1}$.

Table 6.8: Experimental data for CEPDE3-LF cAMP hydrolysis

Experimental data recorded from 5 enzyme assays was used to measure cAMP hydrolysis by CEPDE3-LF. Average values and standard deviation were calculated for each substrate concentration.

Substrate (μM)	Assay 1 (pmol/min)	Assay 2 (pmol/min)	Assay 3 (pmol/min)	Assay 4 (pmol/min)	Assay 5 (pmol/min)	Average Velocity (pmol/min)	Standard deviation
0.1	36	26	30	31	34	31	3.42
0.2	56	29	38	42	59	44	11.2
0.4	66	18	52	61	61	51	17.38
0.8	66	30	54	65	69	56	14.22

A**B****Figure 6.4 CEPDE3-LF cAMP hydrolysis in insect cells**

(A) Saturation curve of cAMP hydrolysis with increasing concentrations of cold cAMP (0.1, 0.2, 0.4 or 0.8 μM) and constant ^3H -cAMP substrate (< 0.01 mCi). (B) Lineweaver-Burk plot, graphed with $1/[S]$ (X-axis) plotted against $1/V$ (Y axis).

6.7.1.3: CEPDE3-SF

6.7.1.3.1: cAMP Hydrolysis CEPDE3-SF

Hydrolysis of cAMP by CEPDE3-SF expressed in insect cells was measured as discussed in section 6.6.1.2.1 for CEPDE3-LF. Data points were obtained from six individual PDE enzyme assays (Table 6.9). Based on the experimental data, graphs were plotted as substrate [S] against velocity (V) (Fig. 6.5A) and the Lineweaver-Burk reciprocal plot ($1/[S]/1/V$) (Fig. 6.5B). Under these experimental conditions, the CEPDE3-SF hydrolysis assay did not reach saturation. Therefore, K_m and V_{max} values cannot be determined experimentally. Qualitatively, the CEPDE3-SF isoform is less efficient at cAMP hydrolysis than CEPDE3-LF. The estimated K_m and V_{max} values were calculated based on the graph equation from Figure 6.5B. Hence the estimated V_{max} for CEPDE3-SF was ~ 56 pmol/min/mg and the K_m value was $0.02 \mu\text{M}$. In addition, the K_{cat} value was calculated from the derived V_{max} . Since the MW of CEPDE3-SF is 54.2 kDa and $15 \mu\text{g}$ of CEPDE3-SF was used, the initial concentration of enzyme was 276.75 pmoles was used. K_{cat} was calculated as follows $K_{cat} = V_{max} (1/\text{initial concentration of enzyme})$. Thus, for CEPDE3-SF, $K_{cat} = 56(1/276.75) = 0.20 \text{ seconds}^{-1}$.

Table 6.9: Experimental data for CEPDE3-SF cAMP hydrolysis

Experimental data recorded from 6 enzyme assays was used to measure cAMP hydrolysis by CEPDE3-SF. Average values and standard deviation was calculated for each substrate concentration. Unit of each assay is expressed in (pmol/min).

Substrate (μM)	Assay 1	Assay 2	Assay 3	Assay 4	Assay 5	Assay 6	Average velocity	Standard deviation
0.1	40.08	43	41	48.08	46.08	46.42	44.11	3.23
0.2	41	43.56	44.02	49	51.04	49.06	46.28	3.95
0.4	45.12	44	46	58.12	56.12	56.45	49.87	6.56
0.8	61.02	59	62	54.02	52.02	52.34	57.61	4.47

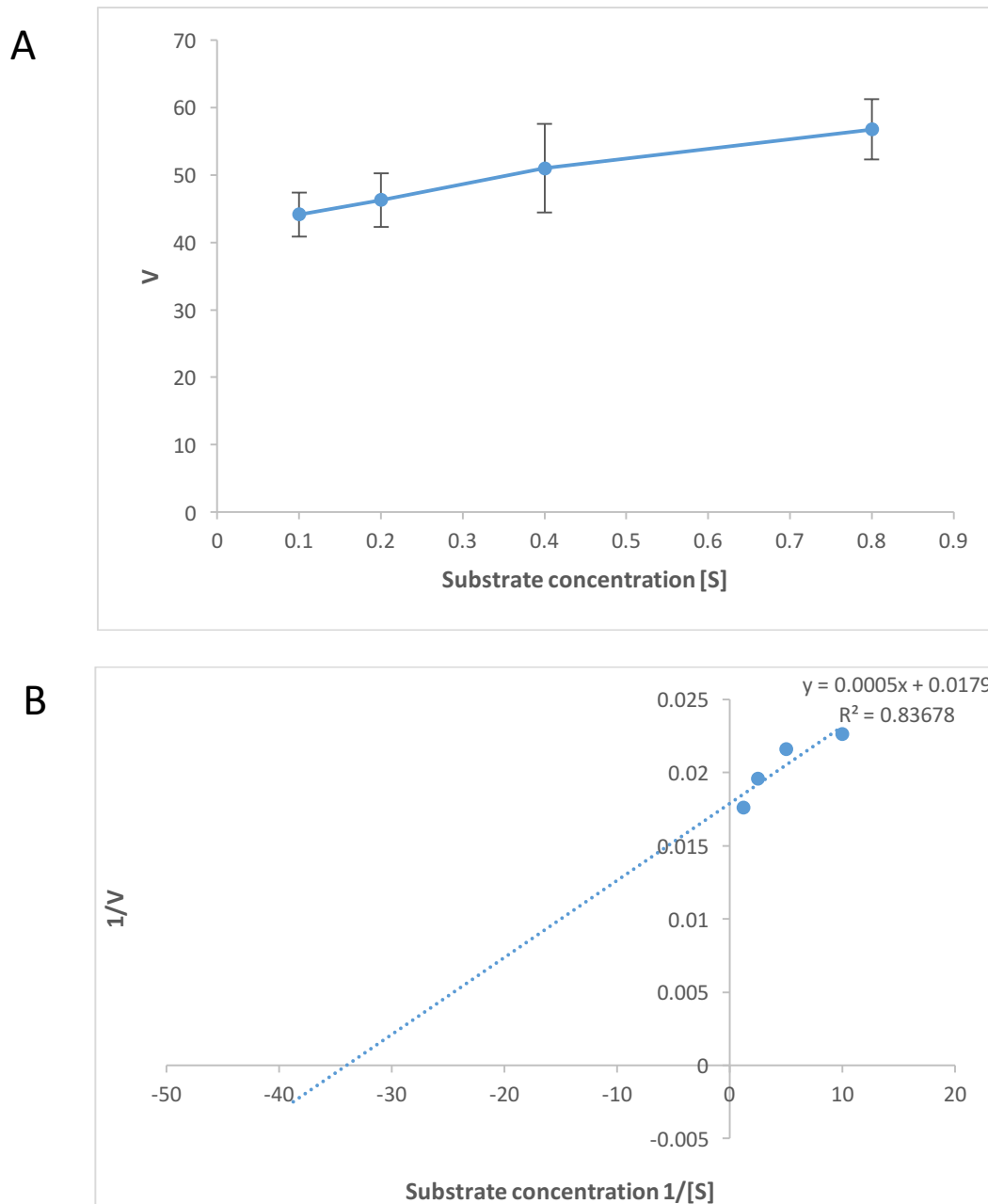


Figure 6.5: CEPDE3-SF cAMP hydrolysis in insect cells

(A) CEPDE3-SF was exposed to increasing concentrations of cold cAMP (0.1, 0.2, 0.4 or 0.8 μM) and constant ^3H -cAMP substrate (< 0.01 mCi) for cAMP hydrolysis. (B) Lineweaver-Burk plot, graphed with $1/[S]$ (X-axis) plotted against $1/V$ (Y axis).

6.7.2: cGMP hydrolysis by CEPDE3-LF and CEPDE3-SF

6.7.2.1: CEPDE3-LF

To determine cGMP hydrolysis by CEPDE3 LF and SF enzymes, ^3H -cGMP, guanosine 3',5'-cyclic phosphate, ammonium salt was used instead of ^3H -cAMP. cGMP substrate preparation was based on the same protocol used for cAMP (described in section 6.7.1). Increasing concentrations of cold cGMP, ranging from 0.1 to 2.4 μM , were prepared (see Table 6.10).

Table 6.10: Preparation of substrate for cGMP hydrolysis

cGMP hydrolysis was performed using constant ^3H -cGMP substrate with a concentration of (< 0.01 mCi) and increasing amounts of cold cGMP. All other components of the buffer were added in ml volume to prepare a total volume of 5 ml.

Components cGMP	0.1 μM	0.2 μM	0.4 μM	0.8 μM	1.2 μM	1.6 μM	2.4 μM
Hepes pH7	2.5	2.5	2.5	2.5	2.5	2.5	2.5
1M MgCl_2	0.041	0.041	0.041	0.041	0.041	0.041	0.04
30 μM cold cGMP	0.050	0.1	0.2	0.4	0.8	1.6	4.8
^3H -cGMP	0.025	0.025	0.025	0.025	0.025	0.025	0.025
DW	2.38	2.34	2.24	2.96	3.76	3.36	4.96
Total	5 ml	5 ml	5ml	5ml	5 ml	5 ml	5 ml

Table 6.11: Experimental data for CEPDE3-LF cGMP hydrolysis

Experimental data recorded from 4 enzyme assays was used to measure cAMP hydrolysis by CEPDE3-LF. Average values and standard deviation was calculated for each substrate concentration.

Substrate (μM)	Assay 1	Assay 2	Assay 3	Assay 4	Average velocity	Standard Deviation
0.2	84	98	161	243	146	72.52
0.4	143	121	181	156.	150	25.07
0.8	262	214	317	279	268	42.75
1.6	325	306	294	314	342	13.05
2.4	415	383	389	407	398	15.03

Experimental data analysis for CEPDE3-LF cGMP hydrolysis

Hydrolysis of cGMP by CEPDE3-LF expressed in insect cells was also studied in the same pattern as discussed in section 6.6.1.2 for cAMP hydrolysis. Data points were obtained from 4 individual PDE enzyme assays (Table 6.11). Based on the experimental data, graphs were plotted as substrate [S] against velocity (V) (Fig. 6.6A) and the Lineweaver-Burk reciprocal plot ($1/[S]/1/V$) (Fig. 6.6B). Under these experimental conditions, the CEPDE3-LF hydrolysis assay did not reach saturation. Hence an estimated K_m and V_{max} values were calculated based on the graph equation from (Figure 6.6B). The V_{max} for CEPDE3-LF was 344.8 pmol/min/mg and the K_m value was 0.17 μM . In addition, the K_{cat} value was calculated from the derived V_{max} . K_{cat} was calculated as follows $K_{cat} = V_{max} (1/\text{initial concentration of enzyme})$. Since the MW of CEPDE3-LF is 63.5 kDa and 17 μg of CEPDE3-LF was used, the initial concentration of enzyme was 267.72 pmoles. Thus, for CEPDE3-LF, $K_{cat} = 344.8(1/267.72) = 1.29 \text{ seconds}^{-1}$. One factor that influenced the shape of the saturation curve was that the lowest concentration of substrate (0.2 μM) had a degree of variability in the calculated V value between experiments, as seen by the large error bars. As a result, the average V value was higher than expected, at this point, and was very similar in value to V at 0.4 μM . The cause of this variability is unknown, but could have been due to a technical error, like column contamination or a pipetting error.

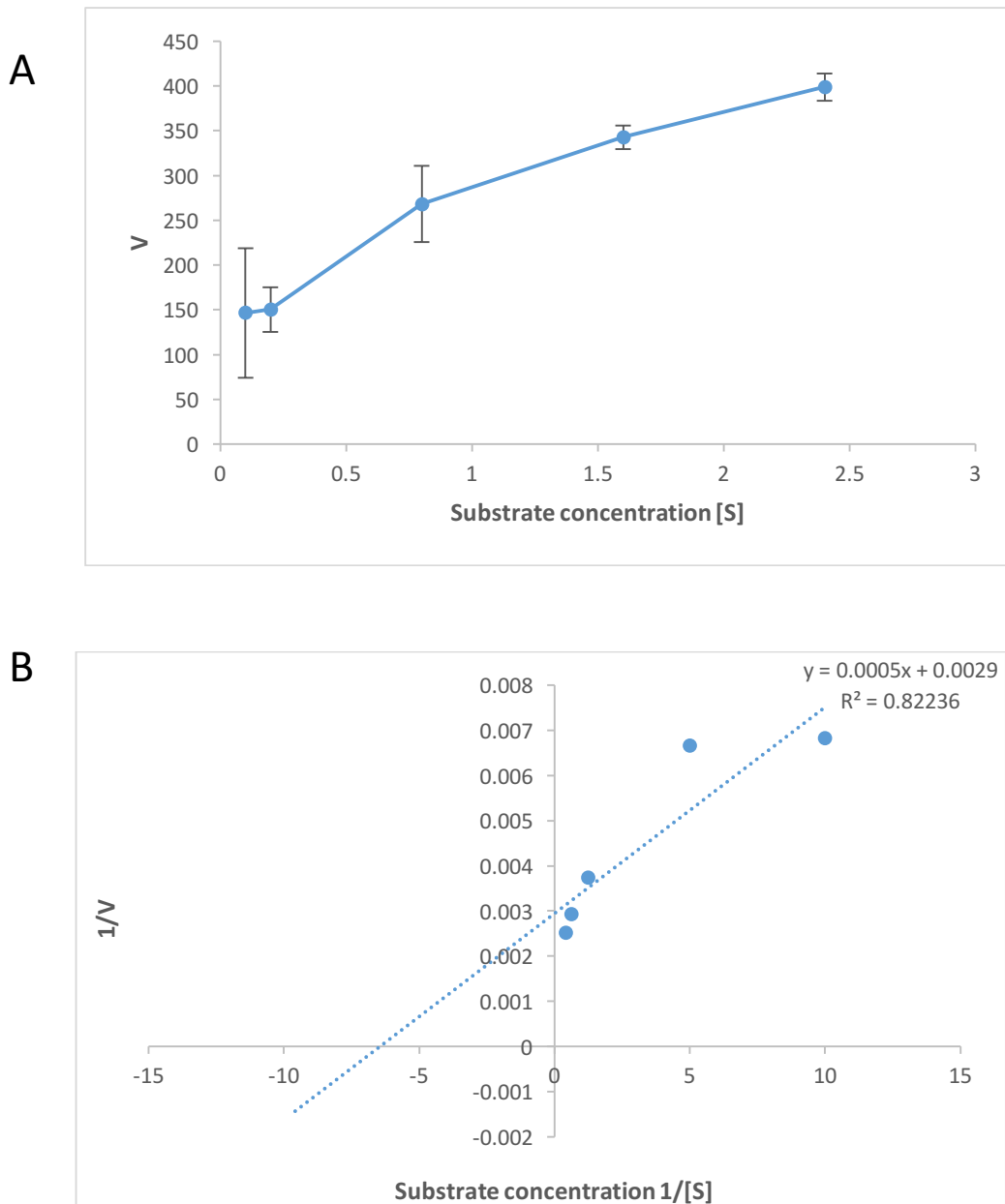


Figure 6.6: CEPDE3-LF cGMP hydrolysis in insect cells

(A) CEPDE3-LF was exposed to increasing concentrations of cold cGMP (0.2, 0.4, 0.8, 1.6, 2.4 μM) and constant ^3H -cGMP substrate (< 0.01 mCi) for cGMP hydrolysis. (B) Lineweaver-Burk plot, graphed with $1/[S]$ (X-axis) plotted against $1/V$ (Y axis).

6.7.2.2: CEPDE3-SF cGMP hydrolysis

Table 6.12: Experimental data for CEPDE3-SF cGMP hydrolysis

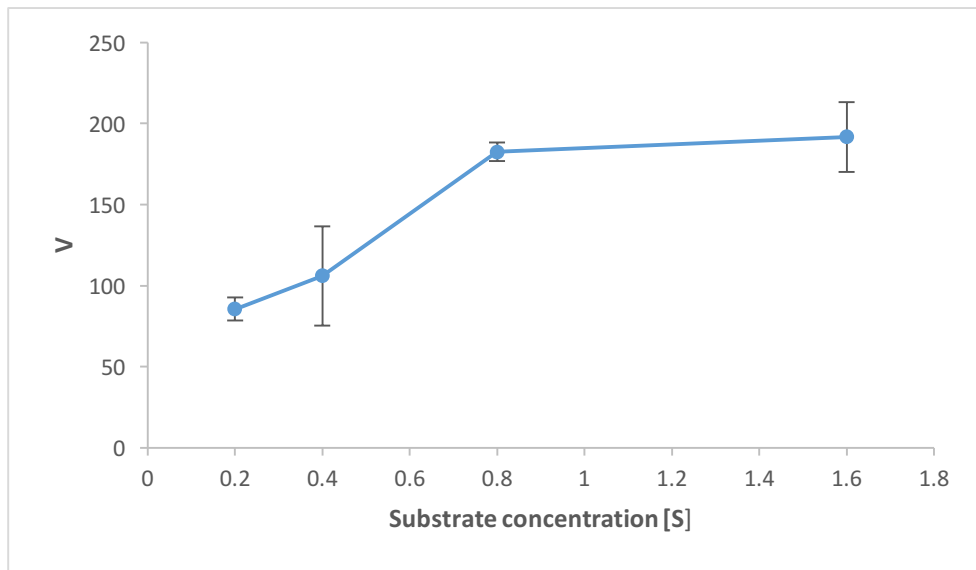
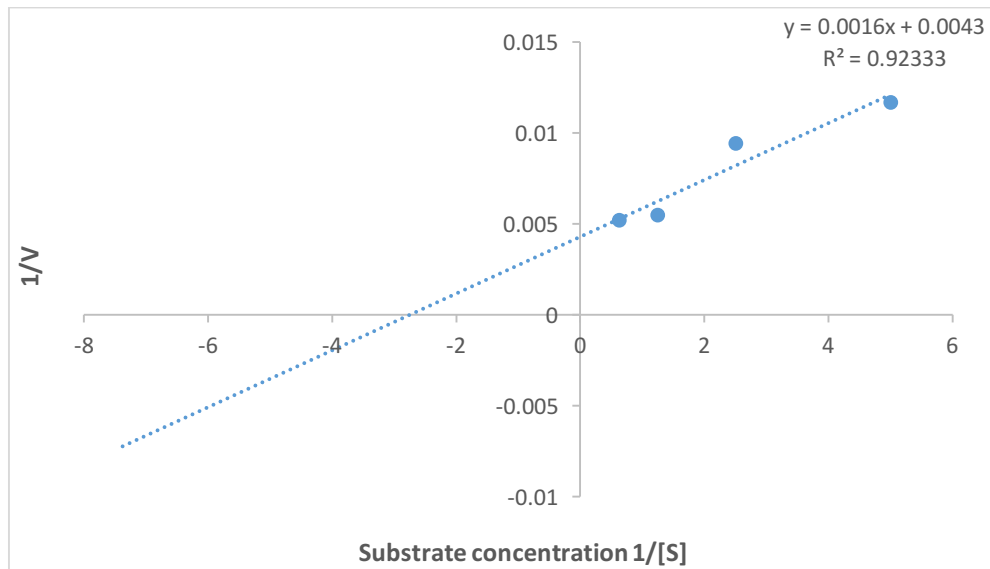
Experimental data recorded from 4 enzyme assays was used to measure cGMP hydrolysis by CEPDE3-SF. Average values and standard deviation was calculated for each substrate concentration.

Substrate [S] (μM)	Assay 1	Assay 2	Assay 3	Assay 4	Average velocity	Standard deviation
0.2	88.4	90.4	75	88.33	85	7.08
0.4	102	82	90	150.06	106	30.49
0.8	191	179	180	182.5	182	5.68
1.6	221	192	170	191.75	191	21.51

Experimental analysis for CEPDE3-SF cGMP hydrolysis

cGMP hydrolysis was performed using the CEPDE3-SF lysates expressed in insect cells with substrate concentrations of 0.2, 0.4, 0.8 and 1.6 μM (listed in Table 6.10). These enzyme assays were carried out 4 times (experimental data summarized in Table 6.11). Graphs were plotted based on the values of increasing substrate concentrations [S] against V (Fig. 6.7A), and the respective Lineweaver-Burk reciprocal plot based on $1/[S]$ against $1/V$ (Fig. 6.7B). Accordingly, the K_m and V_{\max} were recorded based on the graph equation of Fig 6.7B. The V_{\max} for CEPDE3-SF was 232.5 pmoles/min and the K_m was 0.3 μM . Since the MW of CEPDE3-SF is 54.2 kDa, and 15 μg of CEPDE3-SF was used, the initial concentration of enzyme was 276.75 pmoles.

K_{cat} was calculated as follows, $K_{\text{cat}} = V_{\max} (1/\text{initial concentration of enzyme})$. Hence, $K_{\text{cat}} = 232.55(1/276.75) = 0.84 \text{ seconds}^{-1}$.

A**B****Figure 6.7 CEPDE3-SF cGMP hydrolysis in insect cells**

(A) Saturation curve of cGMP hydrolysis with increasing concentrations of cold cGMP (0.2, 0.4 or 0.8 and 1.6 μM) and constant ^3H -cAMP substrate (< 0.01 mCi). (B) Lineweaver-Burk plot, graphed with 1/[S] (X-axis) plotted against 1/V (Y axis).

Experimental analysis of cAMP and cGMP hydrolysis for K_m and V_{max} values in CEPDE3-LF and SF isoforms is summarized in Table 6.13.

Table 6.13: Enzyme kinetics data of cAMP and cGMP hydrolysis by CEPDE3 enzymes

The table below summarizes the K_m , V_{max} and K_{cat} values obtained from cAMP and cGMP hydrolysis by CEPDE3-SF and LF isoforms

CEPDE3 isoforms	cAMP hydrolysis				cGMP hydrolysis			
	K_m (μM)	K_{cat} (sec^{-1})	K_{cat}/K_m ($\mu M^{-1} sec^{-1}$)	V_{max} (pmoles/min)	K_m (μM)	K_{cat} (sec^{-1})	K_{cat}/K_m ($\mu M^{-1} sec^{-1}$)	V_{max} (pmoles/min)
CEPDE3-LF	0.11	0.26	2.36	70	0.17	1.29	7.588	345
CEPDE3-SF	0.02	0.20	10	56	0.37	0.84	2.27	232.5

6.8 Discussion

6.8.1: PDE3 catalytic assay

The PDE3 enzyme acts as a catalyst which speeds up a chemical process or conversion of a cyclic nucleotide to a nucleotide. The enzyme thus acts upon substrates, forming products, and allowing the reaction to go to equilibrium (Fig. 6.8). In the CEPDE3 enzymatic reaction, the PDE3 enzyme acts on substrates by binding them at its active site. The 3'-5' cyclic nucleotide phosphodiesterase activity of the CEPDE3 isoforms allows the enzyme to act as a catalyst and break the 3'phosphodiester bond of cAMP. In the enzyme assay here, 3H -labelled cAMP is converted to 3H -5'-AMP over time. By adding *Crotalus atrox* venom, 3H -5'-AMP is further degraded to 3H -adenosine. However, this treatment does not affect the remaining cAMP present in the sample, as it hydrolyses only nucleotides. Therefore, the amount of adenosine produced is directly proportional to the PDE activity in the reaction. In a similar manner, the conversion of 3H -labelled cGMP to 3H -guanosine can also be measured. Based on these reactions, studies of the CEPDE3 isoforms were performed to determine their catalytic properties and substrate affinity to cAMP and cGMP, as well as the inhibitor specificity of cilostamide (K_m , V_{max} , IC_{50} , K_{cat} values).

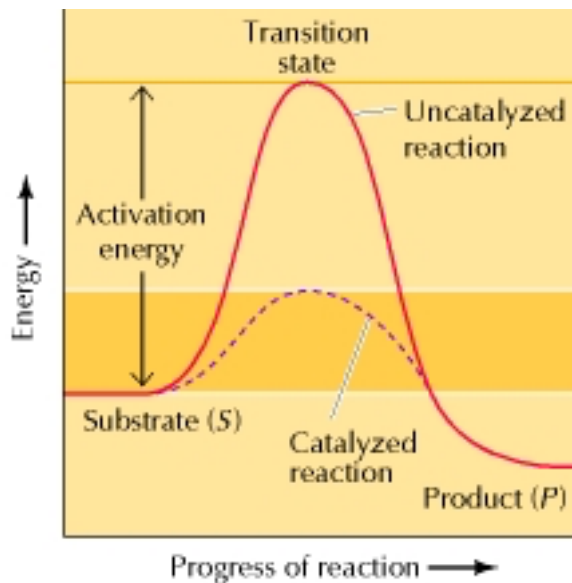


Figure 6.8: Process of enzymatic reactions

Diagrammatic representation of the enzyme catalysis reaction involving the conversion of substrate (S) into product (P). For the reaction to proceed, substrate passes through the transition stage of high energy, the activation energy helps in achieving the transition stage and hence determines the rate of the reaction. In the presence of an enzyme which acts as a catalyst, the activation energy is lower and the reaction therefore proceeds at an accelerated rate (Cooper, 2000).

6.8.1.1: Enzyme activity in CEPDE3 proteins

Initial studies with CEPDE3 isoforms were based on bacterial cell lysates containing recombinant His-tagged CEPDE3 isoforms. Both the long and short isoforms of His-tagged CEPDE3 proteins showed low PDE3 activity (Table 6.1). Attempts carried out to increase the protein expression levels failed. To facilitate purification and characterization of CEPDE3 proteins, the CEPDE3 isoforms were expressed with a GST fusion partner in bacteria. The GST-tagged constructs increased protein expression and solubility; > 80% of the expressed proteins were recovered in a soluble form. However, ~ 20% of the protein remained in the insoluble cell-pellet (Table 6.2). Meanwhile, the PDE activity of the GST-tagged constructs was ~ 15.9% greater than the enzyme activity of the His-tag expressed constructs. In addition, purification experiments with GST-tagged proteins showed that there was ~ 5.10-fold increase in PDE3 activity with purification of the long-form (Table 6.3) and the purified short form protein showed a ~ 3.6-fold increase in enzyme activity (Table 6. 4).

As the CEPDE3 isoforms expressed in *E. coli* were not assayed before using the PDE3-specific inhibitor cilostamide, it was important to study their enzyme inhibition. Therefore, the difference in CEPDE3 activity was calculated with and without inhibitor. In addition, this activity was compared to CEPDE3 specific activity from isoforms expressed in insect cells, for comparison. Inhibitor concentrations ranged from 0.01 μM to 5 μM . Both Flag-tagged CEPDE3-LF expressed

in insect cells and GST-tagged CEPDE3-LF purified from bacteria showed a 90% inhibition with 1 μM cilostamide (Fig. 6.1 and 6.2), while Flag-tagged CEPDE3-SF showed only 80% inhibition with 1 μM cilostamide (Fig. 6.3). However, at the concentration of 5 μM , there was \sim 95% inhibition of CEPDE3-SF by cilostamide. The IC_{50} values for CEPDE3 long and short isoforms expressed in insect cells were 0.1 and 0.3 μM respectively. Hence, the CEPDE3-SF appeared to be less sensitive to cilostamide than the CEPDE3-LF. The IC_{50} of CEPDE3-LF purified proteins expressed in bacteria was 0.1 μM . Therefore, the drug cilostamide inhibits PDE3 proteins expressed in bacteria and insect cells in a similar manner.

6.8.1.2: Enzyme activity of recombinant proteins from bacteria versus insect cells

Previous studies conducted in the Manganiello lab used purified Flag-tagged CEPDE3 isoforms from recombinant baculovirus expression vectors in insect cells. In these cells, 71% recovery of PDE activity from the lysate was achieved. Specific activity of the eluate containing pure long-form protein showed a value of 0.8×10^6 pmol/min/mg. This value was equivalent to > 400 -fold enrichment of the CEPDE3 activity from the insect cell lysate (Samidurai et al., 2015; unpublished data). While using GST-tagged CEPDE3 constructs improved protein yield and solubility over His-tagged constructs, the PDE activity was still low. Several theories could explain the low enzyme activity, despite the proteins being extracted in a soluble form. First, *E. coli* may not be as suitable for correct folding of recombinant proteins, and this may impact high activity performance of the enzymes (Montalben et al., 2007; Rosanno et al., 2013; Yang et al., 2003; Kurokawa et al., 2000). Second, there are no post-translational modifications with *E. coli* expression, and the lack of these modifications might also affect enzymatic activity or protein folding. Post-translational modifications in PDEs, like acetylation and glycosylation, modify PDE enzyme activity. Sphingomyelin phosphodiesterase acid-like 3A (SMPDL3A), a recently identified secreted N-linked glycoprotein, has increased phosphodiesterase activity with N-glycosylation (Traini et al., 2017). In comparison, deglycosylation of purified recombinant SMPDL3A resulted in loss of phosphodiesterase activity. Simultaneously, the phosphorylation in PDEs also plays an important role in their regulation and hydrolytic activity (Sette and Conti, 1996). Insect cells are a higher eukaryotic system and able to carry out more complex post-translational modifications in comparison to other expression systems like the bacteria and yeast. They are also known to have highly efficient machinery for folding recombinant mammalian proteins, and thus can be used for extracting high amounts of proteins from soluble fractions. As a result, these factors may allow expression of a highly active PDE3 when the CEPDE3 isoforms are expressed in insect cells.

6.8.2 cAMP and cGMP hydrolysis

The Michaelis-Menten equation describes the hyperbolic relationship between the rate of enzyme reaction and the substrate concentration. As substrate concentration $[S]$ increases, V approaches the limiting value V_{max} . V_{max} is equal to the rate V that is observed if the enzyme is saturated, i.e. when all the active sites in the enzyme are occupied by the substrate. Hence adding more substrate in the reaction at this point cannot increase the overall rate of reaction.

In this study, the activities of CEPDE3 isoforms expressed in insect cells were measured with respect to hydrolysis of cAMP and cGMP substrates. Experimental data derived from the exposure of CEPDE3-LF enzyme to increasing amounts of cAMP substrate showed a hyperbolic curve, indicating that the CEPDE3-LF enzyme reached its saturation point (Fig 6.4A). By plotting $1/V$ vs $1/[S]$ to derive a linear graph equation based on the reciprocals, V_{max} was calculated and K_m was derived from $V_{max}/2$ (Eisenthal et al., 2007). The V_{max} for CEPDE3-LF was 70 pmoles/min/mg and K_m was 0.11 μM . Similarly, cAMP hydrolysis by CEPDE3-SF was carried out using increasing substrate concentrations (0.1, 0.2, 0.4 and 0.8 μM). However, experimental data demonstrated that the CEPDE3-SF enzyme did not achieve a saturation curve under these conditions (Fig 6.5A) A rising curve was obtained, but a saturation point was not reached by the enzyme. However, an experimental V_{max} and K_m for the short isoform could be determined, but a qualitative estimate of the V_{max} and K_m was calculated from the graph plotted (in Fig. 6.5B) from the reciprocal $1/V$ vs $1/[S]$. Derived from this graph equation, the estimated V_{max} was 56 pmoles/min/mg and K_m was 0.02 μM .

Next, the cGMP hydrolysis study was carried out following the same parameters used for cAMP hydrolysis by both CEPDE3 isoforms. When experimental data was plotted from the exposure of CEPDE3-LF enzyme to increasing amounts of cGMP substrate, it showed a rising curve, which did not reach a plateau, suggesting that the CEPDE3-LF enzyme did not reach a saturation point with the cGMP substrate concentrations used under these conditions (Fig 6.6A). Meanwhile, the CEPDE3-SF assay showed a hyperbolic curve (Fig. 6.7A), suggesting that the CEPDE3-SF enzyme did reach a saturation point. Therefore, a qualitative comparison of the two isoforms indicated that the short isoform more effectively hydrolyzed cGMP than the long isoform. Experimentally, only the short isoform V_{max} and K_m could be determined. The calculated V_{max} of the short isoform was 232 pmoles/min and K_m was 0.3 μM . Based on the qualitative analysis of the Lineweaver-Burk reciprocal plot ($1/V$ vs $1/[S]$) of the long isoform, estimated V_{max} and K_m values were calculated (Fig. 6.6B). The estimated V_{max} for CEPDE3-LF was 345 pmoles/min/mg and K_m was 0.17 μM .

The K_m values for CEPDE3-LF cAMP hydrolysis and CEPDE3-SF cGMP hydrolysis were in the range of 0.1-0.4 μM . A low K_m value indicates strong binding, and less substrate is required for the enzyme to perform hydrolysis at a given rate compared to an enzyme with a high K_m and low affinity for its substrate (Bezerra et al., 2016). Hence, the current CEPDE3-SF and LF studies demonstrated that CEPDE3-LF showed a strong binding for cAMP and CEPDE3-SF showed a strong binding for cGMP. Since the other assays did not reach saturation, only an estimated K_m value could be determined, which was within the same range. Similarly, studies carried out with mammalian PDE3 demonstrated K_m values for cAMP and cGMP hydrolysis in the range of 0.1-0.8 μM (Shakur et al., 2001). Finally, the K_{cat} of the CEPDE3 isoforms were determined. The K_{cat} is the turnover number that indicates the number of times a single enzyme molecule can make a product molecule per time (seconds or minutes) under saturating conditions. The K_{cat} value for CEPDE3-LF was 0.26 seconds⁻¹. Meanwhile, based on the estimated V_{max} for CEPDE3-SF cAMP hydrolysis, the K_{cat} value for CEPDE3-SF was 0.20 seconds⁻¹. For cGMP hydrolysis, the K_{cat} was 1.29 seconds⁻¹ for CEPDE3-LF, based on its estimated V_{max} , and 0.84 seconds⁻¹ for CEPDE3-SF

(Table 6.13). Therefore, in general, the turnover rate for cAMP was faster than cGMP, for both CEPDE3 isoforms.

6.8.3: K_{cat}/K_m ratio in CEPDE3 isoforms

The K_{cat}/K_m , commonly known as specificity constant, was calculated in this study to determine the catalytic efficiency of CEPDE3-LF and CEPDE3-SF for each of their substrates, the cAMP and cGMP. K_{cat}/K_m is an index of the catalytic efficiency of an enzyme, in regards to substrate binding and conversion to the product. The K_{cat}/K_m value for CEPDE3-LF hydrolysis of cAMP was $2.36 \mu\text{M}^{-1} \text{sec}^{-1}$. In comparison, with cGMP hydrolysis, the CEPDE3-LF K_{cat}/K_m value was $7.588 \mu\text{M}^{-1} \text{sec}^{-1}$. These experiments indicate that CEPDE3-LF may hydrolyze cGMP substrate more efficiently than cAMP. Similarly, experimental studies with CEPDE3-SF determined that the K_{cat}/K_m ratio for CEPDE3-SF cAMP hydrolysis was $10 \mu\text{M}^{-1} \text{sec}^{-1}$, and the K_{cat}/K_m ratio for cGMP hydrolysis was $2.27 \mu\text{M}^{-1} \text{sec}^{-1}$. Therefore, the CEPDE3-SF appears to more efficiently hydrolyze cAMP than cGMP.

However, there are some caveats to interpreting the specificity constant. If the ratio of rates is based on different enzymes with identical k_{cat}/K_m values acting on the same substrate, it depends on the ratio of $[S]/K_m$. For a given value of $[S]$, the rate may be directly proportional to the K_m at a given $[S]$ concentration. As the K_{cat} has to increase to maintain the K_{cat}/K_m constant, any changes in K_{cat} mainly affects velocity rather than a change in K_m . An enzyme with a higher (K_{cat}/K_m) at a given concentration of substrate can catalyze an identical reaction at lower rates than one with lower (K_{cat}/K_m). When an enzyme with higher K_{cat}/K_m catalyzes a reaction faster as compared to a reaction with lower catalytic efficiency, the ratio of the two reaction rates is not constant but is dependant on $[S]/K_m$ (Eisenthal et al., 2007).

Another alternative method proposed by Ceccarelli et al. (2008), is based on the theory of catalysis by Albery and Knowles. They describe the efficiency function of an enzyme (E_f) as the ratio between the rate of the catalyzed reaction and maximum theoretical rate, limited by diffusion of substrate to the active site. E_f is a function of the catalytic properties of the enzyme and the actual substrate concentration $[S]$. According to this method, the K_m represents the kinetic parameter for the forward reaction, and K_{cat} represent the rate constant of the reverse reaction (Ceccarelli et al., 2008). Together, it is a measure for estimating conditions under which an enzyme could efficiently catalyze a reaction. It offers advantages based on the interpretation of the catalytic competence used in common practice in the traditional enzyme kinetics approach (Ceccarelli et al., 2008). The E_f function indicates individual enzyme velocities to the maximum obtained, instead of comparing different relative rates derived from each enzymes. Hence, overall, using the K_{cat}/K_m as a measure for comparison of catalytic efficiency may vary for every enzyme reaction.

6.8.3.1: Continued studies in CEPDE3 isoforms

The PDE enzyme assays performed on both CEPDE3 isoforms indicated that CEPDE3-LF reached a saturation curve with cAMP, whereas the CEPDE3-SF did not reach a saturation curve with cGMP hydrolysis. This indicated the long-isoform effectively hydrolyzed cAMP. On the other hand, the SF did not reach a saturation curve with cAMP hydrolysis but reached a saturation curve with cGMP and thus the short isoform effectively hydrolyzed cGMP. However, based on the experimental analysis from PDE enzyme assays, there was a limitation in calculating the K_{cat}/K_m index because the CEPDE3-LF with cGMP hydrolysis and CEPDE3-SF in cAMP hydrolysis did not reach an expected saturation curve. Hence, to further assess the binding affinities of both the enzymes, a binding study using a catalytically incompetent mutant enzyme or using a non-hydrolysing substrate would enable us to assess the binding kinetics in both CEPDE3 isoforms. Two commonly used binding assays include fluorescence intensity and fluorescence anisotropy.

Fluorescence intensity binding assays use the difference in the fluorescence intensity of the product compared with the reactants. While, fluorescence anisotropy measures the rotational diffusion of a molecule. When one reactant binds to the other, the product has a lower rotational diffusion coefficient and a higher fluorescence anisotropy (Pollard, 2010).

In addition, other enzyme assays could be carried out on both isoforms to determine their nucleotide specificity for cAMP and cGMP hydrolysis. A modified two-step method of PDE assay using the ^3H -cAMP and ^3H -cGMP substrates on ion exchange resin could be performed on both the CEPDE3 isoforms (Rybalkin et al., 2013 ; Sette and Conti, 1996 ; Thompson and Appleman, 1971). Alternatively, a PDE assay using the isothermal titration calorimetry could also be performed, where the calorimeter measures the current applied to the cell containing enzymatic mixture to maintain its temperature. As the hydrolysis progresses, due to the heat generated, less current is applied to the hydrolyzed mixture. PDE activities are then recorded based on the heat differences generated in the sample and control (Rybalkin et al., 2013). Overall, analysing PDE assays based on various methods, would enable us to optimize and estimate the affinities of both CEPDE3 isoforms to their substrates, cAMP and cGMP. In addition, studies based on site directed mutagenesis of selected catalytic domain residues at the amino terminus of both CEPDE3 isoforms and using a catalytic incompetent mutant enzyme would also be a helpful index to estimate their catalytic efficiency, thus determining if the CEPDE3 enzymes are catalytically active.

6.8.3.2: Biological importance of CEPDE3 isoforms

The objective of studying the kinetics of the CEPDE3 enzyme isoforms was to determine their substrate specificity, inhibitor sensitivity and binding capacity. Determining the kinetic properties of an enzyme can help us to understand many of its physiological roles. For example, PDEs are known to be important regulators of intracellular cyclic nucleotide signals (Shemarova, 2009). Changes in the concentration of cyclic nucleotides is cell-specific, and may affect differences in the expression of PDE isoforms and their substrates (Atienza et al., 1999). Based

on the level of expression of PDEs, the intracellular concentration of cAMP and cGMP are tightly-regulated and their concentrations and turnover can be functionally compartmentalized. PDE3A and PDE3B are enzymes that hydrolyze cAMP and cGMP with high affinity in a mutually competitive way. Based on this principle, increased activation of guanylyl cyclase is induced by nitric-oxide and causes an increase in cGMP, in certain cells like vascular smooth muscle and platelets (Maurice et al., 2003; Shakur et al., 2001). These changes in the cells can cause inhibition of PDE3 activity, since PDE3 is a cGMP inhibited PDE, which in turn leads to a switch in signaling and an increase in cAMP signaling. Due to this effect, the enzymes can inhibit platelet aggregation and increase vasodilatation in the smooth muscle cells (Maurice et al., 2003; Shakur et al., 2001).

Although the PDE3 has dual specificity for cAMP and cGMP, experimental analysis derived from the enzyme kinetics study on CEPDE3 isoforms demonstrated that both the CEPDE3 long and short isoforms did not show equal specificity in hydrolysis with each of their substrates, cAMP and cGMP. The formation of the enzyme-substrate complex (ES) during the catalysis reaction determines the affinity of the enzyme to the substrate, whereas the reversible reaction of the catalysis in dissociation of the enzyme-substrate complex describes the hydrolysis of the reaction. Thus, enzyme kinetics studies of both CEPDE3 isoforms indicated that the CEPDE3-LF had affinity for cAMP, however its' K_{cat}/K_m index showed that the CEPDE3-LF hydrolyzes the cGMP substrate more efficiently. Simultaneously, the saturation curves of CEPDE3-SF showed that the CEPDE3-SF enzyme has more affinity for cGMP substrate, but based on the K_{cat}/K_m index, the CEPDE3-SF efficiently hydrolyzes cAMP substrate. This difference may in part explain the ability of cGMP to act as a competitive inhibitor of cAMP hydrolysis by PDE3, since the rate of PDE3 hydrolysis of cAMP has been reported to be greater for cAMP in comparison to cGMP, whereas the affinity for cGMP is higher (Azevedo et al., 2014). In addition, the expression levels of CEPDE3 isoforms and the intracellular localization of cAMP and cGMP, may contribute to the varied response of CEPDE3 isoforms in hydrolysis of cAMP and cGMP. Therefore, a detailed knowledge of PDE3 enzyme kinetics can contribute to the design of more effective small molecule modulators, of PDE3 catalytic activity, with clinical relevance.

Chapter 7

Chapter 7: Final Discussion

7.1: Overview

In this thesis, a biochemical study of the *C. elegans* PDE3 nematode gene was performed. The objective of studying the *C. elegans* phosphodiesterase 3 gene was to purify a recombinant fusion protein of the CEPDE3 isoforms (long and short form) for catalytic studies and crystallization. This goal was accomplished by subcloning the CEPDE3 isoforms into the pGEX-6P1 vector, then expressing, extracting, and purifying recombinant CEPDE3 isoforms from *E. coli* using GST-tag purification to analyze their catalytic properties. As discussed in chapter 1, earlier studies performed on CEPDE3 isoforms by A. Samidurai et al. (unpublished data) demonstrated that the *C. elegans* share a ~ 40% homology with the mammalian PDE3 isoforms. Preliminary experimental data also demonstrated that the nematode CEPDE3 isoforms exhibit catalytic properties and inhibitor sensitivities that are characteristic of the mammalian PDE3 gene family. In addition, bioinformatics analysis indicated that there is > 90% homology between the two CEPDE3 isoforms (CEPDE3-SF and CEPDE3-LF) (Fig.1.7 and Samidurai, A. et al., unpublished data). This current study with the CEPDE3 isoforms allowed us to study their biochemical properties and will enable us to carry out comparative studies with the mammalian PDE3 and *C. elegans* isoforms. Most importantly, a crystal structure of the mammalian and worm form may inform us of the critical and structural determinants of the PDE3 catalytic pocket. This work could contribute to the design of more effective small molecule modulators of PDE3 catalytic activity, with clinical relevance, and may also shed light on the evolution of mammalian PDE3 isoforms.

7.2: Studies on CEPDE3 isoforms

The subcloning studies of *C. elegans* PDE3 isoforms into pGEX-6P1, confirmed the length of both the cDNA isoforms to the predicted size (long isoform ~ 1.9 kb and short isoform ~ 1.7 kb). CEPDE3 isoforms were previously expressed as Flag-tag proteins in a baculovirus expression vector, expressed in SF21 insect cells in the Manganiello laboratory by A. Samidurai. The CEPDE3 purified proteins had > 400-fold enzyme activity when compared to cell lysate. Due to the challenges in insect cell expression, bacterial expression in *E. coli* was considered as a suitable alternative expression system for producing high amounts of recombinant proteins. In addition, recombinant protein expression in bacteria also has a relatively low cost and faster growth kinetics. Moreover, the bacterial protein expression is inducible using IPTG, so expression levels can be modified. Accordingly, the His-tag constructs were formed to express recombinant proteins in *E. coli*. The experimental data presented in this thesis in chapter 4, section 4.3 indicated that His-tagged CEPDE3 isoforms had challenges in protein expression, due to low yield of CEPDE3 associated with poor solubility, as protein fractions were not extracted in the soluble form. Alternative methods of optimizing CEPDE3 protein expression resulted in limited success. Attempts of purification using IMAC was ineffective due to poor or no binding of CEPDE3 to the Ni²⁺ and Co²⁺ resin columns. Therefore, sequential analysis and control protein expression experiments were carried out to observe expression levels from a GST construct. As discussed in chapter 3 and chapter 4, a control experiment using a GST-tagged ARH protein resulted in high inducible expression by IPTG.

Considering the sequential analysis of CEPDE3 constructs and the pGEX-6P1 vector design, the vector was considered a suitable vector for subcloning and forming new GST-tagged CEPDE3 constructs to further aid recombinant protein expression. As discussed in Chapter 3, subcloning of CEPDE3 based on traditional cloning was a challenge and initial experiments failed to give the desired results. However, PCR was a successful approach for the CEPDE3 isoforms to be amplified. Following PCR, the CEPDE3 constructs were further studied with two different techniques. Initially, the amplified CEPDE3-LF cDNA was inserted into the TOPO cloning vector and thereafter the long-form was subcloned into pGEX-6P1. Simultaneously, the CEPDE3-SF was codon optimized and further subcloned into pGEX-6P1. Hence, both plasmids were successfully redesigned as GST-tagged constructs using the pGEX-6P1 expression vector. The restriction digestion analysis, with compatible restriction enzymes, confirmed the length of the CEPDE3 inserts size to be the predicted sizes. In addition, both isoforms were confirmed by gene sequencing analysis.

7.2.1: Soluble protein expression

Several aspects of the study related to subcloning, PCR, protein expression, and purification have been discussed in detail in each chapter of this thesis. However, protein expression and solubility remained a major challenge, despite the successful formation of GST-tag constructs. Effective measures were taken to address these challenges in protein expression. Screening studies were conducted with several optimizing conditions, including a range of temperatures, IPTG concentration, induction time, cell-lysis, culture conditions and buffer analysis. Based on screening buffers at different pHs, small scale screening studies determined the optimal buffer for cell-lysis and purification. Cell-lysis of the bacterial cells using French-press was a more effective method for extracting soluble protein fractions than sonication. Optimization with lower temperature resulted in effective induction and solubility. Thus, experimental analysis for CEPDE3 isoforms derived from a range of data, and confirmed that protein expression carried out applying a 'cold-shock' procedure (with a shift of incubation temperature from 37°C to 4°C when OD reached 0.4-0.6) made a significant improvement in extracting soluble CEPDE3 isoforms. This result is supported by several studies suggesting that lower temperature inductions help to improve protein solubility, and expressing proteins with a shift in temperature may induce the cold-shock proteins (Csp) in *E. coli* (Gordon et al., 2008; Khow & Suntrarachun, 2012; Harper and Speicher, 2011). Thus, optimization techniques and strategies based on protein expression, induction time, temperature and cell-lysis methods were effective in allowing the recovery of both the CEPDE3 isoforms from the soluble fractions.

Experimental data derived from western immunoblotting and SDS-PAGE confirmed that the GST-tagged proteins expressed were the predicted size, based on the protein analysis for both isoforms. The GST moiety is ~ 26 kDa, while the estimated size of CEPDE3-LF is ~ 63.5 kDa, for the long isoform, and ~54.2 kDa for the short-isoform, CEPDE3-SF. Therefore, the estimated size of each isoform with the GST-tag was ~ 90 kDa for CEPDE3-LF and ~ 80 kDa for CEPDE3-SF. Taken together, the experimental data on CEPDE3 isoforms showed that the CEPDE3 proteins, were successfully expressed as GST-tagged proteins in the soluble form. In addition, the isoform

specific antibodies generated by the Manganiello laboratory for CEPDE3-LF and SF were specific to each isoform. Experimental analysis derived from reproducible data confirmed detection of each isoform at the predicted length with anti-GST antibody and their respective isoform-specific antibodies, directed to the N or C terminus. The common antibody for both isoforms detected both the long and short isoform proteins. Hence, the screening methods applied in small scale studies and scaling up conditions were determined to have been effective in improving recombinant expression and solubility for both CEPDE3-SF and LF isoforms.

7.2.2: Purifying GST-tagged proteins

Purification studies were aimed to obtain a pure form of the CEPDE3 proteins in order to crystallize them. Though protein expression of the CEPDE3 isoforms resulted in high expression and solubility, further purifying the protein remained a challenge. However, a thorough screening based on various parameters helped in improving the purification conditions. In the batch method, purification using glutathione sepharose 4B resin, reducing viscosity and the addition of up to 10 mM DTT helped to improve binding capacity and was thus considered an effective measure in the purification study. This analysis is also supported by other studies performed using GST-tag protein expression and purification (Harper et al., 2011). The uniqueness of purifying protein lies in obtaining a pure form of the protein, especially if a protein carries a tag. Hence, enzymatic cleavage with PreScission Protease was a critical step for the future studies of the purified protein, as having a tag may be a challenge in performing crystallization as it can alter the protein conformation. Experimental data from our studies demonstrated that using on-column technique for eluting proteins was more efficient than using reduced glutathione as an elution buffer. The eluted protein size of the CEPDE3 isoforms were in agreement with the predicted size of both (CEPDE3-LF ~ 63.5 kDa and CEPDE3-SF ~ 54.2 kDa).

7.2.3: CEPDE3 enzyme study

When the enzyme activity of the new CEPDE3 GST constructs was measured, a 10-15% increase in enzyme activity was observed compared to the CEPDE3 His-tag constructs. The purified CEPDE3-SF and LF proteins showed > 90% enzyme inhibition by cilostamide, at a 5 μM concentration. Due to the low enzyme activity in the CEPDE3 GST-tagged enzymes, cAMP and cGMP hydrolysis was measured using Flag-tagged CEPDE3 isoforms expressed in insect cells, due to their high enzyme activity. Experimental analysis measuring cAMP hydrolysis demonstrated that CEPDE3-LF showed affinity for cAMP. In comparison, CEPDE3-SF hydrolysis did not reach saturation under the same assay conditions. Therefore, CEPDE3-SF was less efficient in cAMP hydrolysis than CEPDE3-LF. On the other hand, CEPDE3-SF showed affinity for cGMP, while the CEPDE3-LF assay did not reach saturation under the same experimental conditions. Therefore, CEPDE3-SF was more efficient than CEPDE3-LF at cGMP hydrolysis. Therefore, the K_m values for CEPDE3-LF and CEPDE3-SF were in the range of 0.1-0.4 μM . An estimated K_m and V_{max} was determined for cGMP hydrolysis by CEPDE3-LF and cAMP hydrolysis by CEPDE3-SF, where saturation was not obtained. The K_{cat}/K_m value for CEPDE3-LF hydrolysis of cAMP was 2.36 $\mu\text{M}^{-1} \text{sec}^{-1}$, with cGMP hydrolysis, the CEPDE3-LF K_{cat}/K_m value was 7.588 $\mu\text{M}^{-1} \text{sec}^{-1}$. Hence the long

isoform effectively hydrolyzed cGMP substrate. Experimental studies with CEPDE3-SF determined that the K_{cat}/K_m ratio for CEPDE3-SF cAMP hydrolysis was $10 \mu\text{M}^{-1} \text{sec}^{-1}$, and the K_{cat}/K_m ratio for cGMP hydrolysis was $2.27 \mu\text{M}^{-1} \text{sec}^{-1}$. Thus the short isoform effectively hydrolyzed the cAMP substrate.

The cAMP and cGMP signaling systems play an important role in signal transduction by regulating a vast number of physiological processes, including cell-differentiation, proliferation, insulin and metabolic pathways. The cAMP and cGMP activated protein kinases act as cellular effectors, along with cyclic nucleotide-gated ion channels, in these signal transduction pathways (Shakur et al., 2001; Manganiello et al., 1995). In addition, an increase in cAMP and cGMP cellular levels affect the actions of these effectors. Therapeutic agents such as exendin-4 for diabetes, bind to GPCRs and affect functions inside the cells by stimulation of adenylyl cyclase, resulting in the catalysis of cAMP (Parkes et al., 2013). On the other hand, agents stimulating guanylyl cyclase, also known as nitric oxide donor drugs, are involved in the catalysis of cGMP and include glyceryl trinitrate, used in the treatment of angina (Boden et al., 2012).

Enzymatic studies with CEPDE3 purified protein fractions demonstrated that the source of the recombinant CEPDE3 proteins and method of tagging influenced enzyme activity. CEPDE3 GST tagged constructs had a 15.9-fold increase in activity as compared to His-tagged proteins. However, the purification of GST-tagged proteins from cell lysate did not result in the same drastic increase in PDE3 enzyme activity, as seen in previous studies (performed by A. Samidurai) using flag-tagged CEPDE3 proteins in using the baculovirus expression vector, which had > 400-fold enzyme activity with purification. There are several reasons why the same protein expressed in a different expression system showed varied activities. It may be due to a protein conformation change or the unavailability of the active site due to improper folding in *E. coli* versus insect cells. In addition, the presence of a GST-tag may change the biochemical nature of a protein, in terms of protein conformation, and thus affect enzyme activity. Although it is an interesting fact to know that the CEPDE3 proteins expressed differently exhibit varied catalytic properties, it was unclear what caused of the lower enzyme activity in the *E. coli* expression system.

Isolation of purified proteins of CEPDE3-SF and LF were further continued, in order to obtain the substantial amount of protein essential for crystallization ($\sim 2\text{-}4 \text{ mg/ml}$). A concentrated form of the purified CEPDE3 protein will be used for crystallization studies in collaboration with Dr. Hengming Ke from the University of North Carolina. While the studies on purified proteins of CEPDE3 are promising, it would be interesting to learn more of the catalytic domains through crystal structure definition and further bioinformatic analysis. Our studies on the CEPDE3 isoforms, and determining their crystal structure, will enable us to understand the evolutionary progression of CEPDE3 to the homolog now found in humans. By studying the biochemical properties of the CEPDE3 isoforms, and understanding that they have different abilities to hydrolyze cAMP and cGMP, it will allow us to understand how differences in the nematode play a role in cell signaling and signal transduction.

7.2.4: Structure of CEPDE3 isoforms

The amino acid sequence of CEPDE3-SF (NP_064683.5) and CEPDE3-LF (NP_182143.2) were analysed as the query protein sequence of CEPDE3 isoforms using the National Center for Biotechnology Information (NCBI) resources, such as 'Gene', a searchable database of genes (<https://www.ncbi.nlm.nih.gov/gene/?term=pde3++caenorhabditis+elegans>). This analysis allowed us to model a probable crystal structure of the CEPDE3 isoforms and identify possible structure-function relationships based on amino acid sequence. The NCBI RefSeq (reference sequences) tab listed on the right side of the page gives a detailed analysis of the nucleotide and amino acid sequences based on updated entries of mRNA at the NCBI webpage. By clicking on the conserved domain tab, it also locates several other proteins which have a similar domain structure to the query and thus can be used to determine the phylogenetic tree or a conserved domain model. Based on these parameters, it generates a probable crystal structure with close resemblance to the query sequence to similar protein structures from other organisms. This is helpful to gain insight into the arrangement of conserved and divergent residues to determine how protein families are interrelated. This analysis was beneficial to identify the similarity between CEPDE3 isoforms (CEPDE3 LF and SF). In addition, a comparison with the mammalian isoforms and PDE proteins from various other organisms can be estimated. (see Fig 7.1 and Fig 7.2).

The model crystal structures for both CEPDE3 isoforms demonstrate several binding sites within the conserved domains, including ones for zinc, magnesium and arsenic. This structure is helpful to gain insight into the pattern of the conserved residues, and also the divergent ones, in families of proteins that are related to several different isoforms within the same family. Based on the amino acid sequence similarity of both CEPDE3 isoforms, a close resemblance was detected between the human *PDE4B2B* sequence and other lower organisms. The conserved residues that matched the human *PDE4B2B* structure were identical in both isoforms, and the predicted CEPDE3 structure for both CEPDE3-SF and LF are close to these template structures generated using the CEPDE3 protein sequences. In addition, alignment of the conserved domain sequence display helps us to identify and analyze the amino acids in a protein sequence that are involved in functions such as catalysis and protein binding, as they are mapped from the conserved domain annotations to the query sequence. As a result, the query protein sequence of CEPDE3 isoforms embedded within the multiple sequence alignments of a domain model can be analyzed based on the display and also be used to locate other proteins which have a similar domain structure to the query, and thus be used to determine the phylogenetic tree for a conserved domain model, and identify unknown family members that are related.

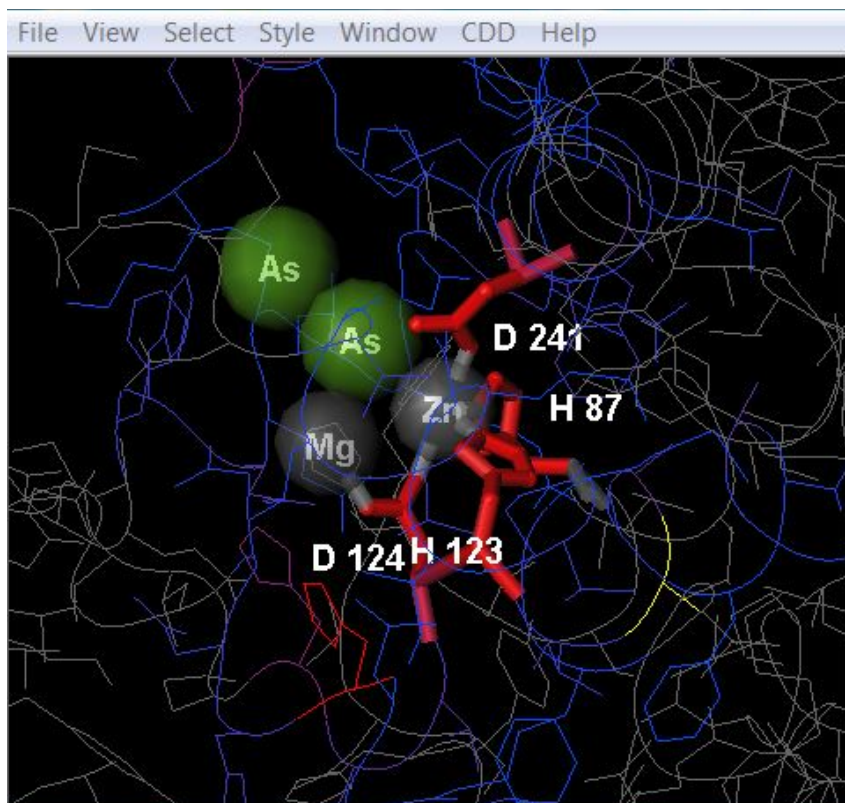


Figure 7.1: Predicted crystal structure template for CEPDE3-SF

Based on the probable conserved amino acid sequences of CEPDE3-SF through the database at NCBI, the sequence similarity of CEPDE3-SF closely matched to the human PDE4B2B, and other lower organisms. The macromolecular crystal structure of PDE4B2B can be viewed using the Cn3D software and this structure was used as a template for a predicted CEPDE3-SF structure. This structure features the Zn-Zinc, M-Magnesium, and A-Arsenic binding sites, as well as the H-Histidine and D-Aspartate residues present at these sites (Ref no: PMID 10846163, reference: <http://www.ncbi.nlm.nih.gov/Structure/cdd/cddsrv.cgi>).

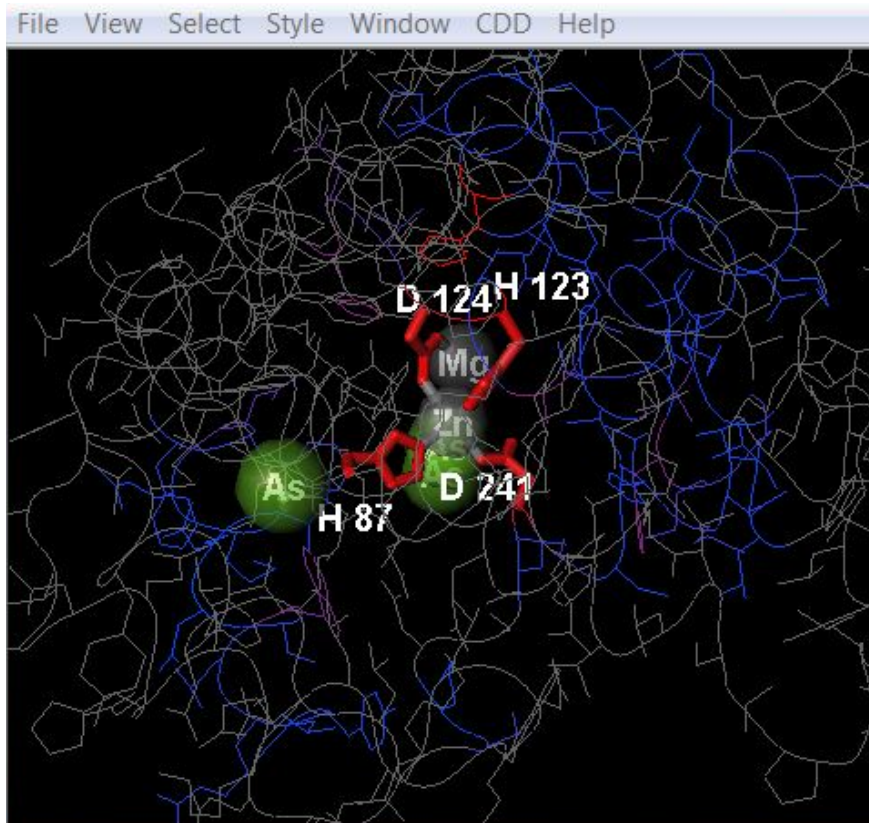


Figure 7.2: Predicted crystal structure template for CEPDE3-LF

Based on the probable conserved amino acid sequences of CEPDE3-LF generated from the NCBI database, the sequence similarities of the long-isoform closely match to the human PDE4B2B and other lower organisms. Accordingly, the macromolecular crystal structure of human PDE4B2B was generated and can be viewed using the Cn3D software, and used as a template for a predicted CEPDE3-LF structure. This structure features the H-Histidine, D-Aspartate, A-Arsenic, Zn-Zinc and M-Magnesium binding sites.

(Ref no: PMID 10846163, reference: <http://www.ncbi.nlm.nih.gov/Structure/cdd/cddsrv.cgi>).

7.2.5: PDE3 inhibitors and functions

PDE3s are targets for many drug actions, including drugs such as cilostamide, amrinone, and milrinone, which demonstrate cardiostimulant, thrombolytic, vasodilatory and anti-platelet aggregation properties. For example, milrinone is used in the treatment of acute heart failure (Francis et al., 2001). Enoximone is used in the treatment of chronic heart failure (Boldt and Suttner, 2007), and cilostamide was the first potent and selective inhibitor known as a platelet anti-aggregant (Maurice and Haslam, 1990). PDE3 is a cardiostimulant agent and milrinone was the first PDE3 inhibitor used in the treatment of acute heart failure. There have been some complications reported with mortality by chronic treatment with milrinone, resulting in tachyarrhythmia and tachycardia, so the drug can only be prescribed to humans for a limited time (Movsesian, 2003). In these conditions, with patients suffering from severe heart failure and diminished cardiac output, the drug does not induce exacerbation of myocardial injury, but is associated with reduced inflammation and apoptotic signaling (Movsesian et al., 2011; Movsesian, 2015). However, continuous treatment with milrinone has proved to be safe with patients having a short waiting time which is <100 days for heart transplant. Cilostazol has been used for treatment of intermittent claudication (Asal and Wojciak, 2017; Castellsague et al., 2017). Pentoxifylline and cilostazol are the only medicines approved by the US Food and Drug administration (USFDA) for the treatment of intermittent claudication, they inhibit platelet aggregation and cause arterial vasodilatation, resulting in dilation of the arteries supplying blood to the legs (Keravis and Lugnier, 2012). PDE3B have been studied extensively in the area of insulin, IGF-1, and leptin signaling (Zhao et al., 1997; Guirguis et al., 2013; Chung et al., 2017). PDE3B activation plays an important role in anti-lipolytic and anti-glycogenolytic actions of insulin (Shakur et al., 2001). The PDE3B KO mice demonstrate alterations in the regulation of energy homeostasis, which include signs of insulin resistance and a number of other alterations in the regulation of energy homeostasis (Guirguis et al., 2013; DiPilato et al., 2015 ;Chung et al., 2017). Administration of PDE3 inhibitors to mice and rats increased lipolysis and insulin secretion, and blocked insulin-induced suppression of endogenous glucose production hence, the absence or inhibition of PDE3B could be associated with the development of insulin resistance, which could be related to dysregulation of insulin signaling and hepatic glucose output (Zhao et al., 2002.; Cong et al., 2007). Absence of PDE3B in beta cells of the pancreas also plays a potential role in insulin secretion, which could be important in patients with type 2 diabetes (Manganiello and Degerman, 2004). Together, these studies suggest that studying the regulation and modulation of PDE3 activity could have a profound impact on the treatment of diseases such as heart failure, stroke, obesity and diabetes.

7.3: Future Studies

The future studies on CEPDE3 isoforms are aimed on crystallizing the isoforms. Crystallization studies will enable us to do comparative studies with the mammalian PDE3 isoforms and identify the structural determinants of the catalytic pocket and inhibitor residues. Identifying their crystal structures which may help to further broaden our understanding of the PDE biology by studying the gene in a nematode. The studies on CEPDE3 expressed in *E. coli* as recombinant proteins demonstrated that the expressed and purified recombinant proteins were markedly inhibited by the PDE3 specific inhibitor cilostamide. PDE3 inhibitors such as cilostamide, enoximone, milrinone and cilostazol are some of the drugs which are currently in use and their physiological actions have been described in detail (see above and Chapter 1, Table 1.1). PDE3 inhibitors are known to be primary therapeutic agents with properties such as cardiotoxic, bronchodilatory and vasodilatory action exhibited in several species. Crystallization of the CEPDE3 isoforms could contribute to the design of more effective small molecule modulators of PDE3 catalytic activity, with clinical relevance, and may also shed light on evolution of the mammalian PDE3 isoforms from the invertebrate forms. In addition, studies of site directed mutagenesis of selected catalytic domain amino acid residues can be performed on the CEPDE3 isoforms. Mutation of these residues could be used to detect the effects on enzyme activity and identify residues that block hydrolysis of cyclic nucleotides. These experiments would allow us to further investigate the CEPDE3 protein structure and determine the biological activity of this enzyme.

References

- Ahmad, F., Cong, L.N., Stenson Holst, L., Wang, L.M., Rahn Landstrom, T., Pierce, J.H., Quon, M.J., Degerman, E., and Manganiello, V.C. (2000). Cyclic nucleotide phosphodiesterase 3B is a downstream target of protein kinase B and may be involved in regulation of effects of protein kinase B on thymidine incorporation in FDCP2 cells. *J. Immunol. Baltim. Md 1950* *164*, 4678–4688.
- Ahmad, F., Lindh, R., Tang, Y., Weston, M., Degerman, E., and Manganiello, V.C. (2007). Insulin-induced formation of macromolecular complexes involved in activation of cyclic nucleotide phosphodiesterase 3B (PDE3B) and its interaction with PKB. *Biochem. J.* *404*, 257–268.
- Ahmad, F., Murata, T., Simizu, K., Degerman, E., Maurice, D., and Manganiello, V. (2015). Cyclic Nucleotide Phosphodiesterases: important signaling modulators and therapeutic targets. *Oral Dis.* *21*, e25–e50.
- Alberts, B., Johnson, A., Lewis, J., Raff, M., Roberts, K., and Walter, P. (2002). Fractionation of Cells.
- Angov, E. (2011). Codon usage: Nature’s roadmap to expression and folding of proteins. *Biotechnol. J.* *6*, 650–659.
- Asal, N.J., and Wojciak, K.A. (2017). Effect of cilostazol in treating diabetes-associated microvascular complications. *Endocrine* *56*, 240–244.
- Aslanidis, C., and de Jong, P.J. (1990). Ligation-independent cloning of PCR products (LIC-PCR). *Nucleic Acids Res.* *18*, 6069–6074.
- Atienza, J.M., Susanto, D., Huang, C., McCarty, A.S., and Colicelli, J. (1999). Identification of Inhibitor Specificity Determinants in a Mammalian Phosphodiesterase. *J. Biol. Chem.* *274*, 4839–4847.
- Azevedo, M.F., Faucz, F.R., Bimpaki, E., Horvath, A., Levy, I., de Alexandre, R.B., Ahmad, F., Manganiello, V., and Stratakis, C.A. (2014). Clinical and molecular genetics of the phosphodiesterases (PDEs). *Endocr. Rev.* *35*, 195–233.
- Baca, A.M., and Hol, W.G. (2000). Overcoming codon bias: a method for high-level overexpression of Plasmodium and other AT-rich parasite genes in Escherichia coli. *Int. J. Parasitol.* *30*, 113–118.
- Bader, S., Kortholt, A., and Van Haastert, P.J.M. (2007). Seven Dictyostelium discoideum phosphodiesterases degrade three pools of cAMP and cGMP. *Biochem. J.* *402*, 153–161.
- Baehr, W. (2014). Membrane Protein Transport in Photoreceptors: The Function of PDE δ . *Invest. Ophthalmol. Vis. Sci.* *55*, 8653–8666.
- Bagorda, A., Mihaylov, V.A., and Parent, C.A. (2006). Chemotaxis: moving forward and holding on to the past. *Thromb. Haemost.* *95*, 12–21.
- Bargmann, C. (2006). Chemosensation in *C. elegans*. *WormBook*.
- Bargmann, C.I., Hartwig, E., and Horvitz, H.R. (1993). Odorant-selective genes and neurons mediate olfaction in *C. elegans*. *Cell* *74*, 515–527.

- Beavo, J.A., Conti, M., and Heaslip, R.J. (1994). Multiple cyclic nucleotide phosphodiesterases. *Mol. Pharmacol.* *46*, 399–405.
- Beavo, J.A., Francis, S.H., and Houslay, M.D. (2010). *Cyclic Nucleotide Phosphodiesterases in Health and Disease* (CRC Press).
- Bezerra, R.M.F., Pinto, P.A., Fraga, I., and Dias, A.A. (2016). Enzyme inhibition studies by integrated Michaelis-Menten equation considering simultaneous presence of two inhibitors when one of them is a reaction product. *Comput. Methods Programs Biomed.* *125*, 2–7.
- Blount, M.A., Zoraghi, R., Ke, H., Bessay, E.P., Corbin, J.D., and Francis, S.H. (2006). A 46-amino acid segment in phosphodiesterase-5 GAF-B domain provides for high vardenafil potency over sildenafil and tadalafil and is involved in phosphodiesterase-5 dimerization. *Mol. Pharmacol.* *70*, 1822–1831.
- Blumenthal, S.A. (2012). Earl Sutherland (1915-1974) [corrected] and the discovery of cyclic AMP. *Perspect. Biol. Med.* *55*, 236–249.
- Boden, W.E., Finn, A.V., Patel, D., Peacock, W.F., Thadani, U., and Zimmerman, F.H. (2012). Nitrates as an integral part of optimal medical therapy and cardiac rehabilitation for stable angina: review of current concepts and therapeutics. *Clin. Cardiol.* *35*, 263–271.
- de Boer, H.A., Comstock, L.J., and Vasser, M. (1983). The tac promoter: a functional hybrid derived from the trp and lac promoters. *Proc. Natl. Acad. Sci. U. S. A.* *80*, 21–25.
- Boldt, J., and Suttner, S. (2007). Combined use of ultra-short acting beta-blocker esmolol and intravenous phosphodiesterase 3 inhibitor enoximone. *Expert Opin. Pharmacother.* *8*, 2135–2147.
- Bornhorst, J.A., Deibel, M.A., and Mulnix, A.B. (2004). Gene amplification by PCR and subcloning into a GFP-fusion plasmid expression vector as a molecular biology laboratory course*. *Biochem. Mol. Biol. Educ. Bimon. Publ. Int. Union Biochem. Mol. Biol.* *32*, 173–182.
- Bounoutas, A., and Chalfie, M. (2007). Touch sensitivity in *Caenorhabditis elegans*. *Pflug. Arch. Eur. J. Physiol.* *454*, 691–702.
- Bucher, M.H., Evdokimov, A.G., and Waugh, D.S. (2002). Differential effects of short affinity tags on the crystallization of *Pyrococcus furiosus* maltodextrin-binding protein. *Acta Crystallogr. D Biol. Crystallogr.* *58*, 392–397.
- Burgess-Brown, N.A., Sharma, S., Sobott, F., Loenarz, C., Oppermann, U., and Gileadi, O. (2008). Codon optimization can improve expression of human genes in *Escherichia coli*: A multi-gene study. *Protein Expr. Purif.* *59*, 94–102.
- Busch, K.E., Laurent, P., Soltész, Z., Murphy, R.J., Faivre, O., Hedwig, B., Thomas, M., Smith, H.L., and de Bono, M. (2012). Tonic signaling from O₂ sensors sets neural circuit activity and behavioral state. *Nat. Neurosci.* *15*, 581–591.
- Carson, S., Carson, S., Miller, H., and Witherow, D.S. (2012). *Molecular Biology Techniques: A Classroom Laboratory Manual* (Academic Press).

Castellsague, J., Perez-Gutthann, S., Calingaert, B., Bui, C., Varas-Lorenzo, C., Arana, A., Prados-Torres, A., Poblador-Plou, B., Gonzalez-Rubio, F., Giner-Soriano, M., et al. (2017). Characterization of new users of cilostazol in the UK, Spain, Sweden, and Germany. *Pharmacoepidemiol. Drug Saf.*

Ceccarelli, E.A., Carrillo, N., and Roveri, O.A. (2008). Efficiency function for comparing catalytic competence. *Trends Biotechnol.* *26*, 117–118.

Chung, Y.W., Ahmad, F., Tang, Y., Hockman, S.C., Kee, H.J., Berger, K., Guirguis, E., Choi, Y.H., Schimel, D.M., Aponte, A.M., et al. (2017). White to beige conversion in PDE3B KO adipose tissue through activation of AMPK signaling and mitochondrial function. *Sci. Rep.* *7*, 40445.

Clark, D.A., Biron, D., Sengupta, P., and Samuel, A.D.T. (2006). The AFD Sensory Neurons Encode Multiple Functions Underlying Thermotactic Behavior in *Caenorhabditis elegans*. *J. Neurosci.* *26*, 7444–7451.

Cobb, B.D., and Clarkson, J.M. (1994). A simple procedure for optimising the polymerase chain reaction (PCR) using modified Taguchi methods. *Nucleic Acids Res.* *22*, 3801–3805.

Colman, R.W. (2004). Platelet Cyclic Adenosine Monophosphate Phosphodiesterases: Targets for Regulating Platelet-Related Thrombosis. *Semin. Thromb. Hemost.* *30*, 451–460.

Cong, L., Chen, K., Li, J., Gao, P., Li, Q., Mi, S., Wu, X., and Zhao, A.Z. (2007). Regulation of adiponectin and leptin secretion and expression by insulin through a PI3K-PDE3B dependent mechanism in rat primary adipocytes. *Biochem. J.* *403*, 519–525.

Conti, M. (2011). Phosphodiesterases and regulation of female reproductive function. *Curr. Opin. Pharmacol.* *11*, 665–669.

Conti, M., and Beavo, J. (2007). Biochemistry and Physiology of Cyclic Nucleotide Phosphodiesterases: Essential Components in Cyclic Nucleotide Signaling. *Annu. Rev. Biochem.* *76*, 481–511.

Conti, M., Mika, D., and Richter, W. (2014). Cyclic AMP compartments and signaling specificity: Role of cyclic nucleotide phosphodiesterases. *J. Gen. Physiol.* *143*, 29–38.

Cooper, G.M. (2000). The Central Role of Enzymes as Biological Catalysts.

Corbin, J.D., and Francis, S.H. (1999). Cyclic GMP Phosphodiesterase-5: Target of Sildenafil. *J. Biol. Chem.* *274*, 13729–13732.

Couto, A., Oda, S., Nikolaev, V.O., Soltesz, Z., and de Bono, M. (2013). In vivo genetic dissection of O₂-evoked cGMP dynamics in a *Caenorhabditis elegans* gas sensor. *Proc. Natl. Acad. Sci. U. S. A.* *110*, E3301-3310.

Daegelen, P., Studier, F.W., Lenski, R.E., Cure, S., and Kim, J.F. (2009). Tracing Ancestors and Relatives of *Escherichia coli* B, and the Derivation of B Strains REL606 and BL21(DE3). *J. Mol. Biol.* *394*, 634–643.

Damak, S., and Bullock, D.W. (1993). A simple two-step method for efficient blunt-end ligation of DNA fragments. *BioTechniques* *15*, 448–450, 452.

- Day, J.P., Dow, J.A.T., Houslay, M.D., and Davies, S.-A. (2005). Cyclic nucleotide phosphodiesterases in *Drosophila melanogaster*. *Biochem. J.* *388*, 333–342.
- Degerman, E., Belfrage, P., and Manganiello, V.C. (1996). cGMP-inhibited phosphodiesterases (PDE3 gene family). *Biochem. Soc. Trans.* *24*, 1010–1014.
- Degerman, E., Belfrage, P., and Manganiello, V.C. (1997). Structure, localization, and regulation of cGMP-inhibited phosphodiesterase (PDE3). *J. Biol. Chem.* *272*, 6823–6826.
- Degerman, E., Ahmad, F., Chung, Y.W., Guirguis, E., Omar, B., Stenson, L., and Manganiello, V. (2011). From PDE3B to the regulation of energy homeostasis. *Curr. Opin. Pharmacol.* *11*, 676–682.
- Demain, A.L., and Vaishnav, P. (2009). Production of recombinant proteins by microbes and higher organisms. *Biotechnol. Adv.* *27*, 297–306.
- Ding, B., Abe, J., Wei, H., Huang, Q., Walsh, R.A., Molina, C.A., Zhao, A., Sadoshima, J., Blaxall, B.C., Berk, B.C., et al. (2005). Functional role of phosphodiesterase 3 in cardiomyocyte apoptosis: implication in heart failure. *Circulation* *111*, 2469–2476.
- DiPilato, L.M., Ahmad, F., Harms, M., Seale, P., Manganiello, V., and Birnbaum, M.J. (2015). The Role of PDE3B Phosphorylation in the Inhibition of Lipolysis by Insulin. *Mol. Cell. Biol.* *35*, 2752–2760.
- Dormiani, K., Khazaie, Y., Sadeghi, H.M.M., Rabbani, M., and Moazen, F. (2007). Cloning and expression of a human tissue plasminogen activator variant: K2S in *Escherichia coli*. *Pak. J. Biol. Sci. PJBS* *10*, 946–949.
- Dragosits, M., Nicklas, D., and Tagkopoulos, I. (2012). A synthetic biology approach to self-regulatory recombinant protein production in *Escherichia coli*. *J. Biol. Eng.* *6*, 2.
- Dugaiczyk, A., Boyer, H.W., and Goodman, H.M. (1975). Ligation of EcoRI endonuclease-generated DNA fragments into linear and circular structures. *J. Mol. Biol.* *96*, 171–184.
- Duong-Ly, K.C., and Gabelli, S.B. (2014). Using ion exchange chromatography to purify a recombinantly expressed protein. *Methods Enzymol.* *541*, 95–103.
- Eisenthal, R., Danson, M.J., and Hough, D.W. (2007). Catalytic efficiency and k_{cat}/K_M : a useful comparator? *Trends Biotechnol.* *25*, 247–249.
- Esposito, D., and Chatterjee, D.K. (2006). Enhancement of soluble protein expression through the use of fusion tags. *Curr. Opin. Biotechnol.* *17*, 353–358.
- Evans, T.C., Benner, J., and Xu, M.Q. (1998). Semisynthesis of cytotoxic proteins using a modified protein splicing element. *Protein Sci. Publ. Protein Soc.* *7*, 2256–2264.
- Fathi-Roudsari, M., Akhavian-Tehrani, A., and Maghsoudi, N. (2016). Comparison of Three *Escherichia coli* Strains in Recombinant Production of Reteylase. *Avicenna J. Med. Biotechnol.* *8*, 16–22.
- Ferrer, M., Chernikova, T.N., Yakimov, M.M., Golyshin, P.N., and Timmis, K.N. (2003). Chaperonins govern growth of *Escherichia coli* at low temperatures. *Nat. Biotechnol.* *21*, 1266–1267.
- Ford, C.F., Suominen, I., and Glatz, C.E. (1991). Fusion tails for the recovery and purification of recombinant proteins. *Protein Expr. Purif.* *2*, 95–107.

- Francis, S.H., Turko, I.V., and Corbin, J.D. (2001). Cyclic nucleotide phosphodiesterases: relating structure and function. *Prog. Nucleic Acid Res. Mol. Biol.* *65*, 1–52.
- Francis, S.H., Conti, M., and Houslay, M.D. (2011). *Phosphodiesterases as Drug Targets* (Springer).
- Frangioni, J.V., and Neel, B.G. (1993). Solubilization and Purification of Enzymatically Active Glutathione S-Transferase (pGEX) Fusion Proteins. *Anal. Biochem.* *210*, 179–187.
- Fu, Y., and Yau, K.-W. (2007). Phototransduction in mouse rods and cones. *Pflug. Arch. Eur. J. Physiol.* *454*, 805–819.
- Fujishige, K., Kotera, J., Yuasa, K., and Omori, K. (2000). The human phosphodiesterase PDE10A gene genomic organization and evolutionary relatedness with other PDEs containing GAF domains. *Eur. J. Biochem. FEBS* *267*, 5943–5951.
- Gecchele, E., Merlin, M., Brozzetti, A., Falorni, A., Pezzotti, M., and Avesani, L. (2015). A comparative analysis of recombinant protein expression in different biofactories: bacteria, insect cells and plant systems. *J. Vis. Exp. JoVE*.
- Geng, L., Xin, W., Huang, D.-W., and Feng, G. (2006). A universal cloning vector using vaccinia topoisomerase I. *Mol. Biotechnol.* *33*, 23–28.
- Gordon, E., Horsefield, R., Swarts, H.G.P., de Pont, J.J.H.H.M., Neutze, R., and Snijder, A. (2008). Effective high-throughput overproduction of membrane proteins in *Escherichia coli*. *Protein Expr. Purif.* *62*, 1–8.
- Gronwald, J.W., and Plaisance, K.L. (1998). Isolation and characterization of glutathione S-transferase isozymes from sorghum. *Plant Physiol.* *117*, 877–892.
- Guirguis, E., Hockman, S., Chung, Y.W., Ahmad, F., Gavrilova, O., Raghavachari, N., Yang, Y., Niu, G., Chen, X., Yu, Z.X., et al. (2013). A role for phosphodiesterase 3B in acquisition of brown fat characteristics by white adipose tissue in male mice. *Endocrinology* *154*, 3152–3167.
- Gustafsson, C., Minshull, J., Govindarajan, S., Ness, J., Villalobos, A., and Welch, M. (2012). Engineering genes for predictable protein expression. *Protein Expr. Purif.* *83*, 37–46.
- Hall, A.L., Franke, J., Faure, M., and Kessin, R.H. (1993). The role of the cyclic nucleotide phosphodiesterase of *Dictyostelium discoideum* during growth, aggregation, and morphogenesis: overexpression and localization studies with the separate promoters of the *pde*. *Dev. Biol.* *157*, 73–84.
- Hambleton, R., Krall, J., Tikishvili, E., Honegger, M., Ahmad, F., Manganiello, V.C., and Movsesian, M.A. (2005). Isoforms of cyclic nucleotide phosphodiesterase PDE3 and their contribution to cAMP hydrolytic activity in subcellular fractions of human myocardium. *J. Biol. Chem.* *280*, 39168–39174.
- Hammarström, M., Hellgren, N., van den Berg, S., Berglund, H., and Härd, T. (2002). Rapid screening for improved solubility of small human proteins produced as fusion proteins in *Escherichia coli*. *Protein Sci. Publ. Protein Soc.* *11*, 313–321.
- Harper, S., and Speicher, D.W. (2008). Expression and purification of GST fusion proteins. *Curr. Protoc. Protein Sci.* Editor. Board John E Coligan Al *Chapter 6*, Unit 6.6.

- Harper, S., and Speicher, D.W. (2011). Purification of proteins fused to glutathione S-transferase. *Methods Mol. Biol. Clifton NJ* 681, 259r, S.
- Harrington, A.J., Hamamichi, S., Caldwell, G.A., and Caldwell, K.A. (2010). *C. elegans* as a model organism to investigate molecular pathways involved with Parkinson's disease. *Dev. Dyn. Off. Publ. Am. Assoc. Anat.* 239, 1282–1295.
- Hillier, L.W., Coulson, A., Murray, J.I., Bao, Z., Sulston, J.E., and Waterston, R.H. (2005). Genomics in *C. elegans*: So many genes, such a little worm. *Genome Res.* 15, 1651–1660.
- Hofmann, F., Bernhard, D., Lukowski, R., and Weinmeister, P. (2009). cGMP regulated protein kinases (cGK). *Handb. Exp. Pharmacol.* 137–162.
- Hou, J., Xu, J., Liu, M., Zhao, R., Luo, H.-B., and Ke, H. (2011). Structural Asymmetry of Phosphodiesterase-9, Potential Protonation of a Glutamic Acid, and Role of the Invariant Glutamine. *PLOS ONE* 6, e18092.
- Houslay, M.D., and Adams, D.R. (2003). PDE4 cAMP phosphodiesterases: modular enzymes that orchestrate signalling cross-talk, desensitization and compartmentalization. *Biochem. J.* 370, 1–18.
- Houslay, M.D., and Milligan, G. (1997). Tailoring cAMP-signalling responses through isoform multiplicity. *Trends Biochem. Sci.* 22, 217–224.
- Houslay, M.D., Schafer, P., and Zhang, K.Y.J. (2005). Keynote review: phosphodiesterase-4 as a therapeutic target. *Drug Discov. Today* 10, 1503–1519.
- Hughes, R.A., Miklos, A.E., and Ellington, A.D. (2011). Gene synthesis: methods and applications. *Methods Enzymol.* 498, 277–309.
- Imai, A., Nashida, T., and Shimomura, H. (1996). Expression of mRNA encoding cAMP-specific phosphodiesterase isoforms in rat parotid glands. *IUBMB Life* 40, 1175–1181.
- Inada, H., Ito, H., Satterlee, J., Sengupta, P., Matsumoto, K., and Mori, I. (2006). Identification of Guanylyl Cyclases That Function in Thermosensory Neurons of *Caenorhabditis elegans*. *Genetics* 172, 2239–2252.
- Insall, R.H., Soede, R.D., Schaap, P., and Devreotes, P.N. (1994). Two cAMP receptors activate common signaling pathways in *Dictyostelium*. *Mol. Biol. Cell* 5, 703–711.
- Jana, S., and Deb, J.K. (2005). Strategies for efficient production of heterologous proteins in *Escherichia coli*. *Appl. Microbiol. Biotechnol.* 67, 289–298.
- Jin, S.L., Swinnen, J.V., and Conti, M. (1992). Characterization of the structure of a low Km, rolipram-sensitive cAMP phosphodiesterase. Mapping of the catalytic domain. *J. Biol. Chem.* 267, 18929–18939.
- Johansson, E.M., Sanabra, C., Cortés, R., Vilaró, M.T., and Mengod, G. (2011). Lipopolysaccharide administration in vivo induces differential expression of cAMP-specific phosphodiesterase 4B mRNA splice variants in the mouse brain. *J. Neurosci. Res.* 89, 1761–1772.
- Jones, P.G., and Inouye, M. (1994). The cold-shock response--a hot topic. *Mol. Microbiol.* 11, 811–818.

- Jung, W.H., Warn, P., Ragni, E., Popolo, L., Nunn, C.D., Turner, M.P., and Stateva, L. (2005). Deletion of PDE2, the gene encoding the high-affinity cAMP phosphodiesterase, results in changes of the cell wall and membrane in *Candida albicans*. *Yeast* 22, 285–294.
- Kataeva, I., Chang, J., Xu, H., Luan, C.-H., Zhou, J., Uversky, V.N., Lin, D., Horanyi, P., Liu, Z.J., Ljungdahl, L.G., et al. (2005). Improving solubility of *Shewanella oneidensis* MR-1 and *Clostridium thermocellum* JW-20 proteins expressed into *Escherichia coli*. *J. Proteome Res.* 4, 1942–1951.
- Ke, H., and Wang, H. (2007). Crystal structures of phosphodiesterases and implications on substrate specificity and inhibitor selectivity. *Curr. Top. Med. Chem.* 7, 391–403.
- Ke, H., Wang, H., and Ye, M. (2011). Structural Insight into the Substrate Specificity of Phosphodiesterases. In *Phosphodiesterases as Drug Targets*, S.H. Francis, M. Conti, and M.D. Houslay, eds. (Springer Berlin Heidelberg), pp. 121–134.
- Kenan, Y., Murata, T., Shakur, Y., Degerman, E., and Manganiello, V.C. (2000). Functions of the N-terminal region of cyclic nucleotide phosphodiesterase 3(PDE 3) isoforms. *J. Biol. Chem.* 275, 12331–12338.
- Kennell, D. (2002). Processing Endoribonucleases and mRNA Degradation in Bacteria. *J. Bacteriol.* 184, 4645–4657.
- Keravis, T., and Lugnier, C. (2012). Cyclic nucleotide phosphodiesterase (PDE) isozymes as targets of the intracellular signalling network: benefits of PDE inhibitors in various diseases and perspectives for future therapeutic developments. *Br. J. Pharmacol.* 165, 1288–1305.
- Khow, O., and Suntrarachun, S. (2012). Strategies for production of active eukaryotic proteins in bacterial expression system. *Asian Pac. J. Trop. Biomed.* 2, 159–162.
- Kimura, K.D., Miyawaki, A., Matsumoto, K., and Mori, I. (2004). The *C. elegans* thermosensory neuron AFD responds to warming. *Curr. Biol. CB* 14, 1291–1295.
- Lanza, A.M., Curran, K.A., Rey, L.G., and Alper, H.S. (2014). A condition-specific codon optimization approach for improved heterologous gene expression in *Saccharomyces cerevisiae*. *BMC Syst. Biol.* 8, 33.
- Lebedenko, E.N., Birikh, K.R., Plutalov, O.V., and Berlin YuA, null (1991). Method of artificial DNA splicing by directed ligation (SDL). *Nucleic Acids Res.* 19, 6757–6761.
- L'Etoile, N.D., and Bargmann, C.I. (2000). Olfaction and odor discrimination are mediated by the *C. elegans* guanylyl cyclase ODR-1. *Neuron* 25, 575–586.
- Li, N., and Baehr, W. (1998). Expression and characterization of human PDEdelta and its *Caenorhabditis elegans* ortholog CEdelta. *FEBS Lett.* 440, 454–457.
- Li, Z., Chen, J.-H., Hao, Y., and Nair, S.K. (2012). Structures of the PelD Cyclic Diguanylate Effector Involved in Pellicle Formation in *Pseudomonas aeruginosa* PAO1. *J. Biol. Chem.* 287, 30191–30204.
- Lichty, J.J., Malecki, J.L., Agnew, H.D., Michelson-Horowitz, D.J., and Tan, S. (2005). Comparison of affinity tags for protein purification. *Protein Expr. Purif.* 41, 98–105.

- Ling, L., Kao, L.-W., and Wang, N.-H.L. (2014). A new general method for designing affinity chromatography processes. *J. Chromatogr. A*.
- Liu, H., and Maurice, D.H. (1998). Expression of cyclic GMP-inhibited phosphodiesterases 3A and 3B (PDE3A and PDE3B) in rat tissues: differential subcellular localization and regulated expression by cyclic AMP. *Br. J. Pharmacol.* *125*, 1501–1510.
- Liu, J., Ward, A., Gao, J., Dong, Y., Nishio, N., Inada, H., Kang, L., Yu, Y., Ma, D., Xu, T., et al. (2010). *C. elegans* phototransduction requires a G protein-dependent cGMP pathway and a taste receptor homolog. *Nat. Neurosci.* *13*, 715–722.
- Luo, L., Clark, D.A., Biron, D., Mahadevan, L., and Samuel, A.D.T. (2006). Sensorimotor control during isothermal tracking in *Caenorhabditis elegans*. *J. Exp. Biol.* *209*, 4652–4662.
- Ma, P., Wera, S., Van Dijck, P., and Thevelein, J.M. (1999). The PDE1-encoded low-affinity phosphodiesterase in the yeast *Saccharomyces cerevisiae* has a specific function in controlling agonist-induced cAMP signaling. *Mol. Biol. Cell* *10*, 91–104.
- Majorek, K.A., Kuhn, M.L., Chruszcz, M., Anderson, W.F., and Minor, W. (2014). Double trouble—Buffer selection and His-tag presence may be responsible for nonreproducibility of biomedical experiments. *Protein Sci. Publ. Protein Soc.* *23*, 1359–1368.
- Malhotra, A. (2009). Tagging for protein expression. *Methods Enzymol.* *463*, 239–258.
- Manganiello, V. (2011). Cyclic nucleotide phosphodiesterases: critical modulators of endocrine, metabolic, and cardiovascular function and appealing therapeutic targets. *Curr. Opin. Pharmacol.* *11*, 646–648.
- Manganiello, V.C., Reed, B.C., Lieberman, F.S., Moss, J., Lane, M.D., and Vaughan, M. (1983). Alterations in cyclic AMP phosphodiesterase activities during differentiation of 3T3-L1 cells. *J. Cyclic Nucleotide Protein Phosphor. Res.* *9*, 143–154.
- Markaki, M., and Tavernarakis, N. (2010). Modeling human diseases in *Caenorhabditis elegans*. *Biotechnol. J.* *5*, 1261–1276.
- Martinez, S.E., Bruder, S., Schultz, A., Zheng, N., Schultz, J.E., Beavo, J.A., and Linder, J.U. (2005). Crystal structure of the tandem GAF domains from a cyanobacterial adenylyl cyclase: modes of ligand binding and dimerization. *Proc. Natl. Acad. Sci. U. S. A.* *102*, 3082–3087.
- Masciarelli, S., Horner, K., Liu, C., Park, S.H., Hinckley, M., Hockman, S., Nedachi, T., Jin, C., Conti, M., and Manganiello, V. (2004). Cyclic nucleotide phosphodiesterase 3A-deficient mice as a model of female infertility. *J. Clin. Invest.* *114*, 196–205.
- Matsumura, I. (2015). Why Johnny can't clone: Common pitfalls and not so common solutions. *BioTechniques* *59*, IV–XIII.
- Maurice, D.H., and Haslam, R.J. (1990). Molecular basis of the synergistic inhibition of platelet function by nitrovasodilators and activators of adenylyl cyclase: inhibition of cyclic AMP breakdown by cyclic GMP. *Mol. Pharmacol.* *37*, 671–681.

- Maurice, D.H., Palmer, D., Tilley, D.G., Dunkerley, H.A., Netherton, S.J., Raymond, D.R., Elbatarny, H.S., and Jimmo, S.L. (2003). Cyclic nucleotide phosphodiesterase activity, expression, and targeting in cells of the cardiovascular system. *Mol. Pharmacol.* *64*, 533–546.
- McCarter, J.D., Stephens, D., Shoemaker, K., Rosenberg, S., Kirsch, J.F., and Georgiou, G. (2004). Substrate Specificity of the *Escherichia coli* Outer Membrane Protease OmpT. *J. Bacteriol.* *186*, 5919–5925.
- Mehats, C., Andersen, C.B., Filopanti, M., Jin, S.-L.C., and Conti, M. (2002). Cyclic nucleotide phosphodiesterases and their role in endocrine cell signaling. *Trends Endocrinol. Metab.* *13*, 29–35.
- Mercado-Pimentel, M.E., Jordan, N.C., and Aisemberg, G.O. (2002). Affinity purification of GST fusion proteins for immunohistochemical studies of gene expression. *Protein Expr. Purif.* *26*, 260–265.
- Movsesian, M. (2015). New pharmacologic interventions to increase cardiac contractility: challenges and opportunities. *Curr. Opin. Cardiol.* *30*, 285–291.
- Movsesian, M.A. (2003). PDE3 inhibition in dilated cardiomyopathy: reasons to reconsider. *J. Card. Fail.* *9*, 475–480.
- Movsesian, M., Wever-Pinzon, O., and Vandeput, F. (2011). PDE3 inhibition in dilated cardiomyopathy. *Curr. Opin. Pharmacol.* *11*, 707–713.
- Niumsup, P., and Wuthiekanun, V. (2002). Cloning of the class D beta-lactamase gene from *Burkholderia pseudomallei* and studies on its expression in ceftazidime-susceptible and -resistant strains. *J. Antimicrob. Chemother.* *50*, 445–455.
- O'Halloran, D.M., Hamilton, O.S., Lee, J.I., Gallegos, M., and L'Etoile, N.D. (2012). Changes in cGMP levels affect the localization of EGL-4 in AWC in *Caenorhabditis elegans*. *PloS One* *7*, e31614.
- Oknianska, A., Zmuda-Trzebiatowska, E., Manganiello, V., and Degerman, E. (2007). Long-term regulation of cyclic nucleotide phosphodiesterase type 3B and 4 in 3T3-L1 adipocytes. *Biochem. Biophys. Res. Commun.* *353*, 1080–1085.
- Omori, K., and Kotera, J. (2007). Overview of PDEs and Their Regulation. *Circ. Res.* *100*, 309–327.
- Palmer, D., Jimmo, S.L., Raymond, D.R., Wilson, L.S., Carter, R.L., and Maurice, D.H. (2007). Protein kinase A phosphorylation of human phosphodiesterase 3B promotes 14-3-3 protein binding and inhibits phosphatase-catalyzed inactivation. *J. Biol. Chem.* *282*, 9411–9419.
- Pang, D.C. (1988). Cyclic AMP and cyclic GMP phosphodiesterases: Target for drug development. *Drug Dev. Res.* *12*, 85–92.
- Parkes, D.G., Mace, K.F., and Trautmann, M.E. (2013). Discovery and development of exenatide: the first antidiabetic agent to leverage the multiple benefits of the incretin hormone, GLP-1. *Expert Opin. Drug Discov.* *8*, 219–244.
- Persson, A., Gross, E., Laurent, P., Busch, K.E., Bretes, H., and de Bono, M. (2009). Natural variation in a neural globin tunes oxygen sensing in wild *Caenorhabditis elegans*. *Nature* *458*, 1030–1033.
- Pollard, T.D. (2010). A Guide to Simple and Informative Binding Assays. *Mol. Biol. Cell* *21*, 4061–4067.

- Pozuelo Rubio, M., Campbell, D.G., Morrice, N.A., and Mackintosh, C. (2005). Phosphodiesterase 3A binds to 14-3-3 proteins in response to PMA-induced phosphorylation of Ser428. *Biochem. J.* *392*, 163–172.
- Qing, G., Ma, L.-C., Khorchid, A., Swapna, G.V.T., Mal, T.K., Takayama, M.M., Xia, B., Phadtare, S., Ke, H., Acton, T., et al. (2004). Cold-shock induced high-yield protein production in *Escherichia coli*. *Nat. Biotechnol.* *22*, 877–882.
- Quick, M., and Wright, E.M. (2002). Employing *Escherichia coli* to functionally express, purify, and characterize a human transporter. *Proc. Natl. Acad. Sci.* *99*, 8597–8601.
- Richards, J.S. (2001). Perspective: The Ovarian Follicle—A Perspective in 2001. *Endocrinology* *142*, 2184–2193.
- Richter, W (2002). 3', 5'-Cyclic nucleotide phosphodiesterases class III: Members, structure, and catalytic mechanism. *Protens Struct.Funct. Bioinforma.* *46*, 278-286.
- Richter, W., Unciuleac, L., Hermsdorf, T., Kronbach, T., and Dettmer, D. (2001). Identification of substrate specificity determinants in human cAMP-specific phosphodiesterase 4A by single-point mutagenesis. *Cell. Signal.* *13*, 159–167.
- Rohan, R.M., King, D., and Frels, W.I. (1990). Direct sequencing of PCR-amplified junction fragments from tandemly repeated transgenes. *Nucleic Acids Res.* *18*, 6089–6095.
- Rondina, M.T., and Weyrich, A.S. (2012). Targeting Phosphodiesterases in Anti-platelet Therapy. *Handb. Exp. Pharmacol.* 225–238.
- Rosano, G.L., and Ceccarelli, E.A. (2014). Recombinant protein expression in *Escherichia coli*: advances and challenges. *Front. Microbiol.* *5*.
- Rossomando, E.F. (1990). [24] Ion-exchange chromatography. In *Methods in Enzymology*, M.P. Deutscher, ed. (Academic Press), pp. 309–317.
- Rybalkin, S.D., Hinds, T.R., and Beavo, J.A. (2013). Enzyme assays for cGMP hydrolysing Phosphodiesterases. *Methods Mol. Biol. Clifton NJ* *1020*, 51–62.
- Sadeghi, H.M.M., Rabbani, M., Rismani, E., Moazen, F., Khodabakhsh, F., Dormiani, K., and Khazaei, Y. (2011). Optimization of the expression of reteplase in *Escherichia coli*. *Res. Pharm. Sci.* *6*, 87–92.
- Sala, E., and de Marco, A. (2010). Screening optimized protein purification protocols by coupling small-scale expression and mini-size exclusion chromatography. *Protein Expr. Purif.* *74*, 231–235.
- Sequeira, A.F., Brás, J.L.A., Guerreiro, C.I.P.D., Vincentelli, R., and Fontes, C.M.G.A. (2016). Development of a gene synthesis platform for the efficient large scale production of small genes encoding animal toxins. *BMC Biotechnol.* *16*.
- Sette, C., and Conti, M (1996). Phosphorylation and activation of a cAMP specific Phosphodiesterase by the cAMP-dependent Protein Kinase involvement of serine 54 in the enzyme activation. *J. Biol. Chem.* *271*. 16526-16534.

- Shakur, Y., Takeda, K., Kenan, Y., Yu, Z.X., Rena, G., Brandt, D., Houslay, M.D., Degerman, E., Ferrans, V.J., and Manganiello, V.C. (2000). Membrane localization of cyclic nucleotide phosphodiesterase 3 (PDE3). Two N-terminal domains are required for the efficient targeting to, and association of, PDE3 with endoplasmic reticulum. *J. Biol. Chem.* *275*, 38749–38761.
- Shakur, Y., Holst, L.S., Landstrom, T.R., Movesesian, M., Degerman, E., and Manganiello, V. (2001). Regulation and function of the cyclic nucleotide phosphodiesterase (PDE3) gene family. *Prog. Nucleic Acid Res. Mol. Biol.* *66*, 241–277.
- Shemarova, I.V. (2009). cAMP-dependent signal pathways in unicellular eukaryotes. *Crit. Rev. Microbiol.* *35*, 23–42.
- Shidara, H., Hotta, K., and Oka, K. (2017). Compartmentalized cGMP responses of olfactory sensory neurons in *Caenorhabditis elegans*. *J. Neurosci.* 2628–16.
- Sivashanmugam, A., Murray, V., Cui, C., Zhang, Y., Wang, J., and Li, Q. (2009). Practical protocols for production of very high yields of recombinant proteins using *Escherichia coli*. *Protein Sci. Publ. Protein Soc.* *18*, 936–948.
- Snyder, P.B., Florio, V.A., Ferguson, K., and Loughney, K. (1999). Isolation, expression and analysis of splice variants of a human Ca²⁺/calmodulin-stimulated phosphodiesterase (PDE1A). *Cell. Signal.* *11*, 535–544.
- Soderling, S.H., and Beavo, J.A. (2000). Regulation of cAMP and cGMP signaling: new phosphodiesterases and new functions. *Curr. Opin. Cell Biol.* *12*, 174–179.
- Soderling, S.H., Bayuga, S.J., and Beavo, J.A. (1999). Isolation and Characterization of a Dual-Substrate Phosphodiesterase Gene Family: PDE10A. *Proc. Natl. Acad. Sci. U. S. A.* *96*, 7071–7076.
- Sørensen, H.P., and Mortensen, K.K. (2005). Advanced genetic strategies for recombinant protein expression in *Escherichia coli*. *J. Biotechnol.* *115*, 113–128.
- Springett, G.M., Kawasaki, H., and Spriggs, D.R. (2004). Non-kinase second-messenger signaling: new pathways with new promise. *BioEssays News Rev. Mol. Cell. Dev. Biol.* *26*, 730–738.
- Stephens, L., Milne, L., and Hawkins, P. (2008). Moving towards a Better Understanding of Chemotaxis. *Curr. Biol.* *18*, R485–R494.
- Stevenson, J., Krycer, J.R., Phan, L., and Brown, A.J. (2013). A Practical Comparison of Ligation-Independent Cloning Techniques. *PLOS ONE* *8*, e83888.
- Struhl, K. (2001). Subcloning of DNA fragments. *Curr. Protoc. Mol. Biol.* Ed. Frederick M Ausubel *AI Chapter 3*, Unit3.16.
- Sudo, T., Tachibana, K., Toga, K., Tochizawa, S., Inoue, Y., Kimura, Y., and Hidaka, H. (2000). Potent effects of novel anti-platelet aggregatory cilostamide analogues on recombinant cyclic nucleotide phosphodiesterase isozyme activity. *Biochem. Pharmacol.* *59*, 347–356.
- Swaffield, J.C., and Johnston, S.A. (2001). Affinity purification of proteins binding to GST fusion proteins. *Curr. Protoc. Mol. Biol.* Ed. Frederick M Ausubel *AI Chapter 20*, Unit 20.2.

- Tang, Y., Osawa, H., Onuma, H., Nishimiya, T., Ochi, M., Sugita, A., and Makino, H. (2001). Phosphodiesterase 3B gene expression is enhanced in the liver but reduced in the adipose tissue of obese insulin resistant db/db mouse. *Diabetes Res. Clin. Pract.* *54*, 145–155.
- Terpe, K. (2003). Overview of tag protein fusions: from molecular and biochemical fundamentals to commercial systems. *Appl. Microbiol. Biotechnol.* *60*, 523–533.
- Thomas, G.M., and Huganir, R.L. (2004). MAPK cascade signalling and synaptic plasticity. *Nat. Rev. Neurosci.* *5*, 173–183.
- Thompson, W.J., and Appleman, M.M. (1971). Multiple cyclic nucleotide phosphodiesterase activities from rat brain. *Biochemistry (Mosc.)* *10*, 311–316.
- Tilley, D.G., and Maurice, D.H. (2002). Vascular smooth muscle cell phosphodiesterase (PDE) 3 and PDE4 activities and levels are regulated by cyclic AMP in vivo. *Mol. Pharmacol.* *62*, 497–506.
- Torphy, T.J., Zhou, H.L., and Cieslinski, L.B. (1992). Stimulation of beta adrenoceptors in a human monocyte cell line (U937) up-regulates cyclic AMP-specific phosphodiesterase activity. *J. Pharmacol. Exp. Ther.* *263*, 1195–1205.
- Traini, M., Kumaran, R., Thaysen-Andersen, M., Kockx, M., Jessup, W., and Kritharides, L. (2017). N-glycosylation of human sphingomyelin phosphodiesterase acid-like 3A (SMPDL3A) is essential for stability, secretion and activity. *Biochem. J.* *474*, 1071–1092.
- Tsunoda, Y., Sakai, N., Kikuchi, K., Katoh, S., Akagi, K., Miura-Ohnuma, J., Tashiro, Y., Murata, K., Shibuya, N., and Katoh, E. (2005). Improving expression and solubility of rice proteins produced as fusion proteins in *Escherichia coli*. *Protein Expr. Purif.* *42*, 268–277.
- Urh, M., Simpson, D., and Zhao, K. (2009). Affinity chromatography: general methods. *Methods Enzymol.* *463*, 417–438.
- Van Haastert, P.J.M., and Devreotes, P.N. (2004). Chemotaxis: signalling the way forward. *Nat. Rev. Mol. Cell Biol.* *5*, 626–634.
- Vang, A.G., Basole, C., Dong, H., Nguyen, R.K., Housley, W., Guernsey, L., Adami, A.J., Thrall, R.S., Clark, R.B., Epstein, P.M., et al. (2016). Differential Expression and Function of PDE8 and PDE4 in Effector T cells: Implications for PDE8 as a Drug Target in Inflammation. *Front. Pharmacol.* *7*, 259.
- Walls, D., and Loughran, S.T. (2011). Tagging recombinant proteins to enhance solubility and aid purification. *Methods Mol. Biol. Clifton NJ* *681*, 151–175.
- Wang, D., O'Halloran, D., and Goodman, M.B. (2013). GCY-8, PDE-2, and NCS-1 are critical elements of the cGMP-dependent thermotransduction cascade in the AFD neurons responsible for *C. elegans* thermotaxis. *J. Gen. Physiol.* *142*, 437–449.
- Wang, H., Liu, Y., Chen, Y., Robinson, H., and Ke, H. (2005). Multiple Elements Jointly Determine Inhibitor Selectivity of Cyclic Nucleotide Phosphodiesterases 4 and 7. *J. Biol. Chem.* *280*, 30949–30955.
- Wang, H., Peng, M.-S., Chen, Y., Geng, J., Robinson, H., Houslay, M.D., Cai, J., and Ke, H. (2007). Structures of the four subfamilies of phosphodiesterase-4 provide insight into the selectivity of their inhibitors. *Biochem. J.* *408*, 193–201.

Waugh, D.S. (2011). An overview of enzymatic reagents for the removal of affinity tags. *Protein Expr. Purif.* *80*, 283–293.

Wechsler, J., Choi, Y.-H., Krall, J., Ahmad, F., Manganiello, V.C., and Movsesian, M.A. (2002). Isoforms of cyclic nucleotide phosphodiesterase PDE3A in cardiac myocytes. *J. Biol. Chem.* *277*, 38072–38078.

Weidner, J.R., and Dunn, B.M. (1991). Development of synthetic peptide substrates for the poliovirus 3C proteinase. *Arch. Biochem. Biophys.* *286*, 402–408.

Yegnasubramanian, S. (2013). Preparation of Fragment Libraries for Next-Generation Sequencing on the Applied Biosystems SOLiD Platform. *Methods Enzymol.* *529*, 185–200.

Zhang, L., Zhang, Z., Zhang, R.L., Cui, Y., LaPointe, M.C., Silver, B., and Chopp, M. (2006). Tadalafil, a long-acting type 5 phosphodiesterase isoenzyme inhibitor, improves neurological functional recovery in a rat model of embolic stroke. *Brain Res.* *1118*, 192–198.

Zhao, A.Z., Zhao, H., Teague, J., Fujimoto, W., and Beavo, J.A. (1997). Attenuation of insulin secretion by insulin-like growth factor 1 is mediated through activation of phosphodiesterase 3B. *Proc. Natl. Acad. Sci. U. S. A.* *94*, 3223–3228.

Zhao, A.Z., Bornfeldt, K.E., and Beavo, J.A. (1998). Leptin inhibits insulin secretion by activation of phosphodiesterase 3B. *J. Clin. Invest.* *102*, 869–873.

Zhao, A.Z., Shinohara, M.M., Huang, D., Shimizu, M., Eldar-Finkelman, H., Krebs, E.G., Beavo, J.A., and Bornfeldt, K.E. (2000). Leptin induces insulin-like signaling that antagonizes cAMP elevation by glucagon in hepatocytes. *J. Biol. Chem.* *275*, 11348–11354.

Zhao, A.Z., Huan, J.-N., Gupta, S., Pal, R., and Sahu, A. (2002). A phosphatidylinositol 3-kinase phosphodiesterase 3B-cyclic AMP pathway in hypothalamic action of leptin on feeding. *Nat. Neurosci.* *5*, 727–728.

Zhou, Z., Schnake, P., Xiao, L., and Lal, A.A. (2004). Enhanced expression of a recombinant malaria candidate vaccine in *Escherichia coli* by codon optimization. *Protein Expr. Purif.* *34*, 87–94.

Addgene: Plasmid Cloning by PCR (with Protocols).

28-Chen-CorA-2003.pdf.

Protein Purification Protocols | Paul Cutler | Springer.